

**PETROLOGICAL STUDIES OF LEWISIAN BASIC AND ULTRABASIC ROCKS NEAR
SCOURIE, SUTHERLAND.**

C. R. BOWDIDGE, M.A. (Cantab.)

Thesis presented for the degree of Doctor of Philosophy

University of Edinburgh

September, 1969



TABLE 2-1

	S	L	G	X
Qz	20.0	25.9	28.7	30.5
Cor	-3.3	-0.6	1.7	3.3
Or	7.5	14.2	26.0	20.0
Ab	26.2	31.0	28.3	32.0
An	31.4	17.3	9.2	3.0
Hy	10.6	6.4	2.3	4.0
Mt	4.5	2.3	1.2	2.0
Il	1.3	0.9	0.6	0.5
<u>Fe</u>	49.6	50.0	55.1	50.8
Fe+Mg				

Modal averages of the normative compositions

of Lewisian rock groups:

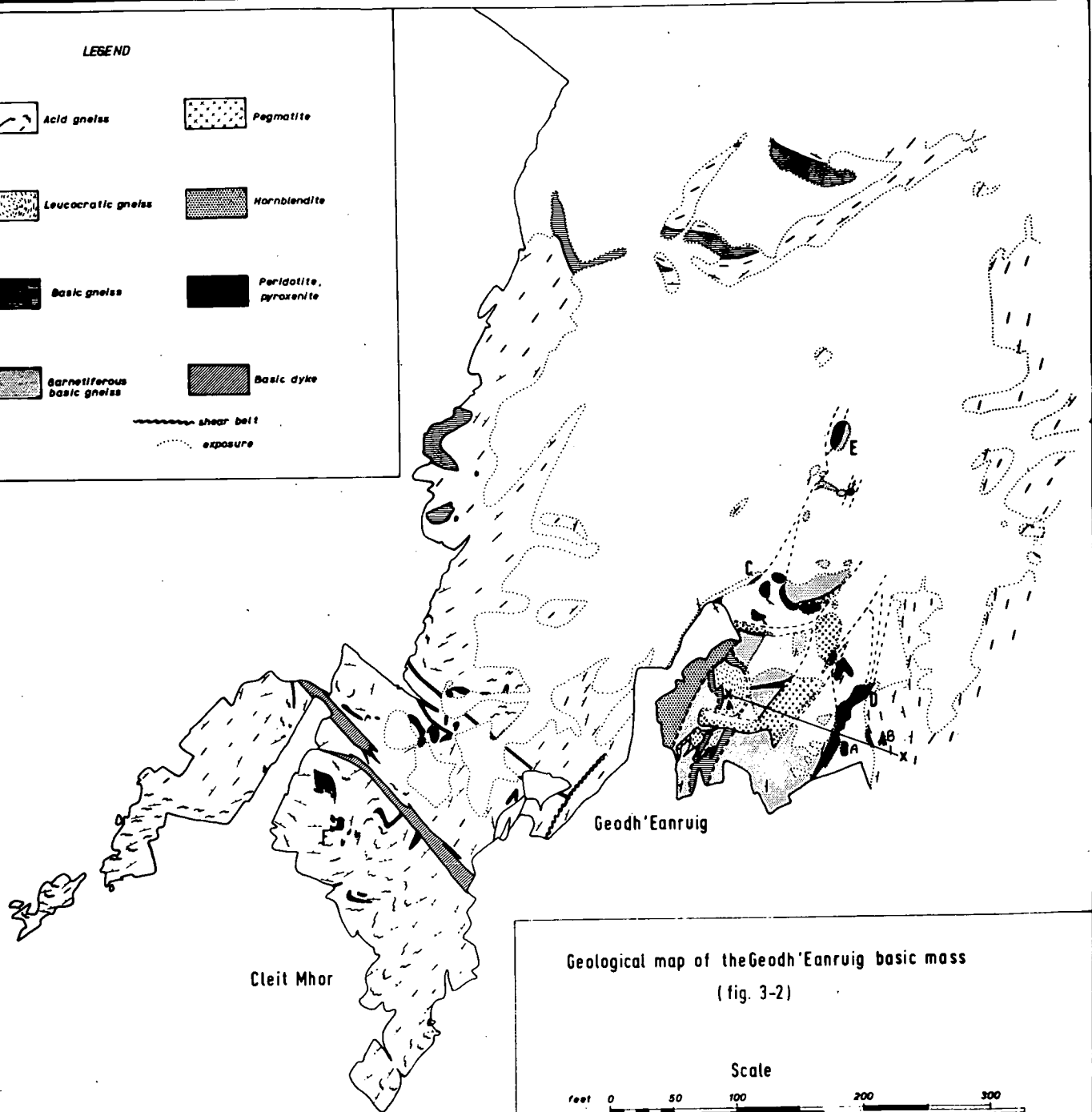
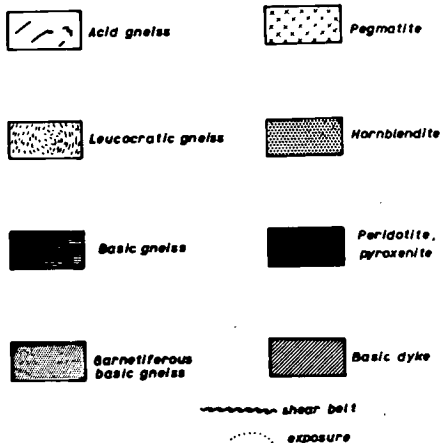
S Average 'pyroxene-granulite' (Holland, 1965)

L Average 'grey gneiss' (Laxfordian) (Holland, 1965)

G Average Laxford Granite (Holland, 1965)

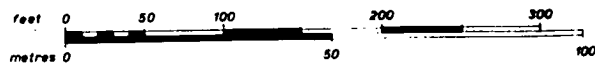
X Material, 49 percent of which subtracted from L
will produce S

LEGEND



Geological map of the Geodh'Eanruig basic mass
(fig. 3-2)

Scale



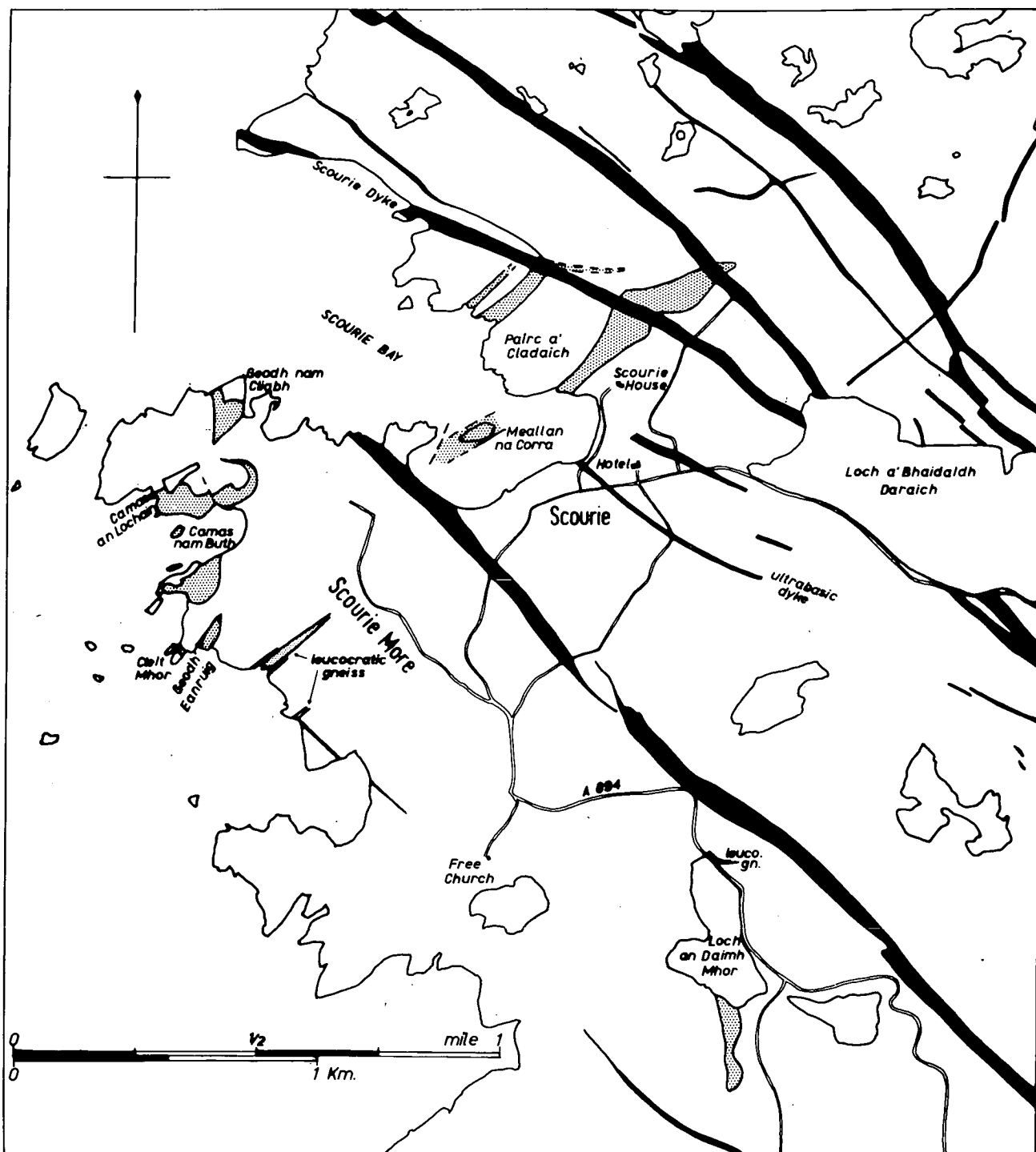


Fig. 3-1. Map of Scourie, showing the basic and ultrabasic masses (heavy stipple) and the separate occurrences of leucocratic gneiss referred to in the text. Other occurrences of similar rocks are not shown. Basic dykes are shown in black and are taken from C.T.Clough (Geol. Surv. of Scotland, 6-inch sheets Sutherland 30 and 39).

	<u>Page</u>
CHAPTER 6 SUMMARY AND CONCLUSIONS	115
6.1 Summary	115
6.2 Conclusions	122
APPENDIX A STRUCTURE OF THE LEWISIAN IN THE SCOURIE AND BEN STROME AREAS	A-1
A.1 Structure of the Ben Strome area	A-1
A.2 Some regional observations	A-8
APPENDIX B POSSIBLE TRACES OF SEDIMENTARY ROCKS IN THE LEWISIAN NEAR SCOURIE	
APPENDIX C CHEMICAL ANALYSES OF ROCKS	
APPENDIX D MINERALOGICAL DATA	
APPENDIX E SIMULATION MODEL FOR DIFFUSION	
APPENDIX F THE INTERPRETATION OF FREE ENERGY-COMPOSITION DIAGRAMS	
APPENDIX G ANALYTICAL METHODS	
REFERENCES	
ACKNOWLEDGEMENTS	

CHAPTER 1

INTRODUCTION

This study is concerned with some aspects of the geology and petrology of the Lewisian Gneiss near Scourie, on the north-west coast of Scotland. The study is directed principally towards the basic and ultrabasic members of the metamorphic complex: in the course of the work it became necessary or desirable to examine certain aspects of the regional geology. A map of the area showing the outline geological features is shown in fig. 1-1.

1.1 History of research

The first major geological study of the area was that of the Geological Survey, which commenced work in the North-West Highlands in 1885, and continued in the area for about 20 years. Although many of their observations were published during that period, the collected results are presented in the memoir "The Geological Structure of the North-West Highlands of Scotland" (Clough et al., 1907), which also summarises all previous studies of the area.

The area between Laxford and Kylesku was critical in the interpretation of the history of the Lewisian. The sequence of events postulated for this region was:

(1) Formation of an Early Complex, now exposed from Scourie southwards at least as far as Lochinver. This complex consists mostly, in the fresh state, of banded pyroxene bearing acid gneisses, together with subordinate amounts of basic and ultrabasic material.

(2) Intrusion of a suite of dykes, mainly N.W.-S.E. trending, and mostly of dolerite.

(3) A late metamorphism, affecting both the rocks of the Early Complex and the basic dykes, regionally to the north of Laxford, and in localised belts of shearing to the south of Scourie. When followed north-eastwards from Scourie, the usually flat-lying gneisses of the Early Complex assume a steep dip and a N.W.-S.E. strike, and become progressively more affected by shearing and folding, until a zone rich in sheet like granite intrusions and pegmatites is reached, which forms the south-western margin of the 'Northern Belt', where the late metamorphism is regional in its effect. The intrusion of these granite sheets was roughly contemporaneous with the late metamorphism.

Following the exhaustive study of the Survey, very little work was done in the North-West Highlands for nearly half a century. Davidson (1943) described the petrology of some of the basic and ultrabasic rocks in S. Harris, which are similar to those near Scourie, observing that they were of granulite facies, but classifying some garnet-clinopyroxene rocks as eclogite.

Resurgence of interest in the Lewisian Gneiss of the mainland began with the study of Sutton and Watson (1950). Many of their conclusions, although framed in more modern terminology, differed little from those of Clough et al. (1907), as was somewhat critically observed by Bailey (1951). The terms 'Scourian' and 'Laxfordian' were introduced as names for the early and late metamorphisms respectively. These terms were used to describe the two metamorphic complexes, and to refer to the metamorphic events which produced them. They were defined as referring to all events which pre-dated and post-dated the intrusion of the N.W.-S.E. basic dykes. So long as only one major metamorphism was recognised in each period of time this definition was

satisfactory, but as the detail of mapping (and, one is tempted to say, the imagination of the mappers) has increased, more metamorphic events and so-called orogenies have been postulated, and a terminology allowing only a two-fold division of Lewisian time no longer seems entirely satisfactory. For instance, Watson (1965) describes evidence subsequently published by Dearnley and Dunning (1967) for the existence of a Pre-Scourian 'orogeny' in Lewis. Both Sutton and Watson (discussion after Sabine and Watson, 1965) reiterate their original definition of the term 'Scourian' to include all events which pre-date the basic dykes, so that, logically, there can be no pre-Scourian events. Neither the 'Pre-Scourian Orogeny', nor a division of the Laxfordian into Early and Late metamorphisms in South Harris (Dearnley, 1963) has yet been substantiated by isotopic dating.

Sutton and Watson (1950) describe the petrology of the acid gneisses of the Scourian Complex near Scourie. These gneisses are characterised, where they are not affected by retrograde metamorphism by: pale blue quartz with minute, needle-like inclusions; antiperthitic plagioclase; augite, often with exsolution lamellae of orthopyroxene; strongly pleochroic hypersthene; and an ore mineral composed of magnetite-ilmenite intergrowth. They were recognised as belonging to the granulite facies, and were termed 'charnockitic'. O'Hara (1960, part 3) has shown that there is little similarity between the Scourie gneisses and the type charnockites of Madras.

Ghose (1958) has studied the petrofabric structure of the rocks between Scourie and Laxford. His observations substantiate the chronology of Sutton and Watson (1950). More recent structural work has been done between Kylesku and Geisgil (Khoury, 1968a, b), around Scourie (Barroah, 1967), and north

(Dash, 1967) and west (Chowdhary, 1969) of Rhiconich.

O'Hara (1961b) has studied the petrology of the dolerite dyke on the north side of Scourie Bay (the 'Scourie Dyke', which Teall (1885) used to demonstrate the metamorphic transformation of dolerite into chemically equivalent hornblende schist), and concluded that it was intruded into rocks which were still at a high temperature. It was therefore unnecessary to postulate a non-orogenic phase between the Scourian and Laxfordian metamorphisms. Burns (1966) studied the geochemistry of similar dykes in the Scourie-Laxford region (the 'Scourie Dykes') and demonstrated their remarkable chemical homogeneity, and the very slight metasomatism which they underwent during Laxfordian metamorphism.

O'Hara (1960, 1961a) has studied the petrology of the gneisses between Scourie and Laxford, with particular reference to the basic and ultrabasic gneisses. The latter have also been the subject of study by Bowes et al. (1961, 1964, 1966), and some controversy has taken place (O'Hara, 1965, 1966), as a consequence of which the present study was felt necessary. The petrology of gneisses and granites near Laxford has been described by Inglis (1966). A geochemical study of the Lewisian rocks of the whole area has been undertaken by Holland (1965), using 400 chemical analyses.

Early isotopic dating (Giletti et al., 1961) dated the early metamorphism at 2460 m.y., and the late metamorphism at 1600 m.y. Subsequent studies (Evans, 1963) demonstrated that, at Lochinver, there were three major metamorphic events: a granulite facies metamorphism at more than 2600 m.y. ('Scourian'); and amphibolite facies metamorphisms at 2200 m.y. ('Inverian'); and 1400-1600 m.y. ('Laxfordian'). The dykes of the Assynt

region (Evans and Tarney, 1964) gave dates from 1400 to 2200 m.y., the broad dolerite or epidiorite dykes (the Scourie Dykes) being dated at 2190 m.y. (i.e. very soon after the Inverian metamorphism).

1.2 A note on terminology

As noted above, the terms 'Scourian' and 'Laxfordian' were introduced by Sutton and Watson (1950) to refer to pre-dyke and post-dyke events, and were defined to include all events which fell into these two divisions of time. In view of the increasing knowledge of the complexity of the history of the Lewisian, mentioned above, as well as the fact that there are several types of basic dyke present in the Lewisian (Tarney, 1963; O'Hara, 1962; Barcoah, 1967; Sutton and Watson, 1950; Clough et al., 1907), and the possibility that these dykes may be of more than one age (Bowes and Ghaly, 1964; Bowes and Khoury, 1965; Evans and Tarney, 1964; Park, 1964), it may be more desirable to have specific names for separate metamorphisms, which are not defined in terms of their relations to any dykes. The method of isotopic dating makes it feasible to adopt such a nomenclature.

For the purposes of this thesis, the terms 'Scourian' and 'Laxfordian' will be used in much the same sense as they were used by Sutton and Watson (1950), but not in the broad sense that their strict definition would imply. They will refer to groups of rocks (Scourian gneisses, Scourian Complex) formed in single metamorphic episodes (i.e. those metamorphisms whose effects are seen at Scourie and Laxford, and which can be dated at about 2600 and 1600 m.y. respectively), and to those metamorphic episodes themselves.

1.3 Basic and ultrabasic rocks

The basic and ultrabasic rocks which form the main object of this study form a minor part of the Scourian Complex, but are widespread, and have been described from Scourie in the north to Achiltibuie in the south, a distance of 25 miles (Bowes et al., 1964). They comprise pyroxene-plagioclase + hornblende rocks (basic gneiss), pyroxene-plagioclase-garnet rocks (garnetiferous basic gneiss), a group of contact gneisses, principally pyroxene-garnet rocks, and various ultrabasic rocks (peridotite, pyroxenite, and hornblendite). They tend to occur intimately associated with each other, and with a group of relatively potash rich quartz-felspar rocks (leucocratic gneisses).

The principal controversy which has arisen over these rocks has been over the extent to which they have been affected by chemical and structural changes during the metamorphism. Bowes et al. (1961) postulate that the basic-ultrabasic masses were unmetamorphosed layered intrusions. The same authors (1964, 1966) conclude that these masses are parts of a larger layered igneous mass(es), disrupted and metamorphosed during the Scourian granulite facies metamorphism, but with the original igneous layering and sequence of rock types still clearly preserved. O'Hara (1960, 1961, 1965, 1966) maintains that the basic, garnetiferous basic, and contact gneisses all originated by reaction between ultrabasic igneous rocks and the acid country rocks during the granulite facies metamorphism.

1.4 Approach to the problem

In Chapter 2, the available evidence relating to the origin of the acid gneisses of the Scourian Complex will be reviewed. A hypothesis involving

partial melting of a supracrustal series of rocks, and loss of the fluid phase will be outlined. The relation between the Scourian and Laxfordian Complexes will be discussed, and if this relation is genetic, certain limits will be imposed on it.

In Chapter 3, descriptions of the field relations of the basic and ultrabasic rocks will be presented, and brief petrographic descriptions of a representative suite of specimens given. Chemical analyses of a series of specimens will be given in Appendix C, and mineralogical data in Appendix D. From this basis, a discussion of the petrogenesis of the basic-ultrabasic association will be made in Chapter 4.

The chemistry and mineralogy of the basic, garnetiferous basic, and ultrabasic gneisses will be reviewed in order to test the rival hypotheses. The chemical variation due to the compositional layering in the ultrabasic gneisses will be discussed, and then the chemistry of the basic members will be discussed in terms of likely igneous compositions. A possible scheme of evolution for magmatic rocks of these compositions will be presented.

The theory of diffusion zone formation will be outlined, and a simple simulation model for reaction between two rock types will be presented. The chemical variation across ultrabasic contacts will be discussed in the light of this theory, and compared with the results of the simulation model, in order to test the hypothesis that the basic members of the association were formed by reaction between the ultrabasic and acid members.

At each stage of the argument, it is not possible to draw firm conclusions, but limits will be placed on the several possible hypotheses, and in

the end, the postulates which have appeared most probable will be brought together into tentative syntheses.

In Chapter 5 the chemistry of the leucocratic gneisses will be discussed, and an attempt made to interpret them as partial melting products of the acid gneisses, dating from an early stage in the evolution of the Complex.

CHAPTER 2

SOME ASPECTS OF THE REGIONAL GEOLOGY

The only aspects of regional geology to be considered in this study are those which bear on the discussion of the origin of the basic and ultrabasic rocks, which follows, or vice versa. The structural history of the Scourian Complex is discussed briefly in Appendix A. In this chapter, some aspects of the petrogenesis of the acid gneisses are examined, and an attempt made to put forward an explanation of their origin.

2.1 Previous studies of the acid gneisses

The opinion of Clough et al. (1907) was that the Scourian gneisses were all primary igneous rocks, the ultrabasic and basic rocks being the product of early, and the acid gneisses of late, consolidation of a single magma. Little or no advance on this hypothesis was made until the now classic study of Sutton and Watson (1950). These authors accepted that all the rocks of the Scourian Complex were metamorphosed. As to the origin of the acid gneisses, they find "it reasonable to consider a migmatitic origin for the complex" (p. 273). As they subsequently state in the discussion that "the authors stated that they used the term 'migmatisation' to describe the formation of mixed rocks," (p. 306), it is not possible to extract a precise petrogenic scheme from their paper. Nevertheless, the term 'migmatitic' now carries overtones of partial melting, without regional metasomatism, amongst a large part of the petrological world.

The next advance was that of O'Hara (1960), who, finding that the Scourian

acid gneisses had an unusual geochemistry, being very poor in potash, and exceptionally poor in rubidium and some other trace elements, postulated "regional metasomatism of a rock series whose main component might have been hornblende schist." (p. 168) and also partial melting with "migration of the fluid phase to regions of lower temperature and/or pressure, leaving the crystalline phases depleted in rubidium relative to potassium" (p. 161).

The extensive geochemical study of Holland (1965) revealed the same geochemical features as that of O'Hara (1960), although with about 20 times as many analyses. It also revealed exceptionally low $\text{Sr}^{87}/\text{Sr}^{86}$ ratios in acid gneisses from Scourie. For these reasons, he postulates that the Scourian Complex represents "a primitive segment of the Earth's crust which separated from the mantle more than 2600 m.y. ago" (p. 274). This statement is not amplified, and might refer to some unidentifiable intra-telluric process, or to more conventional igneous processes of partial melting, and crystal fractionation.

Barooah (1967) describes a number of rocks, which he considers to represent sedimentary relics within the Scourian Complex. For this reason, he postulates a sedimentary, or supracrustal, origin for the whole Complex.

Discussion of the above mentioned hypotheses

It is unlikely that anyone would now dispute that the Scourian Complex has been extensively metamorphosed. As the conclusions of Sutton and Watson are somewhat too allusive to be precisely criticised, the principal problem facing a new worker in the area is the conflict between the conclusions of O'Hara (1960), Holland (1965), and Barooah (1967). To some

extent, these conclusions are based on different lines of evidence, so that it is as well to summarise the features peculiar to the complex, which it is now necessary to explain. They are:

- (1) The 'peculiar geochemistry', particularly the poverty in K, Rb, and Li.
- (2) The very low $\text{Sr}^{87}/\text{Sr}^{86}$ ratios.
- (3) The unusual, possibly sedimentary rocks.

In order to resolve the conflict between the published opinions, it is necessary to answer the following questions:

- (a) Is there definite evidence of the existence of sedimentary relics?
- (b) Does a sedimentary origin for some of the rocks necessitate a similar origin for the whole complex?
- (c) Do the low $\text{Sr}^{87}/\text{Sr}^{86}$ ratios demand a mantle origin? (i.e. is the model of Hurley et al. (1963) valid in detail?).

2.2 The possible sedimentary relics

There are a number of occurrences of somewhat unusual rock types in the Scourie area, which are difficult to explain as of other than sedimentary origin. New data on some of these occurrences are presented in Appendix B. All the known occurrences of such unusual types are summarised below. All except no. (2) are from the Scourian Complex.

- (1) Barcoah (1967) describes three types: 'calc-silicate granulite'; 'meta-arkose'; and 'chlorite schist'. The calc-silicate granulite, a diopside-garnet-calcite-plagioclase rock, is of particularly convincing sedimentary appearance, both in hand specimen and thin section.

(2) Chowdhary (1969) describes two occurrences of quartzite in the Laxfordian Complex near Rhiconich.

(3) Holland (1965) presents approximately 115 analyses of 'pyroxene-granulites or their amphibolitised equivalents', of which six analyses contain between 99 and 100% of SiO_2 . These six analyses are not commented on in the text, but it is possible to infer that they represent quartzitic material.

(4) O'Hara (1960, p. 145) describes a mass of tremolite rock at Loch a'Mhuillin, near Duartbeg, which might represent a calcareous band.

(5) O'Hara (1960, p. 146) describes a quartz-plagioclase granulite with apatite, calcite, epidote, biotite and muscovite, also from Loch a'Mhuillin.

(6) Clough (Geol. Survey of Scotland, 6-inch sheet Sutherland 39) notes an 'irregular sill of saussurite'. The same rock type was described by O'Hara (1960, p. 146) as forming a number of lenticular bodies in the gneiss, on the north shore of Loch Glendhu. Many similar occurrences have been encountered in the present study, and further details are given in Appendix B.

(7) Diopside-apatite-scapolite-sphene-orthoclase rock which occurs near the basic masses at Geodh'Eanruig and Pairc a'Cladaich (O'Hara, 1960, p. 46) is similar in appearance in hand specimen to the calc-silicate granulite described by Barcoah (1967). An analysis is given in Appendix B.

(8) Another rock of atypical composition occurs on the west side of Geodh'Eanruig. It is a garnet-biotite-titanomagnetite rock and is described in Appendix B.

(9) Two occurrences of limestone have been found between Scourie and Kylesku (one is mentioned by Clough et al., 1907, p. 148). They are described in Appendix B.

(10) Clough et al. (1907, p. 153) record the existence of rusty weathering garnetiferous rocks near Ben Stack. They are briefly described in Appendix B, as 'garnet-biotite schist'.

Individually, these occurrences may not be conclusive, but taken together, they strongly suggest that sedimentary rocks are present in the Scourian and Laxfordian Complexes. Such a conclusion might render the hypothesis of direct intratelluric differentiation from the mantle (Holland, 1965?) somewhat less plausible, as it would require that the rocks had ascended to the surface before the Scourian metamorphism.

2.3 The strontium isotope ratios

The relevant data are shown in fig. 2-1, with information extracted from Evans (1963) and Holland (1965). Growth lines for the $\text{Sr}^{87}/\text{Sr}^{86}$ ratios against time are shown for various groups of Lewisian rocks. At the time of the Laxfordian metamorphism (1600 m.y. ago), the Laxfordian gneisses had $\text{Sr}^{87}/\text{Sr}^{86}$ ratios close to 0.705, and the average growth line for these gneisses extrapolated back to 2600 m.y. (the time of the Scourian metamorphism gives a ratio at that time of 0.699, the same as that of the Scourian gneisses at the time. The Scourian gneisses near Lochinver had $\text{Sr}^{87}/\text{Sr}^{86}$ ratios of about 0.706 at 2600 m.y., and the Scourie metadolerite dykes had initial $\text{Sr}^{87}/\text{Sr}^{86}$ ratios of 0.708 to 0.709 at 2200 m.y. (the time of intrusion).

If the tholeiitic magma of the Scourie dykes came from the upper mantle, then it is very likely that the $\text{Sr}^{87}/\text{Sr}^{86}$ ratio of part of the upper mantle

was near 0.708 at 2200 m.y. (contamination by Scourian rocks could only lower the ratio). Part of the crust, at least from Scourie to Lochinver, had $\text{Sr}^{87}/\text{Sr}^{86}$ ratios between 0.700 and 0.705 at that time. These observations, in themselves, are not consistent with the model of Hurley et al. (1963). It seems likely that this model tends to oversimplify matters by not allowing for intra-crustal and intra-mantle fractionation of rubidium relative to strontium. Such fractionation would, by altering the $\text{Rb}^{87}/\text{Sr}^{86}$ ratio, give rise, in time, to variable $\text{Sr}^{87}/\text{Sr}^{86}$ ratios. Allowing for such processes, it no longer seems surprising that some parts of the mantle could have higher $\text{Sr}^{87}/\text{Sr}^{86}$ ratios than some parts of the crust.

2.4 The geochemistry

The particularly barren geochemistry of the Scourian gneisses can be interpreted in a number of ways. Derivation from the mantle, either by way of an intratelluric process (Holland, 1965?), or via andesitic volcanics (D.R. Bowes, verbal communication at the 16th Inter-Univ. Geol. Congr., Glasgow, 1968) is one interpretation. Clastic sediments derived largely from similar pre-existing complexes (however, the latter were formed) would naturally possess similar geochemical features. The other published postulate, that of O'Hara (1960) may require a little explanation.

Fig. 2-2 illustrates diagrammatically the effects of partial melting on the dehydration of a series of rocks undergoing progressive metamorphism. In stage 1, removal of water vapour can produce rocks with compositions lying along the line A-B, but none less hydrous than these. On the reasonable assumption that partial melting ensues before, or simultaneously with (Lundgren, 1966),

the breakdown of hydrous phases, compositions less hydrous than those along the line A-B which will be pyroxene-bearing on cooling can only be produced by abstraction of the paligenetic liquid phase. Incidentally, such a process may help to explain metamorphic segregation, since the mafic rock C, whose composition lies on the line joining the liquid and ultramafic compositions, will, by total loss of the liquid phase, become ultramafic in composition, while the felsic rock D will become more felsic. This might be a possible mechanism for the production of ultramafic knots in the banded gneiss complex.

Any elements which readily enter the liquid phase will be removed with it. The remarkable paucity of the Scourian gneisses in such elements could possibly be explained by this mechanism. Table 2-1 shows the (modal) average normative compositions of the Scourian and Laxfordian gneisses, and the Laxford Granites (from the data of Holland, 1965), and the normative composition of a material, which could be subtracted to the extent of ^{49%}~~42%~~ from the average Laxfordian gneiss to produce the average Scourian gneiss. (In the calculation of this composition, normative diopside was reckoned as the equivalent weight of normative hypersthene, anorthite, and negative corundum.) The composition of this subtracted material does not differ greatly from that of the average Laxford Granite, interpreted by Holland (1965), as a partial melting product of the Laxfordian gneisses. The latter have compositions consistent with their being a normal sedimentary series (Holland, 1965).

The coincidence of the $\text{Sr}^{87}/\text{Sr}^{86}$ ratios of the Scourian and Laxfordian gneisses at the time of the Scourian metamorphism very strongly suggests a link between the two groups of rocks, which was broken at that time. Holland (1965) suggests a sedimentary derivation of the Laxfordian rocks from the

Scourian in immediately post-Scourian times. Another possible interpretation is that the Scourian Gneisses were derived from what are now the Laxfordian gneisses by partial melting and loss of a fluid, granitic, phase, during the Scourian metamorphism.

There are two objections to this apparently feasible proposal. The basic rocks (amphibolites) of the Laxford region are substantially different in composition from the basic and garnetiferous basic gneisses of the Scourian Complex (Table 4-3, and fig. 4-13). Furthermore, ultrabasic intrusions enclosed in biotite bearing acid rocks (the Laxfordian gneisses are uniformly biotite bearing) normally react to produce diffusion zones, amongst which a biotite zone is prominent (fig. 4-31), but no representatives of such a zone have been found near the ultrabasic gneisses at Scourie, Ben Strone, or elsewhere. For these reasons, it is not entirely likely that the present Laxfordian Complex was parental to the present Scourian Complex. The evidence thus favours the conclusion of Holland (1965), that the Laxfordian rocks were derived by a sedimentary process from the Scourian Complex.

As to the Scourian Complex itself, the arguments presented above suggest that the acid gneisses comprising the majority of it were formed from sediments derived from an earlier complex, of somewhat similar composition, but richer in potassium and especially rubidium, and a similarly low $\text{Sr}^{87}/\text{Sr}^{86}$ ratio. Such a complex could have been composed predominantly of intermediate igneous rocks. Occasional calcareous and other sediments of slightly exotic composition are still preserved. The Scourian Complex would, in this way, have been hornblende and chlorite, and not biotite bearing at low metamorphic grade. Most of the

water, and most of the (minor) potash, rubidium, and lithium would have been lost in the palingenetic fluid which has been removed.

CHAPTER 3DESCRIPTIONS OF THE BASIC AND ULTRABASIC MASSES3.1 Occurrence of basic and ultrabasic rocks in the Scourian Complex

Basic gneisses, composed of hypersthene, augite and plagioclase, with or without hornblende, and without garnet are common in the granulite facies Scourian Complex. They occur as generally concordant bodies in the acid gneiss. They are of all sizes, from distinct units hundreds of feet thick, to bands only a few cm. thick within the acid gneiss, at which point they may be said to comprise no more than mafic folia in the banded gneiss. Where they form mappable units, as near Loch Clach a'Chinn Dubh (fig. 3-9) they commonly contain conformable bands and streaks, a few cm. thick, rich in quartz and plagioclase. These bands and streaks increase in thickness and number outwards, so that the basic rock interdigitates with and passes by gradations into the acid gneiss. All intermediate types between acid and basic gneisses are found, and the boundaries shown on fig. 3-9 are somewhat arbitrary.

In their more massive and quartz-free central portions, these bodies are quite often poorly garnetiferous. Garnet rich basic gneisses and ultrabasic gneisses are of rarer occurrence, but may occur within the larger basic masses (e.g. garnetiferous basic gneiss E. and S.W. of Loch Clach a'Chinn Dubh, and ultrabasic gneiss W. of the summit of Ben Strome, both in fig. 3-9). They may also be found as detached bodies in the acid gneiss, with only subordinate amounts of basic gneiss (e.g. garnetiferous basic gneiss E. of the Badcall-Scourie road, NC 167425, and ultrabasic gneiss at Poll Banruig, on the S.W. side of Ben Stack, NC 270414).

The most common occurrence of ultrabasic and garnetiferous basic gneisses however, is in distinct masses, associated with each other, and with minor amounts of garnet-free basic gneiss. Such masses are common near Scourie, both near the roads (Bowes et al., 1964, fig. 8), and elsewhere (Geol. Survey of Scotland, 6-inch sheets, Sutherland nos. 30, 31, 39, 40, 49, 50).

It is these basic and ultrabasic masses which form the principal object of this study. Their widespread occurrence, from Ben Stack in the North to Achiltibule in the South, has led Bowes et al. (1964) to suggest that they are parts of a layered igneous intrusion or series of intrusions, disrupted during the metamorphism. O'Hara (1961), by contrast, regards them as ultrabasic intrusions which have reacted with the enclosing acid gneiss during the metamorphism, the basic rocks forming a series of zones around the original intrusions.

The features emphasised by Bowes et al. (1964) are: the mineral banding in the rocks; the occurrence of sedimentary structures, indicative of crystal accumulation; and the consistently upward sequence from ultrabasic through basic rocks, all of which were taken as evidence of a layered igneous origin. O'Hara (1965), using evidence from the masses near Scourie only, disputes the nature of the sedimentary structures, and considers that they are likely to be tectonic in origin. Further, he lists four possible modes of origin of mineral banding, only one of which is igneous, and observes that in many of the masses, the garnetiferous basic member occurs as often below as above the ultrabasic gneiss.

The divergence of these conclusions illustrates the difficulties which arise in any attempt to discover the original nature of a group of rocks in

such a high grade metamorphic terrain. This study, which was commenced as an attempt to reconcile the conclusions of Bowes et al. (1964, 1966), with those of O'Hara (1961, 1965, 1966), concentrated on a detailed chemical study. It was desirable, however, to re-examine the field evidence, as even this has been interpreted very differently by different authors.

The two localities chosen for study in detail were: around Scourie Bay, and the Ben Strome area (figs. 3-1 and 3-9). The petrology of the basic and ultrabasic rocks near Scourie Bay has been studied in detail by O'Hara (1960, 1961). These rocks are very well exposed at several localities on the shore. The Ben Strome basic and ultrabasic rocks form the largest mass in the area, and are in the region of the flattest lying and least retrogressively altered gneisses of the whole complex. Many similar basic-ultrabasic masses in the area are less suitable for study because of indifferent exposure or retrograde metamorphism.

The only other petrological work in this thesis is mineral analysis on a specimen from Loch an Daimh Mhor, one mile South of Scourie (O'Hara, 1961 specimen UA), which was made available by Dr. O'Hara. This basic and ultrabasic mass is poorly exposed, and the relations of the rock types are too complex for an interpretation to be definite (Bowes et al., 1964, 1966; O'Hara, 1961, 1965).

3.2 Presentation of data

Data will be presented in the following order:

Summary of the principal rock types

Field relations: maps with brief descriptions referring to the most important features.

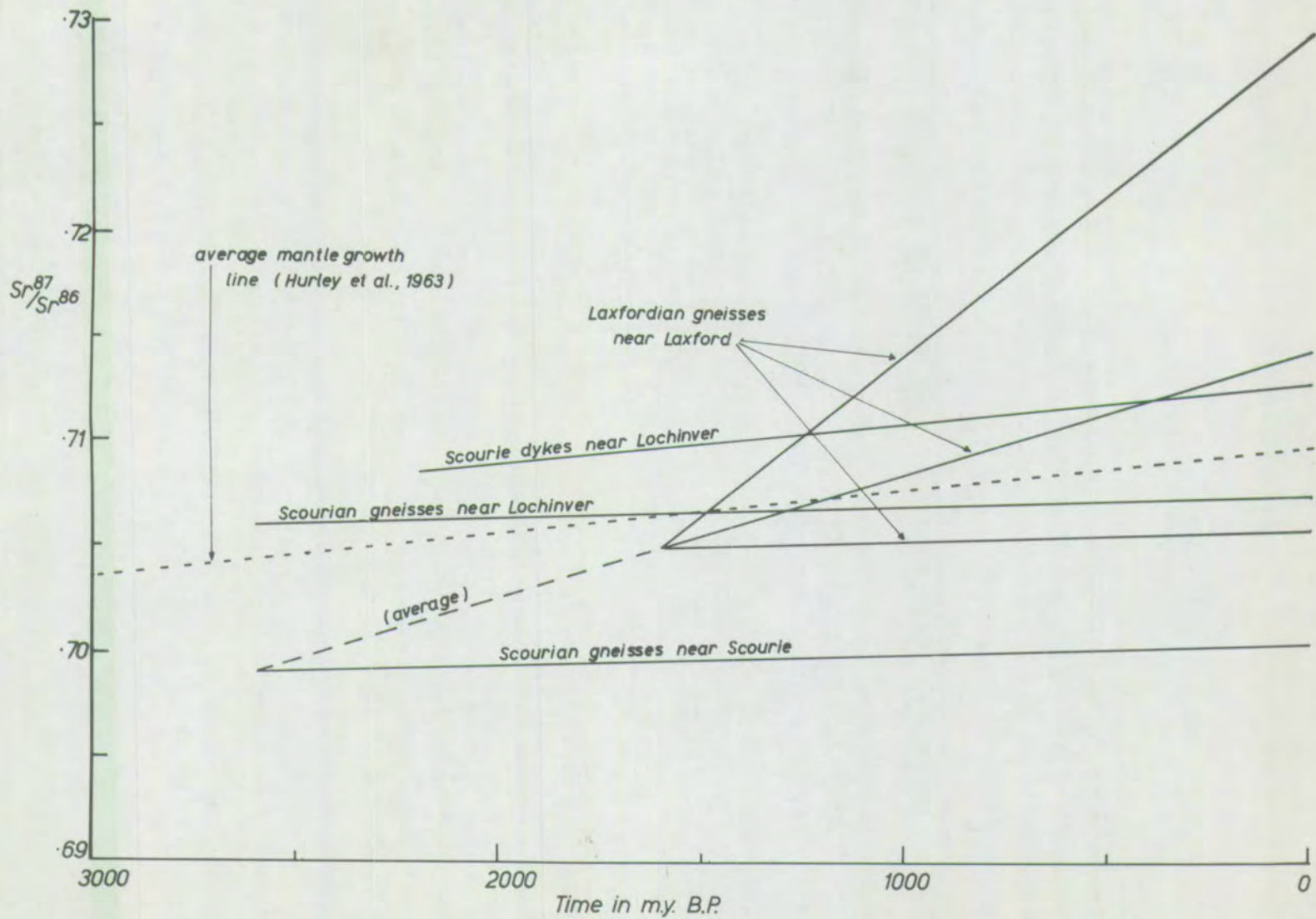


Fig. 2-1. Growth lines for the $\text{Sr}^{87}/\text{Sr}^{86}$ ratios of various groups of Lewisian rocks.

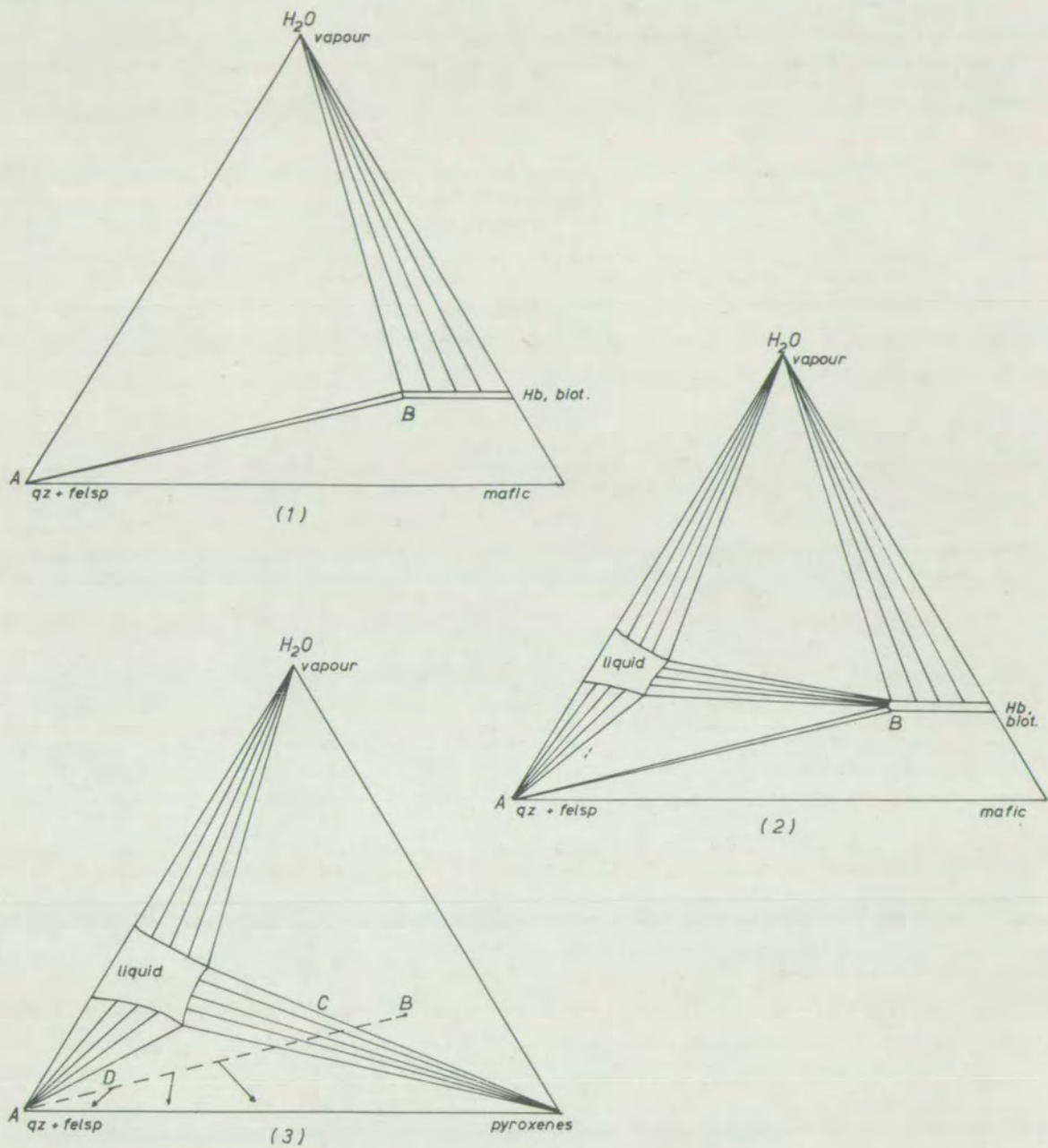


Fig. 2-2. Schematic isotherms of the 'system' (quartz + felspar) - (pyroxenes) - H_2O , at increasing temperatures.

(a stage intermediate between 2 and 3, in which hydrous phases coexist with pyroxenes, does not affect the argument and is omitted)

Petrography: descriptions of a suite of specimens from Geodh'Eanruig. The majority of the petrographic features of the whole association are seen in these specimens. For the other localities studied, brief descriptions in terms defined in this section, accompany the chemical data in Appendix C. Chemical and mineralogical data are presented in tabular form in Appendices C and D. Graphical representations of relevant parts of the data are given at appropriate places in the text of Chapters 4 and 5.

3.3 Summary of the principal rock types

The ultrabasic gneisses are medium grained rocks, of a massive appearance on a broken surface, but on weathered surfaces a prominent banding is commonly seen, due to variations in the proportions of the component minerals: only the most olivine rich types are free from this banding. Folds, generally with axes parallel to the folds in the adjacent acid gneisses, often affect this banding, and structures reminiscent of current bedding and 'wedge-bedding' are also common (Bowes et al., 1964). The rocks consist of olivine, hypersthene, augite, hornblende, spinel and magnetite. Serpentinous alteration is common. O'Hara (1961) has used the terms dunite gneiss, peridotite gneiss, and pyroxenite gneiss to distinguish rocks of varying olivine content. Bowes et al. (1964) use the terms metaperidotite and metapyroxenite. The implications of these terms about modes of origin are clear. In this thesis, the terms peridotite and spinel-pyroxenite will be used, without implying similarity to any igneous rocks.

Spinel-free pyroxenites and hornblendites appear to represent a distinct group, often restricted to the margins of ultrabasic bands, or to very clearly defined bands within them. It is in these olivine-free bands that the

'wedge-bedding' structures of Bowes et al. (1964) are most common.

The contact gneisses are poorly exposed, and form bands from 1 mm. to about 5 feet thick, at the contacts between ultrabasic and garnetiferous basic gneisses. They may, in some cases, be absent from these contacts. They are coarse grained rocks, rich in garnet and/or augite, with hypersthene, plagioclase, amphibole, spinel, and ore minerals. Clinopyroxenite and garnet-augite gneiss are recognisable as distinct types: the division between them is an arbitrary one. The latter type has been referred to as 'eclogite' (Davidson, 1943; Harker, 1939, p. 308). This group includes the 'transition gneiss' and 'ariegite' of O'Hara (1961). The latter is a type rich in garnet and titanomagnetite. The contact gneisses contain only minor plagioclase, which distinguishes them from the garnetiferous basic gneisses.

The basic and garnetiferous basic gneisses (O'Hara, 1961), also referred to as (garnet-) pyriclasite by Bowes et al. (1964), are grey or brownish rocks of medium to coarse grain. The garnetiferous varieties are pale weathering, and there is little foliation, except in the basic gneiss where it occurs as part of the predominantly acid gneiss sequence. Deep red garnets form rounded porphyroblasts up to 5 cm. across and rarely larger. Their appearance is often enhanced by rims of plagioclase grains. Augite and hypersthene are also major, and hornblende, ore minerals, and rarely spinel, minor, minerals.

The plagioclase gneisses are coarse grained pale pink or grey rocks, poor in quartz and mafic minerals (augite, hypersthene, hornblende, ore minerals, and rare biotite). They grade into both acid and basic gneisses, but can often be mapped as separate units. They seldom show a distinct foliation.

The other groups of leucocratic rocks associated with the basic and ultrabasic masses have been defined by O'Hara (1960). These are the garnetiferous

leucocratic and potash-rich leucocratic gneisses. The former are very coarse grained rocks, with quartz, plagioclase, garnet, and ore minerals in varying proportions. The latter are pink or pale grey medium grained rocks of a sugary appearance, with a foliation defined by lenticular, pale blue quartz grains; the plagioclase and/or alkali feldspar occurs as more equant grains. Both types form well-defined layers, or more irregular bodies, normally within the basic or garnetiferous basic gneisses. They may be related to a group of (quartz-) plagioclase veins which often cut the basic and ultrabasic gneisses. These are coarse grained, white rocks, seldom with any sign of a foliation. The quartz, where present, is very often pale blue, as it normally is in the acid gneisses.

The sequence of rock types is emphasised by O'Hara (1961, 1965), and Bowes et al. (1964, 1966). On making a traverse from ultrabasic to acid gneiss the following sequence is encountered: peridotite, spinel-pyroxenite, clinopyroxenite, garnet-augite gneiss, garnetiferous basic gneiss, basic gneiss, plagioclase gneiss, acid gneiss. The relative thicknesses of the several members vary greatly, and some may be absent. In some cases, as at the Geodh'Eanruig lower contact (B on fig. 3-2), there are no garnetiferous rocks present, and the sequence is: peridotite, pyroxene-hornblendite, plagioclase gneiss, acid gneiss.

3.4 Field relations

O'Hara (1961) has emphasised the zoned nature of the masses, outward from a core of peridotite to acid gneiss, which he interprets as a result of reaction between original ultrabasic and acid materials under granulite facies

conditions. Bowes et al. (1964), by contrast, emphasise the stratiform nature of the masses, and relate this to a hypothesis involving disruption and metamorphism of a layered igneous intrusion(s).

The conflict between these divergent conclusions cannot be resolved without decisive field data. For this study, the masses were mapped using 1:10560 Ordnance Survey maps (Ben Strome), enlarged aerial photographs on a scale of approximately 1:2000 (Scourie Bay area), or by direct measurement on a scale of 1:576 (Geodh'Eanruig). The results are presented in figs. 3-2 and 3-4 to 3-9.

Geodh'Eanruig (fig. 3-2)

This is one of the smaller masses studied, being about 500 ft. long and 150 ft. broad (i.e. about 130 ft. thick); its overall shape is lenticular and concordant with the banding of the acid gneisses. There is one band of ultrabasic gneiss, up to 25 ft. thick which is folded sigmoidally. Poles to the banding in the ultrabasic gneiss are plotted in fig. 3-3a, showing that it is folded about an axis plunging at 54° towards 238° . Poles to the banding (fig. 3-3b.), and lineations (fig. 3-3c.) from the nearby acid gneisses clearly show that these rocks are folded on axes plunging at about 35° to the North. Axial planes of the folds in the acid gneiss are parallel to the dominant N.N.E.-S.S.W. foliation. Those of the fold in the ultrabasic band are steep, and trend E.N.E.-W.S.W.

At A (fig. 3-2) the banding in the ultrabasic gneiss and its contact with the garnetiferous basic gneiss are discordant. From the map it is apparent that the ultrabasic band as a whole is also discordant to its contact with the

At E (fig. 3-2) olivine-pyroxenite (10719) overlies a one foot thick layer of coarse garnet-augite gneiss (10720), described by O'Hara (1961, specimen X 646), which passes down to plagioclase-poor garnetiferous basic gneiss (10721-2).

At the West side of the mass, the leucocratic gneiss passes out through basic gneiss into garnetiferous basic gneiss, which in turn passes into very coarse hornblendite; the hornblende is black and lustrous. It is quite different from the hornblende at A and B, which is greenish in hand specimen. On the East side of the mass, at the contact (transitional) between the plagioclase and acid gneisses, occurs the irregular mass of diopside-apatite-scapolite-sphene-orthoclase rock described by O'Hara (1960, specimen X 812). For an analysis and further details of this rock, see Appendix B.

On Cleit Mhor, the small peninsula West of Geodh'Eanruig are abundant strips and layers of ultramafic material, often in fold cores. The majority are iron rich pyroxenites and hornblendites (O'Hara, 1961, p. 272) and they may be in chemical equilibrium with the mafic minerals of the acid gneiss. A few, however, seem to be of ultrabasic composition, and one (F on fig. 3-2) is olivine-rich in the centre (GE 22). This passes out through hornblende-pyroxenite (GE 31, 34), and basic gneiss (GE 25), to acid gneiss, with no garnet appearing.

Geodh nam Cliabh

This mass, composed predominantly of basic rocks, is about 600 ft. by 400 ft. in plan, and about 150 ft. thick. It is poorly exposed, except in the sea cliffs, where there is no ultrabasic material. The contacts of the ultrabasic layers are nowhere adequately exposed.

acid gneiss.

The ultrabasic gneisses consist everywhere of olivine-bearing types, except at B and C (fig. 3-2), where ultrabasic material passes directly to coarse plagioclase gneiss (at B), or to acid gneiss (at C). Here, coarse pyroxenites and hornblendites are developed at the margins of the ultrabasic band (specimens GELA to GELF from locality B), which occur adjacent to plagioclase gneisses, which are quartz bearing (GELJ and GE2 to GE5), without the development of any garnetiferous rocks. The contact between the pyroxene-hornblendite and the plagioclase gneiss is quite sharp.

At locality A (the upper contact) contact gneisses are well developed. Through a vertical interval of 11 ft. peridotite passes through spinel-pyroxenite, clinopyroxenite, garnet-augite gneiss, to garnetiferous basic gneiss (specimens Z 727 to Z 718). The garnetiferous basic gneiss persists for a thickness of some 50 ft. (B 285) until garnet becomes gradually less abundant, and the grain size is reduced (B 286). Garnet is virtually eliminated (B 287), and the basic gneiss becomes richer in plagioclase, and passes through plagioclase gneiss, to a relatively potash-rich leucocratic gneiss (B 288), over an interval of about 3 ft. This leucocratic gneiss forms a lenticular mass about 20 ft. by 50 ft. A large and massive pegmatite which cuts the basic body has a sharp Northward contact with the leucocratic gneiss, but Southwards, passes by gradations into it.

At D (fig. 3-2) a different type of sequence occurs. The thin layer of basic gneiss which intervenes between the plagioclase and ultrabasic gneisses is only poorly garnetiferous (B 168), and passes without any contact gneiss through hornblende-spinel-pyroxenite (B 167) to peridotite (B 165-6).

Throughout most of the garnetiferous basic part of the mass, quartz bearing, plagioclase rich streaks a few cm. thick which define the foliation are common, and in the basic gneiss, to which the garnetiferous basic is transitional, the more mafic layers often contain a little garnet in large grains rimmed by hornblende and/or plagioclase.

The ultrabasic gneiss is well layered, and in the Northern part of the main ultrabasic band, where there is no garnetiferous basic gneiss adjacent to it, it contains well defined layers composed of olivine-free pyroxenite and hornblendite, some of which contain a thin central layer of plagioclase-pyroxene-hornblendite.

The basic gneiss passes outwards to the West, and along the strike, to the N.N.E., into plagioclase gneiss, which contains abundant lumps and blocks of ultramafic material (pyroxene-hornblendite). It also contains a number of sometimes broken or contorted basic bands, some with garnet. There is one block 8 ft. by 10 ft. of plagioclase-hornblendite, in which there are plagioclase-rich clusters (seen in thin section to consist of plagioclase, hypersthene, garnet, and spinel in vermicular intergrowth) which appear to pseudomorph garnets, and in which there is a foliation discordant to that in the plagioclase gneiss. To the North, the plagioclase gneiss interfingers with acid gneiss, and it also grades into acid gneiss Westwards.

In a single isolated exposure on the East side of the mass is seen the garnetiferous leucocratic gneiss described by O'Hara (1960). Its relations to the other rocks of the mass are not clear.

The basic and ultrabasic rocks of Geodh nam Cliabh give the impression that they have been disrupted and modified by what is now plagioclase gneiss

(and perhaps was once acid gneiss material).

Meallan na Corra (Fig. 3-1)

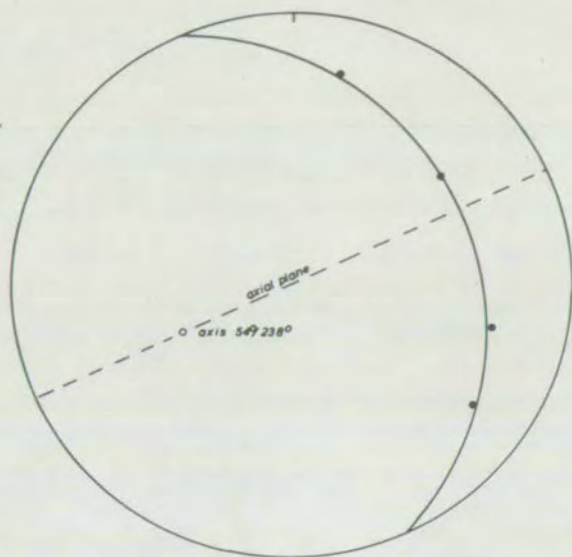
This is a well layered body about 70 ft. thick, concordant with the nearby acid gneisses. It is surrounded by beach deposits, or water, except to the West, where it appears, through indifferent exposure, that the ultrabasic gneiss passes along the strike, through pyroxenite to garnet-free basic gneiss which contains plagioclase rich bands. This basic gneiss is faulted against acid gneiss.

At its lower contact, the peridotite passes downwards through 6 inches of garnet-augite gneiss, 1 ft. of spinel-pyroxenite, 1 ft. of garnetiferous basic gneiss, and 5 ft. of basic gneiss, into acid gneiss.

There are two layers of garnet-augite gneiss within the ultrabasic body. The lower is up to 15 ft. thick, the upper up to 5 ft. The former thins to the N.E. to a vein only a few inches thick, in which the garnet is a strikingly pale pink (specimen B 521).

Scourie House (Fig. 3-5)

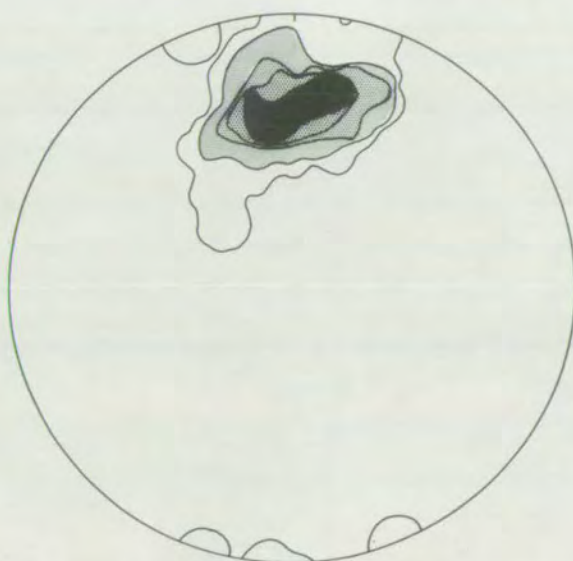
Sporadic exposure prevents exact delimitation of this body. It is a concordant lenticular mass, unusual among those studied in that it consists predominantly of ultrabasic rocks. It is 2000 ft. long and 600 ft. wide and up to 250 ft. thick. The ultrabasic gneisses are well layered and are isoclinally folded on a small scale. A mass of garnetiferous basic gneiss in the Northern part is 300 ft. wide and 400 ft. long. It appears to be entirely enclosed by ultrabasic gneisses. Garnet and hornblende rich rocks are developed near the contact between the two, which is not exposed, but is apparent.



(a)



(b)



(c)

Fig. 3-3.

Stereographic (equal-area) projections
of structural elements from Gneiss'Eanruig.

- (a) Poles to banding in ultrabasic gneiss.
- (b) 172 poles to banding in acid gneiss.
Contours at 10, 8, 6, 4, 2, and 0.6%.
- (c) 63 lineations and linear structures.
Contours at 20, 15, 10, 5, and 1.5%.

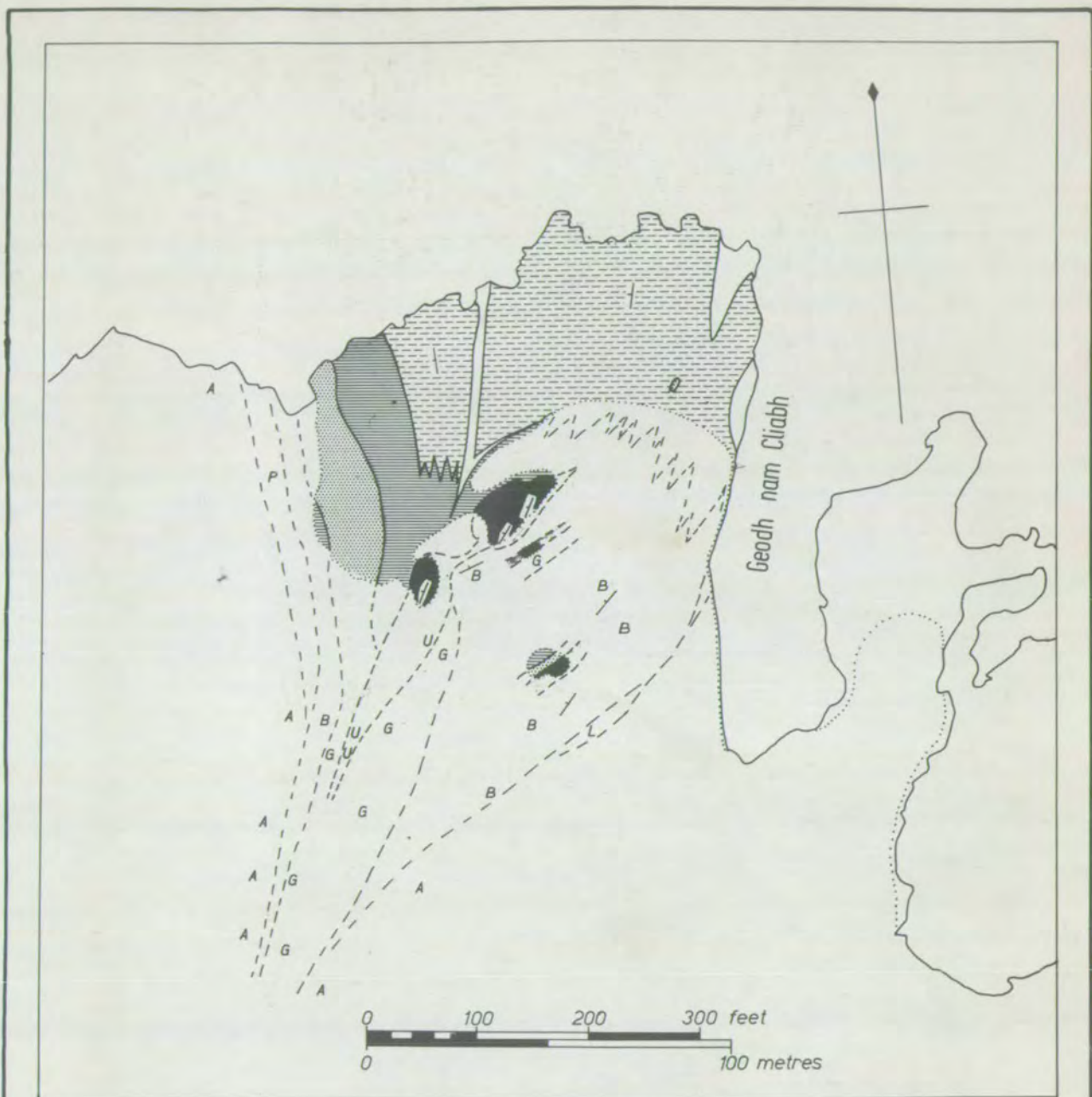
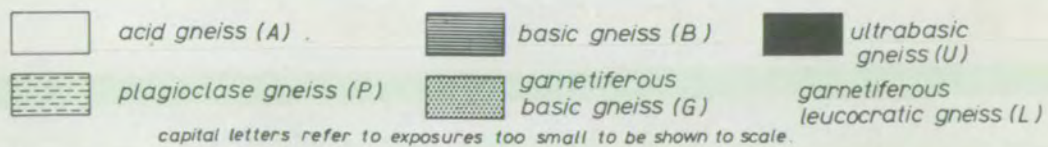


Fig. 3-4. Geological map of the Geodh nam Cliabh basic mass



ABSTRACT

This study is concerned with a group of basic and ultrabasic rocks involved in the granulite facies Scurian Complex of the Lewisian (c. 2600 m.y.). A brief review of the literature concerning the acid gneisses (the major constituents of the Complex) is presented. The salient features are: unusually low $\text{Sr}^{87}/\text{Sr}^{86}$ ratios, somewhat unusual geochemistry, in particular poverty in K, Rb, and Li, and the local occurrence of what may be metasediments. It is concluded that these gneisses may have been formed from a series of acid to intermediate volcanics and/or sediments derived from them by a process of partial melting and loss of the fluid phase containing most of the water, K, Rb, and Li.

The field relations and petrography of the basic and ultrabasic rocks are described. There is a persistent association between garnetiferous basic (opx-cpx-garnet-plag) and ultrabasic (opx-cpx-oliv-spinel) gneisses. Traverses from ultrabasic to acid gneiss may encounter one of two types of sequence: peridotite/spinel-pyroxenite/contact gneiss (garnet and augite rich types)/garnetiferous basic gneiss/basic gneiss/acid gneiss, or: peridotite/pyroxene-hornblende/plagioclase gneiss/acid gneiss. Any sequence intermediate between these two types may be developed.

The structural evidence is reviewed and it is concluded that the formation of the contact gneisses probably post-dated the juxtaposition of the basic and ultrabasic rocks. The best estimate of the P and T of formation of the present assemblages is 1000°C. and 17 Kb. The chemistry of the layering in the ultrabasic gneisses is discussed and found to be consistent with an origin of the gneisses as olivine-opx-amphibole cumulates, or, more probably, by the metasomatic introduction of acid material into an originally homogeneous peridotite. The chemistry of the basic and garnetiferous basic gneisses shows no great variation. The present slight variation can be largely explained by the fraction-

ation of hornblende in a series of magmas at a late stage in their evolution, while the whole range of compositions is consistent with a magmatic origin involving: partial melting of garnet-peridotite at 30-40 Kb., and fractionation of olivine at pressures steadily decreasing to 10-15 Kb. They are not inconsistent with an origin as hornblende-rich cumulates. The basic gneiss is considered to have formed from the garnetiferous basic by a small amount of metasomatic interchange with the acid gneiss, the two assemblages being almost in equilibrium.

The chemical variation across ultrabasic contacts is summarised. The development of contact gneisses seems to be associated with a considerable thickness of garnetiferous basic between the ultrabasic and acid gneisses. The garnet reaction rims of the contact gneisses are probably due to the instability of magnesian garnet at a late stage in the metamorphism, and its breakdown to $\text{opx} + \text{plag} + \text{spinel}$. The theory of diffusion zone formation is outlined, graphical tests for a series of diffusion zones proposed, and a simulation model for diffusion outlined. Both methods of analysis indicate that the contact gneisses may have formed by reaction between ultrabasic and garnetiferous basic gneisses. Reaction between ultrabasic and acid gneisses is likely to produce contacts of the pyroxene-hornblendite type, and not a substantial amount of basic material, under granulite facies conditions.

A group of relatively potash-rich leucocratic gneisses is considered to represent liquids generated during the partial melting of the regional acid gneisses and trapped in and near the basic-ultrabasic masses.

NOTE ON TERMINOLOGY

A few terms are used in this thesis without introduction. 'Foliation' and 'gneiss' are used in the sense of Harker (1939), i.e. to apply to any planar structure, and any coarse grained metamorphic rock showing this structure. 'Banding' is considered a variety of foliation. 'Layering' is a particular type of banding, in which bands of different composition are relatively homogeneous and are separated by fairly distinct contacts. 'Granulite' is used exclusively to refer to the granulite facies, and only as a rock term where a direct quote is made from the literature.

Plagioclase compositions, wherever quoted, were determined by the Michel-Levy method.

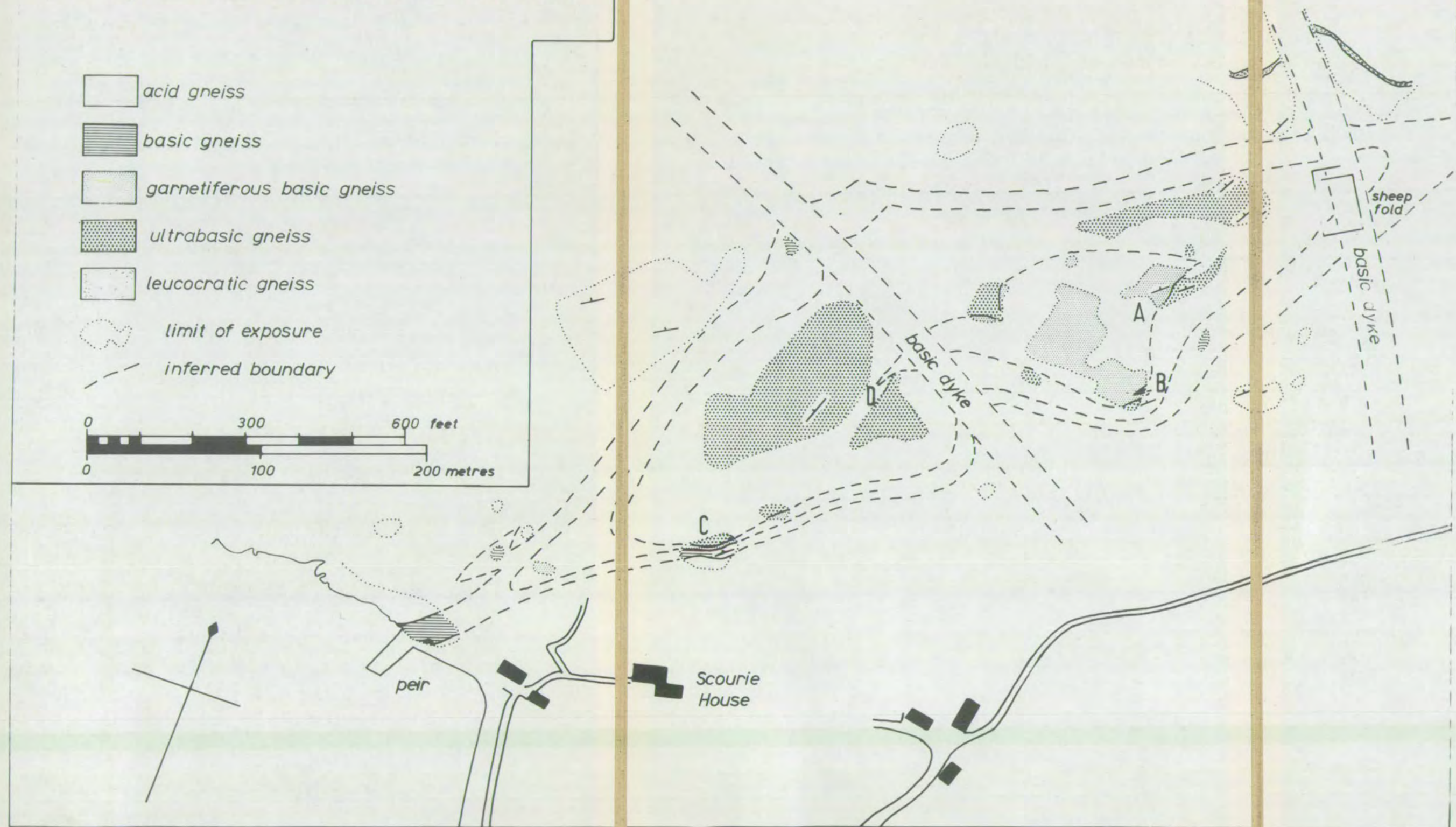
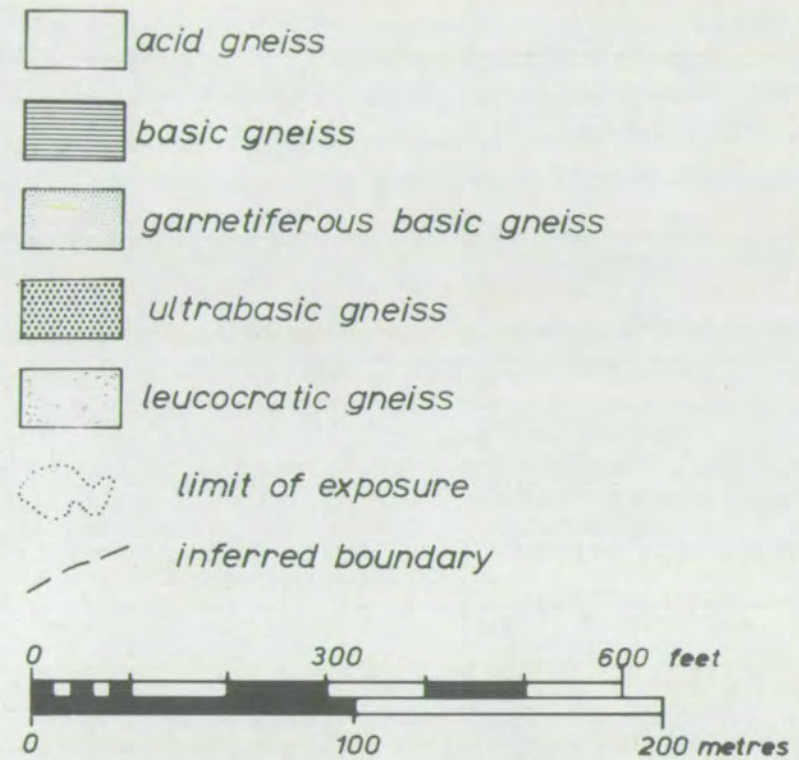
Abbreviations used are either conventional or self-explanatory.

TABLE OF CONTENTS

	<u>Page</u>
CHAPTER 1 INTRODUCTION	1
1.1 History of research	1
1.2 A note on terminology	5
1.3 Basic and ultrabasic rocks	6
1.4 Approach to the problem	6
CHAPTER 2 SOME ASPECTS OF THE REGIONAL GEOLOGY	9
2.1 Previous studies of the acid gneisses	9
2.2 The possible sedimentary relics	11
2.3 The strontium isotope ratios	13
2.4 The geochemistry	14
CHAPTER 3 DESCRIPTIONS OF THE BASIC AND ULTRABASIC MASSES	18
3.1 Occurrence of basic and ultrabasic rocks in the Scourian Complex	18
3.2 Presentation of data	20
3.3 Summary of the principal rock types	21
3.4 Field relations	23
3.5 Petrography	35
CHAPTER 4 PETROGENESIS OF THE BASIC AND ULTRABASIC ROCKS	42
4.1 General remarks	42
4.2 Structural evidence	45
4.3 Mineral facies	48
4.4 Rock and mineral chemistry of the ultrabasic gneisses	50
4.5 Geochemistry of the basic and garnetiferous basic gneisses	57
4.6 Relationship between the basic and garnetiferous basic gneisses	65
4.7 Chemical variation across the ultrabasic contacts	67
4.8 Mineral chemistry of the contact gneisses	71
4.9 Diffusion zone formation	77
4.10 Prediction of the sequence of zones in a com- plex system	88
4.11 Application of theory to the contact sequences	93
4.12 Summary	99
4.13 Discussion	101
4.14 Conclusions	103
CHAPTER 5 THE POTASH RICH LEUCOCRATIC GNEISSES	105
5.1 Petrography	105
5.2 Chemistry	106
5.3 Field relations	106
5.4 Petrogenesis	108

Fig. 3-5.

Geological Map of the Scourie House basic mass



discordant to the foliation in both types at A (fig. 3-5) (specimens SH 12-16). Elsewhere (B on fig. 3-5), the two types interdigitate.

The external relations of the ultrabasic gneisses are obscured by lack of exposure, but isolated exposures of basic gneiss on both sides of the mass may be parts of a continuous layer surrounding the ultrabasic gneiss. At the S.W. end of the mass there is some garnetiferous basic gneiss, and at C (fig. 3-5) there is exposed a continuous sequence from ultrabasic to acid gneiss. The sequence from peridotite through hornblende-rich spinel-pyroxenite, poorly garnetiferous basic gneiss, and basic gneiss grading into acid gneiss, occupies about 10 ft.

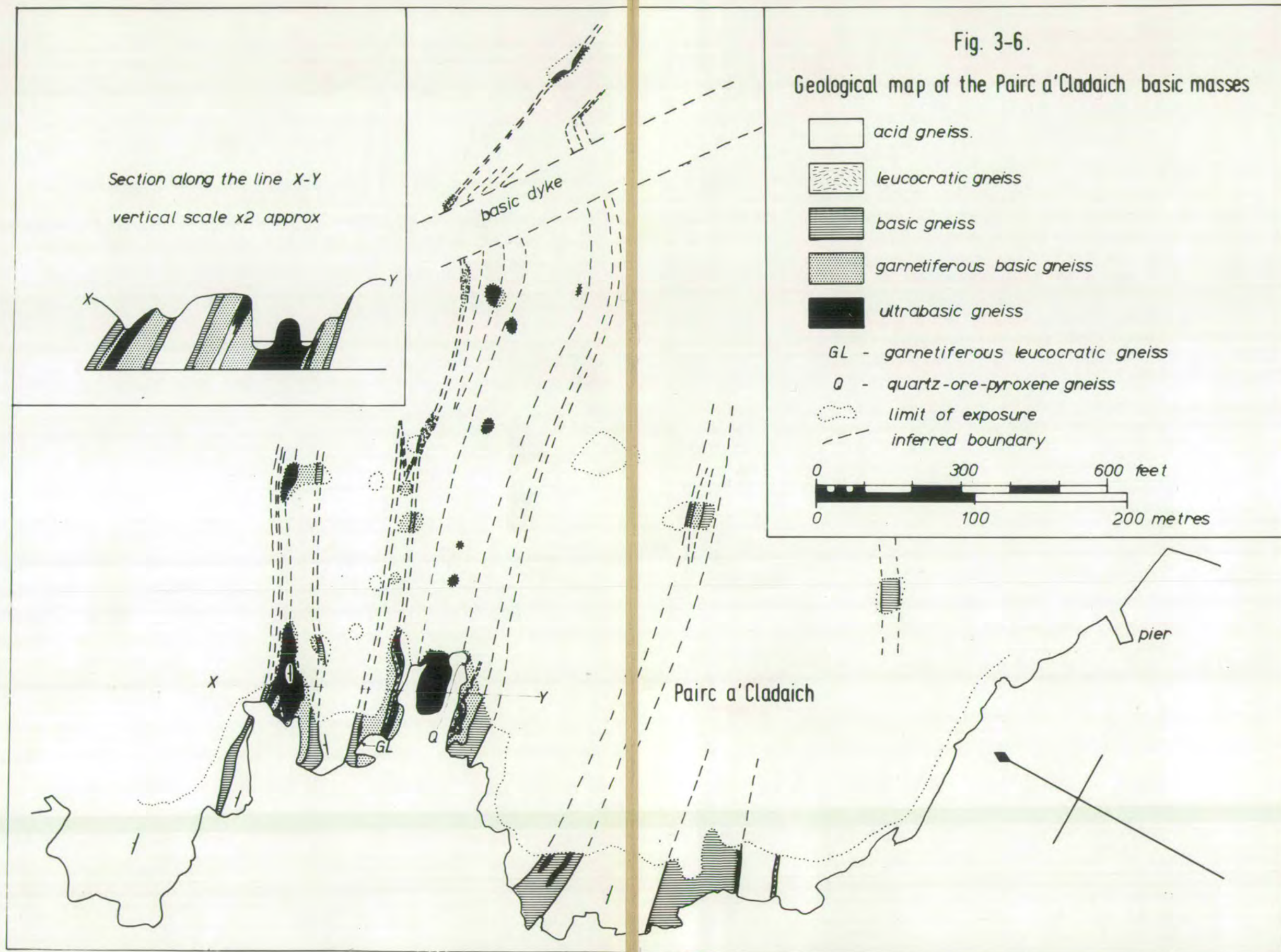
Approximately on the strike extension of the large garnetiferous basic gneiss mass a two inch vein of garnet-augite gneiss occurs, in a very hornblende-rich part of the ultrabasic gneiss (D on fig. 3-5).

In a prominent crag above the N.E. end of the mass is exposed a 25 ft. thick layer of brick red, potash rich leucocratic gneiss. This is a strike continuation of the similar layers seen inside the basic gneisses at the inlets West of Pairc a'Cladaich (see below), the three layers having coalesced into one.

Inlets West of Pairc a'Cladaich (Fig. 3-6)

This mass is in two parts, parallel and separated by 100 ft. of normal acid gneiss. The larger, Eastern part is 250 ft. wide, and may be 1500 ft. long (exposure is poor inland). The western part is 100 ft. wide, and exposed for a length of 500 ft.

The main, eastern part contains four separate ultrabasic layers. The eastern two are thin (less than 5 ft.), carry no olivine, and are strongly folded on axes plunging at 60° to the S.W. The contacts of these two bands



with the garnet poor basic gneiss which encloses them, feature a thin zone of pyroxenite and plagioclase-hornblendite, in which the plagioclase appears to pseudomorph garnet. It is thus possible that contact gneisses were once present at these contacts, but have been destroyed.

The largest ultrabasic layer, consisting of peridotite in the inland part where exposure is poor, consists of spinel-pyroxenite at the shore, where it contains two 2 ft. layers, conformable with the banding, of quartz-plagioclase rock, which have sharp contacts with the pyroxenite. The garnetiferous basic gneiss on the west side of this ultrabasic layer, is thicker and richer in garnet than that on the east. It encloses three separate layers, up to 8 ft. thick, of potash-rich leucocratic gneiss (O'Hara, 1960), which continue for half a mile inland.

Garnetiferous leucocratic gneiss forms a small irregular mass at the contact between the garnetiferous and garnet-free basic gneisses (fig. 3-5a.), and two concordant bands in the garnetiferous basic gneiss a few feet below. Rusty weathering, pyrite and chalcopryrite bearing bands are common in this part of the body. Apart from the presence of the sulphides, they are normal garnetiferous basic gneisses.

The western part of the mass contains only one ultrabasic layer, which consists largely of peridotite, and is bordered by garnet poor basic gneiss on both sides. The lower contact between ultrabasic and garnetiferous basic gneisses has a very thin zone rich in garnet, at the contact between spinel-pyroxenite and garnetiferous basic gneiss (specimen Z 702B). The upper contact is not exposed.

The marginal plagioclase gneiss contains abundant lumps of hornblendite up to 3 ft. across, particularly near its transitional contact with the acid

gneiss. These and the gneiss are strongly folded, also on axes plunging at 60° to the S.W.

Camas an Lochain (Fig. 3-7)

This mass, which is very well exposed near the shore, is 1200 ft. long and 500 ft. wide (i.e. 200 ft. thick). It consists predominantly of garnetiferous basic gneiss, but contains numerous ultrabasic gneiss layers, and also masses of leucocratic gneiss.

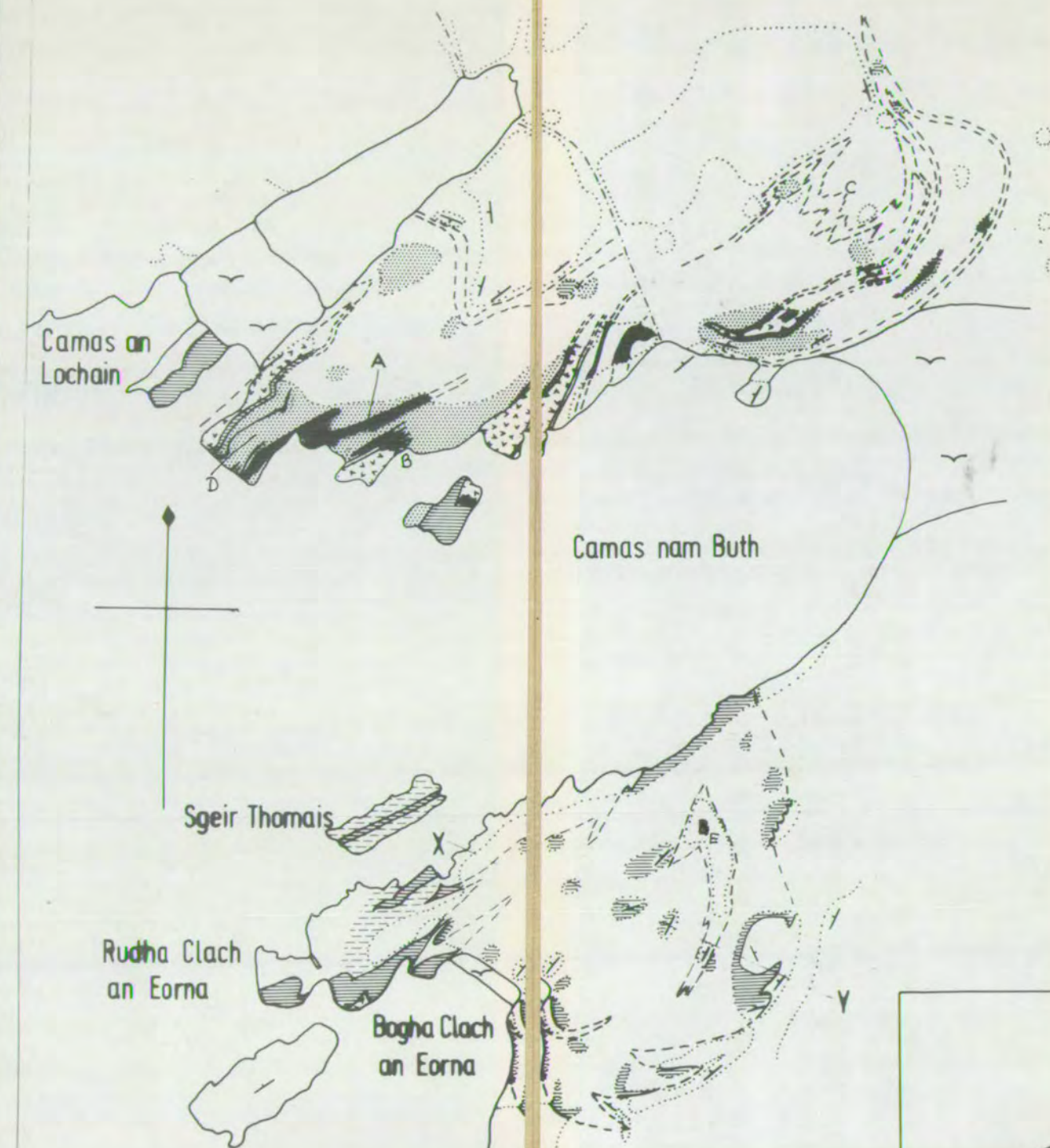
For 3 to 4 ft. near the ultrabasic contacts, the garnetiferous basic gneiss is very poor in plagioclase, but the garnets are not rimmed by fine grained aggregates of hypersthene, plagioclase, and spinel, as normally occurs in the garnet-augite gneisses; they are clear and deep red, and of a very attractive appearance. Where the garnetiferous basic-ultrabasic gneiss contact is exposed, the sequence garnet-augite gneiss/clinopyroxenite/spinel-pyroxenite/peridotite is condensed into a few cm. or less (specimens B 241-2, from A on fig. 3-7).

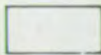



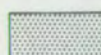

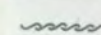
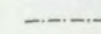
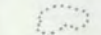

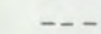
The ultrabasic layers, although thin (1 ft. to 10 ft.), are uniformly olivine-rich, and spinel-pyroxenite occurs either as rare bands, sometimes irregular, and oblique to the contacts (O'Hara, 1961, p. 249), or near the contact with the garnetiferous basic gneisses. Layering is virtually absent from most of the ultrabasic gneisses, and the foliation is defined by a preferred orientation of the olivine and pyroxene crystals. The thin ultrabasic bands at B (fig. 3-7) are olivine poor or olivine-free, however, and are isoclinally folded.

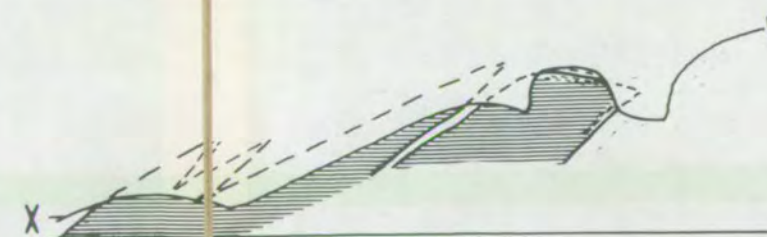
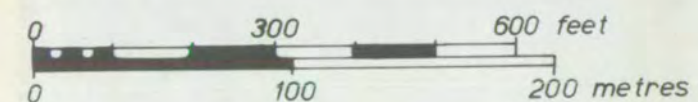
Away from the ultrabasic gneiss, the basic gneiss becomes progressively poorer in garnet. Within the garnetiferous basic gneiss are two distinct

Geological map of the Camas an Lochain
and Camas nam Buth basic masses

Figs. 3-7. & 3-8.



-  acid gneiss
-  leucocratic gneiss
-  basic gneiss
-  plagioclase gneiss
-  garnetiferous basic gneiss
-  ultrabasic gneiss
-  shear belt
-  probable line of fault
-  limit of effectively continuous exposure
-  beach deposits
-  inferred boundary



Section along the line X-Y. To scale

bands of red, unfoliated leucocratic gneiss. They are poorly banded near their margins and grade into basic gneiss over a thickness of about 3 ft. Externally, the garnetiferous basic gneiss grades through basic gneiss into acid gneiss. At C (fig. 3-7) the basic and acid gneisses interfinger, and the contact is irregular.

At D (fig. 3-7) a 2 ft. thick vein of coarse, garnet-bearing plagioclase rock pinches out southwards, and a few feet along its strike extension its place is taken by a thin layer of garnet-augite gneiss.

Camas nam Buth (Fig. 3-8)

This mass consists of evenly banded and homogeneous basic gneiss. Garnet is common in the central parts, but forms only a small proportion of the rock. Mafic and ultramafic bands are also common, particularly in the plagioclase gneisses at the margins of the body, where they are usually folded and boudinaged. The impression is given that a homogeneous basic rock has segregated into mafic rich and plagioclase rich components near these margins.

The contact between the basic and acid gneisses at the S.E. corner of the mass features a band of agmatitic rock, in which angular blocks of pyroxenite and hornblendite are set in a plagioclase rich matrix. On the eastern side of the mass, a band of basic gneiss is seen to wedge out into the acid gneiss. It is evenly banded in the centre, but near the contact a crude, new banding, formed by thin quartz-plagioclase veins parallel to the contact, obscures the older banding. The banding of the acid gneiss flows smoothly around the basic rock.

A prominent crag is formed by a discordant band of massive acid gneiss within the basic mass (^E on fig. 3-8). From this band, concordant wedges of

acid gneiss penetrate the basic gneiss. They finger out into quartz-plagioclase veins, which merge into the banding of the basic gneiss.

Ben Strome (Fig. 3-9)

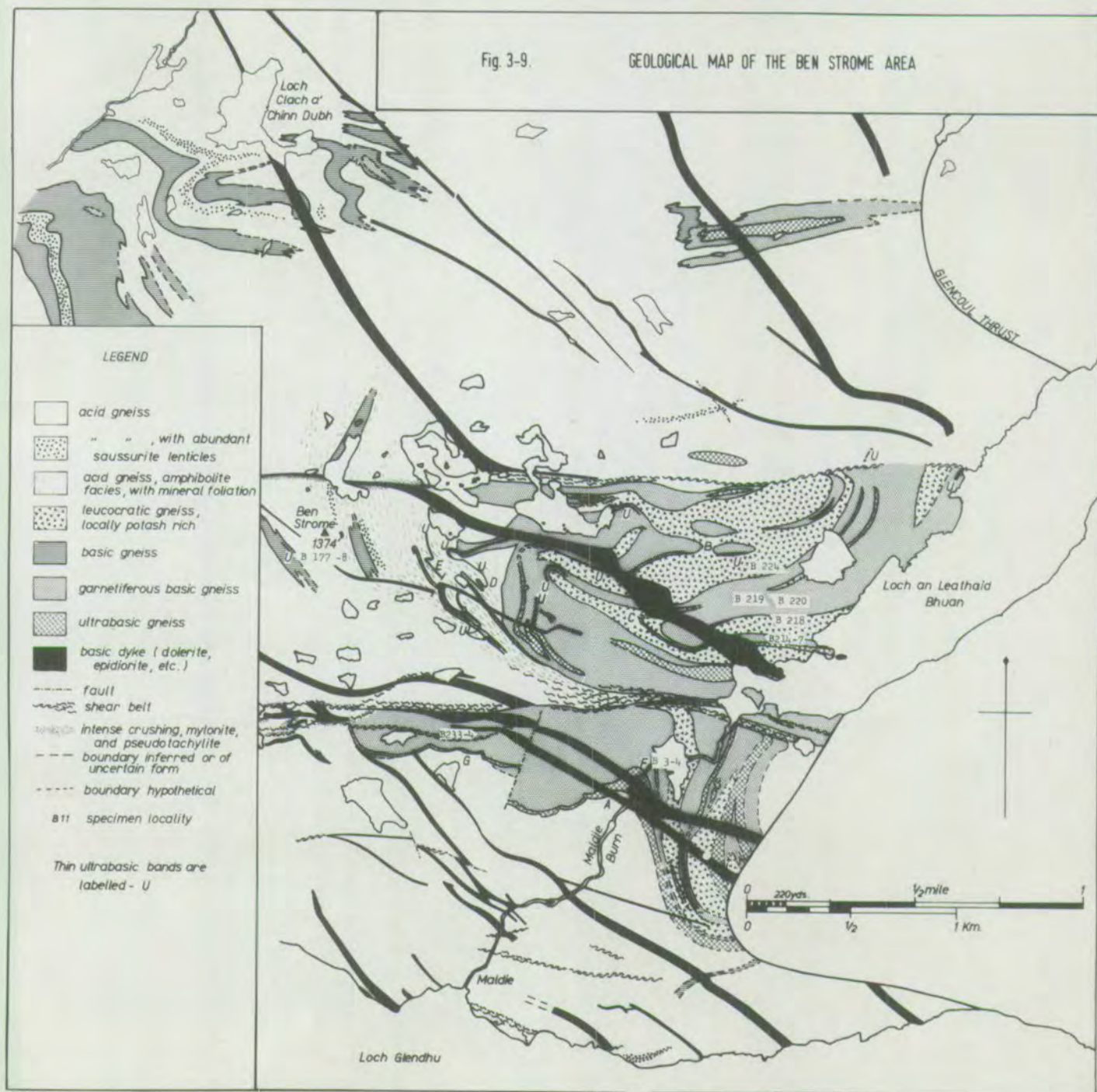
The area of basic and ultrabasic rocks exposed on Ben Strome is approximately 1 sq. km. The mass is divided into two parts by a major E.-W. Laxfordian shear belt. The southern part dips at $5-10^{\circ}$ to the north, and more steeply eastwards east of the Maldie Burn. The northern part dips consistently north at $20-40^{\circ}$.

The northern edge of the mass is formed by another E.-W. shear belt. The southern margin lies mostly along the lower edge of a major ultrabasic band. Where this contact is exposed just west of the Maldie Burn (A on fig. 3-9) there is a wedge of garnetiferous basic gneiss between the acid and ultrabasic gneisses. It is separated from both by gently dipping surfaces, with slickensides. This margin cannot be a Caledonian thrust, similar to the nearby Glencoul Thrust, as the dykes, of intra-Lewisian age, which cut it are not substantially displaced. West of the normal fault which cuts the southern margin of the mass, there is a considerable development of garnetiferous basic gneiss beneath the ultrabasic layer.

The dominant rock type at Ben Strome is massive garnetiferous basic gneiss. The main layer of this rock in the southern part of the mass is over 500 ft. thick, and its upper contact is not seen. Well banded ultrabasic layers are common, and are up to 100 ft. thick. Poorly foliated leucocratic gneiss, which is occasionally potash-rich, forms several layers within the basic parts of the mass, and appears to have separated disrupted portions of it (B on fig. 3-9). The basic gneiss is free of garnets near its contact with the leucocratic gneiss.

Fig. 3-9.

GEOLOGICAL MAP OF THE BEN STROME AREA



A major isocline folds the northern part of the mass (C on fig. 3-9). The banding in the nearby acid gneiss is not affected by this fold, and seems to be an axial plane structure. The thin and remarkably persistent ultrabasic layers west of this locality all have thin garnetiferous basic gneiss margins. They are probably involved in two sets of folds. At D (fig. 3-9) the banding in the acid gneiss is an axial plane structure to the folds, which are isoclinal, and may thus belong to the same set of folds as that at C. At E the foliation in the acid gneiss is parallel to that in the ultrabasic, and both are folded together. This folding may be of the same age as the nearby pre-dyke folds, of possible Inverian age (see Appendix A). Retrograde metamorphism has strongly affected the rocks in this part of the mass.

Contacts between the ultrabasic and garnetiferous basic gneisses are exposed in the Maldie Burn (F on fig. 3-9), and on the southern slopes of Ben Strome (G on fig. 3-9). At both localities there are contact gneisses, the former showing clinopyroxenite and garnet-augite gneiss; the latter has garnet-augite gneiss only. Neither development of contact gneiss is more than 2 ft. thick.

Summary of the field relations

The evidence presented in this chapter demonstrates that neither the description of the masses as 'zoned' (O'Hara, 1961) nor as 'layered' (Bowes et al., 1964), adequately describe them. The relations are more complex than either term would suggest. The masses are predominantly stratiform, but the frequent repetition of the ultrabasic to basic sequence is not consistent with their simple interpretation as a layered intrusion. Rhythmic layering on a large scale in an ultrabasic intrusion in Rhum has been described by Brown

(1956). In this case there is virtually no cryptic variation from top to bottom of each rhythmic layer. The upward sequence from olivine-rich to plagioclase (bytownite) rich rocks is gradual; the downward sequence comprises a sharp discontinuity. There is no such asymmetry between the upward and downward sequences from ultrabasic to garnetiferous basic gneisses.

The absence of garnetiferous rocks from some ultrabasic to acid gneiss sequences, and the different degrees of development of contact gneisses are not wholly consistent with the conclusion that the garnetiferous basic and contact gneisses are the product of simple reaction between the ultrabasic and acid gneisses. At least two stages of reaction are necessary to explain all the observed sequences.

3.5 Petrography

The brief petrographic descriptions in this section will summarise the majority of the microscopic features of the rocks studied. More detailed petrography, including such information as refractive indices, other optical data, pleochroic schemes, exsolution phenomena, and secondary alteration are available in O'Hara's (1960, 1961) description of a representative series of specimens. Certain features common to all the rocks may be summarised first.

The primary assemblages of the rocks all belong to the granulite facies; the assemblages present are shown in fig. 4-32 (together with postulated assemblages for lime and alumina rich compositions). Hornblende may be present in all assemblages except that of the acid gneisses. Titano-magnetite may occur in all except the ultrabasic assemblages.

Grain size: most of the rocks in the Scourian Complex are of coarse to medium grain, the average grain size of the principal minerals (pyroxenes,

plagioclase, hornblende, quartz, olivine) being about 1-2 mm. Garnets are of larger size, forming porphyroblasts commonly up to 1 cm. across. Spinel and the ore minerals occur as grains about 0.2 mm. across. The contact gneisses may be of considerably coarser grain size, however. The terms coarse and fine or large and small, therefore, will indicate values substantially different from the above.

Olivine: the olivines are forsterite-rich and colourless. Alteration to serpentine minerals and magnetite is very common.

Augite: all the clinopyroxenes of the basic and ultrabasic rocks are green augites. Exsolution of hypersthene is ubiquitous, and in some coarse gneisses, exsolution lamellae composed of plagioclase, hypersthene, and titanomagnetite have been observed by O'Hara (1961, fig. 7).

Hypersthene: all the orthopyroxenes are hypersthene with the following pleochroic scheme: α - pale red, β - pale yellow, γ - apple green.

Amphibole: all the primary amphiboles are hornblendes, generally green to brown in colour. The secondary amphiboles are often blue-green.

Garnet: is always pink and isotropic, being a pyrope-almandine with about 17% of the grossular molecule (O'Hara, 1961, fig. 9).

Plagioclase: varies from andesine in the acid and plagioclase gneisses to bytownite in the contact gneisses (O'Hara, 1961, p. 254). Twinning on the albite and pericline laws is ubiquitous in the larger grains, the twin lamellae being usually lenticular. Fine grained, obviously recrystallised plagioclase is often untwinned. Sericitic alteration is very common in the plagioclase of the contact gneisses. In the more acid rocks, antiperthitic exsolution of orthoclase is also common.

Spinel: the green spinel of the ultrabasic gneisses is crowded with minute inclusions of magnetite (O'Hara, 1961, p. 251). This, and the close association in composite grains with magnetite, suggests the exsolution of a single, hercynitic, spinel phase. The spinel of the contact gneisses is clear and green, or sometimes blue-green.

Ore: is a bar-like intergrowth of ilmenite and magnetite (O'Hara, 1961, fig. 6), except in the ultrabasic gneisses, where magnetite occurs alone. Locally, sulphides (pyrrhotite, pyrite, chalcopyrite) are abundant (O'Hara, 1961, p. 253).

Quartz: contains minute rod-like inclusions of a phase presumed to be rutile (Sutton and Watson, 1950, p. 268). Quartz grains, or sometimes eye-shaped aggregates of grains, are frequently flattened parallel to the foliation, and in these cases the inclusions show a preferred orientation, also parallel to the foliation: those inclusions lying most nearly in the plane of the foliation may be boudinaged. Rarely, epitaxial growth parallel to $\{10\bar{1}0\}$ of the quartz is shown. The quartz commonly shows undulose extinction, but where the quartz is obviously recrystallised to a fine grained aggregate, neither inclusions nor undulose extinction are present.

Geodh'Eahruig specimens

A series of specimens taken along the line of section (X-X) of fig. 3-2 are typical of many rocks in the region. They are described briefly below, starting from the top, from leucocratic gneiss, through basic and garnetiferous basic gneisses, contact gneiss, ultrabasic gneiss, pyroxene-hornblende, plagioclase gneiss, to acid gneiss.

B 288, leucocratic gneiss (fig. 3-10a.) consists of a coarse aggregate

of equant grains of andesine-antiperthite (An_{30} , with coarse blebs of orthoclase) and quartz. The quartz grains are lenticular and alone define the foliation. The quartz is strained, with prominent undulose extinction, but many grains are surrounded by a narrow zone of small, unstrained quartz granules. Accessory zircon occurs as small rounded grains.

B 287, basic gneiss (fig. 3-10b.) consists largely of granoblastic augite, with minor ore and hypersthene, and small grains of plagioclase. In this granoblastic matrix are set many rounded areas, likely to be pseudomorphs after garnet, consisting of fine grained plagioclase (An_{58}), hypersthene, and ore (titano-magnetite). Even within the garnet pseudomorphs, the ore grains, which are large and abundant, occur as clusters, surrounded by poikiloblasts of green hornblende, or sometimes of garnet. A few grains of blue-green spinel also occur in the garnet pseudomorphs.

B 286, poorly garnetiferous basic gneiss (fig. 3-10c.) is similar in some respects to B 287, consisting largely of a granoblastic aggregate of augite and plagioclase, with minor hypersthene and green hornblende, in which are set rounded pink garnets up to 5 mm. across, each with a rim, about $\frac{1}{2}$ mm. wide, of plagioclase grains. Subhedral grains of titano-magnetite are common, and are usually surrounded by a fringe of garnet (see O'Hara, 1960, fig. 14).

B 285 and Z 718, garnetiferous basic gneisses (fig. 3-10d.), consists of a matrix of granoblastic augite, with a few small grains of hypersthene, plagioclase, ore, and green hornblende, in which are set rounded garnets, with rims of fine grained plagioclase (An_{54}). In the augite rich matrix

near these rims, hypersthene is more abundant than away from them. Minor green hornblende and some garnet occur as ragged fringes on the few grains of titanomagnetite.

Z 719, garnetiferous basic gneiss transitional to garnet-augite gneiss (fig. 3-11a.), is similar to Z 718, but the plagioclase is a minor constituent, and is more calcic (An_{62}). The garnets lack granular plagioclase rims, such as occur in the garnetiferous basic gneisses, but have wide rims in which the garnet is pseudomorphed by a complex vermicular intergrowth of garnet, plagioclase, hypersthene, and green spinel (fig. 3-11b^{and (c)}_Λ). Only the cores of the larger garnets are free from the development of this sort of intergrowth. The structure of the pseudomorphs is generally radiating, with plates and rods of the four minerals in intimate intergrowth. The intergrowth is, however, systematic. The plagioclase, and particularly the hypersthene, tend to form poikiloblasts, up to 1 mm. across, which are in optical continuity, although apparently discontinuous. These poikiloblasts enclose vermicules of garnet, within each of which is a smaller vermicule of spinel, with a thin sheath of plagioclase between the garnet and spinel, where the garnet vermicule is enclosed by a poikiloblastic hypersthene, but not where it is enclosed by a plagioclase poikiloblast. Spinel is never seen in contact with hypersthene, nor with a poikiloblast of plagioclase. This structure is called the garnet reaction rim, and is very characteristic of the garnet-augite gneisses.

Z 720, garnet-augite gneiss (fig. 3-12a.), is coarser grained than Z 719, with large garnets in an almost plagioclase free matrix of granoblastic augite, with minor hypersthene and spinel. The augite crystals are largest

close to the garnets, where they are accompanied by a little plagioclase (An_{59}) as smaller grains. Reaction rims, as described for Z 719, form thin margins to the garnets.

(fig. 3-12b)
Z 721 is very similar to Z 720, but in this case the garnets are almost entirely converted to reaction rim.

Z 722-3-4, garnet-augite gneiss, passing to clinopyroxenite (fig. 3-12, ~~and c.~~), are parts of a continuous specimen 9 inches long. The overall appearance is similar to that of Z 721, but the garnet pseudomorphs decrease in number downwards towards Z 724. Two types of garnet pseudomorphs can be recognised: those (the majority) which contain garnet, either as a small, distinct core and/or as part of the hypersthene-plagioclase-spinel aggregate, and those with no garnet at all. Neither have the vermicular structure of the garnet reaction rims, but consist of a fine grained and granoblastic aggregate of plagioclase, hypersthene, and spinel. There are occasional small poikiloblasts of hypersthene, in the pseudomorphs, which contain a few vermicules of spinel, suggesting that these pseudomorphs have passed through the reaction rim stage. The size and shape of the aggregates are the same as in the garnet-augite gneisses, and leave no doubt that they are pseudomorphs of garnet.

Z 725, hornblende-spinel-pyroxenite (fig. 3-12d.), is a granoblastic aggregate of hypersthene, augite, and green hornblende, in that order of abundance, with some small grains of magnetite-spinel intergrowth.

Z 726, olivine-pyroxenite, is similar to Z 725, but has a few grains of colourless olivine, intermediate in size between those of the pyroxenes and spinel.

Z 727, peridotite (fig. 3-13a.), is also very similar to Z 726, but olivine is here more abundant than either pyroxene. Magnetite and magnetite-spinel intergrowth are abundant, the two forming distinct but closely associated grains. The distribution of spinel is effectively random, and does not suggest the pseudomorphing of any other aluminous phase (fig. 3-13b.). The texture described by O'Hara (1961, p. 252), in which hypersthene forms a narrow rim between olivine and hornblende, is not present in this rock.

GE 1A, pyroxene-hornblendite, consists of granoblastic green hornblende, with hypersthene and augite. The appearance is very clean in thin section, because of the absence of both spinel and magnetite.

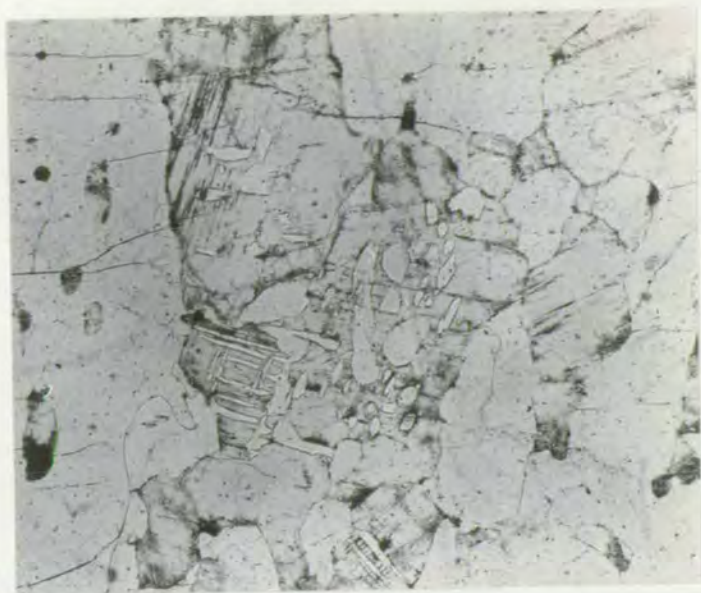
GE 1D, pyroxene-hornblendite, is very similar to GE 1A, but is cut by a 3-inch plagioclase vein (GE 1D3). This latter is coarse granular rock composed of antiperthitic plagioclase (An_{35}), with a little hypersthene and interstitial grains of quartz. A contact zone, at the edge of the vein, is 1 cm. wide, and consists entirely of large plates of hypersthene and hornblende. It has no augite (fig. 3-14a.).

GE 1J, plagioclase gneiss, is a coarse rock composed largely of large crystals of andesine-antiperthite (An_{32}), with minor interstitial hornblende, hypersthene, and augite.

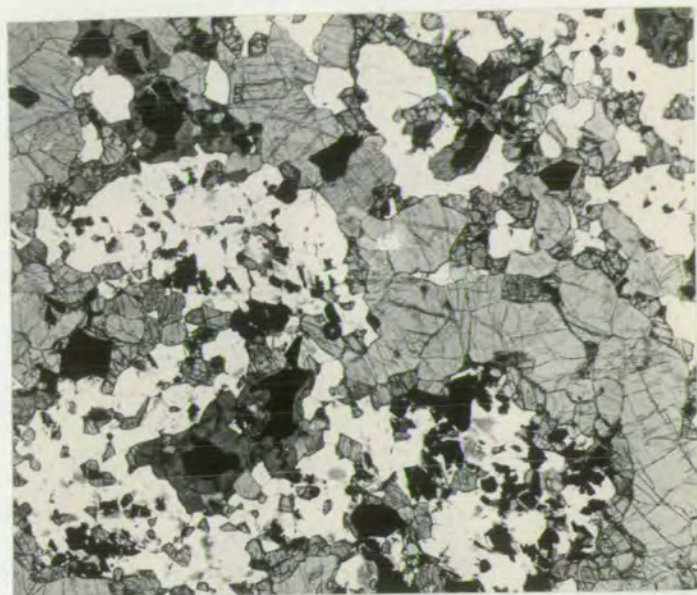
GE 2-5, plagioclase gneisses, are similar to GE 1J, but they also carry a little iron ore, around which biotite flakes have grown, and some quartz (up to 10%). Apatite, in short euhedral prisms, occurs as an accessory mineral (fig. 3-14b.).

Fig. 3-11

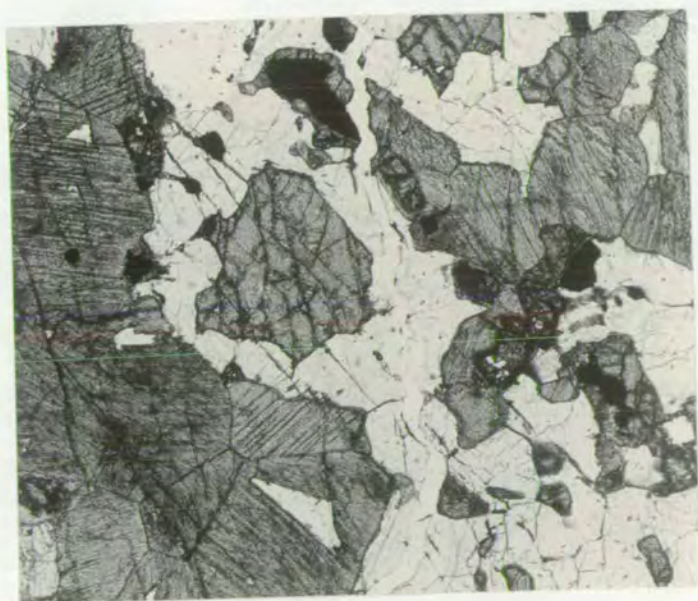
- (a) Z 719 Garnetiferous basic transitional to garnet-augite gneiss.
Augite rich matrix with large garnets almost completely made over
to reaction rim.
- (b) Z 719 and (c) B 230 showing the intimate intergrowth of garnet,
hypersthene, plagioclase (altered in (b)), and spinel (dark).



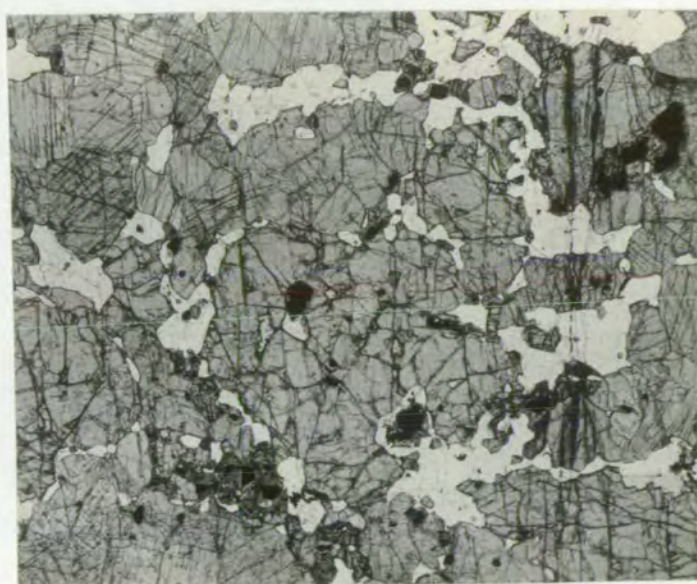
(a) x20



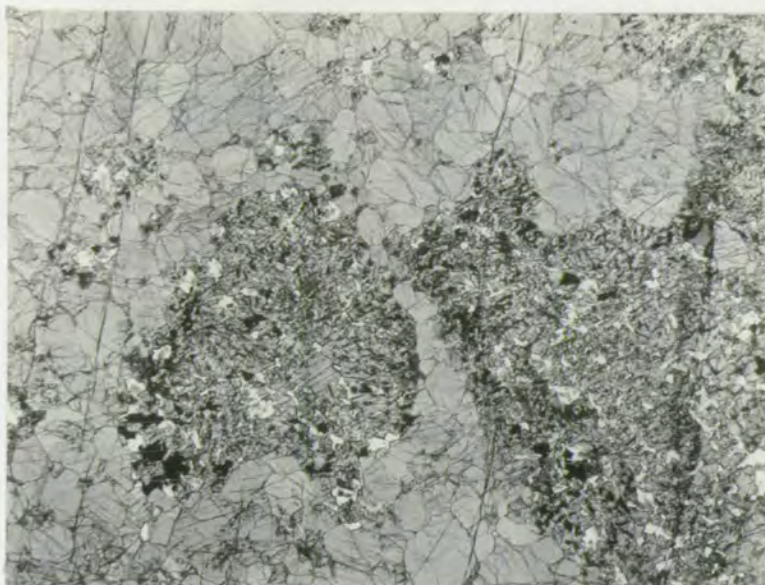
(b) x10



(c) x17



(d) x10



(a) x 7



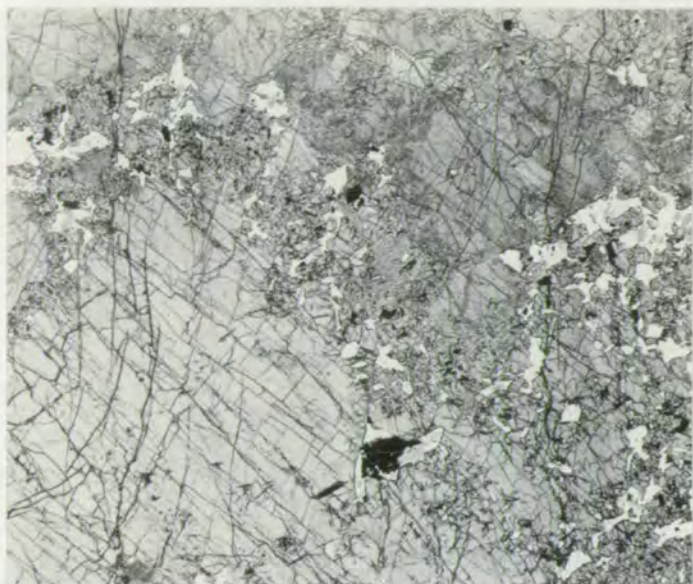
(b) x 27



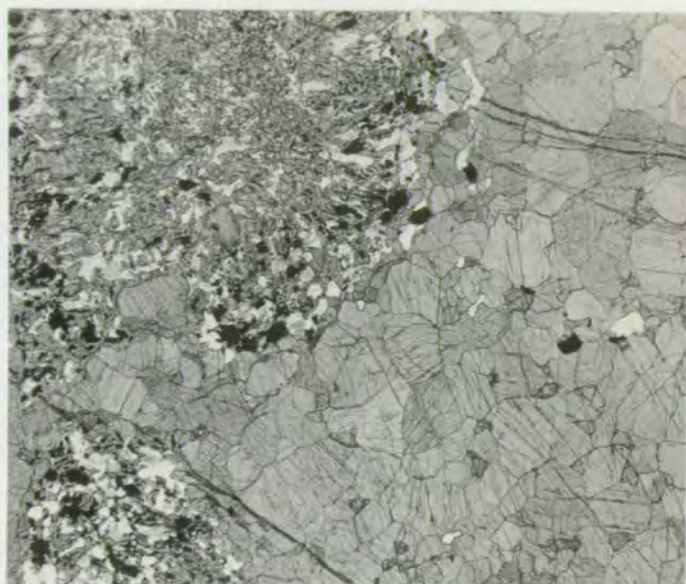
(c) x27

Fig. 3-12

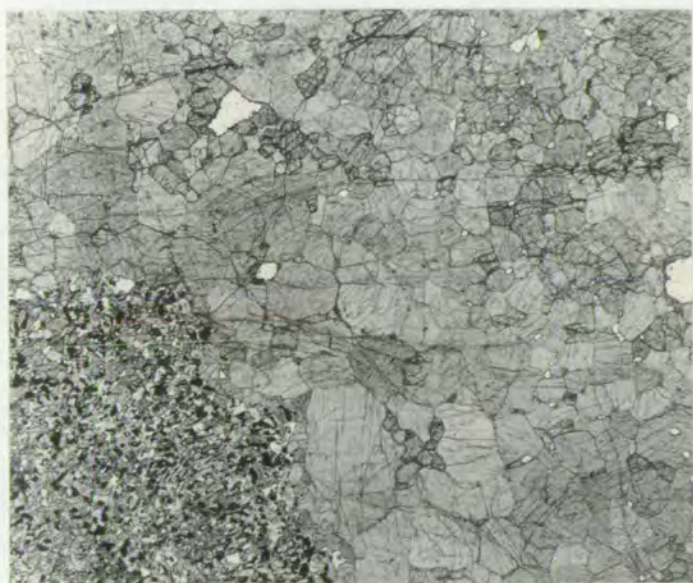
- (a) Z 720 Garnet-augite gneiss. Large garnets, surrounded by narrow reaction rims, in an augite-rich matrix.
- (b) Z 721 The garnets almost completely made over to reaction rims.
- (c) Z 724 as Z 721, but the garnet pseudomorphs are only locally vermicular in texture, and are mainly granoblastic.
- (d) Z 725 Spinel-pyroxenite augite (light), hypersthene (with prominent cleavages), and hornblende (darker) with spinel and magnetite.



(a) x7



(b) x7



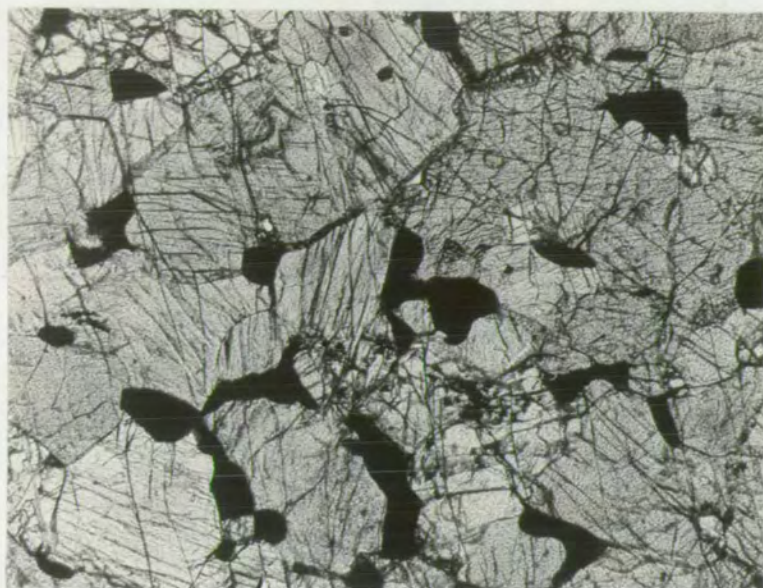
(c) x7



(d) x7

Fig. 3-13

- (a) Z 727 Peridotite. Olivine (light), augite, hypersthene, hornblende, spinel and magnetite.
- (b) Tracing from a projection showing the distribution of spinel in Z 727.



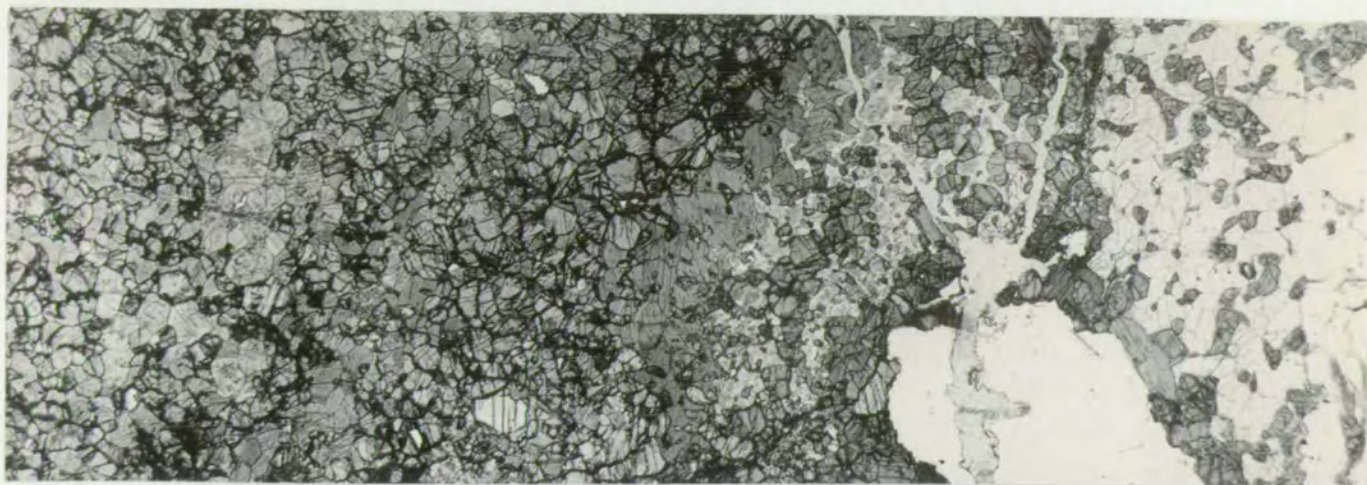
(a) x 20



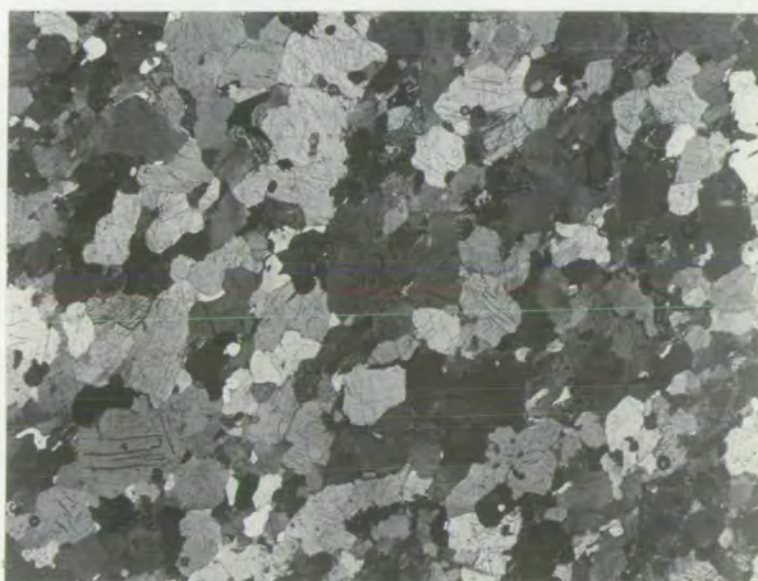
(b) x 3

Fig. 3-14

- (a) GE 1D Left; hornblende-pyroxenite. Centre; coarse hypersthene rich contact zone, rich in hypersthene and hornblende (darker). Right; plagioclase vein with minor augite and hypersthene.
- (b) GE 4 (crossed polars) Plagioclase gneiss. Coarse antiperthitic plagioclase with minor quartz, and ferromagnesian clusters.



(a) x7



(b) x7

CHAPTER 4

PETROGENESIS OF THE BASIC AND ULTRABASIC ROCKS4.1 General Remarks

The problem of the origin and evolution of the basic and ultrabasic rocks of the Scourian Complex may be resolved into a number of separate questions: the pre-metamorphic nature of the several rock types; their pre-metamorphic relation to the acid gneiss and to each other; the extent of the metamorphic changes they have undergone; and the nature and extent of their interaction with the acid gneiss and each other.

Several spatial associations of rock types may be distinguished, as described above (pp. 24 -34), by their more or less persistent occurrence:

- (1) The association of ultrabasic with basic and garnetiferous basic gneisses.
- (2) The association between basic and garnetiferous basic gneisses.
- (3) The sequence: peridotite/spinel-pyroxenite/clinopyroxenite/garnet-augite gneiss/garnetiferous basic gneiss/basic gneiss/(plagioclase gneiss)/acid gneiss.
- (4) The sequence: peridotite/pyroxene-hornblendite/(basic gneiss)/plagioclase gneiss/acid gneiss.

To some extent, the nature of these associations may be regarded as separate problems. Answers to each must nevertheless form a coherent synthesis for the whole.

Statement of Possibilities

There can be little doubt that the ultrabasic gneisses of the Scourie area represent original ultrabasic igneous rocks (a possible alternative origin involving dehydration of serpentinites formed from dolomite may be discounted because of the consistently high Cr and Ni contents (cf. Matthews (1967))). Conflicting opinions have been expressed about the extent of metamorphic modification of the ultrabasic rocks, and about the origin of all the other rock types in the area (this remark does not apply to the leucocratic gneisses, mentioned only by O'Hara (1960), or the 'meta-anorthosite', mentioned only by Bowes, Wright and Park (1964, 1966), which has not been encountered at Scourie or Ben Strome).

The following list gives a series of possibilities for the origin of the different rock types, mostly taken from the literature.

Ultrabasic gneisses

(1) Originally peridotites, poor in Ca and Al, and enriched in these and other elements during the metamorphism (O'Hara, 1961).

(2) Originally picritic rocks, or parts of a layered intrusion, the compositions essentially unmodified (Bowes et al., 1964, 1966).

Basic and Garnetiferous Basic Gneisses

(1) Originally basic igneous rocks (Bowes et al. 1964, 1966).

(a) Both originally igneous.

(b) Garnetiferous basic originally igneous: basic gneiss produced by the influence of the acid gneiss upon it.

(c) Basic gneiss originally igneous: garnetiferous basic produced by the influence of the ultrabasic gneiss upon it.

(2) Both produced by reaction between the ultrabasic and acid gneisses (O'Hara, 1961, 1965, 1966).

Contact Gneisses

(1) Produced by an igneous process and related to the ultrabasic and/or the garnetiferous basic gneiss by this process (Bowes et al., 1961, 1964).

(2) Produced by reaction between the ultrabasic gneiss and adjacent rocks - of acid or basic composition (O'Hara, 1961, 1965, 1966).

Pyroxenite-Hornblendite Sequence

(1) Produced by reaction between the ultrabasic and acid gneisses.

These several possibilities may be grouped into a number of syntheses, and these will vary from the extreme 'igneous' hypothesis of Bowes et al. (1964), to the extreme 'metasomatic' hypothesis of O'Hara (1961). The conclusion of Bowes et al. (1961), that the rocks comprise unmetamorphosed and, presumably, separate layered igneous intrusions, was not reiterated by the same authors (1964, 1966), and may have been abandoned. It is not in accord with any field or petrographic features encountered in the present study.

Approach to the Problem

Firstly, the available evidence bearing on time relations will be reviewed, and a tentative sequence of events put forward. The mineral facies of the rocks will be defined, and the pressure and temperature of their formation determined as closely as possible. The chemistry of the basic and ultrabasic rocks will be examined to determine the likelihood or otherwise of an igneous origin. The relation between the basic and garnetiferous basic gneisses will be discussed.

The chemical and mineralogical variation through selected contact sequences will be summarised, and the nature of the reaction rim texture developed around the garnets examined. The theory of diffusion zone formation will be outlined, and an attempt made to apply this theory to the observed contact sequences.

4.2 Structural Evidence

In an attempt to construct a time sequence, the events to be considered are:

- A: Formation of the ultrabasic rocks.
- B: Formation of the garnetiferous basic gneisses.
- C: Formation of the basic gneisses.
- D: Juxtaposition of the ultrabasic and what is now garnetiferous basic gneiss.
- E: Formation of the contact gneisses.
- F: Formation of the marginal pyroxenites and hornblendites.
- G: Formation of the banding in the ultrabasic gneisses.
- H: Formation of the banding in the acid gneisses.
- J: Formation of the leucocratic gneisses.
- K: Formation of the plagioclase (-quartz) veins.
- L: Formation of the garnetiferous leucocratic veins.
- M: Formation of the garnet-augite layers within the ultrabasic gneisses.
- N: Tectonic slicing of the complexes (suggested by Bowes et al. (1964, 1966)).
- P: First folds at Ben Strome.
- Q: Second folds.
- R: Folds within the ultrabasic mass at Geodh'Eanruig.

See Appendix A.

Some of the following observations do not bear directly on time relations, but point out similarities between rock types, tending to suggest that similar processes operated in their formation. In the absence of more rigorous criteria, this may be used to tentatively indicate a contemporaneous formation. The expressions $A > B$ or $A = B$ will be taken to mean that event A is later than event B, or simultaneous with it.

(1) At Geodh'Eanruig, the basic gneiss (e.g. B 287) appears to have formed from garnetiferous basic (p. 38). O'Hara (1961) observed that garnet has developed from ore in some basic gneisses. These two processes may have operated simultaneously in different places.

$B = C ?$

(2) Also at Geodh'Eanruig (A on fig. 4-1), the composite body of basic and ultrabasic gneisses and its banding are folded by a fold, whose axial trace is truncated abruptly by the margin of the body. Where ultrabasic gneiss approaches this contact pyroxene-hornblendite is developed. Thus, any 'slicing' of the mass post-dated the fold which itself post-dated the formation of a composite basic and ultrabasic, layered body. In view of the occurrence of small masses of peridotite on Cleit Mhor (see fig. 3-9 and (8), below), it seems likely that unaltered peridotite must have been exposed to the acid gneisses on the Western margin of the Geodh'Eanruig body, and the formation of the marginal hornblendite must post-date the tectonic action which resulted in this exposure.

$F > N > R \begin{cases} < D \\ < G \end{cases}$

(3) At B (fig. 4-1), there is no apparent representative of contact gneiss between the ultrabasic and (poorly garnetiferous) basic gneisses. This can

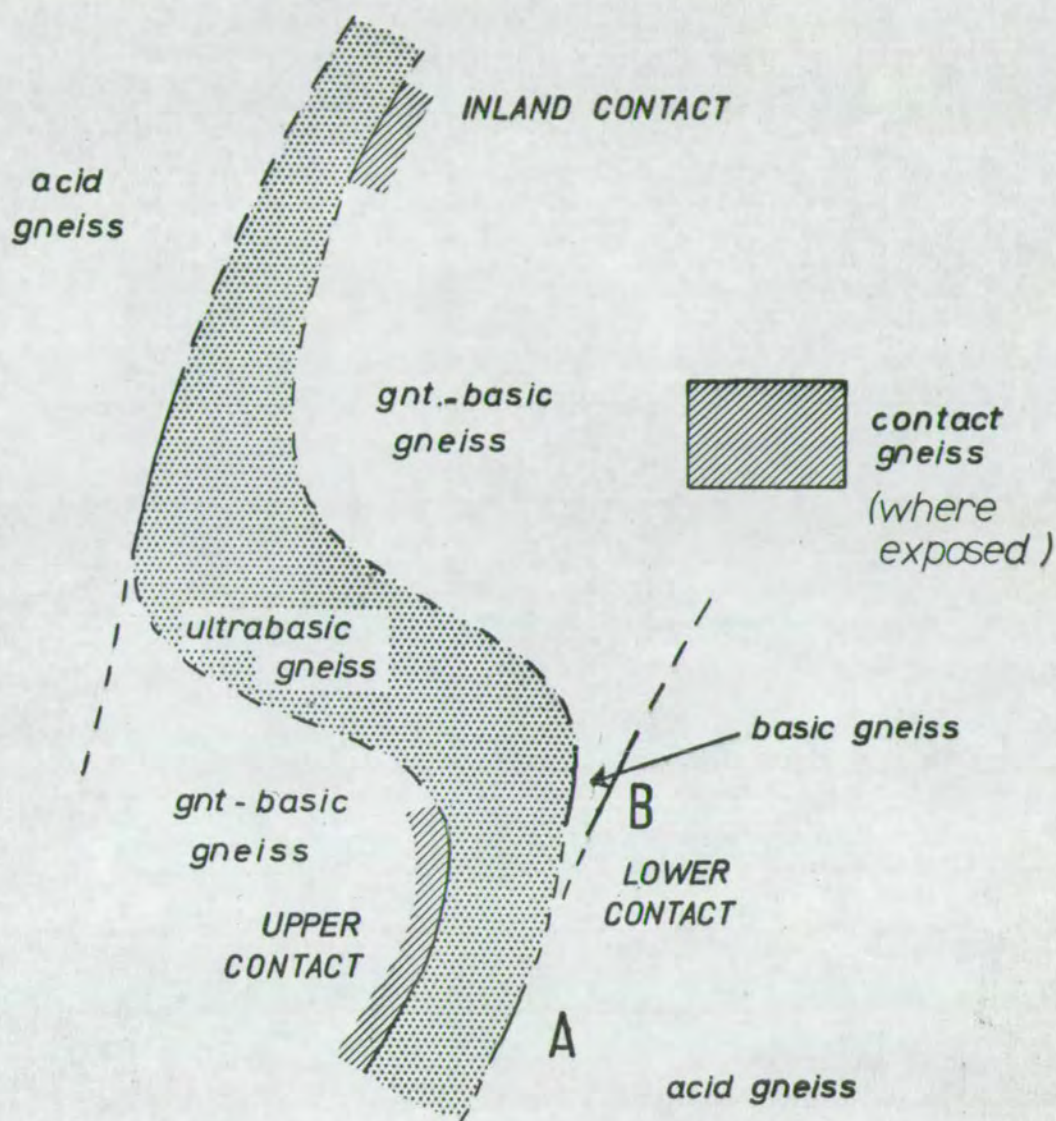


Fig. 4-1. A sketch showing the relations between the ultrabasic, garnetiferous basic, and contact gneisses at Geodh'Eanruig. (from fig. 3-1)

The contact gneiss occurs at ultrabasic-garnetiferous basic gneiss contacts, but disappears as these contacts approach the margins of the mass.

best be explained by assuming that the formation of contact gneiss was here inhibited by the presence of acid gneiss, and that the contact gneisses post-dates the action which brought the acid and ultrabasic gneisses close together at this locality.

$E > N$

(4) At Ben Strome the banding in the acid gneiss is an axial plane structure to the first folds (see Appendix A) which affect both basic and ultrabasic rocks and their banding.

$$H = P \begin{cases} > D \\ > G \end{cases}$$

(5) The occurrence of pyroxene-hornblendite as layers in the ultrabasic gneiss suggests a similar origin for this type of banding to that of the marginal pyroxene-hornblendite. Where, as at Geodh nam Cliabh, or the West side of Ben Strome, these layers pass internally to plagioclase-hornblendite (above, p. 27), a possible relation to the plagioclase (-quartz) veins is suggested.

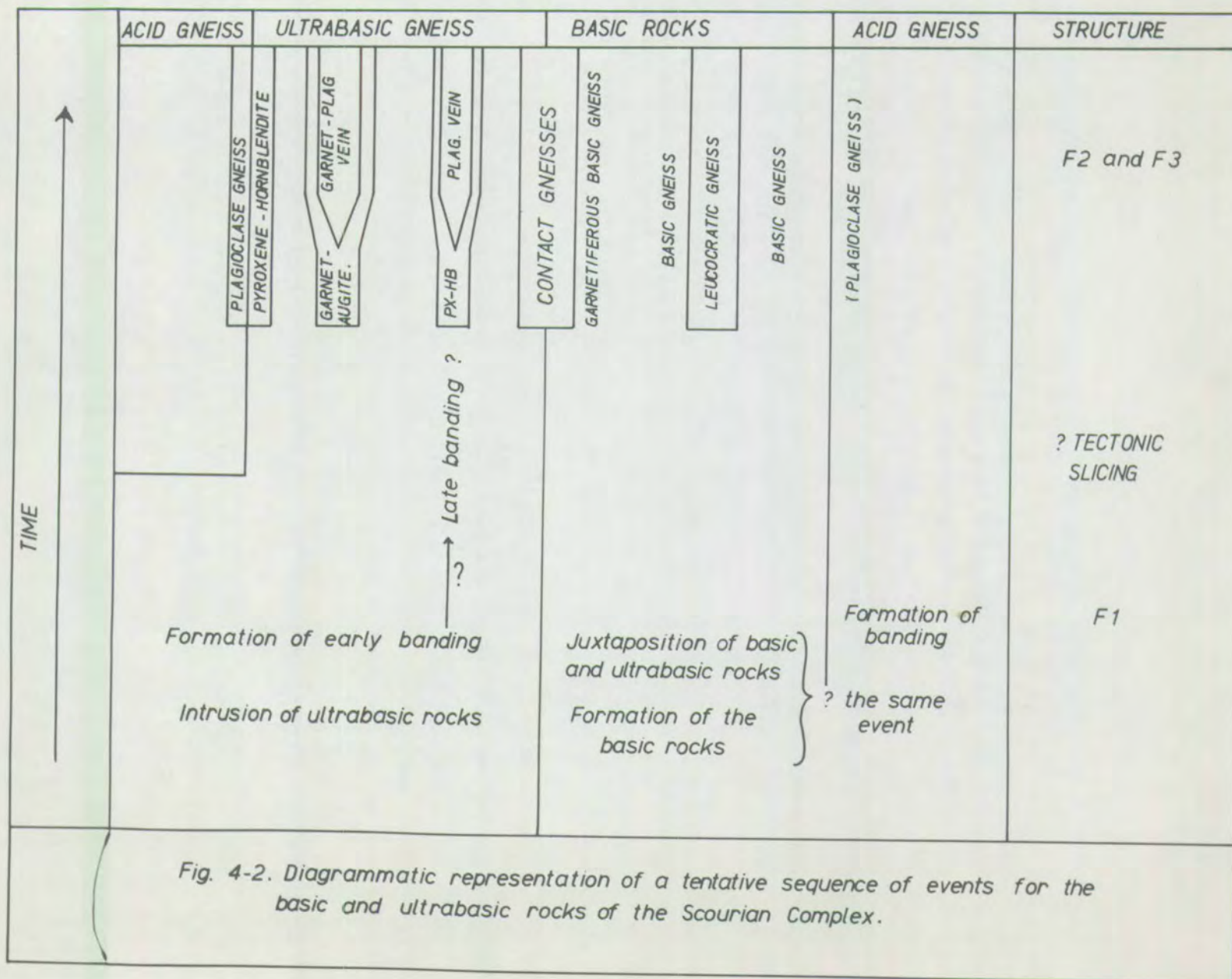
$K = F = G ?$

(6) Similarly, the relation between the garnet-augite layer and the garnetiferous leucocratic vein at Camas an Lochain (above, p. 32) appears to be causal, and the similarity of this layer to the garnet-augite type of contact gneiss also suggests a similar origin.

$L = M = E ?$

(7) All three types of leucocratic vein occur in similar situations and appear to grade into each other. They may be of the same age and of similar origin (O'Hara, 1960, p. 71).

$J = K = L ?$



(8) The small peridotite mass on Cleit Mhór is affected by second folds, which must post-date its separation from the Geodh'Eanruig body.

$Q > N$

A tentative synthesis may be made from these observations:

LATEST

Q

$E = F = G = J = K = L = M$

N

$R = ? P = H$

$$\left. \begin{array}{l} D = \\ ? G = \\ A = \end{array} \right\} ? B/C$$

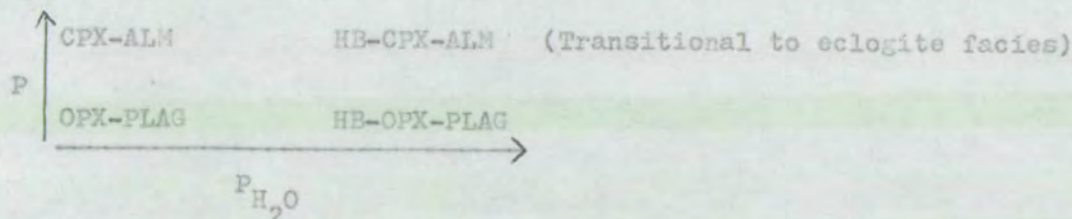
EARLIEST

This synthesis is shown diagrammatically in fig. 4-2.

4.3 Mineral Facies

All the primary mineral assemblages at Scourie are of the granulite facies, as defined by Eskola (1921). The diagnostic assemblage is orthopyroxene-plagioclase; use of the term 'eclogite' for rocks from the area by Harker (1939, p. 308), and Davidson (1943) is misleading: no eclogite or any rock of eclogite facies is present (O'Hara 1960). *

De Waard (1965) gives four sub-divisions of the granulite facies, for silica-saturated rocks:



* See note at foot of p. 49.

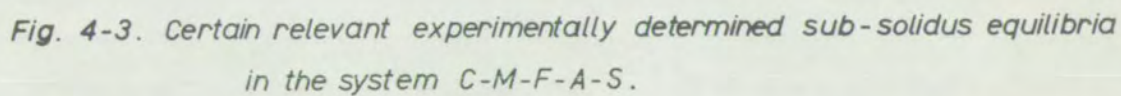
At Scourie, in the acid gneisses, the assemblage quartz-plagioclase-hypersthene-augite-titanomagnetite is ubiquitous (O'Hara, 1960). The silica-undersaturated assemblage of the garnetiferous basic gneisses is garnet-hypersthene-augite-plagioclase-hornblende. The existence, in the same area, of the two assemblages would imply, by the petrogenetic scheme of De Waard (1965), a higher P_{H_2O} in the garnetiferous basic gneisses. The absence of hornblende from the acid gneisses might be more satisfactorily explained by the higher Fe/Fe + Mg ratio in these rocks (Boyd, 1959).

For ultrabasic assemblages from Scourie, O'Hara (1967) has suggested a pressure of c. 17 Kb, and a temperature of c. 1000°C ^{on} the basis of the pyroxene paragenesis. Although the published results of Kushiro and Yoder (1966) indicate that ultrabasic assemblages would carry garnet and ^{not} spinel, under these conditions, another determination of the spinel-peridotite to garnet-peridotite reaction (Green and Ringwood, 1967) indicate that spinel-peridotite would be the stable assemblage. The published results for these and a few other relevant reactions are shown in fig. 4-3.

The texture described by O'Hara (1961) in which hypersthene, plagioclase, and iron ore have exsolved from augite, suggests that at the climax of metamorphism, the augite of the basic and garnetiferous basic gneisses was more aluminous and less calcic than those analysed. If this is also true of the ultrabasic gneisses, the estimated temperature of formation would be higher, but the pressure probably not much different (O'Hara, 1967, fig. 12-4).

It is clear that the available data do not serve to refine the estimates of O'Hara (1967) of 17 Kb and 1000°C.

Note: A recent description of a garnet-spinel-peridotite from South Harris (Livingstone, 1967) indicates that rocks transitional from granulite to eclogite facies are present in the Outer Hebrides.



(2a is an alternative line through the same data points)

4 from Yoder (1955)

6 from MacGregor (1964)

☉ Estimate of the conditions of formation of ultrabasic gneisses from
Scourie (O'Hara, 1967)

4.4 Rock and Mineral Chemistry of the Ultrabasic Gneisses

Thirteen analyses of rocks from the interior parts of ultrabasic layers in two of the masses (Geodh nam Cliabh and Ben Strone) were performed to investigate the nature of the banding, and the variation in composition of the ultrabasic rocks away from the margins of the layers. Minerals were separated from the Geodh nam Cliabh specimens. All six augites and five amphiboles were obtained pure and in sufficient quantity to analyse. One amphibole was obtained pure but in small quantity, and it was not possible to separate the hypersthene to better than 95% purity. Trace element determinations and X-ray diffraction determination of some lattice parameters were performed on these specimens. Estimates of the hypersthene compositions were made using charts derived by Hancock (1964). The olivines were too altered to allow any chemical or X-ray diffraction estimates of their composition to be made. The results of these studies are given in Tables 1, 6, 17, and 18.

Examination of the whole rock chemical analyses in Table 1 shows that there is considerable variation in all the major and trace element contents of these rocks. In Table 4-1 the average of the twelve complete analyses is compared with two picritic lavas, quoted by Miyashiro (1965) as being of similar composition to some alpine serpentinites, and the average peridotite and pyroxenite of Nockolds (1954). The average composition of the Scourie ultrabasic gneisses is not dissimilar to those of the other rocks quoted, the values for most of the major elements lying between those of each of the other pairs. The $\text{Fe}_2\text{O}_3/\text{FeO}$ ratio is high, reflecting the high degree of serpentinisation of olivine. The other analyses of Table 4-1, averages of serpentinites from the Altai-Sayan orogenic belt (Pinus et al. 1958), and the Sanbagawa metamorphic

TABLE 4-1

	A	B	C	D	E	F	G	H
SiO ₂	45.46	46.83	47.50	47.15	43.88	50.50	45.78	45.11
TiO ₂	0.19	2.12	0.31	0.09	0.81	0.53	1.04	tr.
Al ₂ O ₃	4.90	8.21	6.47	3.58	4.02	4.10	3.59	4.93
Fe ₂ O ₃	2.56	2.7	4.32	4.00	2.53	2.44	2.97	4.36
FeO	6.84	9.62	7.15	10.08	9.16	7.37	10.30	7.45
MnO	0.16	0.14	0.19	0.18	0.21	0.13	0.16	n.d.
MgO	35.36	20.51	26.55	30.54	34.28	21.71	30.62	31.04
CaO	4.22	7.48	6.65	3.42	3.49	12.00	4.95	7.12
Na ₂ O	0.26	1.74	0.71	0.01	0.56	0.45	0.39	n.d.
K ₂ O	0.05	0.35	0.14	0.02	0.56	0.21	0.19	n.d.

(Analyses recalculated to 100 percent, water-free)

- A Picritic pillow lava, Cyprus (Gass, 1958)
- B Average Oceanite, Hawaii (Macdonald, 1949)
- C Average ultrabasic gneiss from Table 1
- D Most basic possible end member of the ultrabasic series,
calculated from fig. 4-4 (see text)
- E Average Peridotite }
F Average Pyroxenite } Nockolds (1954)
- G Average of 17 'serpentinities derived from basaltic
magma', Altai-Sayan Mountains, U.S.S.R. (Pinus et al., 1958)
- H Average of 3 serpentinities, Sanbagawa Metamorphic Belt,
Japan (Nakayama, 1960)

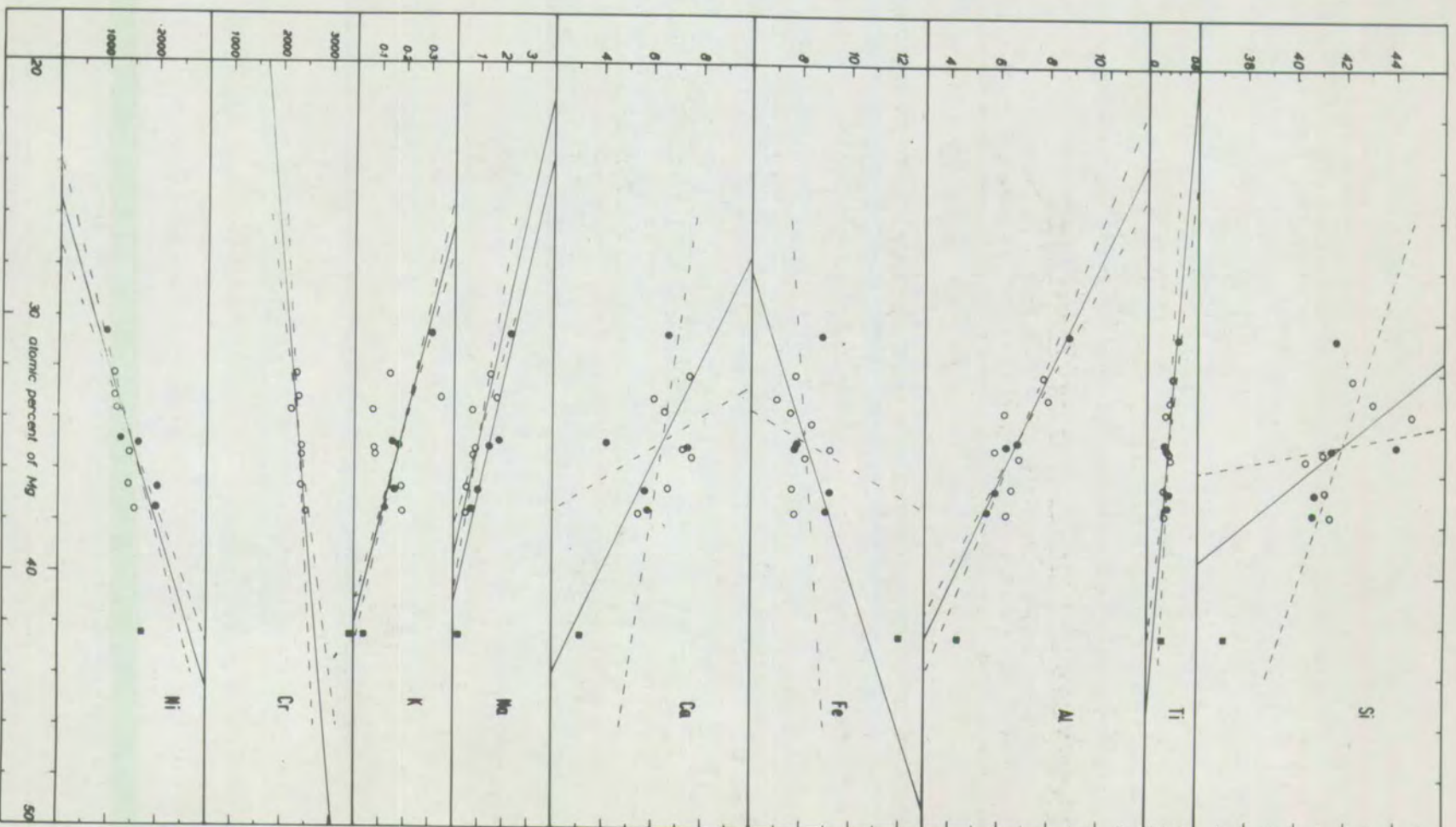
Fig. 4-4

Variation diagrams for the ultrabasic gneisses

Cation atomic percent, and trace element values in p.p.m. are plotted against atomic percent of Mg. Regression lines (dashed) and best fit lines (continuous) are shown on each diagram. Where only a continuous line is shown, the regression lines are virtually coincident with it.

Symbols:

- - ultrabasic gneiss, Geodh nam Cliabh
- - " " , Ben Strome
- - " " , B 241 (Camas an Lochain)



belt of Japan (Nakayama, 1960), also show a general similarity to the Scourie rocks.

The atomic percent variation diagrams in fig. 4-4 show that the most basic rock from which the other compositions can be produced by a single addition process is that which has no sodium - the sodium vs. magnesium line being the first to intersect the magnesium axis. This composition, with the silicon content derived by subtraction from 100%, and recalculated to weight percent, is given in Table 4-1 (D). Its composition is also similar to the others given in Table 4-1.

It is clear from Table 4-1 that rocks of similar composition to the Scourie ultrabasic gneisses are not of uncommon occurrence. Metasomatic alteration of dunitic or harzburgitic rocks is not necessary to explain their compositions.

Nature of the layering

The compositions of ultrabasic rocks may be satisfactorily expressed, in terms of the five components CaO , $(\text{MgO} + \text{FeO})$, $\text{Al}_2\text{O}_3 (+ \text{Fe}_2\text{O}_3)$, SiO_2 , and H_2O . Under isofacial conditions five-phase assemblages in this system will be invariant, according to Goldschmidt's (1911) mineralogical phase rule. Variation in mineral composition is possible only in constituents which are not any of the above components. Thus changes in the Fe/Mg ratio, and in the trace element contents are permissible.

In figs. 4-6 and 4-7 the values of the Fe/Fe + Mg ratio, and the Ni and Cr contents are plotted for mineral pairs and for minerals vs. host rocks for the Geodh nam Cliabh specimens. In fig. 4-5 the rocks and minerals are plotted on Ca-Mg-Fe and CS-MS--A diagrams. The points in the latter



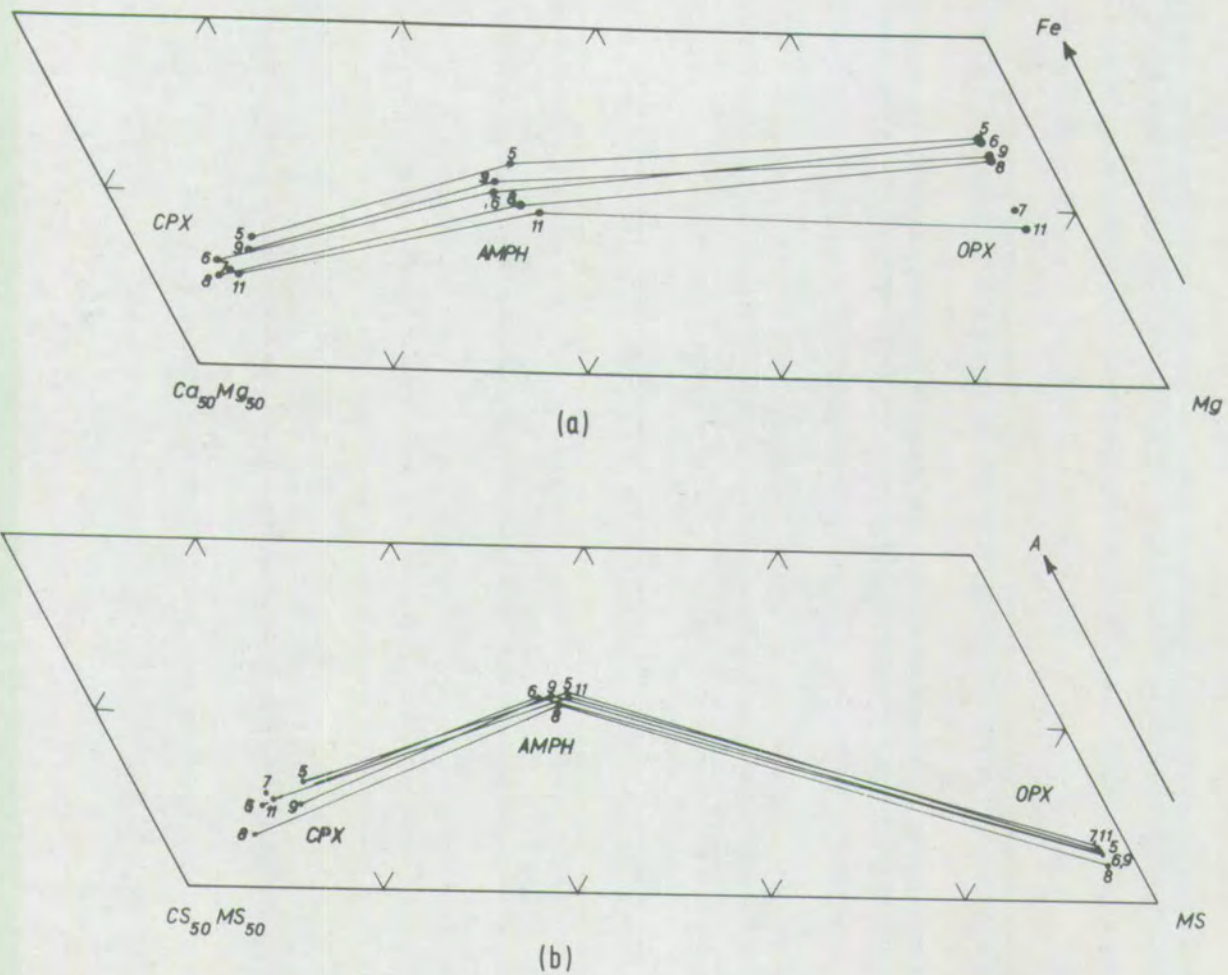


Fig. 4-5. (a) Ca-Mg-Fe and (b) CS-MS-A diagrams for the analysed minerals of ultrabasic gneisses from Geadh nam Clabh.

Diagrams plotted in molecular percent: CS-MS-A coordinates obtained by the data reduction scheme of O'Hara (1988a)

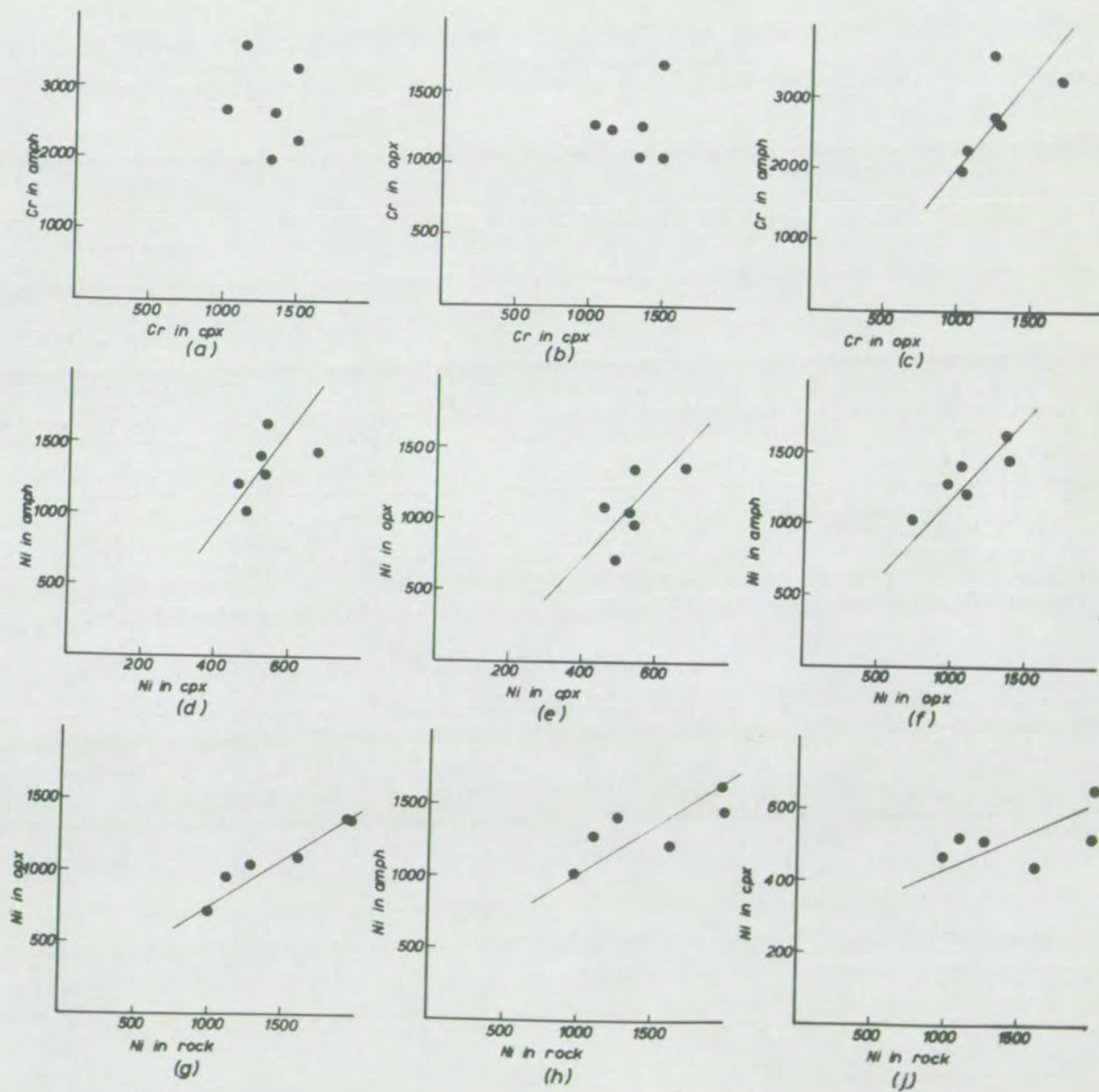


Fig. 4-6. Trace element contents in co-existing minerals, and rocks; ultrabasic gneisses, Geodh nam Clabh. Values are in p.p.m.

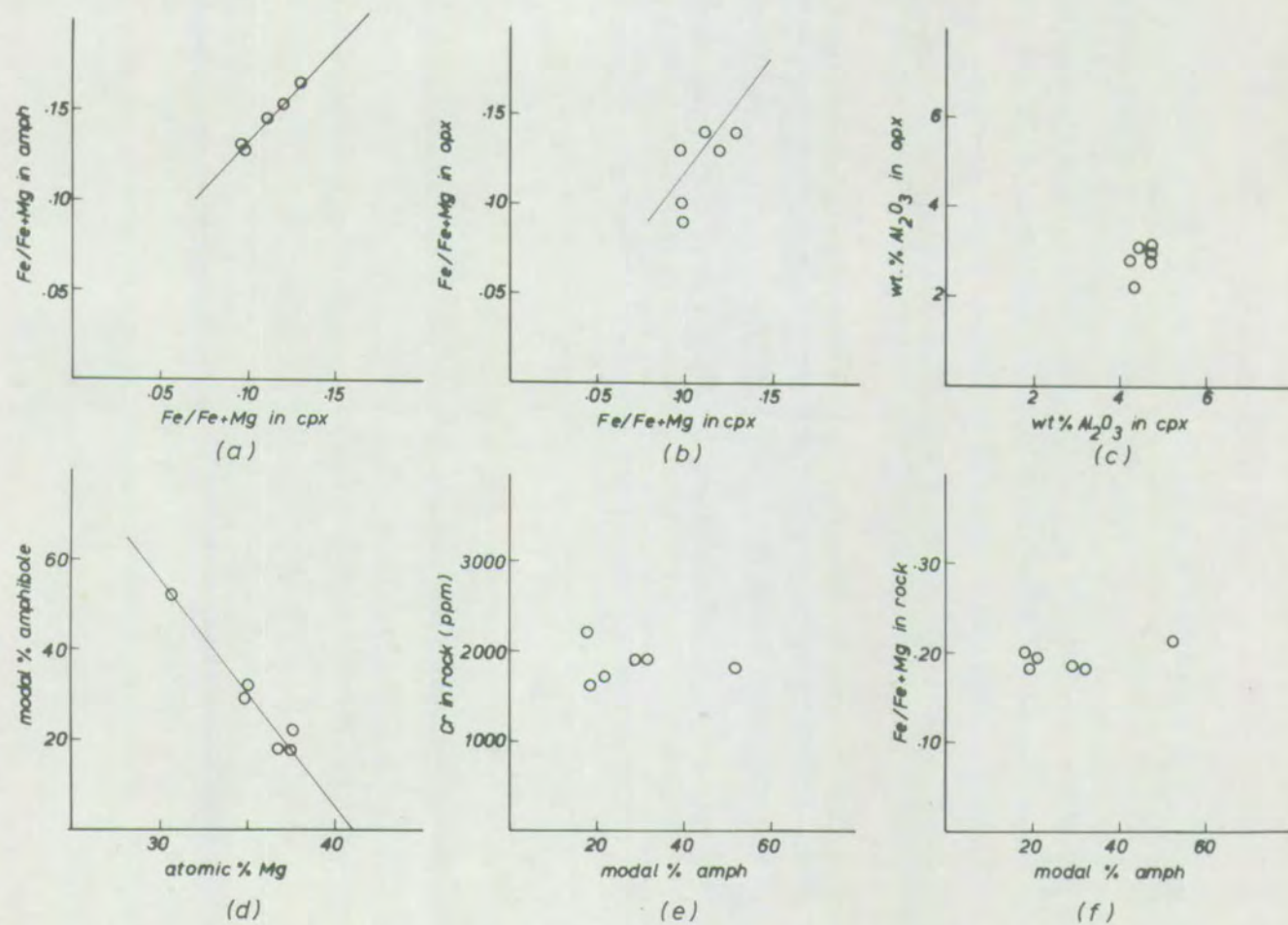


Fig. 4-7. Ultrabasic gneisses, Geodh nam Cliabh.

(a) to (c): Fe/Fe+Mg ratios and Al_2O_3 contents in co-existing minerals.

(d) to (f): variation vs. the amphibole content.

(The Cr contents in (e) were determined using the K_{β} peak and are approximate.)

diagram were obtained by the data reduction scheme of O'Hara (1968a). In fig. 4-7(c) the alumina content of the augites is plotted against the same quantity, estimated by X-ray diffraction measurements, for the hypersthene.

In view of the small extent of the variation in mineral composition, the general coherence of the trace element distributions in figs. 4-6 and 4-7, and the parallelism of the tie-lines in fig. 4-5 are impressive. They imply that there is a variation in mineral composition from one band to the next, which is greater than the analytical error, and that there is attainment of equilibrium between the minerals of each band, but not, clearly, between adjacent bands.

Fig. 4-4 shows variation diagrams for the analysed ultrabasic rocks, plotted in terms of cation atomic percent, against atomic percent Mg. Certain trends are apparent, and in the case of the Na and K contents, the points for rocks from different localities fall on different lines. Regression lines and best fit lines are shown on each diagram. A large angle between the regression lines indicates a low level of confidence for the gradient of the best fit lines.

Using fig. 4-4 as an addition-subtraction diagram, it is possible to calculate the extreme compositions which would produce the observed trends by simple mixing. The most basic possible end member is given in Table 4-2 (X). The least basic possible rock which could have been added to the ultrabasic rocks to produce the trends is that with no Ni. It would have 25% Mg, 1900 p.p.m. Cr, about 4% Na, 11.5% Al, and less certain amounts of Ca, Fe, and Si. Simple mixing of ultrabasic and acid gneiss compositions cannot therefore produce the observed distribution.

O'Hara (1965) lists four possible modes of origin of the layering of banding in the ultrabasic gneisses:

- (1) Mechanical sorting of the existing minerals during deformation.
- (2) Variation in the amount of water present, leading to variation in the amount of amphibole present.
- (3) (a) Metasomatic introduction of material during metamorphism, or
(b) Local internal diffusion of material within the mass.
- (4) Recrystallisation of original igneous layering.

Mechanism (1) cannot have operated alone: it is not possible to produce differences in mineral compositions in this way. Because of the variation in all the major elements in the rock analyses, mechanism (2) cannot have operated alone. Mechanism (3b) cannot have operated alone as it is not possible to produce differences in mineral composition in a homogeneous rock, which would involve diffusion of material up an activity gradient.

As shown above, simple addition of country rock material cannot account for the variation in the ultrabasic gneisses. However, metasomatic alteration is unlikely to be so simple. If diffusion is part of the process, the differences in activity gradient and diffusion coefficient between the several molecular or atomic species involved cause very different rates of penetration. This subject will be discussed more fully later.

The inward passage of some amphibole-rich bands to hornblende-plagioclase rocks of basic composition, and the similarity of both to rocks developed at ultrabasic-acid contacts has already been mentioned (p. 27), and it strongly suggests that these layers represent bands of more extreme penetration of acid material, possibly either as an acid, paligenetic melt which became solidified by reaction with the ultrabasic rock, or by enhanced diffusion along certain tectonically active planes.

The existence, at Camas an Lochain, of peridotites virtually free from

banding, but which still have a strong mineral orientation, suggests that at this locality the process which formed the banding did not operate. In Table 4-2 an analysis of a peridotite from this mass (B 241) is compared with the most basic possible of the ultrabasic series also given in Table 4-1. The silica content of the latter has been assumed, and for the other constituents the two analyses are very similar. Identity would be unlikely, as B 241 is a specimen from close to the margin of the ultrabasic band. This observation lends support to the hypothesis that the layered ultrabasic rocks were formed from a more massive type by metasomatic addition of acid material along the foliation planes.

The close relation between the modal content of amphibole and the Mg content (fig. 4-7d.) shows that the increase in amphibole, and thus the combined, primary water, content is also associated with the other chemical variations (increase in K, Na, Al, Ca, Ti, and Si, and decrease in Mg, Fe, Ni, and Cr). This suggests that they are due to the same underlying process. The line in fig. 4-7d. also intersects the Mg axis at the composition shown to be the most basic possible end member of the ultrabasic series. These observations are entirely consistent with the metasomatic hypothesis outlined above.

If the predominant chemical differences between the ultrabasic layers are caused by an igneous process, then this relation is important, as it seems to require that the water content was determined at the igneous stage. This implies primary crystallisation of an amphibole. This 'igneous' hypothesis could in principle explain the variation in Fe-Mg and trace element distribution in the minerals by the change of distribution coefficients during

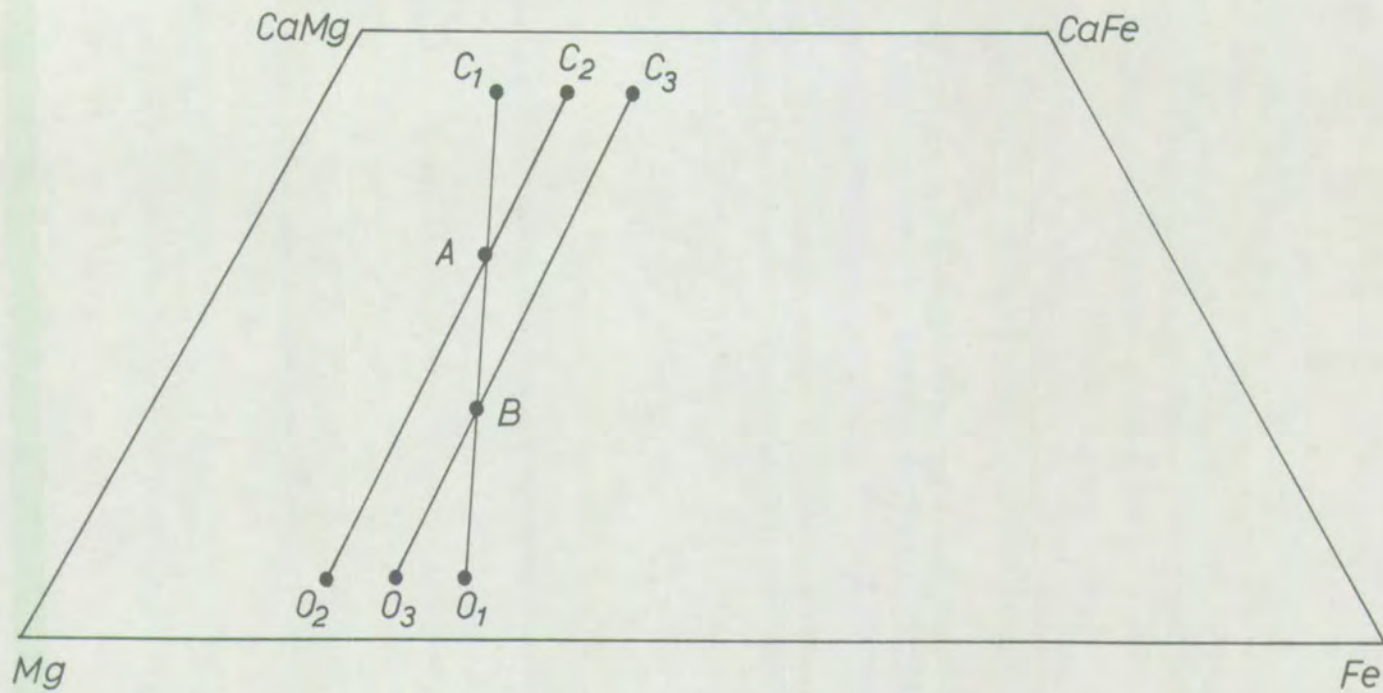


Fig. 4-8. Change in mineral compositions due to a change in Mg-Fe distribution.

Two rocks, A and B, composed of different proportions of cpx C_1 and opx O_1 , are subjected to a change in conditions, and are converted to two different assemblages, O_2-C_2 , and O_3-C_3 . In this way, it is possible to produce differences in mineral composition in an originally banded, but mineralogically homogeneous, rock.

the metamorphism in rocks with varying proportions of the minerals (illustrated in fig. 4-8).

If, as postulated by Bowes et al. (1964), the ultrabasic gneisses are igneous cumulates preserving original igneous layering, then it must be demonstrated that their chemistry is consistent with the sorting of likely cumulus phases. Four phase cumulates are rare, and the analyses should be expressible as mixtures of three or fewer phases to convincingly represent cumulates. As demonstrated above, amphibole would probably have had to have been present at an igneous stage. Olivine would be another likely cumulus phase.

Recalculation of the rock analyses and projection from the olivine composition in the system C-M-A-S by the method of O'Hara (1968a) (fig. 4-9a.) shows that the analyses, in this projection, form a roughly linear trend. The important rock B 241, hypersthene, the amphiboles of the ultrabasic gneisses, and two primary amphiboles from ultrabasic igneous rocks all plot near the extension of the trend. In another projection, from enstatite (fig. 4-9b.), a similar distribution is seen. From these two diagrams it is apparent that the analyses all plot near the plane olivine-hypersthene-amphibole, in this system. It is thus possible, so far as major oxides are concerned, that the rocks represent cumulates formed from varying proportions of these three minerals.

In fig. 4-6a. and c. it is shown that all the present amphiboles are richer in Cr than the other silicate phases and, in fig. 4-7e., that there is no systematic change in Cr content of the rock with modal amphibole content. Fig. 4-7f. shows a similar lack of correlation with Fe/Fe + Mg ratio, while figs. 4-7a. and b. show that the present amphiboles are richer in Fe relative to Mg than the other silicates. These distributions can be produced by

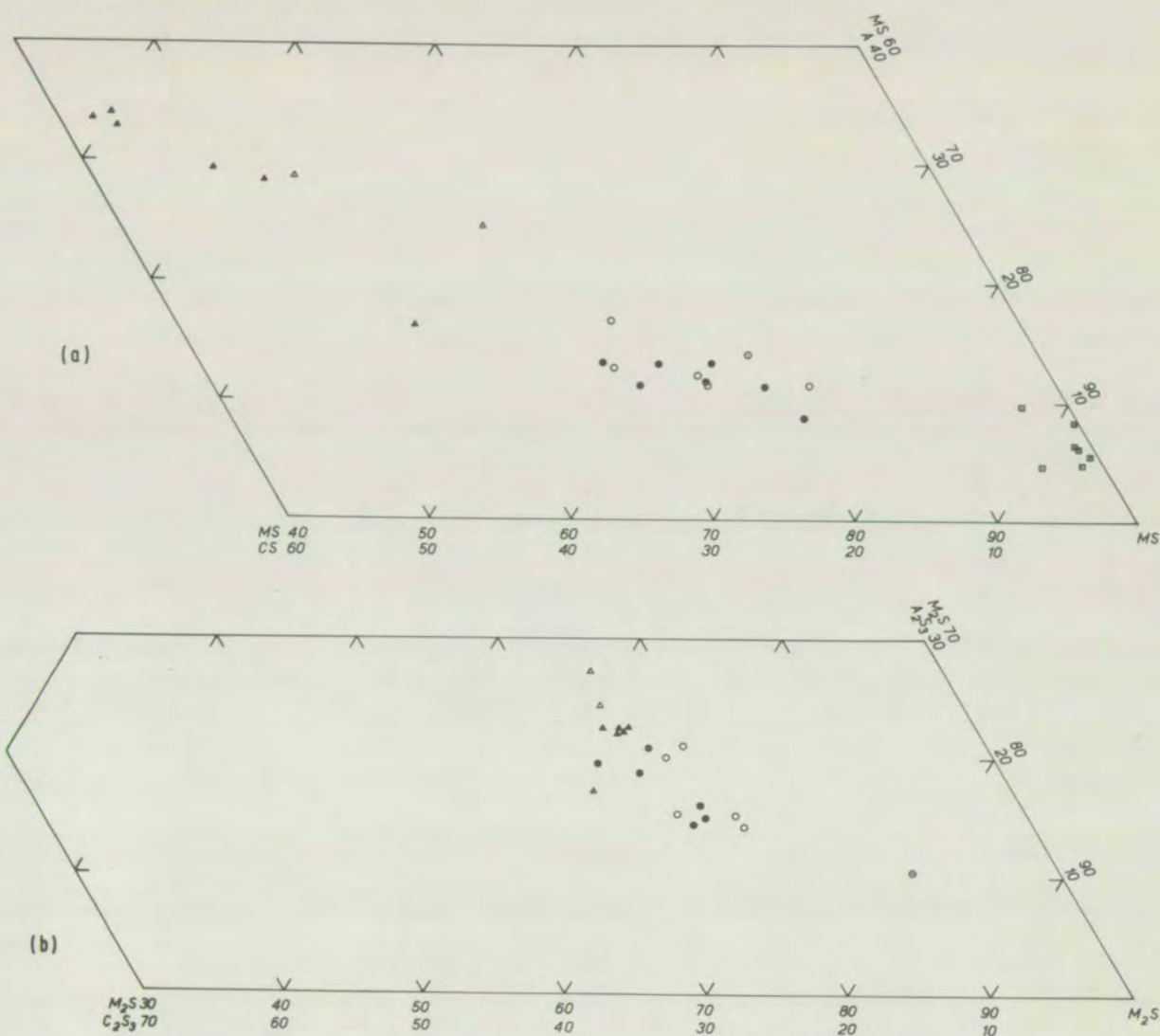
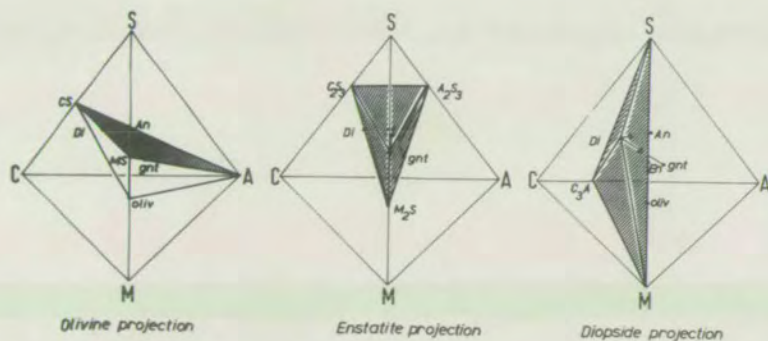


Fig. 4-9. Projections from (a) olivine and (b) enstatite in the system C-M-A-S of ultrabasic gneiss compositions.



- ultrabasic gneiss, Geodh nam Clabh.
- " " " Ben Strone.
- ⊙ " " " Camas an Lochain (B 241)
- ▲ amphibole of ultrabasic gneiss: present study.
- △ " " " " O'Hara (1961)
- △ " " " igneous rock (Deer et al., 1963, Table 40)
- hypersthene of ultrabasic gneiss (O'Hara, 1961)

Left: projections in the system C-M-A-S used in this and subsequent figures.
All projections are in weight percent.

variation in original amphibole proportion only if the amphibole had essentially the same Cr content and $Fe/Fe + Mg$ ratio as the other phases crystallising. Alternatively, a fourth phase could be postulated, rich in Cr and Fe, whose amount varied conversely with that of amphibole (as is the case with spinel in the present metamorphic assemblage).

Sedimentary structure

Bowes et al. (1964) have described structures in the ultrabasic rocks, and also in the basic rocks, of the area, which they regard as of sedimentary origin, and therefore of an accumulative igneous origin. Their sedimentary nature was queried by G.M. Brown (discussion after Bowes et al., 1964), and disputed by O'Hara (1965). The present study revealed no structures at Scourie or Ben Strome, which were directly comparable with those seen during an earlier field season, spent on the layered ultrabasic intrusion of Rhum (Brown, 1956; Wadsworth, 1961).

Conclusions

It has been shown that the compositions of the ultrabasic rocks are similar to those of some known igneous rocks, and that these compositions form a distinct geochemical trend, whose extreme ultrabasic end defines a composition similar to that of a poorly layered peridotite from Camas an Lochain.

Evidence has been produced which supports two hypotheses: that the layering and chemical variation in the ultrabasic gneisses is either of igneous or metamorphic origin. The 'igneous' hypothesis requires that the rocks be olivine-hypersthene-amphibole cumulates. No such types appear to have been described, but there is no theoretical reason why they should not

form from basic magmas under relatively wet conditions. This hypothesis also requires that the distribution of Cr, Fe and Mg between the three minerals be radically different under the conditions of the igneous accumulation and of the metamorphism.

If the layering is of igneous origin, then the poorly layered peridotites of Camas an Lochain represent parts of the intrusion(s) where hypersthene and olivine were the only cumulus phases. If it is of metasomatic origin, then they have escaped the metasomatic process.

In view of the conditions placed on the 'igneous' hypothesis, it may seem preferable to accept that the layering is of metasomatic origin. The lack of similar strictures on this hypothesis may be because it cannot be formulated so precisely.

4.5 Geochemistry of the Basic and Garnetiferous Basic Gneisses

In this section the chemistry of the basic and garnetiferous basic gneisses is examined and compared with that of some basic igneous rocks in an attempt to decide whether they are likely to be the metamorphosed equivalents of such rocks. Table 2 presents analyses of 20 garnetiferous basic gneisses, 16 from Ben Strome, and 2 each from Geodh'Eanruig and Scourie House. Table 3 presents 6 analyses of basic gneisses, 2 from Geodh'Eanruig, and one each from Scourie House, Pairc a'Cladaich, Camas nam Buth, and Ben Strome (the last a composite specimen).

Variation in composition

The range of compositions of the analyses of Tables 2 and 3 is not great. Variation diagrams of cation atomic percent against the $Fe/Fe + Mg$ ratio reveal a few trends (fig. 4-14), none very well defined. Principal component analysis (Kendall, 1968) of the analyses of the garnetiferous basic group was undertaken

by means of a computer programme written by Dr. R.F. Cheeney (Westoll, 1968). No very significant linear trends in multi-dimensional space were revealed by this method. The most significant transformed variable accounted for 34% of the variation, over 90% of which consisted of variation in the silica content. This may be real but may also be a reflection of the poor quality of silica determination by X-ray fluorescence analysis. All the other transformed variables accounted for less than 20% of the variation and were trivial.

Comparison with igneous rocks

Normatively, all the rocks of Tables 2 and 3 are olivine basalts or olivine tholeiites. Normative hypersthene varies from 0.06 to 29%. In Table 4-3 the average analyses of the basic and garnetiferous basic gneisses are compared with other tholeiitic rocks, selected as being averages of, or described as parental to, magma series. The chemical differences between the average basic and garnetiferous basic gneisses is not great: the basic is slightly richer in silica, poorer in ferrous iron, magnesia and lime, and has a slightly higher oxidation ratio. The two are not greatly different from the other analyses shown, although the ocean floor tholeiites are more magnesian, and the other Lewisian rocks more iron rich. Apart from these differences, all the compositions are close enough to be described as 'similar', a practice common in geological literature.

To reveal any significant differences which might not be seen in such a casual inspection, the analyses were plotted on diagrams of the type used by Wager (1956) and O'Hara (1968a). These are shown in figs. 4-10 and 4-11.

On the albite-iron enrichment diagram (fig. 4-10), the normative plagioclase is seen to lie between An_{53} and An_{76} for all but two, and $Fe^{II}/Fe^{III} + Mg$

TABLE 4-2

	B 241	X
SiO ₂	42.2	47.2
TiO ₂	0.2	0.1
Al ₂ O ₃	4.2	3.6
Fe ₂ O ₃	9.0	4.0
FeO	8.2	10.1
MnO	0.2	0.2
MgO	32.5	30.5
CaO	3.3	3.4
Na ₂ O	0.12	0.01
K ₂ O	0.03	0.02
total Fe	18.1	15.2

B 241 Peridotite, Camas an Lochain

(see also Table 11)

X Most basic possible end member of the
ultrabasic series (see also Table 4-1
and text)

TABLE 4-3

	1	2	3	4	5	6	7	8	9	10
SiO ₂	47.0	48.3	49.8	50.7	51.3	49.2	48.9	49.0	48.6	43.3
TiO ₂	0.97	0.87	2.5	0.8	1.2	1.3	1.9	1.4	1.7	1.7
Al ₂ O ₃	14.4	14.3	12.5	16.6	14.9	15.2	12.6	13.9	15.5	13.1
Fe ₂ O ₃	2.5	2.7	1.7	0.6	1.9	2.1	4.5	4.4	2.6	2.0
FeO	11.2	9.8	10.2	9.6	8.5	7.7	11.2	10.2	8.7	6.8
MnO	0.2	0.2	-	-	-	0.2	0.2	0.2	0.2	0.1
MgO	8.9	8.4	8.8	7.3	7.0	9.3	6.4	6.0	8.4	15.6
CaO	12.1	11.4	10.9	12.5	11.8	10.8	9.7	8.9	10.3	12.1
Na ₂ O	1.8	1.8	2.6	1.6	2.1	2.7	2.5	2.9	2.3	2.0
K ₂ O	0.15	0.75	0.6	0.1	0.8	0.27	0.56	0.9	0.6	1.1
H ₂ O	0.8	-	-	-	-	1.3	-	-	0.9	1.9
<u>Fe_x100</u> <u>Fe+Mg</u>	45.9	45.0	42.8	43.8	45.0	37.4	57.2	57.0	42.5	23.7
Cr	315	285	500	425	250	430	70	110	-	4225
Ni	180	140	350	150	60	160	90	75	-	455

- 1 Average garnetiferous basic gneiss. } This thesis (Tables 2 and 3).
 2 Average basic gneiss. }

- 3 Parental magma, Hawaii
 4 Parental magma, Karroo Dolerites
 5 Parental magma, British Tertiary Prov. } Nockolds and Allen (1956)

- 6 Ocean floor tholeiites, average of 8 analyses from Nicholls (1965),
 3 analyses from Nicholls et al. (1964)
 8 analyses from Muir and Tilley (1964)
 9 analyses from Muir and Tilley (1966)

Trace elements - average of six analyses from Muir and Tilley (1964)

- 7 Average analysis of least-altered Scourie Dykes, Burns (1956)
 Trace elements from O'Hara (1961b) and Holland (1965)
 8 Average metamorphosed basic rock, Gairloch (Park, 1965)
 9 Average olivine-tholeiite (Manson, 1967)
 10 Average of 2 amphiboles from pyroxenite, Brae Complex, Shetland (Gill, 1965)

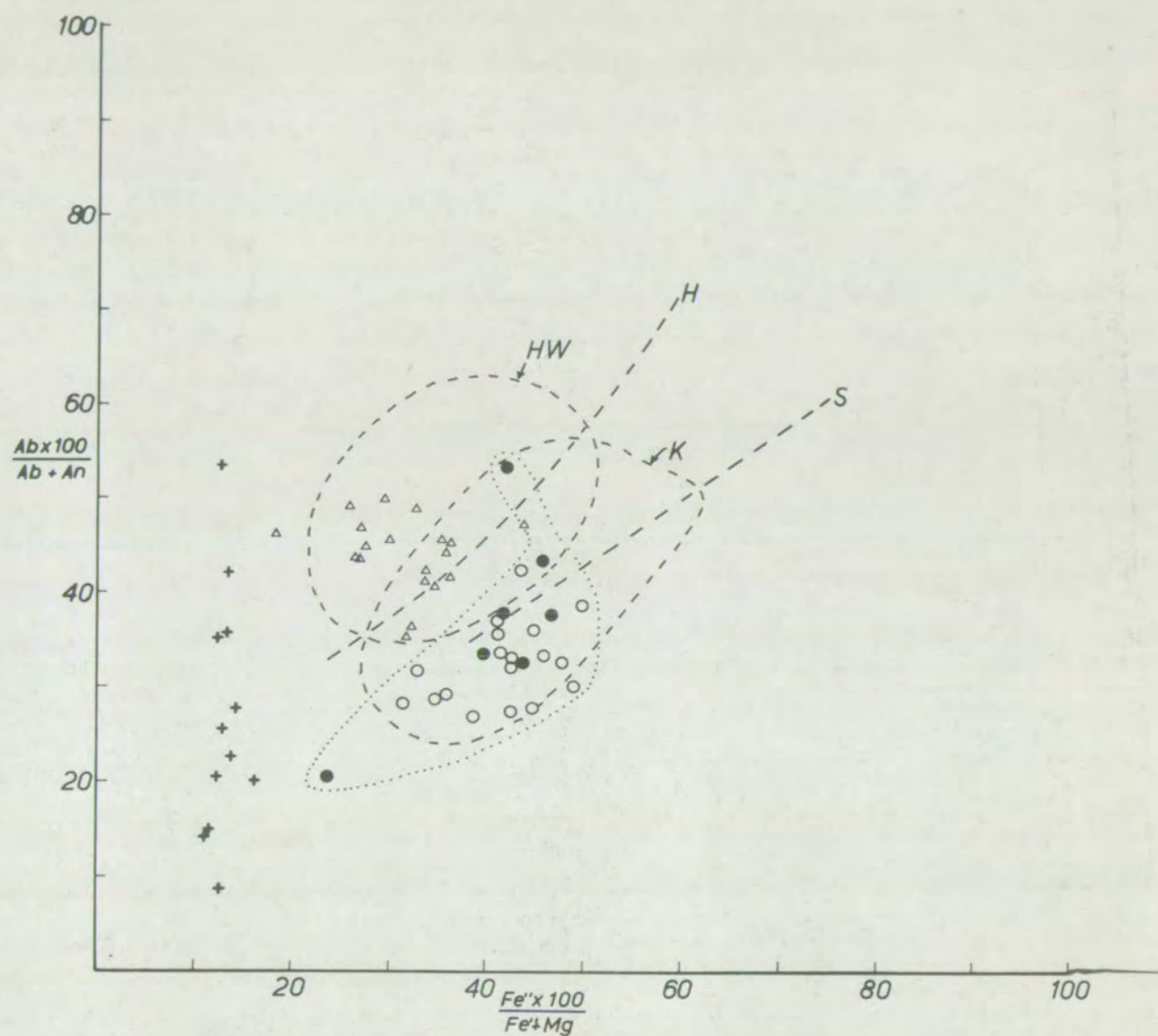


Fig. 4-10. Albite-iron enrichment diagram for the Scourie rocks.

- garnetiferous basic gneiss.
 - basic gneiss
 - + ultrabasic gneiss.
 - △ ocean floor tholeiites. (see text)
- | | | | |
|----|-----------------------------|---|-------------------|
| S | trend of Skaergaard liquids | } | from Wager (1956) |
| H | " " Hebridean magmas | | |
| K | field of Karroo rocks | | |
| HW | " " Hawaiian rocks | | |

between 30% and 50% for all but one of the analysed rocks. The basic gneisses mostly lie to the albite and iron rich end of the area occupied by the garnetiferous basic gneisses. Also shown are some magma trends, and the areas occupied by some groups of rocks, from Wager (1956).

The Scourie basic and garnetiferous basic gneisses form an elongated cloud, whose long axis is parallel to that of the Karroo and Hawaiian fields and the Skaergaard and Hebridean trends. This elongation is characteristic of magma series in which fractionation of both plagioclase and ferromagnesian minerals has taken place. The calcium-rich, sodium-poor character of the rocks is shown by the fact that they plot in an area below that of all the other groups of rocks mentioned. The ocean floor tholeiites plot in two fields: again both are elongated parallel to the others. This group of rocks has much lower $Fe^{II}/Fe^{II} + Mg$, and higher $Ab/Ab + An$ than the Scourie rocks.

On the diagrams (figs. 4-11 - 4-13) showing sub-projections within the system C-M-A-S (O'Hara, 1968a), the field occupied by the basic and garnetiferous basic gneisses is also restricted and close to those of the other groups of rocks plotted. In the diopside projection (fig. 4-12a.) all the areas are virtually coincident, but in the enstatite and olivine projections a significant difference emerges: both the ocean floor tholeiites and the Scourie rocks plot slightly away from the other groups, towards the diopside projection point. The Scourie rocks plot closer to the diopside point than the ocean floor tholeiites, but there is considerable overlap - more between the two fields than between either one and any of the others shown.

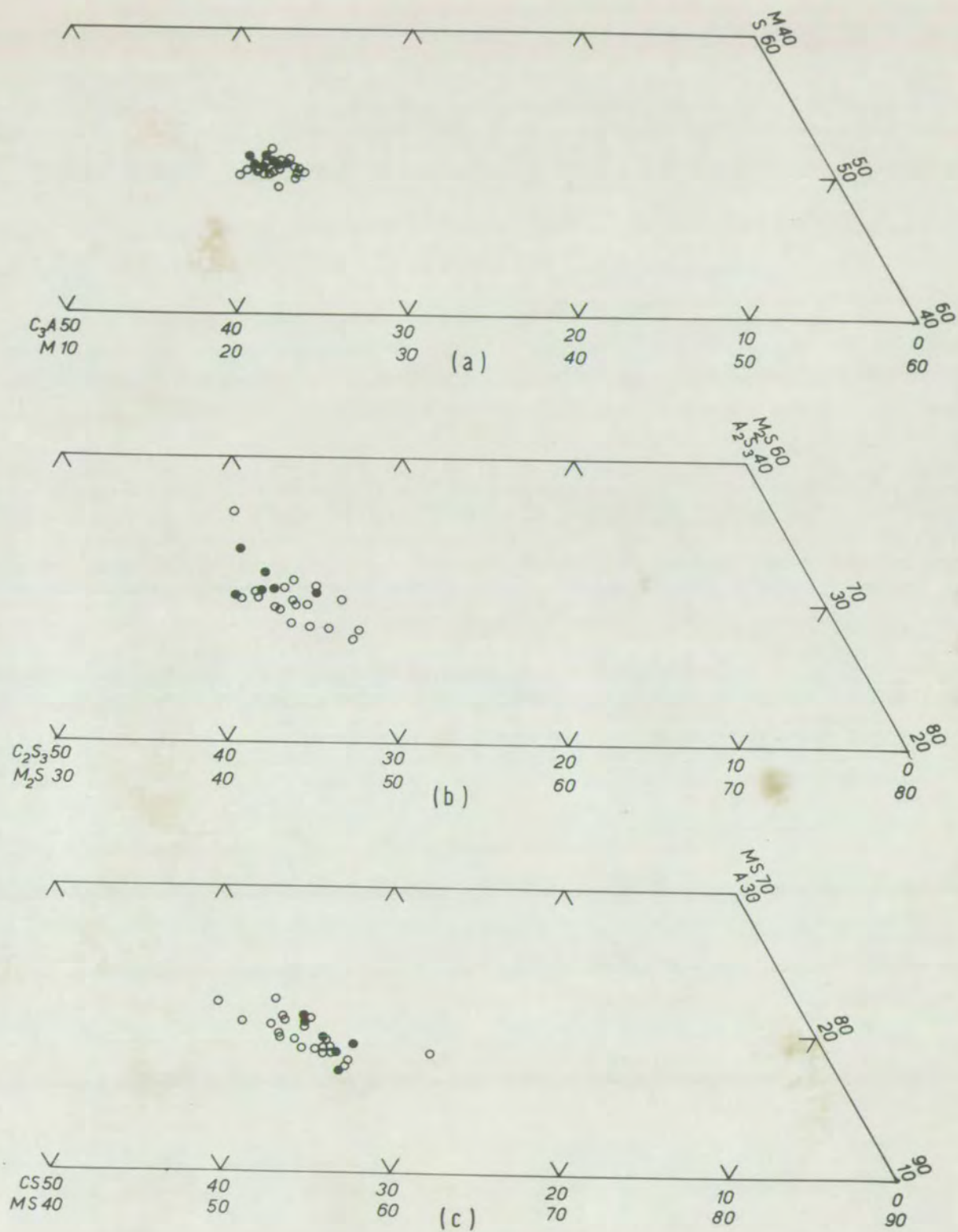
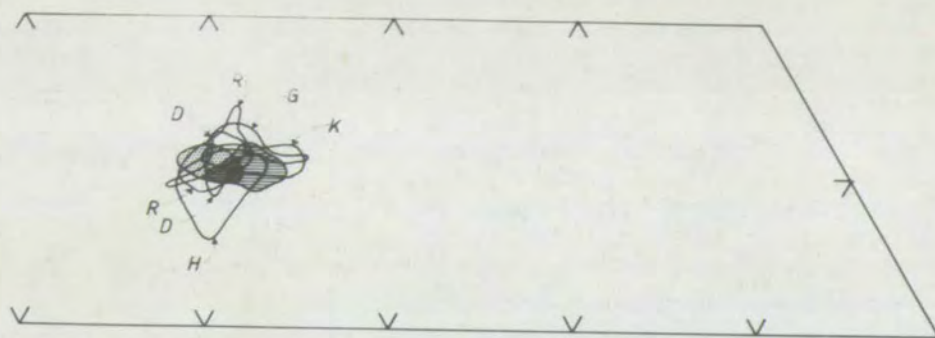
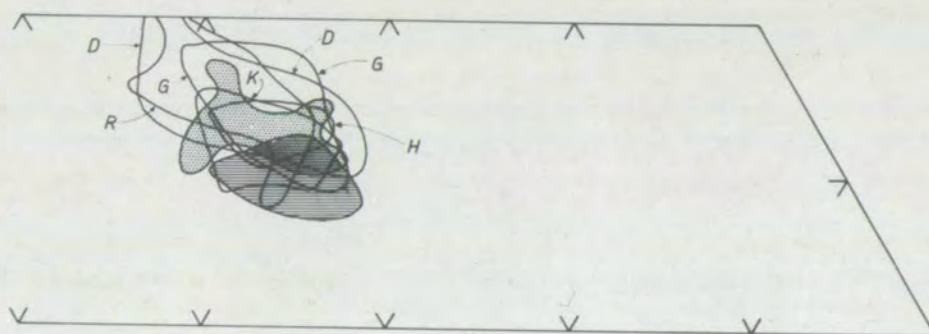


Fig. 4-11. Projections from (a) diopside, (b) enstatite, and (c) olivine in the system C-M-A-S, of compositions of basic and garnetiferous basic gneisses.

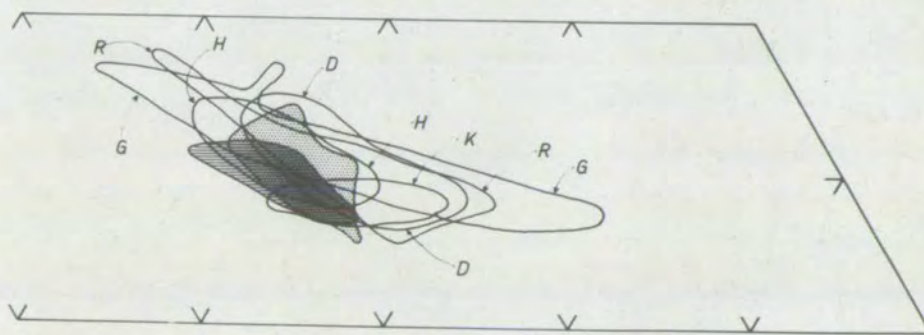
- basic gneiss
- garnetiferous basic gneiss



(a)



(b)



(c)

Fig. 4-12. Projections, as in fig. 4-11, of the compositions of basic and garnetiferous basic gneisses, compared with those of various basic igneous rocks.

D - Scourie dykes (Burns, 1956)

R - Amphibolites in the Laxfordian near Rhiconich (Chowdhary, 1969)

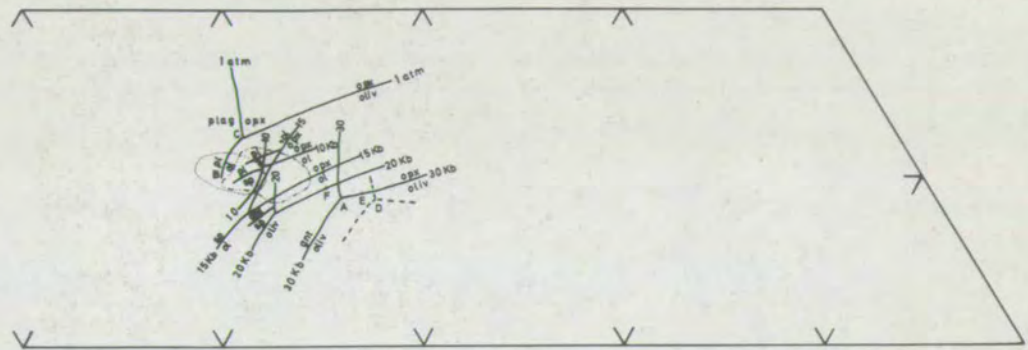
G - " " " " Gairloch (Park, 1966)

H - Olivine-tholeiites from Hawaii (Macdonald, 1949)

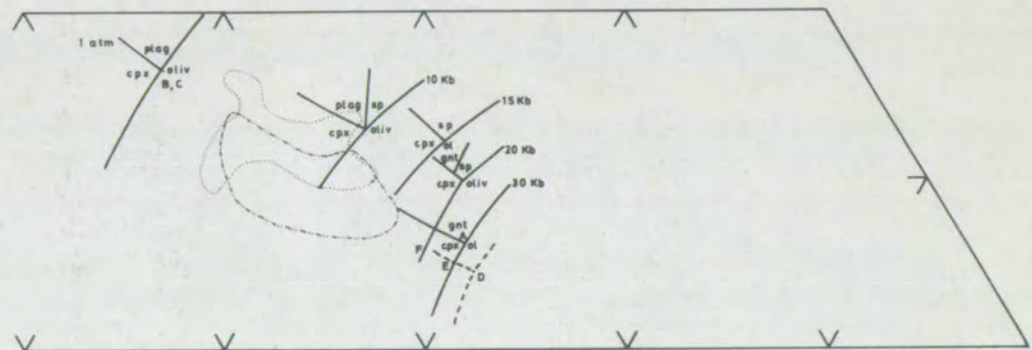
K - " " " the Karroo province (Walker and Poldervaart, 1949)

□ Ocean floor tholeiites (for sources see text)

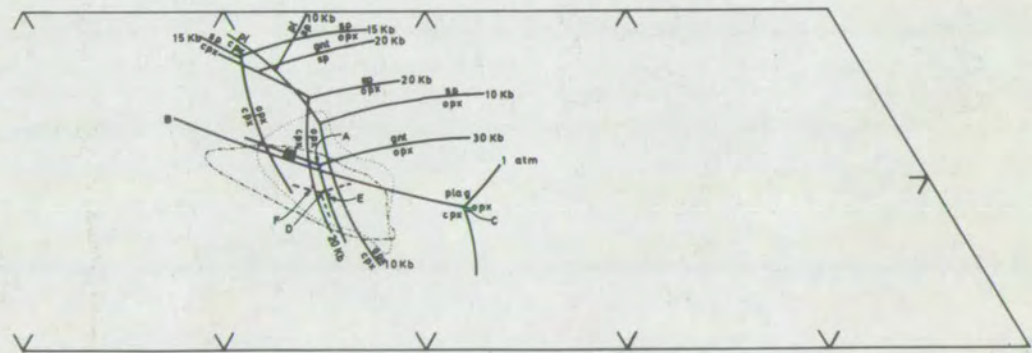
■ basic and garnetiferous basic gneisses



(a)



(b)



(c)

Fig. 4-13. Projections, as in fig. 4-11, of the composition fields of basic and garnetiferous basic gneisses (dash-dot lines) and deep ocean tholeiites (dotted lines) with possible phase relations from O'Hara (1968a).

In fig. 4-13 the same projections are shown with the tentative phase relations deduced from available experimental data (O'Hara, 1968a). The basic and garnetiferous basic gneisses plot inside the olivine primary phase volume at 1 bar, and inside the clinopyroxene primary phase volume between about 15 and 25 Kb.

O'Hara (1968b), to explain what is essentially the same anomaly for the ocean floor tholeiites, has proposed the following fractionation scheme; partial melting of garnet-peridotite at 30 Kb. to give liquid A (fig. 4-13). This magma is erupted towards the surface at a sufficiently rapid rate to keep the composition within the olivine primary phase volume, but with enough halts on the way so that the fractionation of olivine keeps the composition close to the margin of this volume. Final eruption at low pressures finds the magma composition either on or close to the olivine-orthopyroxene-plagioclase cotectic (B-C on fig. 4-13). A halt at any pressure between 10 and 20 Kb. long enough to allow the liquid to fractionate to a composition in equilibrium with four crystalline phases, will render it nepheline-normative, a state from which it could only become tholeiitic again by continuous fractionation and reaction with the wall rock at decreasing pressure, following the liquid + four phases composition to the low pressure eutectic C (fig. 4-13).

The evidence that this is a feasible mechanism for the generation of the ocean floor tholeiites is that the liquid A, olivine, and the rocks are collinear in the system C-M-A-S (they are collinear in the enstatite and diopside projections and coincident in the olivine projection).

An exactly analogous explanation could be advanced for the origin of the Scourie basic and garnetiferous basic gneisses as igneous rocks. The initial

liquid from which to fractionate olivine to obtain their compositions is slightly different from A, and might be derived by melting of garnet-peridotite at 30 to 40 Kb. (D on fig. 4-13, an extrapolation of the data of O'Hara, 1968a), or by more advanced partial melting at 20-30 Kb. (E or F on fig. 4-13), with loss of the aluminous phase. If such a liquid were subjected to olivine fractionation under reducing pressure, it would produce liquids plotting in the same area as the basic and garnetiferous basic gneisses. The pressure cannot be reduced below 10-15 Kb. while continuous fractionation is occurring, since these rocks plot in an area covering the boundary of the olivine primary phase volume at these pressures (they lie astride the olivine-orthopyroxene-clinopyroxene cotectic). It is thus possible, from this method of petrogenetic analysis, that these rocks represent basaltic liquids generated by partial melting at about 100 Km. depth, and intruded in the upper 30 Km. of the crust.

Since, as just mentioned, the rocks plot astride the olivine-orthopyroxene-clinopyroxene cotectic at 10-15 Kb., it may be possible that they represent liquids generated by partial melting of a lherzolite (2-pyroxene peridotite) at these pressures. Any aluminous phase (spinel and/or plagioclase) would require to have been lost during earlier partial melting. This process requires an origin in the lower crust or uppermost mantle, with geothermal gradients of about $40^{\circ}\text{C}/\text{Km}$.

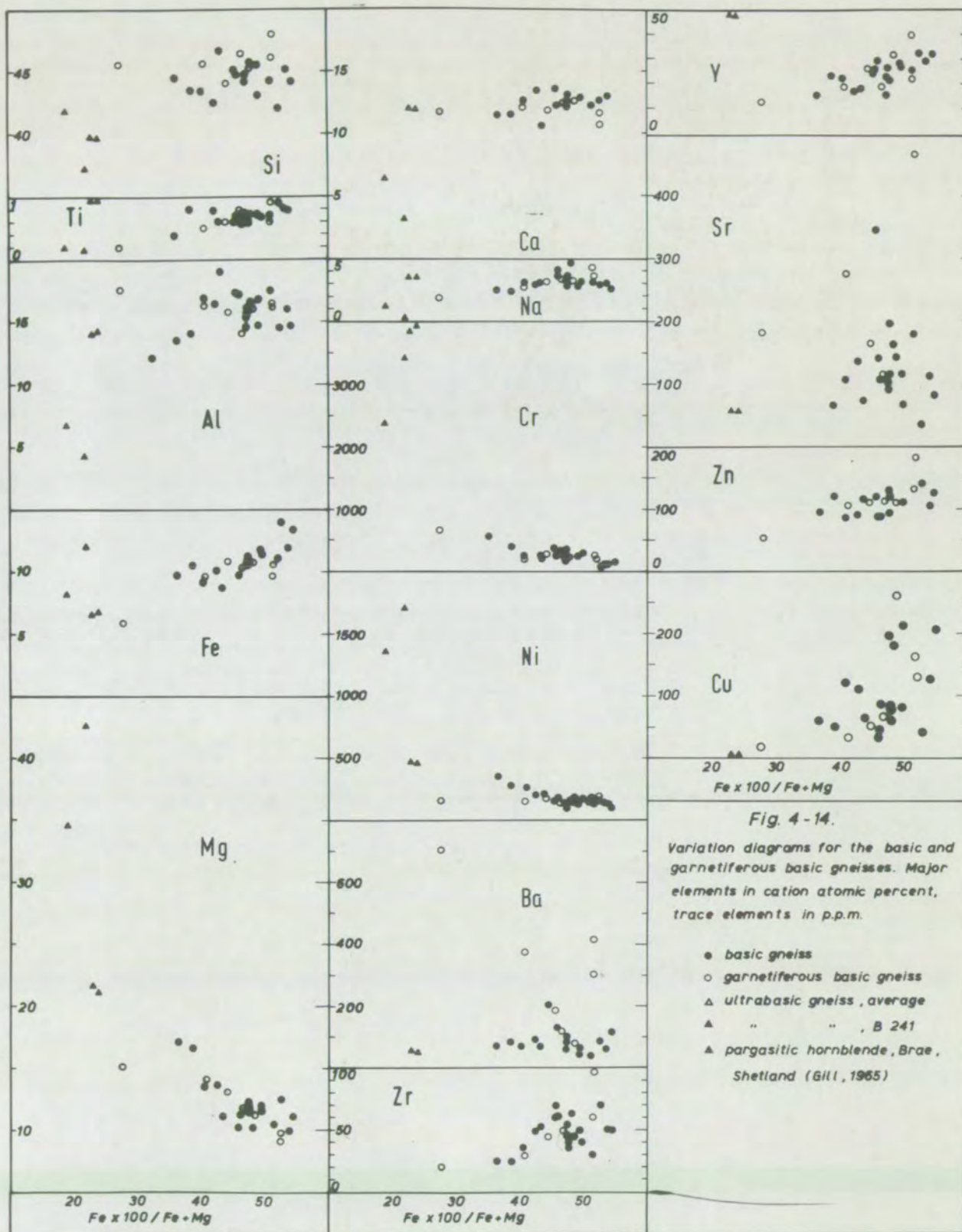
The hypothesis of olivine fractionation, as outlined above, is capable of explaining the geochemical features of the rocks as seen in the reduced system C-M-A-S. The fractionation of olivine alone would increase the $\text{Fe}/\text{Fe} + \text{Mg}$ ratio, without increasing the $\text{Ab}/\text{Ab} + \text{An}$ ratio. This is consistent with the

unusually high anorthite content of the normative plagioclase, for the degree of iron enrichment. It does not explain, however, the apparent evidence of fig. 4-10 that there was simultaneous fractionation of plagioclase and ferromagnesian minerals.

The possibility that hornblende fractionation in a basic magma series might explain the compositions of this group of rocks should not be overlooked. Petrological opinion is currently favouring this mechanism as one way of generating the calc-alkaline magma series in orogenic environments (e.g. Best and Mercy, 1967). Unfortunately the effects of amphiboles on the phase equilibria in the system C-M-A-S are totally unknown.

Table 4-3 gives the compositions of two hornblendes which appear to have crystallised directly from a gabbroic magma, which is part of a calc-alkaline magma series (Gill, 1965). They have considerable amounts of normative anorthite, and low $Fe/Fe + Mg$ ratios. Fractionation of such hornblendes from a basic magma would produce a simultaneous increase in both $Fe/Fe + Mg$ and $Ab/Ab + An$ ratios. Since the basic and garnetiferous basic gneisses do not plot in or near the field of plagioclase crystallisation in fig. 4-13 such a process is a necessity if the rock compositions are to be explained as igneous liquids, and if this relationship is not fortuitous.

Fig. 4-14 shows the effect of fractionation of the above mentioned hornblendes on the chemistry of the basic rocks. All the (poorly defined) trends in the major element chemistry of the rocks, except for that of Ti, could be explained by subtraction of these hornblendes. The trace element variation cannot be so satisfactorily explained, but it is clear that a possible amphibole could be envisaged whose fractionation alone could account for all the chemical variation in the basic group of rocks.



The basic rocks as cumulates

This possibility, raised by Bowes et al. (1964, 1966), has been considered by O'Hara (1965, 1966), who demonstrated the incompatibility of the chemistry of four adjacent samples from Drumbeg (Bowes et al., 1964) with an origin as olivine-orthopyroxene-clinopyroxene-plagioclase cumulates. The data presented in this thesis throw little new light on the matter.

The chemical variation in the basic group is not great; neither is it systematic in any of the masses studied. The rock compositions can be expressed in three ways as likely igneous assemblages: olivine-opx-cpx-plagioclase (the normative minerals); garnet-opx-cpx-plagioclase (the present minerals of the garnetiferous basic gneisses); or opx-cpx-plagioclase-ore (the present mineralogy of the basic gneisses ignoring the minor hornblende). In view of their basic composition, they may also be expressable as assemblages consisting very largely of amphibole.

In a four phase cumulate, the average composition of the cumulate will be very nearly coincident with that of the parent liquid, when plotted in the reduced system C-M-A-S. The failure of the rock compositions to coincide with any liquid + four phase compositions in this system (fig. 4-13), means that they are unlikely to represent four phase cumulates either, unless amphibole was a cumulus phase.

It is therefore possible that the rocks could be derived from cumulates rich in amphibole. The lack of any data on the effects of amphiboles in the system, and the lack of descriptions of rocks of the postulated type, means that the hypothesis is not open to precise criticism, either for or against.

Possible igneous relationships between the basic, garnetiferous basic and ultrabasic gneisses

If an igneous relationship is postulated between these three rock types, it could be one of several types:

(1) The basic types represent magmas from which the ultrabasic rocks are cumulates.

(2) The rocks are all cumulates, which are in their original positions relative to each other (Bowes et al., 1961, 1964).

(3) The rocks are all cumulates, the basic and ultrabasic members having been brought together by tectonic action (Bowes et al., 1966).

In addition, there are two possibilities for the origin of the ultrabasic types:

(a) The ultrabasic rocks are derived from an originally more homogeneous peridotite similar to B 241 in composition (above, p. 54).

(b) The ultrabasic rocks retain their original igneous compositions (Bowes et al., 1964, 1966).

In the former case, the composition of B 241, will control the liquid line of descent in the basic series, while in the latter, it is the average composition of the ultrabasic gneisses which will exert this control.

Figs. 4-10 and 4-14 show that where distinct geochemical trends exist in the basic series, neither the average ultrabasic gneiss, nor B 241 have compositions lying systematically on the extensions of these trends. Thus the basic rocks cannot represent liquids whose composition has been controlled by fractionation of the nearby ultrabasic rocks.

It has been shown above that the basic and garnetiferous basic gneisses may possibly represent cumulates in which an amphibole was a major phase.

The ultrabasic gneisses have been shown to represent possible olivine-orthopyroxene-amphibole cumulates (pp. 54 - 56). In this case, the great difference in the Fe/Fe +Mg ratio of the minerals between the two groups (this ratio varies from 16% to 32% between the augites of Z 726 and Z 718, at Geodh'Eanruig) cannot be explained by their being adjacent parts of a layered intrusion, with a now, iron rich mineral, now no longer present, appearing as a major cumulus phase in the garnetiferous basic member. Magnetite could be such a mineral, but no cumulus magnetite appears to have been described.

It is therefore necessary to presume that, if both basic and ultrabasic rocks represent cumulates, that they are parts of a layered intrusion, once separated by a considerable thickness of intermediate cumulates, brought together by tectonic action, as suggested by Bowes et al. (1966). The apparent absence of any representatives of such intermediate cumulates means that the evidence for a layered igneous origin of all the rocks present in the masses under study rests on observations from each member: their occurrence side by side does not suggest such an origin.

4.6 Relationship between the basic and garnetiferous basic gneisses

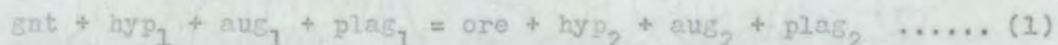
As shown above (Tables 2 and 3), the differences in composition between basic gneisses with abundant garnet and those with little or no garnet are not great. They do not seem, on a superficial examination, sufficient to account for the differences in modal composition. In order to test this observation more rigourously, the analyses were recalculated to give proportions of idealised, anhydrous granulite facies minerals, using the reduced compositional parameters of O'Hara (1968a), and part of the computer programme used for the simulation model (Appendix E). All Fe_2O_3 was considered as FeO, to compensate

for variations in the oxidation state.

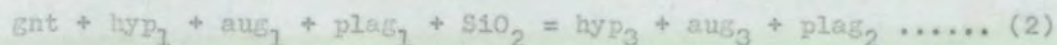
To account for the observed variation in the amount of titanomagnetite, the recalculation was again performed, with increasing amounts of TiO_2 and FeO , equivalent to magnetite with 50% ulvöspinel, subtracted from the analyses. When all the TiO_2 had been used in this way, further FeO was subtracted, and the recalculation performed again. The results of this analysis are shown graphically in figs. 4-15 and 4-16.

At each stage of the recalculation, the basic gneisses give, on average, more hypersthene and plagioclase, and less augite and garnet than the garnetiferous basic. The differences do not suffice to account for all the difference in modal composition, however. The occurrence of different mineral assemblages in rocks of similar composition could be due to differences in the physical conditions. It seems unlikely, however, that the pressure and temperature could have varied significantly between the basic and garnetiferous basic gneisses. More probable is that rather subtle chemical differences, obscured by the reduction to four components are responsible for the modal differences between the two groups of rocks.

It is possible to express the change from garnetiferous basic to basic gneiss assemblage by the reaction:



The hypersthene and augite of the right hand side being more magnesian, and the plagioclase more calcic, than those of the left. The same transformation can be effected by the introduction of silica:



In this case the hypersthene and augite of the right hand side being less

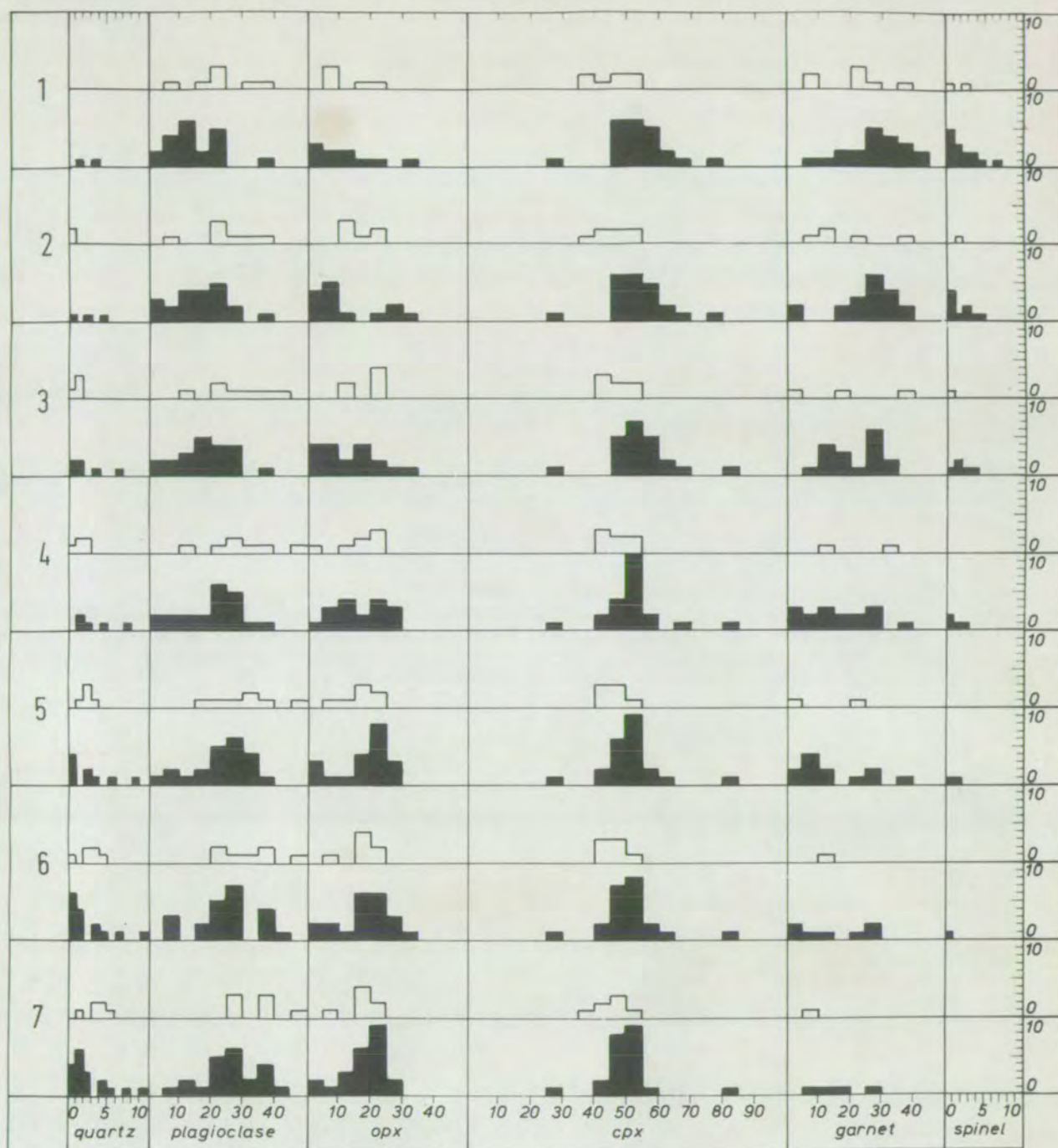


Fig. 4-15. Histograms showing the compositions of basic (open) and garnetiferous basic (solid) gneisses, recalculated to molecular proportions of ideal granulite facies minerals.

Stages 1 to 7 represent subtraction of increasing amounts of FeO and TiO₂ to form titanomagnetite (see fig. 4-16)

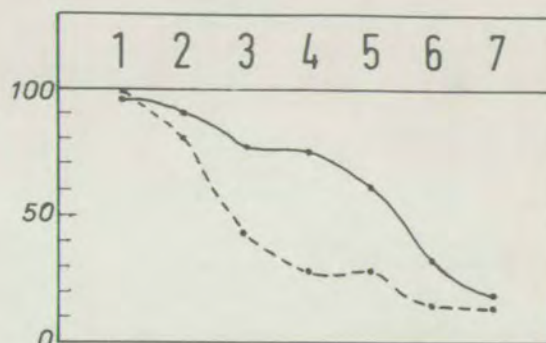
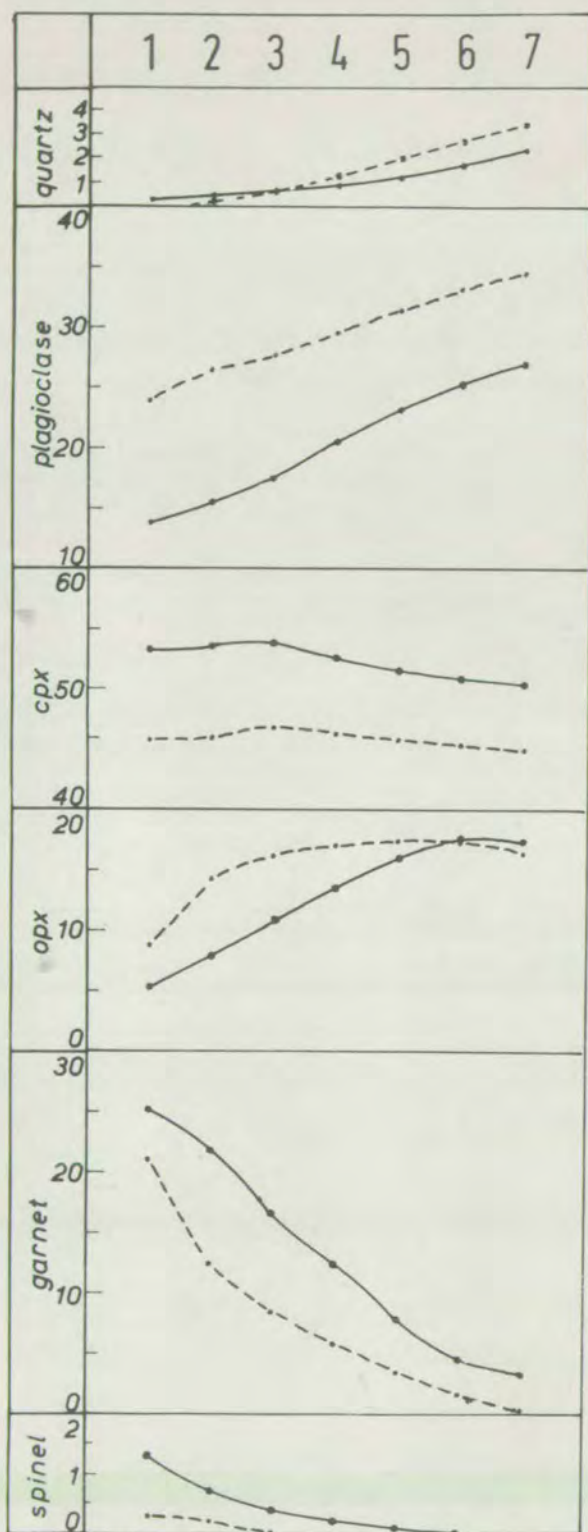


Fig. 4-16.

(above) The proportion of the recalculated analyses of basic gneiss (broken line) and garnetiferous basic gneiss (solid line) which give garnet. (left) Average of the same analyses after recalculation (not the average analyses recalculated)

Stage 1: analyses unmodified (all Fe_2O_3 as FeO)

Stage 2: 50 % available TiO_2 and FeO equiv. to magnetite 50% + ulvöspinel 50 % subtracted from each analysis.

Stage 3: all TiO_2 and equivalent FeO subtracted.

Stages 4 to 7: 1% (mol.) additional FeO subtracted at each stage.

see text for further details.

magnesian than those of the left.

These two reactions would interplay, so that the compositions of the pyroxenes in a basic or garnetiferous basic gneiss will be strongly dependent on its silica content. They will also be dependent on the Fe/Mg and Na/Ca ratios. A small amount of metasomatic change could alter the relative free energies of the basic and garnetiferous basic assemblages so that either becomes the stable state. The reaction in equation (1) would not involve a change in bulk composition so that it would not be detectable in the results of figs. 4-15 and 4-16, while that in equation (2) would. It is for this reason that the recalculations summarised in these figures express only part of the modal differences between the two rock types.

It may be assumed that, as the basic gneiss has more variable compositions than the garnetiferous basic (Tables 2 and 3), that if either type represents original igneous rock, it is the latter, and that the basic gneiss has formed from it by an interchange of material with the acid gneiss sufficient to convert it to basic gneiss. The above argument is also consistent with both rock types being parts of a unified sequence of diffusion zones from ultrabasic to acid gneiss. The existence of chemical potential gradients within and between zones is an essential requirement of such a process.

4.7 Chemical variation across the ultrabasic contacts

Chapter 3 has described the sequence of petrographic types encountered on a traverse from ultrabasic to acid gneiss. To summarise, there are two types of sequence: those in which garnetiferous gneisses are developed; and those in which they are absent. All intermediate types are observed, with varying

degrees of development of basic, garnetiferous basic and contact gneisses.

Two contacts exemplify the extreme types:

<u>Geodh'Eanruig, Lower</u>	<u>Loch an Daimh Mhor</u>
<u>contact (GE 1-5)</u>	<u>contact (UA)</u>
Peridotite	Peridotite
(Hb-sp-pyroxenite?)	Hb-sp-pyroxenite
Px-Hornblendite	Clinopyroxenite
Plagioclase gneiss	Gnt-augite gneiss (ariegite)
Acid gneiss	Garnetiferous basic gneiss
	Basic gneiss
	(Plagioclase gneiss?)
	Acid gneiss

The purpose of this section is to examine the chemical variation associated with the different petrographic types of contact.

The overall chemical homogeneity of the basic, garnetiferous basic, and acid gneisses (Tables 2 and 3, and Holland, 1965) indicates that the majority of chemical variation is to be found at the ultrabasic contacts. In order to make a chemical study of the contact sequences, without a prohibitively large number of analyses, specimens were taken from the ultrabasic to the garnetiferous basic gneiss, where the latter was present in substantial quantities, and from the ultrabasic to the basic or plagioclase gneiss where it was not.

67 rock analyses are presented in Tables 4 to 14 of which 10 are from O'Hara (1961, specimen UA). Of the 57 new analyses, 30 are from Geodh'Eanruig (the main mass and a small peridotite body on Cleit Mhor, GE 22-34). Brief petrographic summaries accompany the chemical data. Fig. 4-17 shows the chemical data in graphical form, cation atomic percent being plotted against

distance for each sequence of specimens. Tables 4a-14a, and fig. 4-18 present the same data, reduced to four components by the method of O'Hara (1968a), but with 'MgO' separated to 'MgO' and 'FeO', and recalculated to proportions of ideal granulite facies minerals (cf. p. 65). Fig. 4-20 shows three of the reduced components plotted on "A-C-F" diagrams. Fig. 4-19 shows cation atomic percent plotted against the Fe/Fe + Mg ratio. In some cases, the diagrams have been extended, using average values for other petrographic types which were not analysed.

The two garnet-free sequences analysed show different types of variation. In the Geodh'Eanruig lower contact, GE 1-5, the zone of pyroxene-hornblendite passes into plagioclase gneiss with a simple discontinuity in all the constituents. In the Cleit Mhor contact, GE 22-34, there is a very nearly linear variation in all the constituents from ultrabasic to basic gneiss, after which we may presume a discontinuity to the acid gneiss. In GE 25, garnet appears as an idealised mineral, in place of modal hornblende.

In the Loch an Daimh Mhor contact, UA, the variation is complex. In rocks of steadily ^{increasing} Fe/Fe + Mg ratio, there is first a culmination in the Ca content, then a depression. Following the Ca culmination, there is a culmination, first in Al, then in Fe, with a concomitant depression in Si. These changes are reflected in the ideal minerals by zones rich in hypersthene, augite, garnet, and spinel (modal magnetite).

The features of the Loch an Daimh Mhor contact are duplicated by the Geodh'Eanruig upper contact, Z 718-Z 726, but to a slighter extent, the culminations and depressions are replaced by more gentle rises and falls in the curves. The

same is true of the other garnetiferous sequences, which approximate more and more closely to a pattern of linear variation from ultrabasic to garnetiferous basic gneiss. The only exception to this is the Geodh'Eanruig inland contact, 10719-10722, which shows an extreme iron culmination, a feature it shares with Loch an Daimh Mhor.

The features described above are well seen in the "A-C-F" plots of fig. 4-20. The trend for the Loch an Daimh Mhor contact shows calcium enrichment, before bending back to the 'A'-'F' side of the triangle, after which it passes to the field of garnetiferous basic gneiss. This same sigmoidal trend is shown by the Geodh'Eanruig upper contact, Z 718-726, and by the Maldie Burn contact, B 204-211. It may be inferred in the Geodh'Eanruig inland contact, 10719-10722, and in B 226-230 from Ben Strone, and to a lesser extent in the Pairc a'Cladaich contact, Z 701-706. The other sequences show a linear trend in these plots.

The analysed sequences in which chemical enrichments and depletions, and sigmoidal trends in triangular plots, occur, all come from localities where a considerable thickness of garnetiferous basic gneiss intervenes between the ultrabasic and acid gneisses. Those in which there is little basic or garnetiferous basic gneiss show more nearly linear trends, and at the Geodh'Eanruig lower contact there is no rock of basic composition at all and there is a major chemical discontinuity.

To summarise, the two petrographic types of contact sequence are also distinct chemically. The occurrence of all intermediate types of contact is also substantiated chemically, and it appears that the development of garnet- and augite-rich contact gneisses is associated with a considerable thickness of

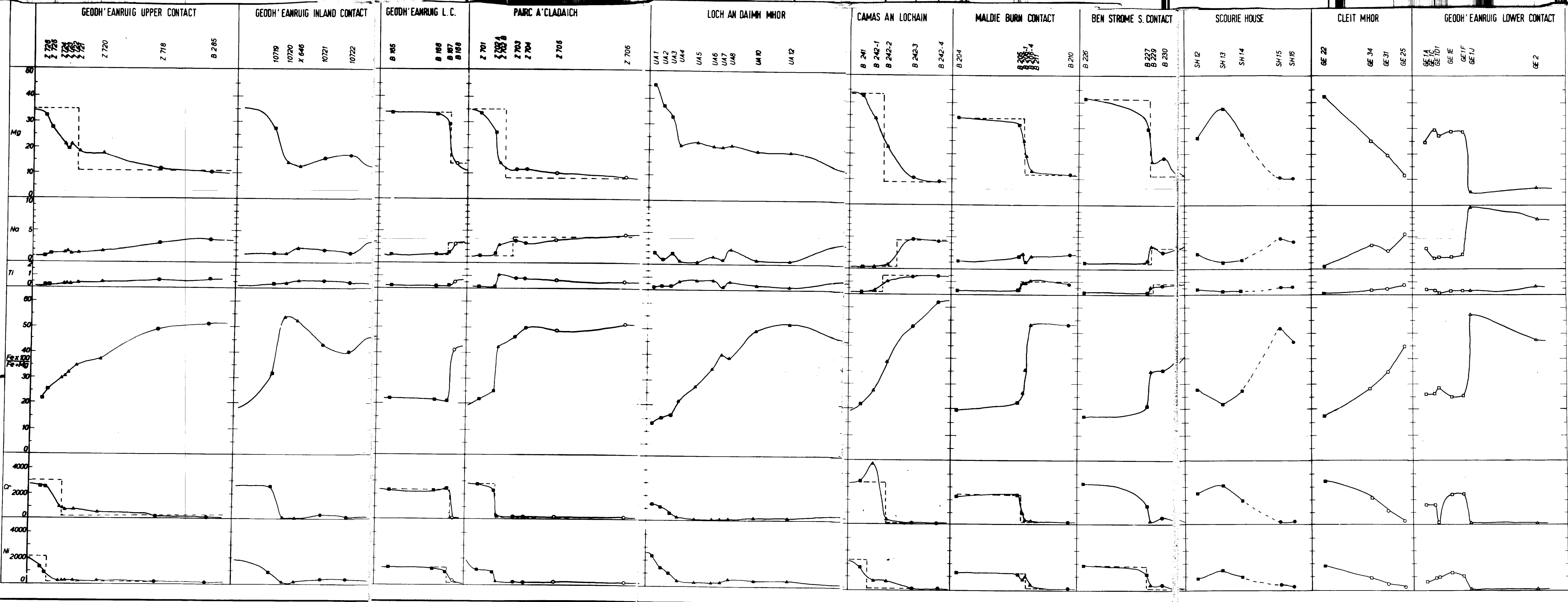
Fig. 4-17

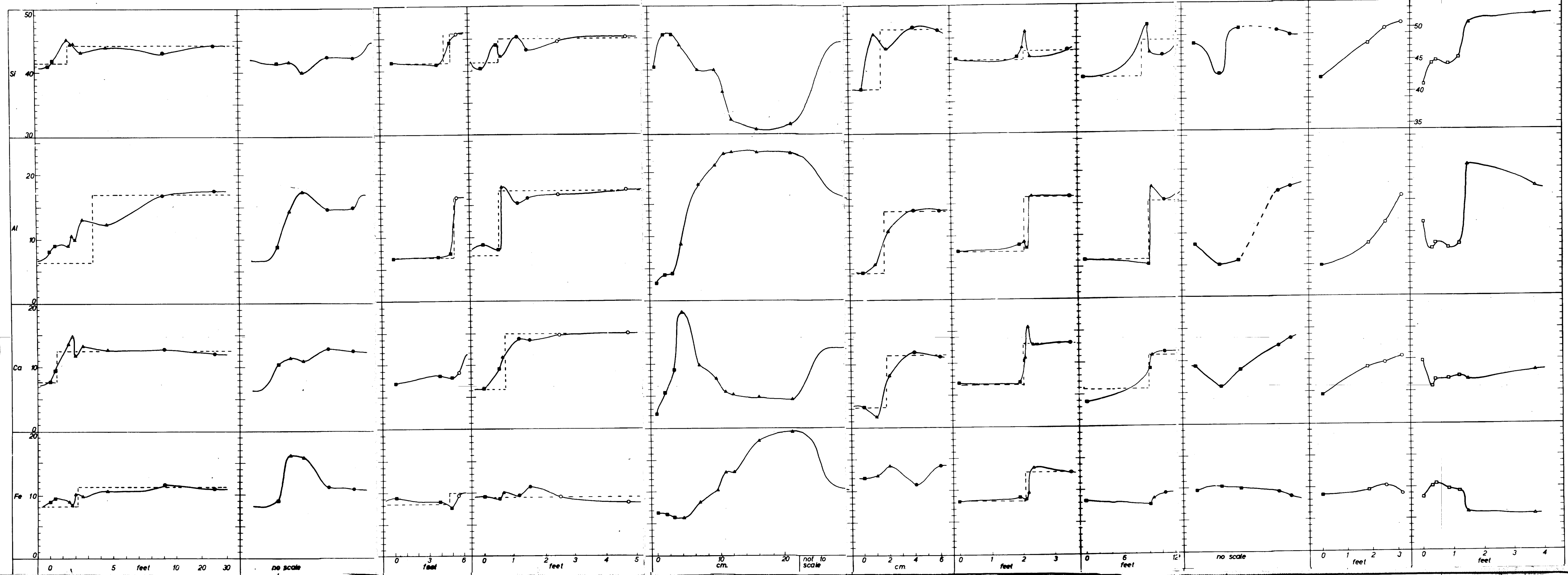
Chemical variation across ultrabasic contacts

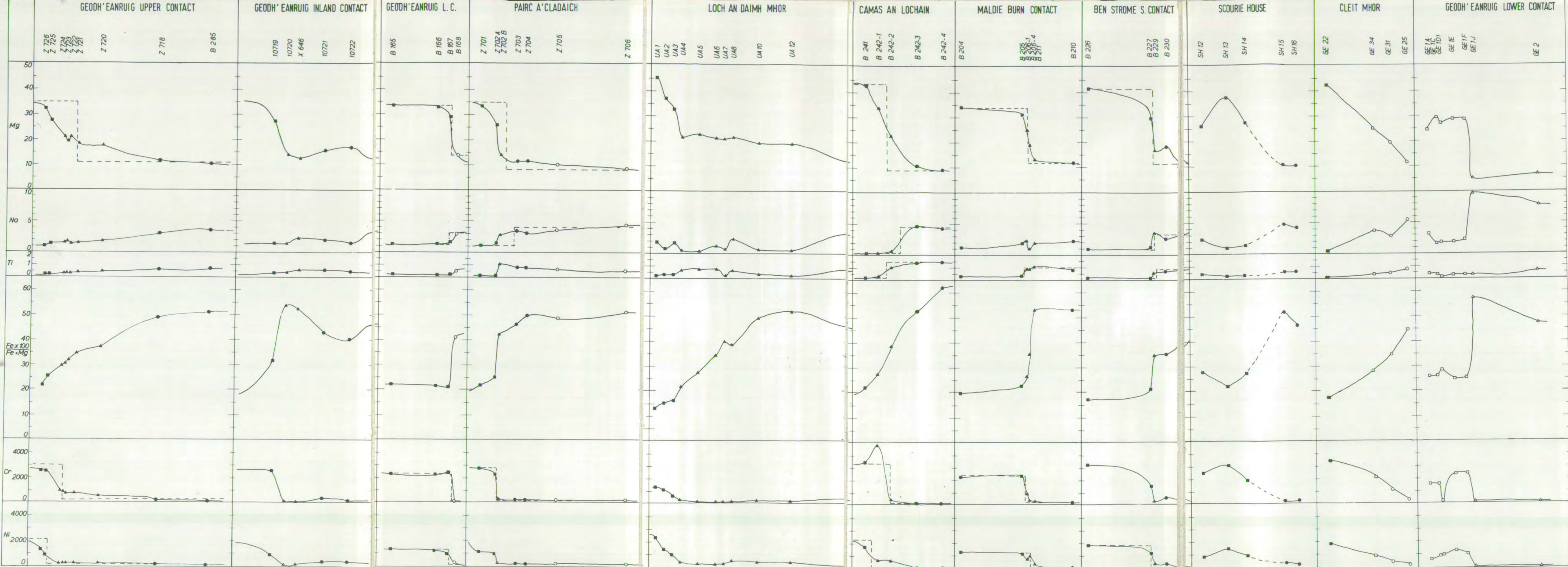
The analyses of Tables 4 to 14 are shown graphically, with cation atomic percent, and trace element contents in p.p.m., plotted against distance, except for those contacts where the samples are not on a single traverse, and no scale is given.

Symbols:

- - ultrabasic gneiss
- - pyroxene-hornblendite
- ▲ - contact gneiss
- - garnetiferous basic gneiss
- - basic gneiss
- △ - plagioclase gneiss







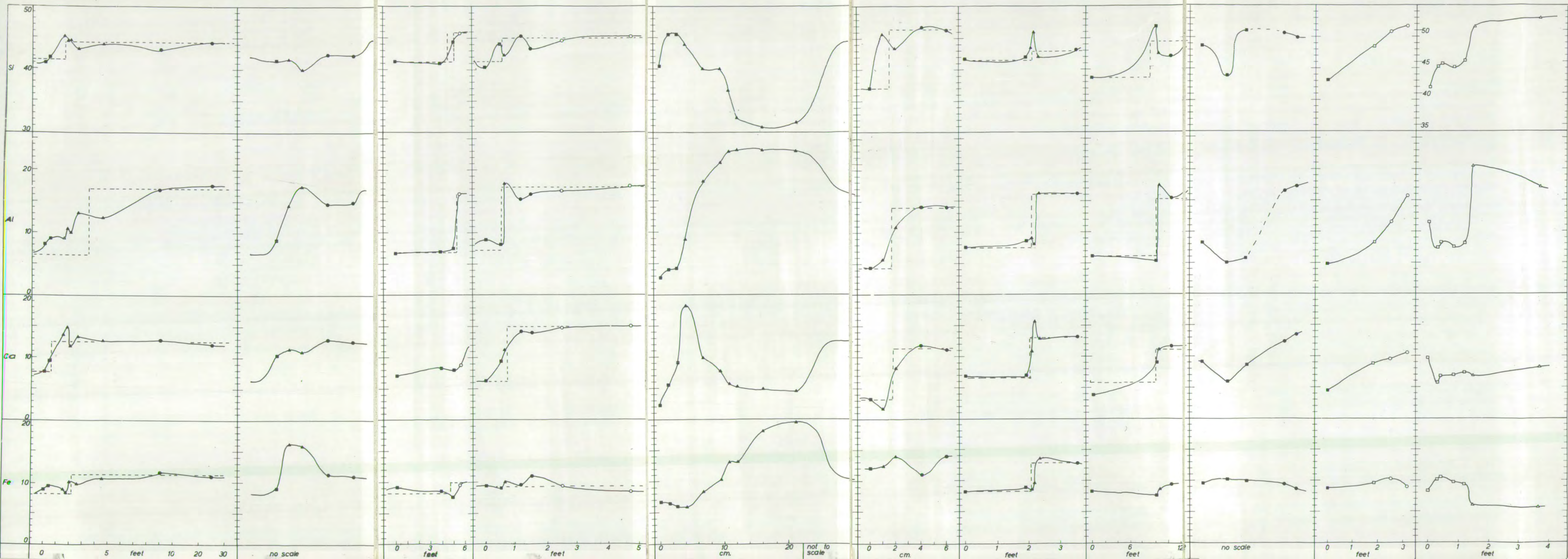
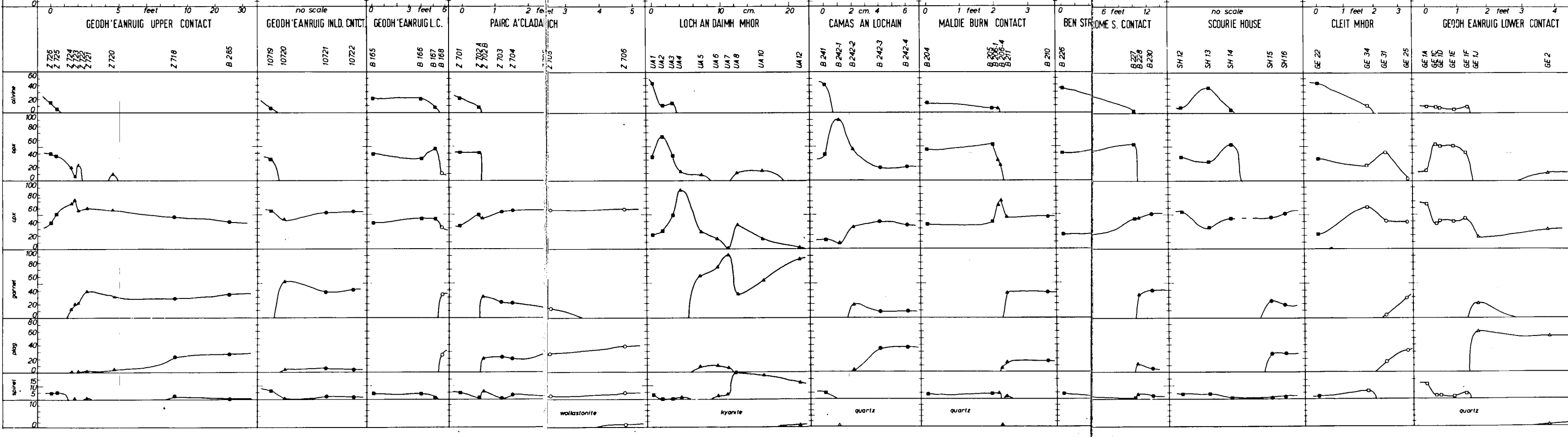
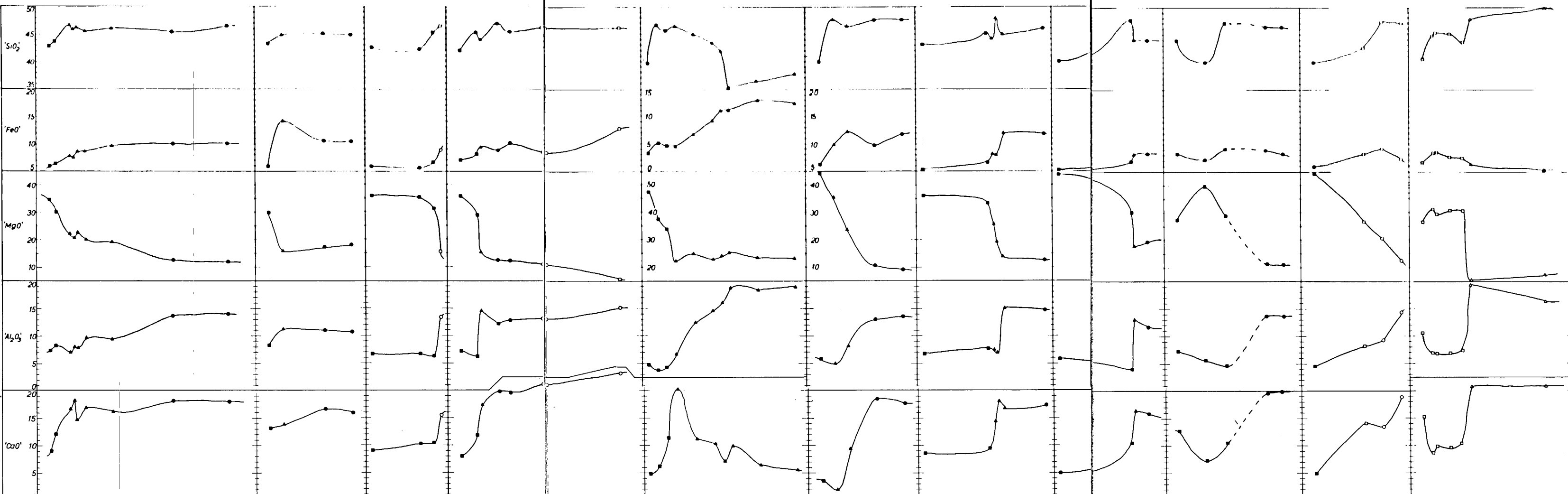


Fig. 4-18

Chemical variation across ultrabasic contacts

The analyses of Tables 4a to 14a (chemical analyses reduced to four components and recalculated to ideal granulite facies minerals) plotted against distance, as in fig. 4-17).

Symbols as in fig. 4-17.



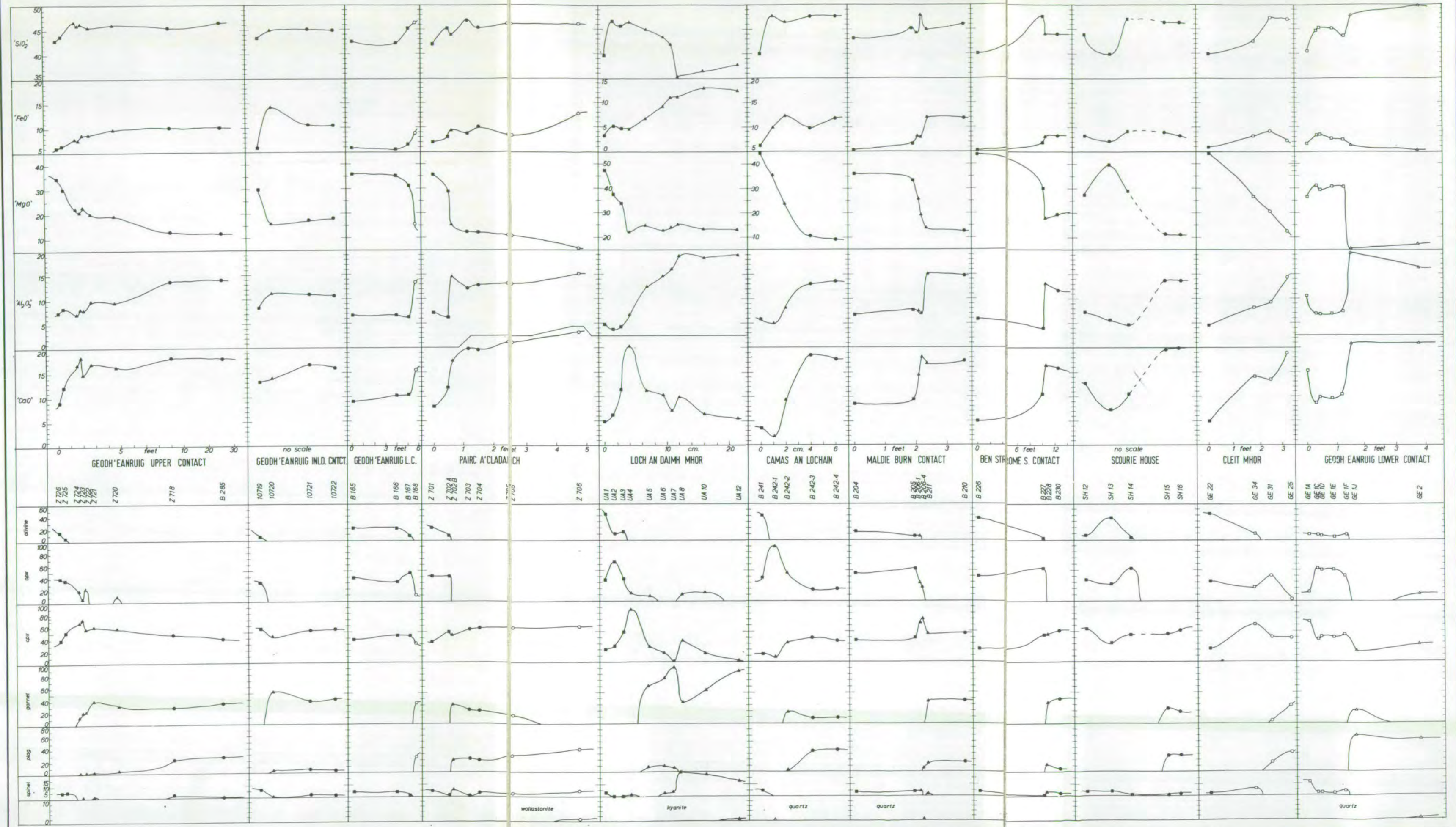
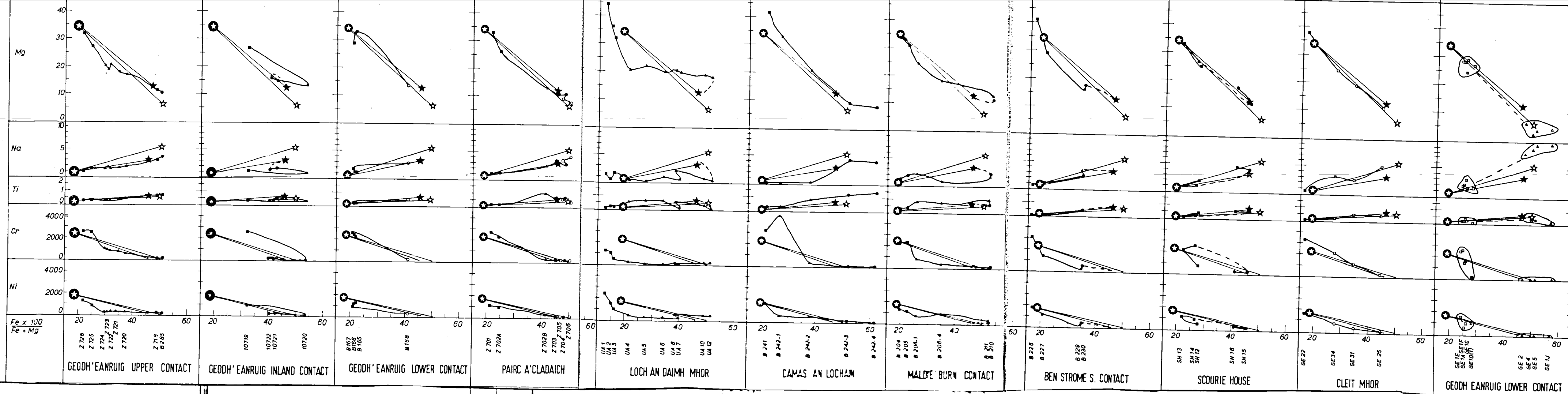


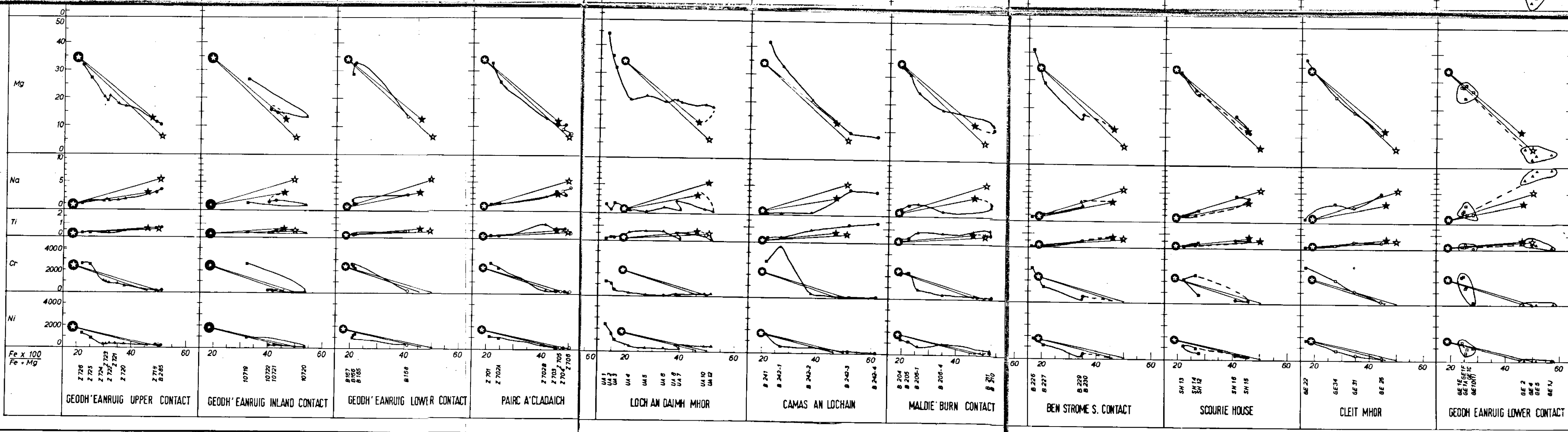
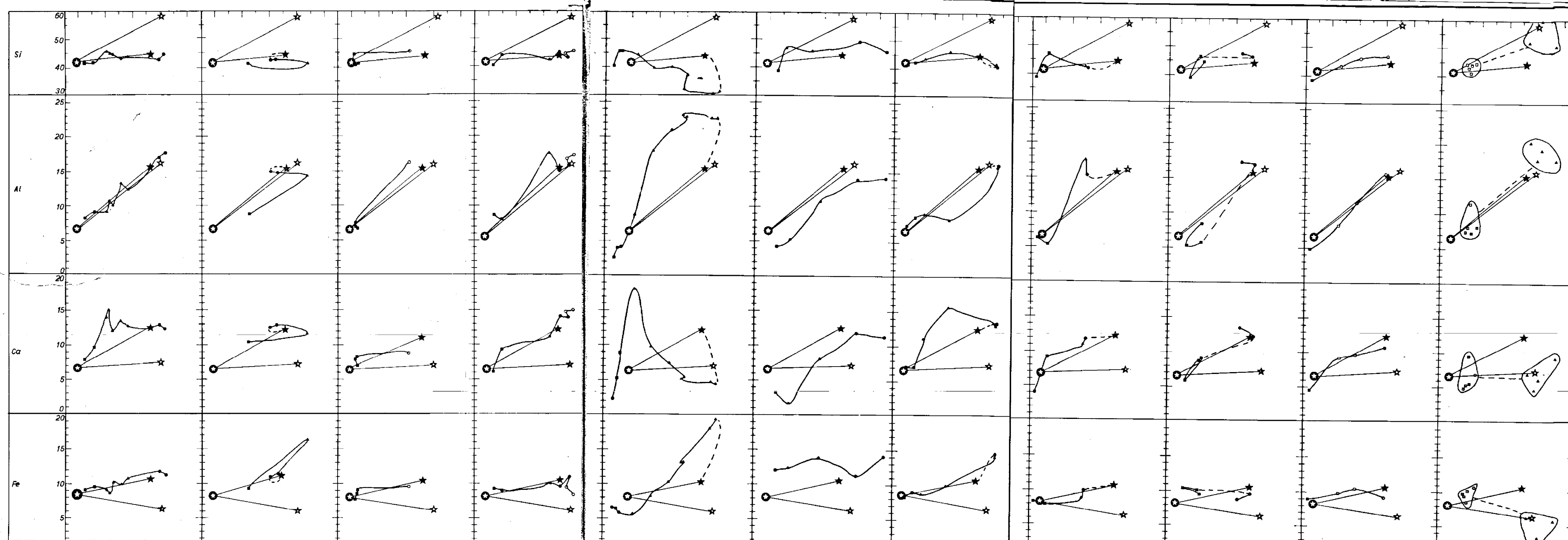
Fig. 4-19

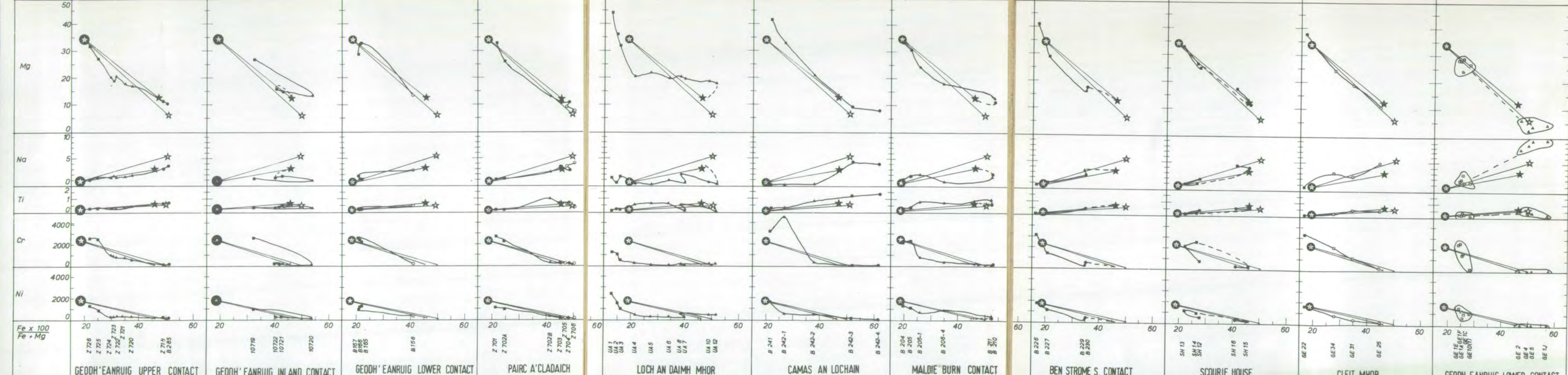
Chemical variation across ultrabasic contacts

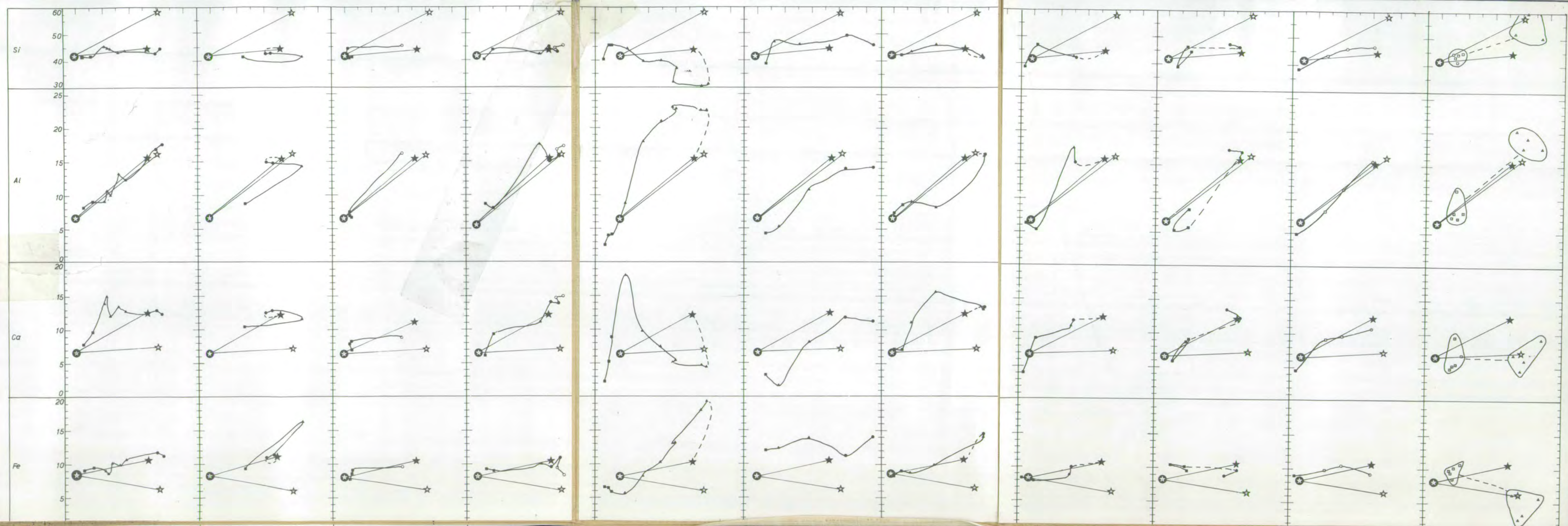
The analyses of Tables 4 to 14, shown in fig. 4-17, are plotted against the $\text{Fe}/(\text{Fe} + \text{Mg})$ ratio (total Fe).

Symbols as in fig. 4-17.









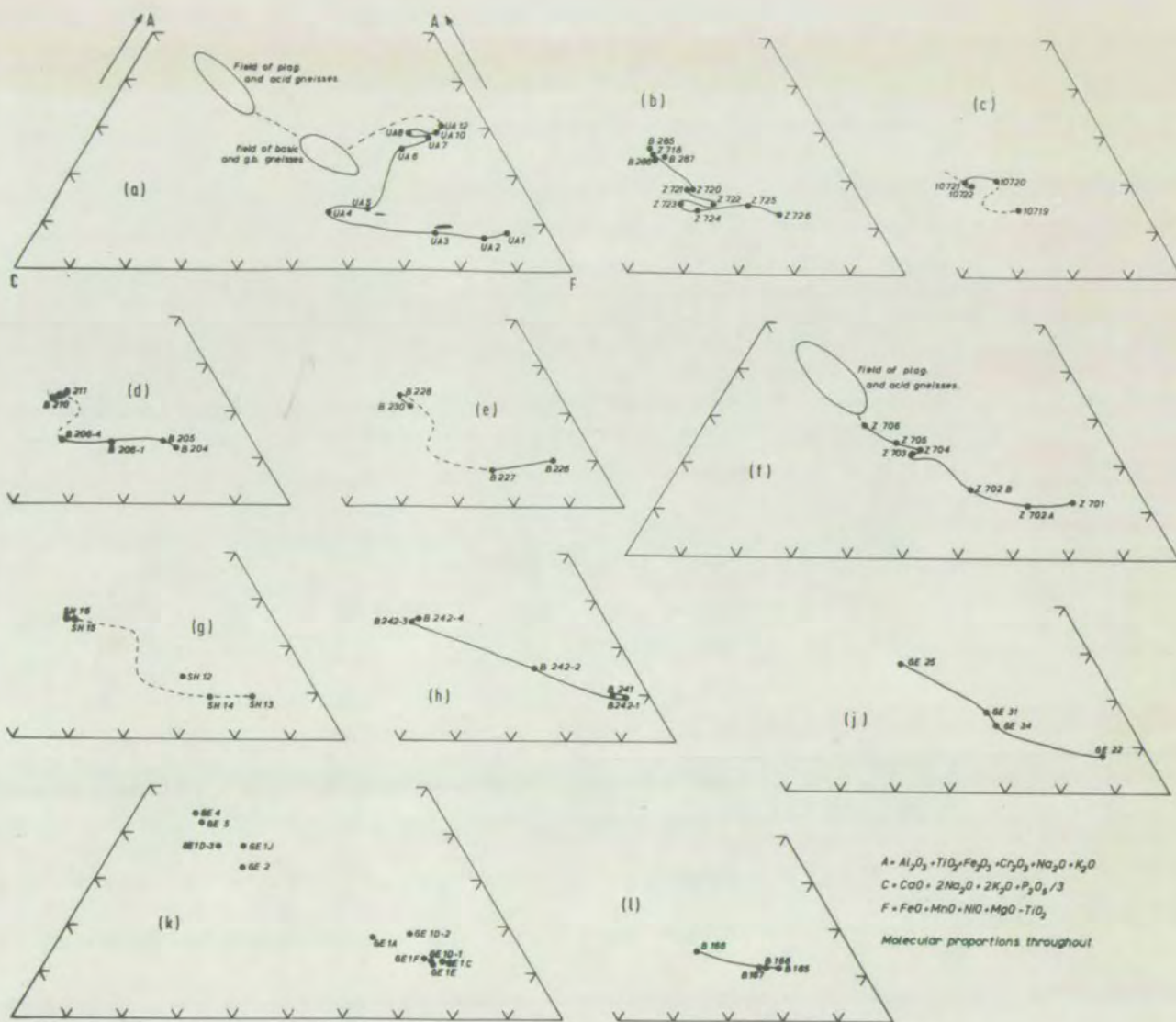


Fig 4-20. A-C-F plots of the chemical variation across ultrabasic contacts

- a - Loch an Dairh Mhor
- b - Beadh'Eanruig - upper contact
- c - " " - inland
- d - Mairdie Burn
- e - South side of Ben Strame
- f - Pairc a'Cladaich
- g - Scourie House
- h - Camas an Lochain
- j - Cleit Mhor
- k,l - Beadh'Eanruig - lower contact

basic rock between the ultrabasic and acid gneisses. Change in type with a change in thickness is not a character of a single series of diffusion zones (below, pp.79 -81).

4.8 Mineral Chemistry of the Contact Gneisses

10 augites were separated from specimens Z 718 to Z 726, from the upper contact at Geodh'Eanruig, and analysed chemically. Analyses were also made of a magnesian garnet and augite from a layer of garnet-augite gneiss in the ultrabasic mass of Meallan na Corra (B 521). Specimens Z 721 to Z 724 from Geodh'Eanruig, and parts of specimen UA from Loch an Daimh Mhor were examined by means of an electron probe micro-analyser, to obtain mineral compositions. Compositions of some garnets from Geodh'Eanruig were estimated from refractive index measurements and X-ray diffraction determinations of unit cell dimensions.

Results for the two localities are discussed separately.

Geodh'Eanruig

Table 19 gives analyses of the augites, and Table 22 gives optical and X-ray data for the garnets. Electron probe analyses are not tabulated, but the results are presented in the following diagrams. Fig. 4-21 shows the variation in some important compositional parameters for the rocks and minerals, and Table 4-4 gives the same parameters for the minerals of the contact gneisses Z 721 to Z 724.

Fig. 4-22 shows a Ca-Mg-Fe projection of mineral equilibria in rocks from Geodh'Eanruig, with the garnet and augite of B 521, and the mineral pairs analysed by O'Hara (1961). Fig. 4-23 shows a similar projection, and fig. 4-24 an Al-Mg-Fe projection for the contact gneisses. The garnet A, of Z 721, is surrounded by a reaction rim (above, p. 39), composed of a much more almandine

TABLE 4-4

Fe/Fe+Mg ratios of minerals in contact gneisses, Upper Contact,
Geodh'Eanruig.

	Z 721	Z 722	Z 723	Z 724
Rock (chemical analysis)	34.8	32.1	30.6	29.8
cpx (chemical)	28.2	25.5	25.2	24.9
cpx (electron probe)	26.5	25.6	24.3	23.4
opx outside garnet rim	36.0	32.8	33.6	31.9
opx in garnet rim (or pseudomorph)	26.8	33.5	-	32.4
spinel in garnet rim	54.7	65.6	-	63.5
garnet in garnet rim	58.9	53*	54*	52*
garnet (unaltered cores in Z 721)	45*			
0.8opx + 0.2spinel (i.e. equivalent to garnet)	32.4	39.9	-	38.4

All determinations by electron probe unless stated.

* optical estimate of garnet composition

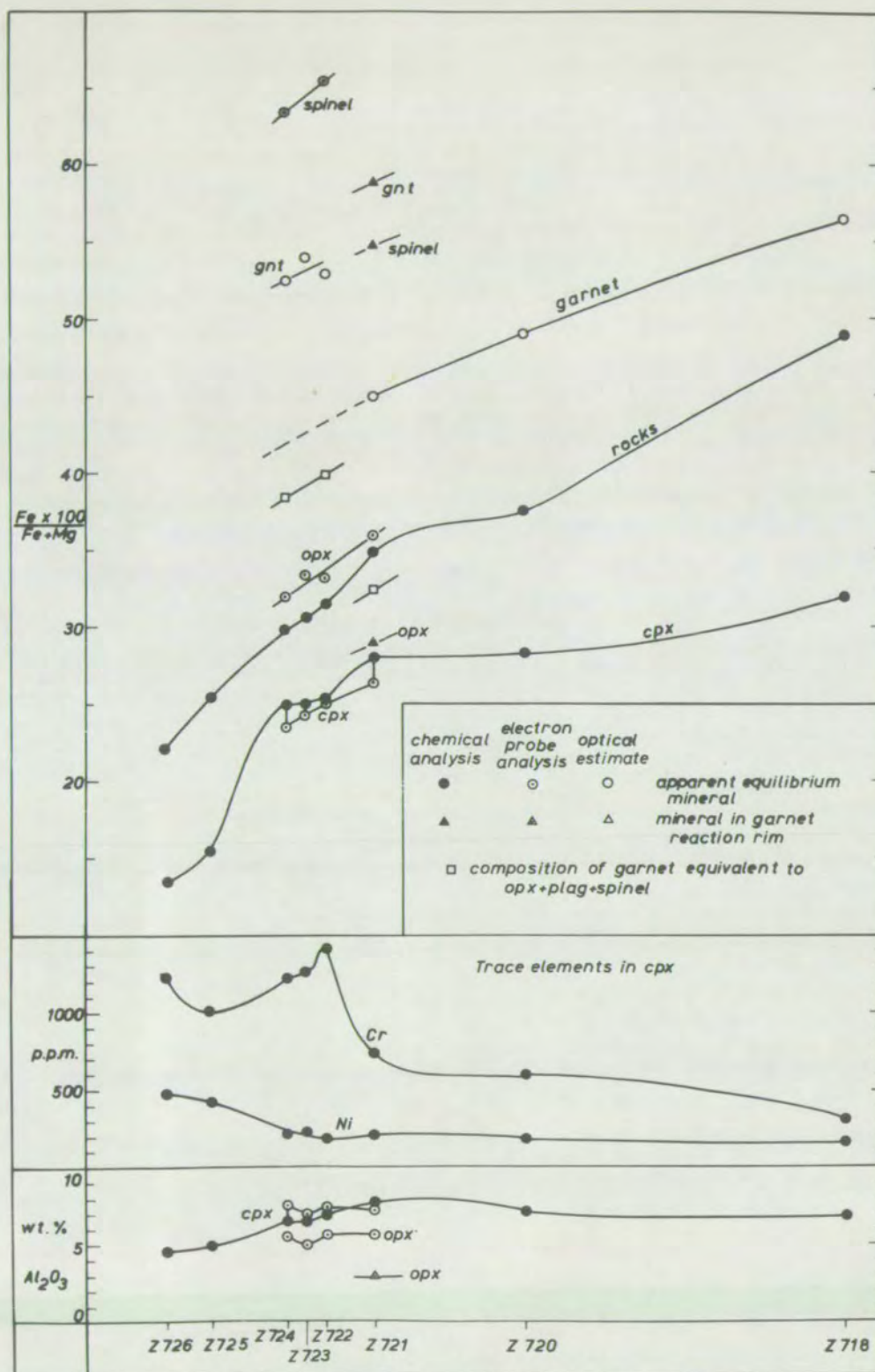


Fig.4-21.
Chemical variation in
minerals, upper
contact, Geodh'Eanruig.

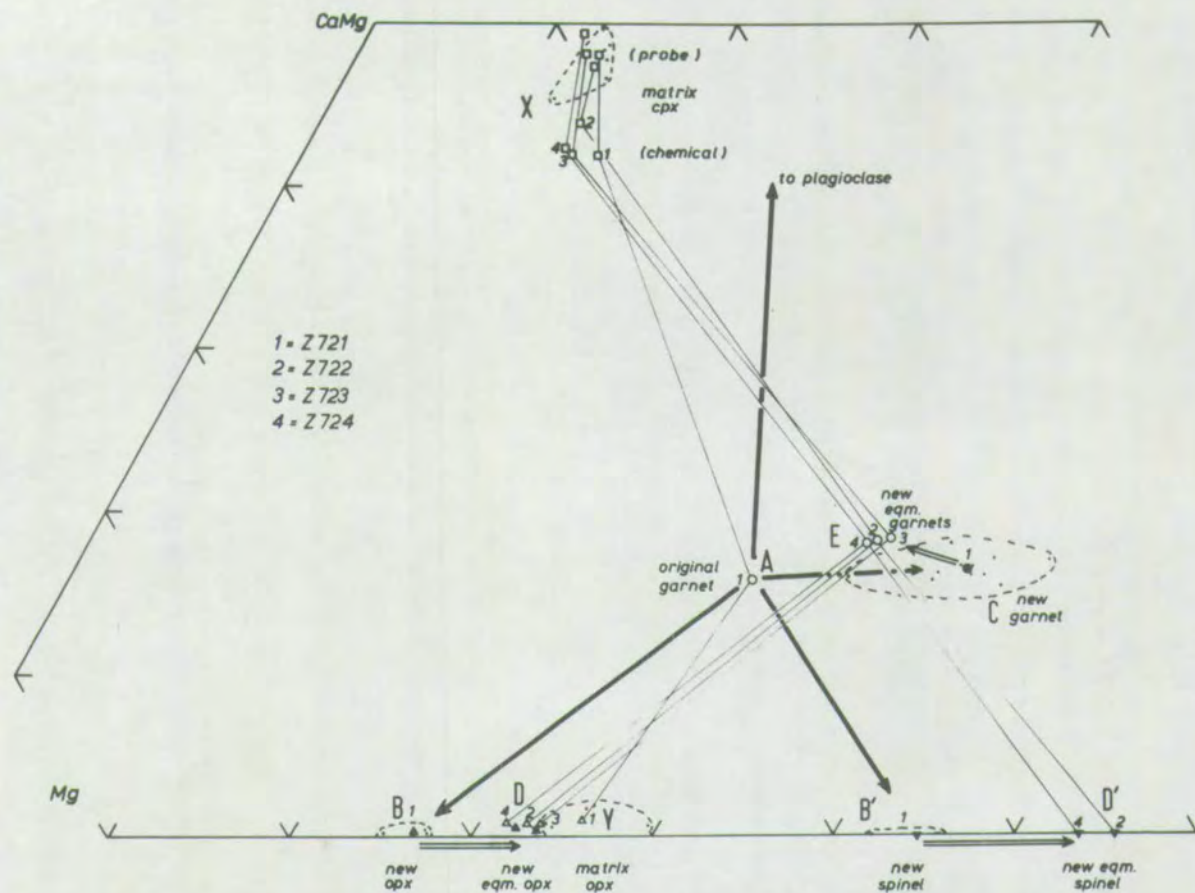


Fig. 4-23. Ca-Mg-Fe plot for minerals of contact gneisses, Geodh'Eanruig.

- (dotted circle) compositions of individual crystals in Z 721 (average of from 2 to 9 electron probe determinations)
 □ Δ - - composition of mineral in the clinopyroxenite matrix of garnet-augite gneiss (chemical analysis or average of electron probe determinations)
 - ▲ ● ▼ composition of mineral in garnet reaction rim (Z 721) or garnet pseudomorph (Z 722-4)
 ○ optical estimate of garnet composition
- reaction observed in Z 721
 = = = = = → reaction inferred in Z 722-4, assuming they have passed through a stage similar to that seen in Z 721

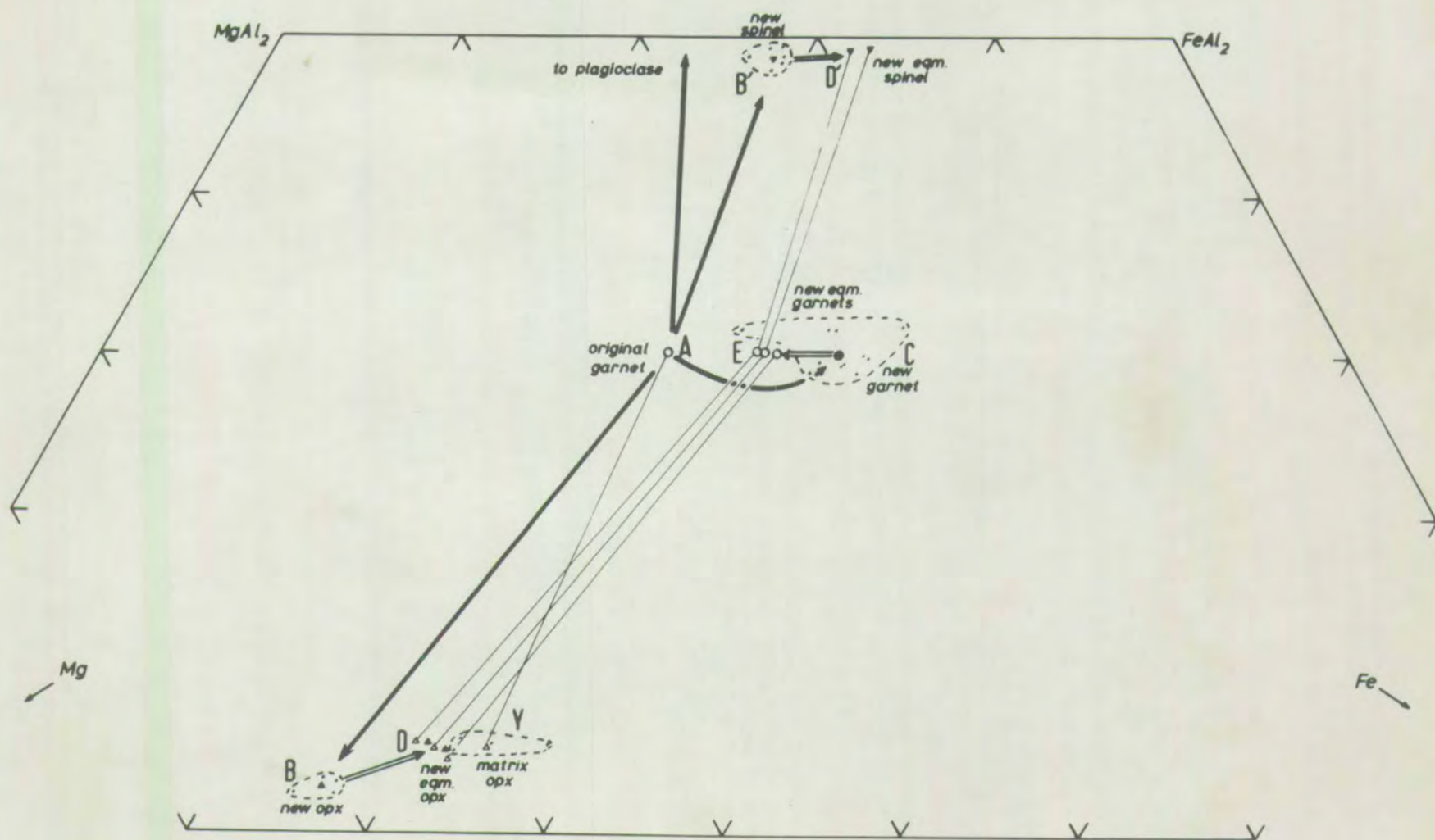


Fig. 4-24. Al-Mg-Fe plot for minerals of contact gneisses, Geodh'Eanruig. (Legend as in fig. 4-23)

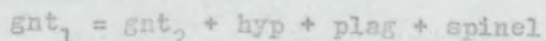
rich garnet C, a magnesian hypersthene B, and spinel B'. The hypersthene B is much more magnesian than the augite X and the hypersthene Y of the granoblastic matrix in which the garnets are set.

In specimens Z 722 to 724 the texture of the garnet pseudomorphs is not vermiform in the way that it is in Z 721; they are very fine grained but granoblastic in texture. The grain boundary angles, as far as they can be determined in so fine an aggregate, are indicative of the attainment of equilibrium (R.H. Vernon, personal communication). The hypersthene D is of very similar composition to the hypersthene Y of the matrix and the spinel D' and garnet E are respectively more and less magnesian than B' and C'. (The differences referred to are so gross that the differences in Fe/Fe + Mg ratio between Z 721 and Z 724 are slight in comparison.)

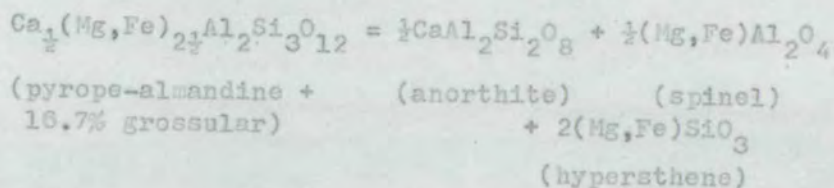
Discussion

It is apparent from fig. 4-21 that there is a smooth and continuous variation in the augite composition from ultrabasic to garnetiferous basic gneiss. We may suppose that the concentrations of Al, Cr, Ni, and the Fe/Fe + Mg ratio in this phase reflect the activities of these elements, and thus conclude that there is a smooth and continuous variation in these activities, which is maintained through the pyroxenite matrix of the contact gneisses. The coherence of the Fe-Mg distribution between augite and hypersthene (Figs. 4-22 and 4-23) emphasises that local equilibrium obtains (the exception of X 646, in ^{which} the pyroxene tie-line is distinctly skew, may be attributable to the presence of plagioclase and iron ore lamellae in the augite (O'Hara, 1961), relics of an earlier equilibrium). The anomalous mineral compositions of Z 721 clearly represent disequilibrium on the grain size scale.

This disequilibrium is due to the breakdown of garnet at a relatively late stage in the formation of the rocks. The reaction in the contact gneisses is:



In the system $\text{CaO}-(\text{MgO} + \text{FeO})-\text{Al}_2\text{O}_3-\text{SiO}_2$ the garnet of these rocks is almost co-planar with hypersthene, spinel, and plagioclase, as can be seen from the reaction:



The assemblage hypersthene-plagioclase-spinel (in the correct proportions) can be envisaged as a second 'polymorph' of garnet, an analogy which may clarify the following discussion.

As a consequence of the chemical equivalence of garnet and hypersthene-plagioclase-spinel (subsequently referred to as hyp-plag-sp) assemblages, the reaction by which garnet breaks down to this assemblage needs to involve only a change in Fe-Mg distribution. It is simple to calculate from the hypersthene and spinel compositions the Fe/Fe + Mg ratio of the garnet which is equivalent to a particular hyp-plag-sp assemblage ($(\text{Fe/Fe} + \text{Mg})_{\text{gnt}} = 0.8(\text{Fe/Fe} + \text{Mg})_{\text{hyp}} + 0.2(\text{Fe/Fe} + \text{Mg})_{\text{sp}}$).

Assuming that the large garnet cores of Z 721 preserve their original compositions, they have broken down into an intimate intergrowth of a garnet much richer in iron, and a hyp-plag-sp assemblage much more magnesian than themselves. In Z 722 to Z 724 the texture, and the similarity in composition of the hypersthene inside and outside the garnet pseudomorphs suggest that local equilibrium on the grain size scale has been re-established, following

such a breakdown. The contrast between the magnesian hyp-plag-sp assemblage and the iron rich garnet is still present, but is not so marked as in Z 721.

Fig. 4-28a. shows a hypothetical free energy-composition diagram (see Appendix F) for the system $\text{Ca}_2(\text{Mg,Fe})_{2\frac{1}{2}}\text{Si}_3\text{O}_{12}$. Two free energy curves are shown, for garnet and for a hyp-plag-sp assemblage equivalent to garnet. Garnet A is unstable, and the stable state for its composition is now garnet E + hyp-plag-sp D. Insofar as the minerals of Z 721 to Z 724 are similar in composition, it is possible to say that garnet A has broken down to garnet C + hyp-plag-sp B, and that these have subsequently equilibrated to D and E. The first step releases most free energy, the second less.

The reason for this two-stage process may be kinetic rather than thermodynamic, so that the free energy production consequent on the change is most rapid in the first stage, where the free energy gain is large. The chemical potentials will arrange themselves so that the material transfer necessary to effect the transformation is the most rapid possible. For the Mg component the chemical potentials in the states A, B, C and D + E respectively are $\mu_1 > \mu_2 > \mu_4 > \mu_3$, and for the Fe end member they are $\mu'_3 > \mu'_4 > \mu'_1 > \mu'_2$ (fig. 4-28a.). As far as it is possible to say that the states A, B and C form concentric zones in a single 'garnet', and as far as it is possible to say that Mg and Fe will diffuse in response to differences in the chemical potentials of $\text{Ca}_2\text{Mg}_{2\frac{1}{2}}\text{Al}_2\text{Si}_3\text{O}_{12}$ and $\text{Ca}_2\text{Fe}_{2\frac{1}{2}}\text{Al}_2\text{Si}_3\text{O}_{12}$, the process can be illustrated as in fig. 4-28b.

The outer edge of garnet C is being depleted in Fe and enriched in Mg, as it is made over to hyp-plag-sp B, while the outer edge of garnet A is being enriched in Fe and depleted in Mg as it is being made over to the more iron

rich garnet C. In this way, the compositions of the phases, and the diffusion of material adjust themselves to give the most effective transformation and the maximum rate of free energy production. A similar explanation could perhaps be devised to account for the alumina content of the hypersthene B, which is much lower than that of the hypersthene in equilibrium with garnet, such as D.

Loch an Daibh Mhor

Variation in mineral composition through 10 cm. of specimen UA is shown in fig. 4-25, and Ca-Mg-Fe and Al-Mg-Fe plots of the same minerals in figs. 4-26 and 4-27. The unusual features of this contact are a zone of nearly pure garnet, outside the clinopyroxenite zone, which passes out through ariegite (O'Hara, 1961) to garnetiferous basic gneiss.

Furthermore, the pyroxenes of the garnet rich zones are more magnesian than those of either the ultrabasic or garnetiferous basic gneisses. The electron probe analyses of fig. 4-25 substantiate the observation of O'Hara (1961), that there is a steady increase of the $Fe/(Fe + Mg)$ ratio of the hypersthene from the peridotite up to the incoming of garnet, where there is a sudden drop, followed by a further steady increase. The augite shows a similar variation, but it is very significant that in a small isolated patch of clinopyroxenite at 6 cm. (fig. 4-25) the augite is as rich in iron as that of the ultrabasic part of the specimen.

Discussion

In the light of the observations at Geodh'Eanraig, the unusual features just described can be simply explained. The hypersthene, plagioclase, and spinel of the garnet rich zone may have been formed from a magnesian garnet which subsequently became unstable. So that the present garnet corresponds to C or E, the hypersthene to B or D, and the spinel to B' or D' (figs. 4-22

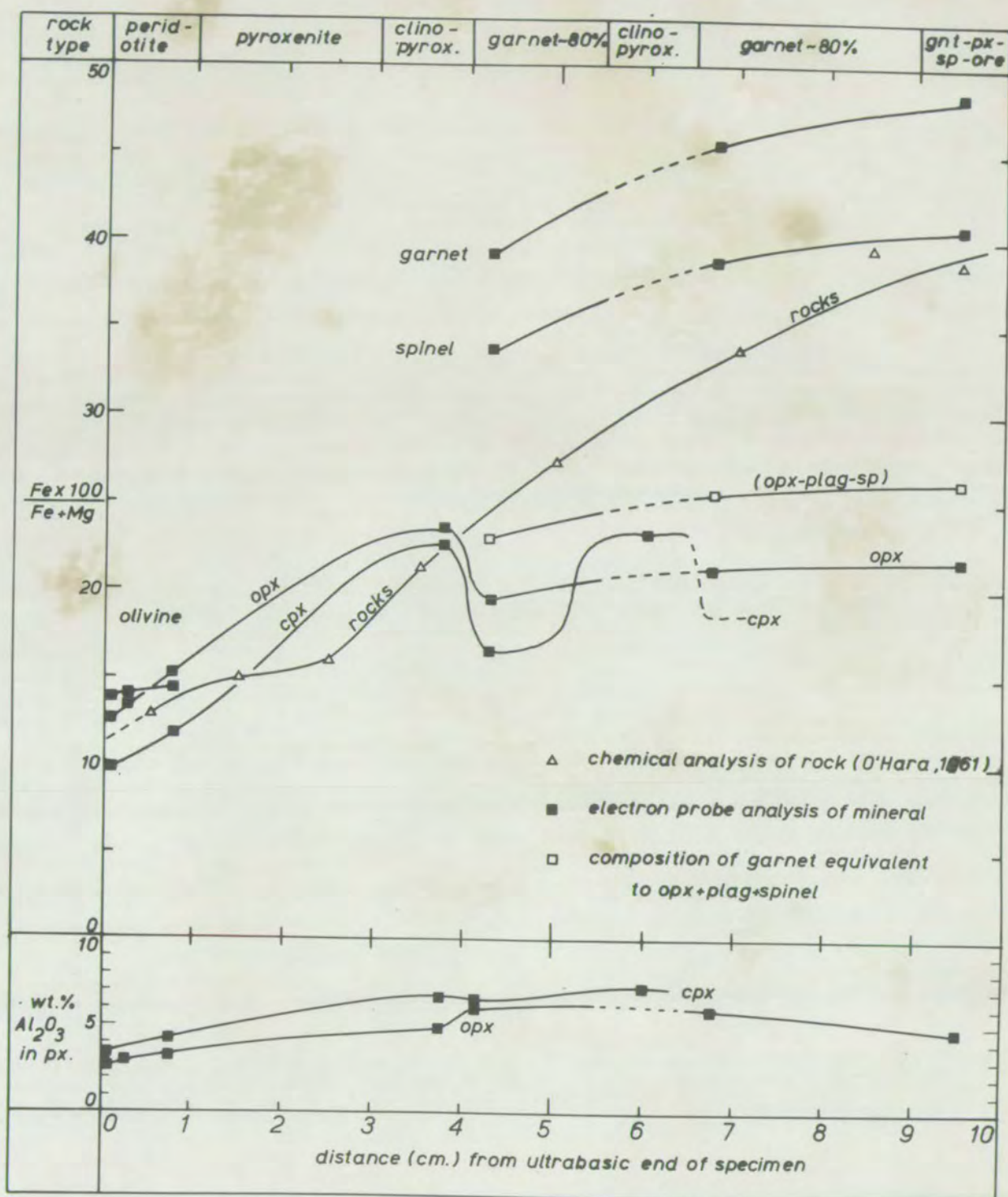


Fig. 4 - 25. Variation in mineral composition through 10 cm. of specimen UA (Loch an Daimh Mhor contact)

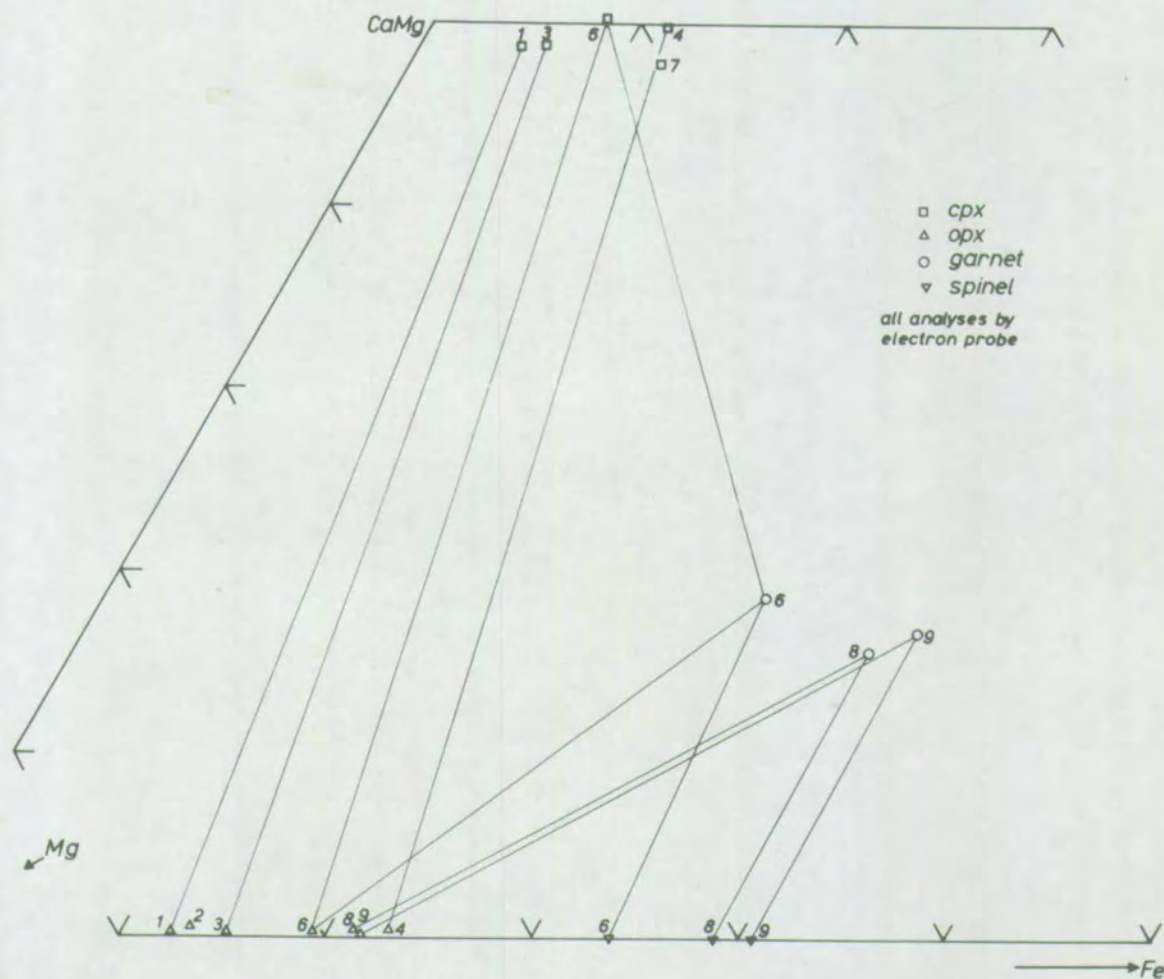


Fig. 4-26. Ca-Mg-Fe plot of mineral compositions from the Loch an Daimh Mhor contact.

Numbers refer to position in specimen UA :

No. Distance from ultrabasic end of specimen (cm.)

1	0
2	0.25
3	0.75
4	3.75
6	4.25
7	6.0
8	6.75
9	9.5

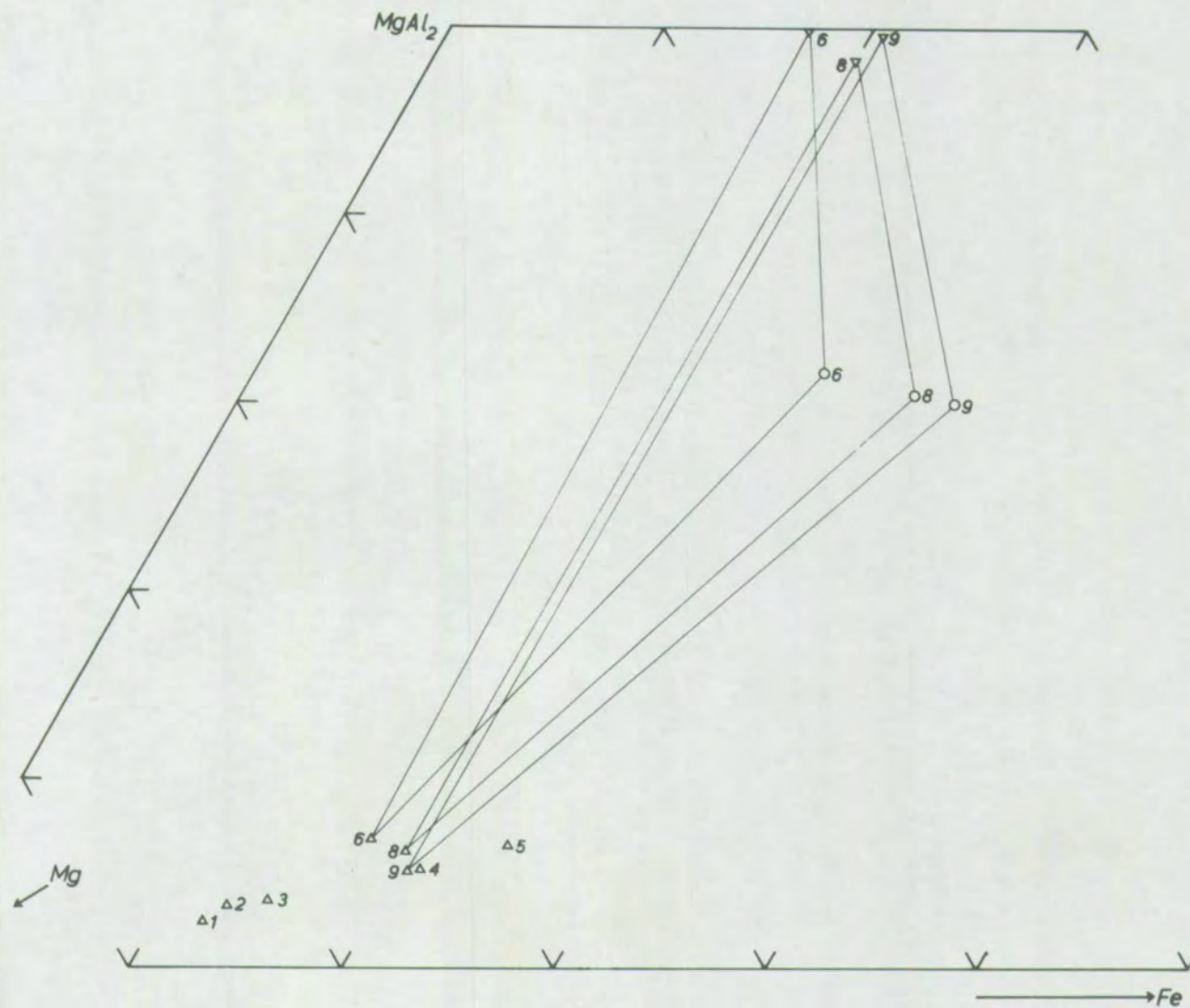


Fig. 4-27. Al-Mg-Fe plot for the minerals of the Loch an Daimh Mhor contact.

Legend as in fig. 4-26

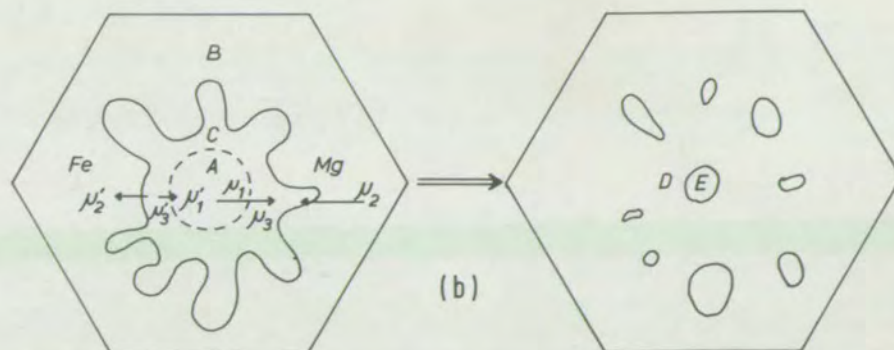
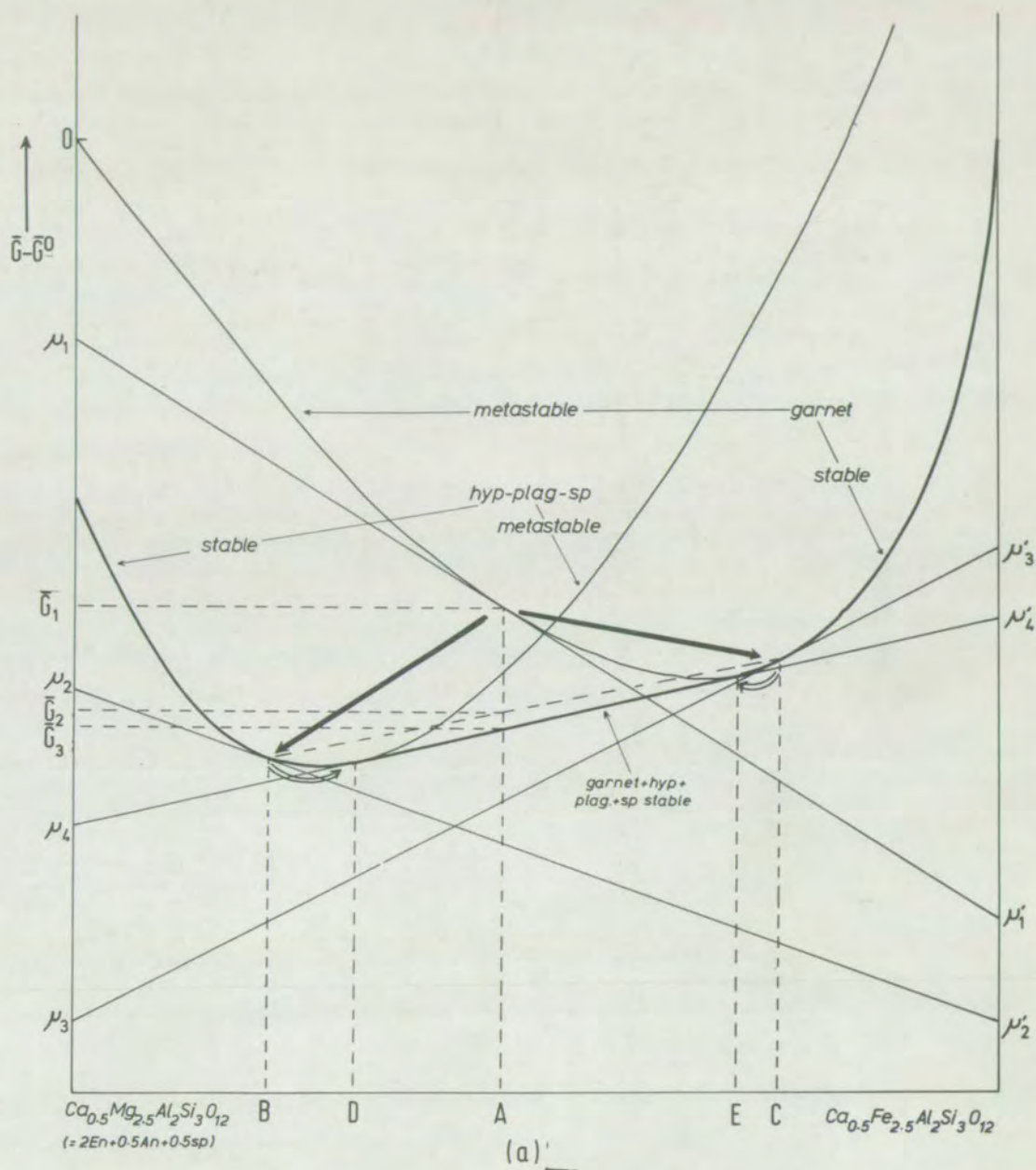
to 4-24). The small proportion of augite in the garnet rich zone has been made over to a composition as magnesian as the coexisting hypersthene, while the cluster of augite grains at 6 cm. has remained iron rich. The range of diffusion at this stage has thus been 1-2 mm.

Whether the garnet, hypersthene, spinel, and plagioclase of the garnet rich part of specimens UA represent states B and C, or D and E of fig. 4-28, it is clear that they are substantially more magnesian than the corresponding minerals at Geodh'Eanruig. Under isofacial conditions the compositions of D and E should be invariant, as is apparent from fig. 4-28, and from the phase rule (5 components: CaO , Al_2O_3 , MgO , FeO , and SiO_2 , and 5 phases. The variance = 2, i.e. P&T). Variance could be allowed by the presence of components not considered above. The plagioclase composition might vary (as far as the sodium content of the original garnet permits), and the oxidation state of the iron and the Cr content might vary. None of these would have been detected, as the plagioclase is too altered to determine its composition, and the oxidation state of iron cannot be determined by the electron probe. In these cases, Fe_2O_3 , Cr, or Na_2O would be components.

If the compositions D and E are effectively invariant the Fe-Mg distribution between garnet, hyp-plag-sp equivalent to garnet, and augite will be as shown in fig. 4-29a, and if substantial variance is possible in their compositions, it will be as in fig. 4-29b. In each case, a garnet-augite equilibrium (1) is rendered unstable by a change in physical conditions, and is replaced by a garnet-augite equilibrium (2), and an equilibrium between augite and hyp-plag-sp equivalent to garnet (3). In the first case, different values of the invariant compositions D and E are produced by differences in the new physical conditions,

Fig. 4-28

- (a) Hypothetical free energy-composition diagram for the system $\text{Ca}_2(\text{Mg,Fe})_{2\frac{1}{2}}\text{Al}_2\text{Si}_3\text{O}_{12}$. (Standard state - garnet at T and P). Garnet A, with molar free energy \bar{G}_1 changes first to (hyp-plag-sp) B, and garnet C, with molar free energy \bar{G}_2 , then to the stable assemblage (hyp-plag-sp)D and garnet E, with molar free energy \bar{G}_3 .
- (b) Illustration showing the diffusion of Mg and Fe required in the conversion of garnet A to (hyp-plag-sp)B and garnet C. The chemical potentials, taken from (a), are seen to be arranged for the most rapid transfer of material.



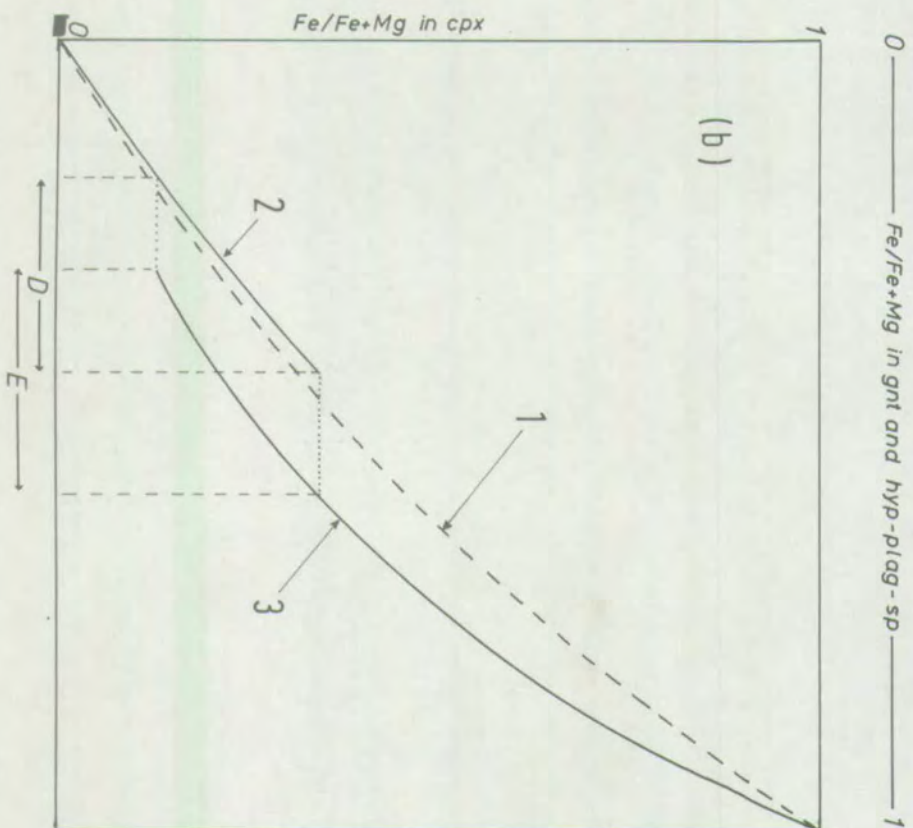
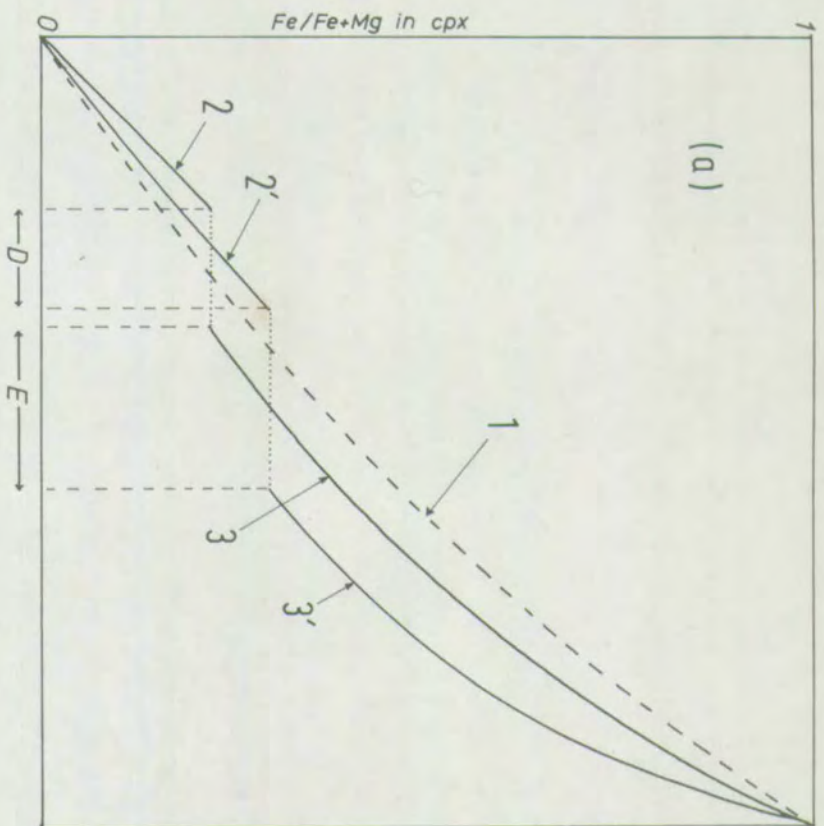


Fig. 4-29

Change in Fe-Mg distribution between garnet and augite

Distribution curve (1) has become unstable, due to a change in physical conditions, and has been replaced by separate distribution curves for garnet and augite (3), and for hyp-plag-sp (chemically equivalent to garnet) and augite (2).

In (a), the new physical conditions for 2 and 3 are different from those of 2' and 3'. The compositions D and E are invariant in each case.

In (b), the new physical conditions are uniform, and the compositions D and E have a variance resulting from one or more degrees of freedom. Where the compositions D and E overlap, the distribution curves, are non-ideal.

D and E correspond to the equilibrium compositions of fig. 4-28.

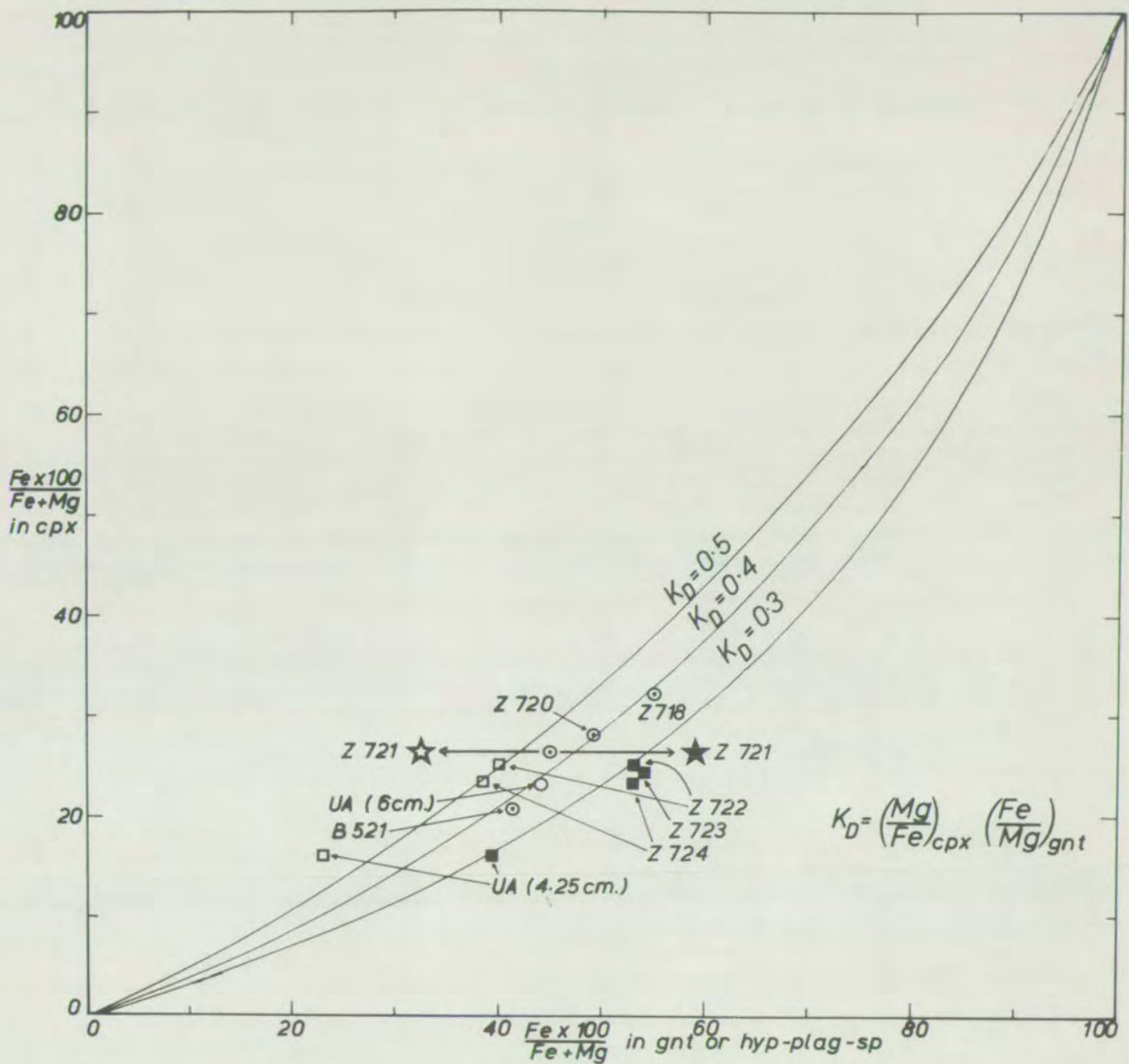


Fig. 4-30. Fe-Mg distribution between garnet, hyp-plag-sp, and augite.

with correspondingly different Fe-Mg distributions. In the second case the compositions D and E can vary, as the system has one or more degrees of freedom.

In fig. 4-30 all the available garnet-augite and (hyp-plag-sp)-augite pairs are plotted. All the garnet-augite pairs which have not been modified by the development of reaction rims plot close to the same curve. It is also apparent that the minerals from the Geodh'Eanruig specimens, in which local equilibrium appears to have been re-attained, plot close to the same curve as the garnet-augite pair from Loch an Daimh Mhor.

In view of this observation it is likely that the physical conditions at the two localities were essentially the same, and that the differences in the Fe/Fe + Mg ratios of the coexisting garnet, hypersthene, and spinel from the two places are the result of more subtle chemical variations, possibly the albite content of the plagioclase, the $\text{Fe}_2\text{O}_3/\text{FeO}$ ratio, or the Cr content in some of the minerals, allowing the system one or more degrees of freedom.

4.9 Diffusion Zone Formation

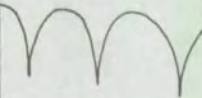
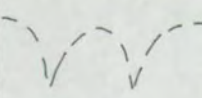
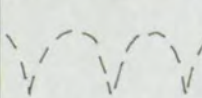
In order to critically assess the conclusion of O'Hara (1961), that the basic, garnetiferous basic, and contact gneisses were formed by solid state reaction between an ultrabasic intrusive and the surrounding acid gneiss, it is necessary to investigate the theory of reaction between a pair of solids, not in chemical equilibrium with each other, which have been placed in contact. Such a process may be expected, and has been observed, to produce a sequence of zones of different composition between the original materials, which will gradually grow at their expense. The nature of these zones is determined by the diffusion of material across the contact.

Previous studies of zoned ultrabasic bodies

Ultrabasic igneous masses, usually serpentinites, surrounded by a series of zones, often of unusual composition, have been described from many localities. Some of the more thorough studies have been by Read (1934), Phillips and Hess (1936), Chidester (1962), Sørensen (1954), and Matthews (1967). The majority of the bodies described appear to have developed their zones during a regional metamorphism.

The feature which has captured the attention of all the above authors is the persistent occurrence of mono- or bi-mineralic zones, frequently with sharp margins, between the ultrabasic rock and the country rock. The principal types of zoned sequence described are summarised in fig. 4-31.

Since the studies of Read (1934) and Phillips and Hess (1936), it has been generally accepted that the zones are genuinely the result of reaction between two rock types, and that all the material in them is of purely local derivation. Sheppard (1968) has produced a brief summary of the existing state of opinion on such occurrences, not complicated by any attempt to explain the monomineralic zones as a fundamental property of such systems.

N-Central Vt.	Central Vt.	Roxbury, Vt.	Thetford, Que.	Unst	Chester, Vt.	Skye	Siorarssuit
(Chidester, 1962)	(Phillips & Hess, 1936)	(Phillips & Hess, 1936)	(Phillips & Hess, 1936)	(Read, 1934)	(Phillips & Hess, 1936)	(Matthews, 1967)	(Sørensen, 1954)
Qz-sericite-chlorite schist	Qz-mica schist ----- chloritised	Schist ----- chloritised	Phyllite	Bi-musc-ep-plag-qz-ore gneiss	musc-qz-gnt gneiss	Felspathic amphibolite ----- bi-qz-fels-gn.	Hyp-plag (qz-diops) gneiss
CHLORITE	CHLORITE	CHLORITE	CHLORITE	BIOTITE CHLORITE	BIOTITE	BIOTITE	PHLOGOPITE
TALC	TALC	TALC ACT.	ACTINOLITE TALC	ACTINOLITE TALC	ACTINOLITE TALC	ACTINOLITE	ENSTATITE
Talc-carb.  Serpentine (antigorite)	Serpentine	Serpentine	Serpentine	Serpentine (antigorite)	Talc-carb.  ? Serpentine	Talc-dolomite  ? Serpentine	Dunite


Approximate scale of increasing metamorphic grade 

Fig. 4-31. Diagrammatic summary of some descriptions of zoned ultrabasic bodies.

Fundamental aspects of diffusion

The basic law of diffusion in any system is Fick's first law, which states that the diffusion flux is proportional to the negative concentration gradient:

$$J = -D \frac{\partial c}{\partial x} \quad \dots\dots\dots (1)$$

where J is the flux per unit area, c the concentration of the diffusing substance, and D the diffusion coefficient. Fick's second law is a consequence of the relation

$$\left(\frac{\partial J}{\partial x} \right)_t = - \left(\frac{\partial c}{\partial t} \right)_x \quad \dots\dots\dots (2)$$

and states that

$$\frac{\partial c}{\partial t} = \frac{\partial}{\partial x} \left(D \frac{\partial c}{\partial x} \right) \quad \dots\dots\dots (3)$$

It was observed by Einstein that the driving force for diffusion of a chemical species is the gradient of the chemical potential of that species, and that the flux can be expressed in terms of the absolute mobility of the species, B_1 :

$$J_i = -\frac{1}{N} \cdot \frac{\partial \mu_i}{\partial x} \cdot B_i \cdot c_i \quad \dots\dots\dots (4)$$

Assuming unit activity coefficient this leads to the relation

$$D_1 = kTB_1 \quad \dots\dots\dots (5)$$

$$\text{or, more generally, } D_1 = kTB_1 \gamma_1 \quad \dots\dots\dots (6)$$

where k is Boltzmann's constant.

This observation makes it clear that the diffusion coefficient D of Fick's laws is dependent on the activity coefficient, and hence will vary with concentration in non-ideal solutions. In multiphase systems, where there is no

simple, general relationship between concentration and chemical potential, Fick's laws will be of little use, and the modification used by Onsager (1949) is likely to be more applicable:

$$J_i = - \sum_k L_{ik} \frac{\partial \mu_k}{\partial x} \quad \dots\dots\dots (7)$$

or, alternatively, the diffusion in response to activity gradients may be used:

$$J_i = - \sum_k L_{ik} \frac{\partial a_k}{\partial x} \quad \dots\dots\dots (8)$$

where L_{ik} and L'_{ik} are the diffusion fluxes of constituent X_i in response to negative unit gradient in the chemical potential or the activity of constituent k . It is likely that L_{ik} and L'_{ik} will be negligible except when $i = k$ (Kirkaldy and Brown, 1963, p. 93).

Diffusion in semi-infinite couples

Pick's laws for the case of diffusion in a semi-infinite couple (two members extending infinitely in opposite directions from a finite value of x) were first considered by Boltzmann (1894), who obtained solutions of the equations in terms of a single parameter $\lambda = x / t$. (x = distance from original contact, t = time). The important consequence of this is that solutions of the equations giving c in terms of λ are not time-dependent, and are thus characteristic of a particular couple and of the physical conditions involved. That such a relationship holds for each zone, and the whole sequence of zones, in ternary, multiphase, systems has been verified theoretically (Kirkaldy and Brown, 1963, and references therein) and experimentally (Clark and Rhines, 1958).

The non-time dependent character of a sequence of diffusion zones is important when only the end products are available for study, as in geological situations, since the sequence, composition, and relative thicknesses of the zones are independent of the time for which the process has operated. This ceases to be true if one end member comes near to exhaustion, as the couple is then no longer semi-infinite.

The attainment of equilibrium in a diffusing system

For diffusion to take place from one part of a system to another, it is necessary for there to be a finite difference in chemical potential between the parts of the system. This can only exist if the system as a whole is not in equilibrium. The diffusion is an irreversible process, and none of the laws of classical thermodynamics which depend on equilibrium or reversibility can be applied to the system as a whole.

From equation (4), it follows that there can be no discontinuities in chemical potential of any species in a system where diffusion is possible for all constituents, since these will immediately be eradicated by an infinite flux. For this reason, the differences in chemical potential between all the phases in one small part of the system, and between adjacent small parts of the system, must be small. The equality of chemical potentials is one criterion of equilibrium, and to a first approximation adjacent thin layers (in a system which varies only in one dimension) may be considered to be in equilibrium with each other. The system as a whole then consists of a series of 'infinitesimal equilibria', each of which conforms to the laws of classical thermodynamics. This concept was introduced by Thompson (1959) as a means of applying a thermodynamic treatment to metasomatic processes: it is a fundamental part of the recently developed science of the thermodynamics of irreversible processes.

A particularly important consequence of the attainment of local equilibrium is that the Gibbs Phase Rule can be applied to every small part of the system. This is preferable to the treatments of Khorzhinskii (1950) and Thompson (1959), who present modification of the Gibbs Phase Rule for systems with 'fixed' and 'mobile' components. These modified phase rules were devised as an explanation of the common occurrence of monomineralic zones in situations involving mass transport diffusion. A fundamental postulate in their derivation is the division between fixed and mobile components. Confusion arises when they are applied to systems where this division is not possible.

This criticism is essentially that of Weill and Fyfe (1964), who point out that any phase rule derived from considerations of equilibria cannot be applied to a system which is not in equilibrium, and that "The Gibbs Phase Rule may be

applied to each part of the system small enough to be considered in equilibrium" (p. 575). Furthermore, as is apparent from the diffusion equations, the compositions and sequence of zones formed by diffusion is determined by the relative diffusion rates of those constituents which diffuse independently, which are dependent on the chemical potentials of each constituent. The chemical potentials are dependent on the compositions of the phases, and these depend on the bulk composition of each layer, and on the compositions and combinations of phases which are possible. No purely thermodynamic analysis can describe fully situations involving an interplay of thermodynamic and kinetic processes.

The number of degrees of freedom necessary to allow all the chemical potentials in a zone to satisfy the boundary conditions imposed by adjacent zones may vary from one, up to the number of independently diffusing constituents. The latter case results in the case of infinite or perfect mobility of all but one component, to which the Khorzhinskii and Thompson Phase Rules can be applied.

Use of the phase rule in diffusing systems

As observed above, the Gibbs Phase Rule, or, in geological systems, the Goldschmidt Phase Rule, can be applied to a small part of a system in which local equilibrium prevails. In applying the phase rule, very careful attention must be given to the choice of what are to be considered as components.

In a diffusing system, each element is diffusing in response to its own chemical potential gradient, according to its own absolute mobility (equation (4) p. 79). In geological situations where there is little change in oxidation state, we may speak of individual oxides diffusing, thereby simplifying our thinking a little. The chemical potential of a species i is given by

$$\mu_i = \left(\frac{\partial G}{\partial n_i} \right)_{P, T, n_j}$$

and to allow for this equation to have meaning, we must allow for a potential variation in the mole fraction of the species i . For this reason, even in parts of the system composed of a single phase of fixed composition, we are required to consider as many components as there are independently diffusing constituents (elements or oxides), even though for many purposes a single phase may be considered as a one-component system. The variation in mole fraction required to define a chemical potential is, of course, minimal, but its existence appears to make the consideration of that constituent as a phase rule component a necessity.

This argument is similar to that of Weill and Fyfe (1964, p. 568), who state that "the chemical potential of part of a phase of fixed composition has never been defined by Gibbs or Khorzhinskii, and is not measurable." The same authors (1967, p. 1170) find it necessary to consider the chemical potential of water in the system $\text{Al}_2\text{O}_3\text{-H}_2\text{O}$, which, at one stage of the argument, consists only of diaspore. It is evident that there must be a chemical potential of water in diaspore (fig. 4-32). This quantity could vary between the limits μ_1 and μ_2 , over a composition range which is probably not detectable. Even in pure diaspore, therefore, it is necessary to consider two components, as long as, in the same argument, the chemical potential of water or Al_2O_3 is being used.

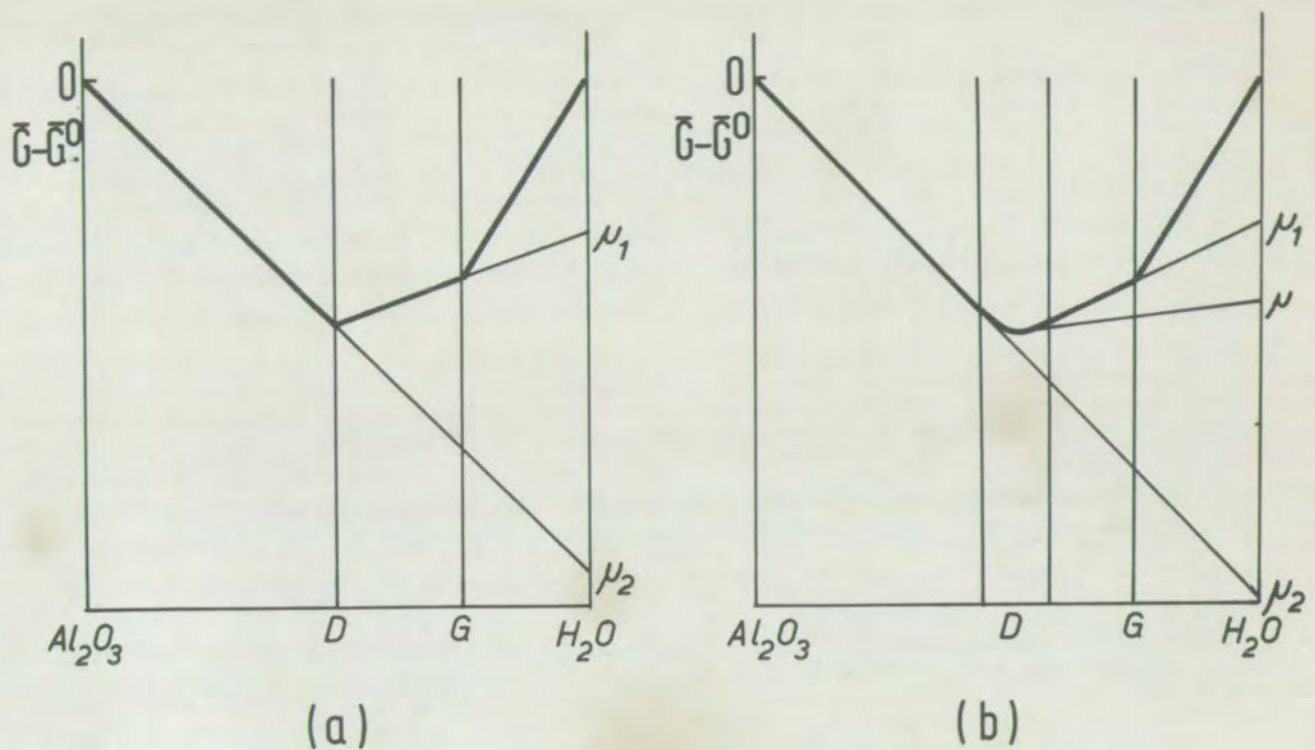


Fig. 4-32. Free energy-composition diagrams for the system $Al_2O_3 - H_2O$.

(a) Reproduced from Weill and Fyfe (1967)

(b) The composition range of diaspore expanded to show the necessary dependence of μ_{H_2O} on composition, even in an effectively stoichiometric compound.

D = diaspore G = gibbsite

Standard state - the oxides at T and P .

Diffusion in multi-component systems

Diffusion in ternary systems has received some attention in metallurgical literature. Most of the relevant information and references to relevant work is contained in the detailed experimental study of the Al-Mg-Zn system by Clark and Rhines (1958), and the review by Kirkaldy and Brown (1963).

Figs. 4-33, 4-34, and 4-35 are from Clark and Rhines (1958), and show the results of reaction between various Mg-Zn alloys and Al, with the quite striking variations in composition produced. Many of the conclusions of the two papers mentioned are relevant to this study and they are reproduced below, except for those conclusions of Clark and Rhines (1958) which are contradicted by those of Meijering (1958) and Kirkaldy and Brown (1963). The numbering is that of the original papers.

From Clark and Rhines (1958):

(1) The layers in a ternary diffusion couple correspond to a connected series of phase equilibria linking the terminal compositions of the couple on the phase diagram.

(4) The diffusion composition path of any couple tends, as a whole, to bend away from the fastest diffusing component of the system.

(5) One phase equilibria result in the formation of single-phase layers in the diffusion structure.

(6) The composition path across a one-phase layer is normally curved and turns away from the composition of the most rapidly diffusing component.

(7) Two-phase equilibria result in the formation of two-phase layers, or interfaces between single-phase layers of the conjugate phases.

(8) The interface type of two-phase structure (corresponding to parallelism of the composition path and a two-phase tie-line) occurs with unexpected

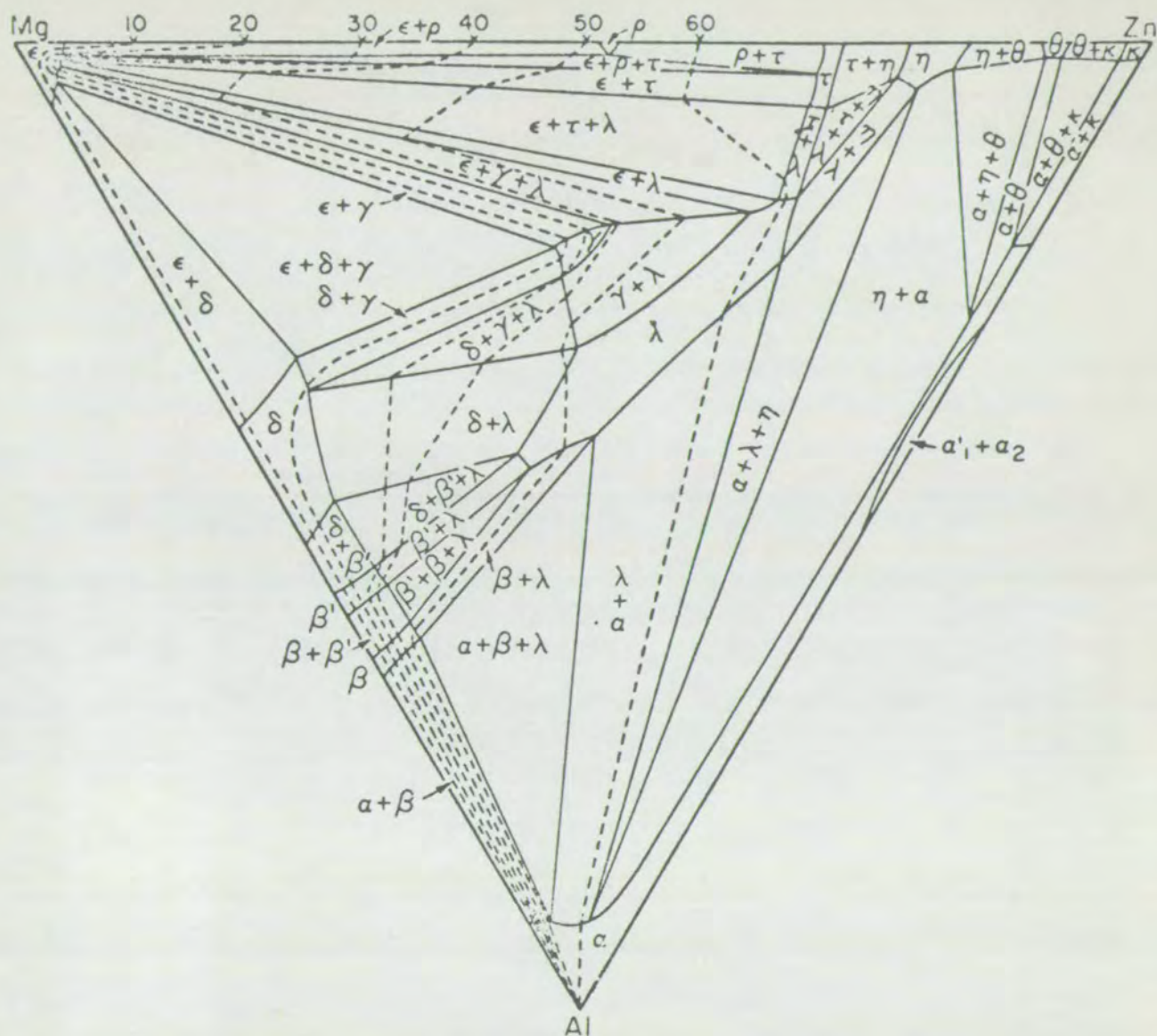


Fig. 1—The Redetermined 335 °C (635 °F) Isotherm of the Al-Mg-Zn Phase Diagram Showing the Paths of Composition in the Diffusion Zones of the Al-Mg-Zn Couples. The ρ and τ fields have been enlarged slightly in their vertical dimension in order to clarify the diagram.

Fig. 4-33. From Clark and Rhines (1958)

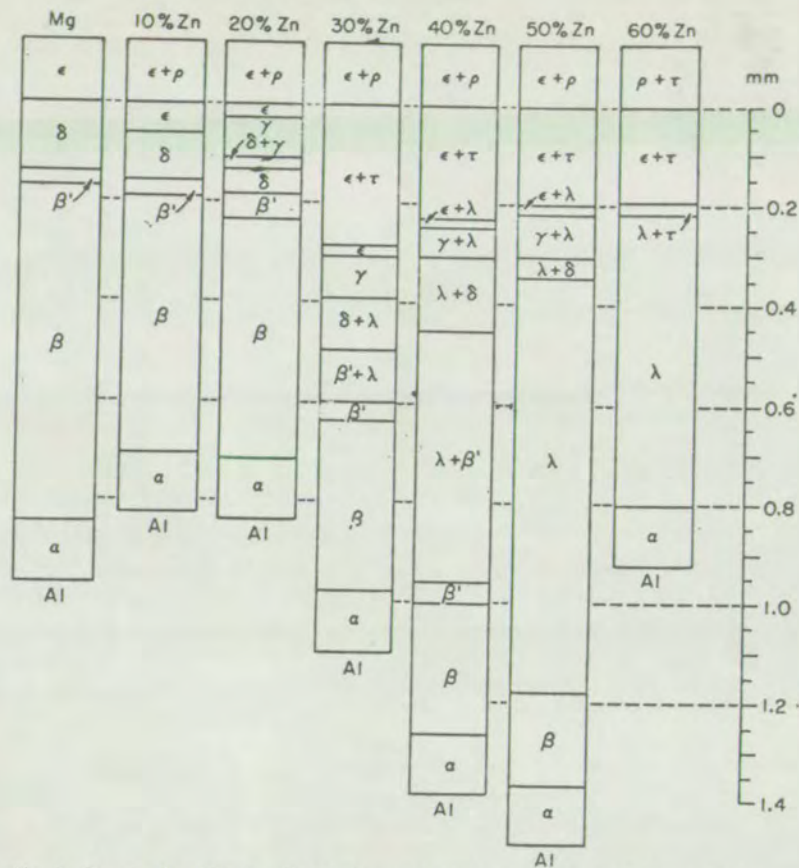


Fig. 2—Key to the Diffusion Layer Structures and the Relative Thickness of the Al-Mg-Zn Diffusion Couples Listed in Table I After a 1000 Hour Anneal at 335 °C (635 °F).

Fig. -4-34.

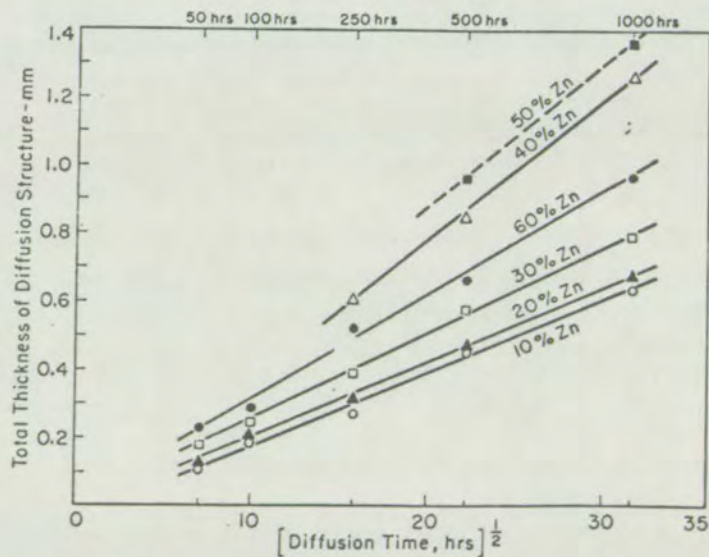


Fig. 4-35.

frequency, suggesting that there may be a tendency to suppress two-phase layer formation in order to minimise the interfacial area in the microstructure, (or, where necessary, to increase the variance?).

(9) The relative proportions of the phases in a two-phase layer correspond with a unique composition path across the two-phase region of the phase diagram; the path may be curved (i.e. crossing the tie-lines is possible).

(10) Three-phase equilibria are represented by interfaces between two layers having a total of three phases.

(11) The composition path commonly turns sharply as it passes through a three phase interface, the direction of rotation being determined by the relative rates of diffusion of the components of the system.

(12) The particles of mid-system two-phased layers are normally acicular, those of terminal two-phase layers tend to be the same as those of the terminal alloy.

(13) Two-phased layers tend to be composed of coarser particles the faster the rate of growth.

(14) Diffusion zone growth in ternary couples obeys the parabolic law.
From Kirkaldy and Brown (1963):

(12) To the extent that lateral diffusion and non-uniformity of layer composition can be ignored or averaged out, the diffusion paths involving two-phase regions may be approximated by a stationary path connecting a continuous series of local equilibria (i.e. a more fastidious re-statement of conclusion (1) of Clark and Rhines, above).

(2) Calculated paths on ternary isotherms remain invariant as the four diffusion coefficients are varied in direct proportion (the four diffusion

coefficients are L_{11} , L_{12} , L_{21} and L_{22}).

(3) Diffusion paths cannot be mapped back into C_1 - C_2 - λ space without the reintroduction of diffusion data. (C_1 and C_2 are the concentrations of two constituents, which uniquely define a ternary composition).

(4) A diffusion path on the ternary isotherm must cross the straight line joining the terminal compositions at least once (Meijering, 1958).

(8) A diffusion path on the ternary isotherm is defined uniquely only by its terminal compositions.

(9) There is no theoretical restriction that prevents diffusion paths radiating from one terminal composition from crossing.

(13) A diffusion path that passes through a two-phase region coincident with a tie line contains a planar interface whose local equilibrium specification is given by that tie-line.

(14) A diffusion path that passes into a two-phase region from a single-phase one at an angle to the tie-lines and returns immediately to that same single phase describes a region of isolated precipitation.

(15) A diffusion path that passes into a two-phase region from a single-phase one at an angle to the tie-lines and exits into another phase represents a two-phase zone.

(16) A diffusion path in a two-phase region may not reverse its order of crossing of the tie-lines.

Finally, Kirkaldy and Brown (1963) conclude that the principle that the rate of entropy production should be a minimum exercises an ultimate control over the choice between diffusion paths with equal rates of free energy production.

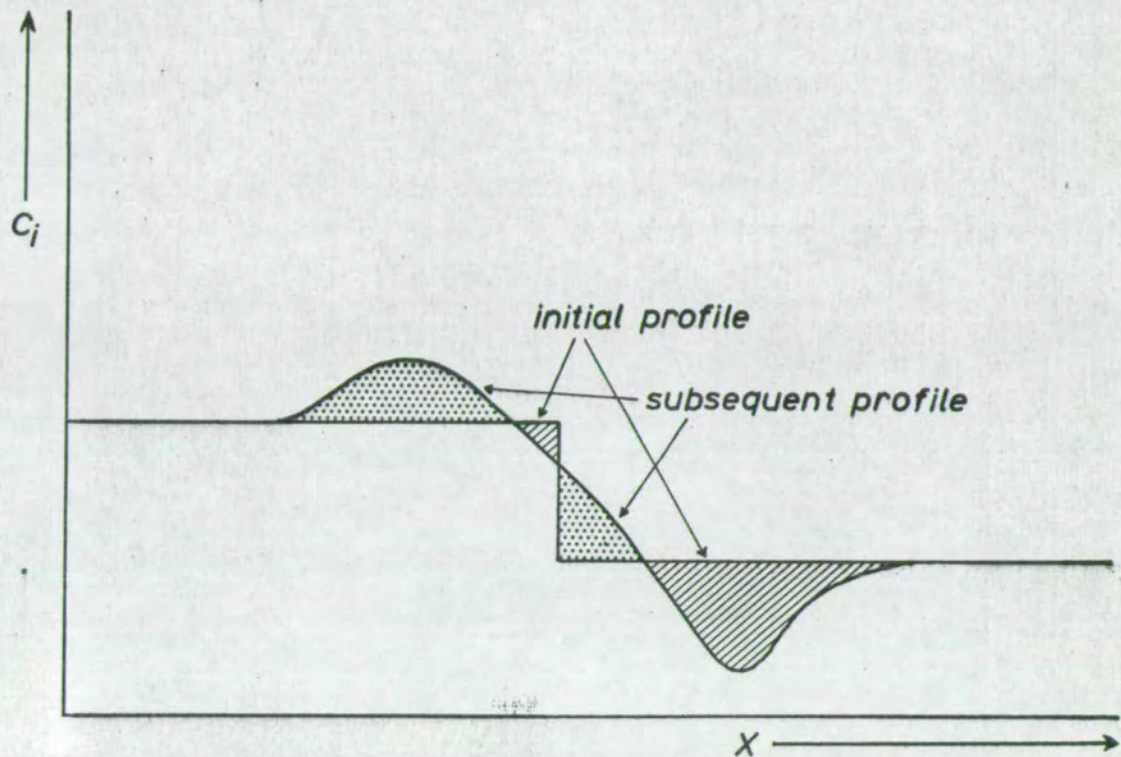


Fig. 4 - 36.

Illustration showing the conservation of mass during diffusion. The concentration-distance profile changes with time, but the area under it is constant.

Many of the conclusions of Kirkaldy and Brown (1963) are axiomatic, and result from the necessity for continuous variation in the chemical potentials of the components across the diffusion zones, while those of Clark and Rhines (1958) are empirical.

Of particular interest is conclusion (3) of Kirkaldy and Brown (1963). This means that consideration of the composition path alone can reveal little about the diffusion processes and leads only to qualitative conclusions such as (4) and (6) of Clark and Rhines (1958). Information about relative diffusion rates can be extracted only from the variation of composition against λ .

Also of importance is conclusion (4) of Kirkaldy and Brown (1963) that curved composition paths must cross the line joining the terminal compositions. This is a simple consequence of the fact that mass must be conserved during the diffusion process, for each component. This conclusion does not apply to systems of four or more components, since in three or more dimensional space the curve may spiral round the straight line without intersecting it. However, it does apply to any planar representation of multi-component data.

The conservation of mass will also be reflected in the plot of concentration versus x or λ (fig. 4-36). The total mass at any time is given by the area under the concentration curve. This area must therefore be the same for all times, and the algebraic sum of the shaded areas in fig. 4-36 must be zero.

4.10 Prediction of the sequence of zones in a complex system

The complexity of natural multi-component systems is such that prediction of the sequence of zones, even with an exact knowledge of the phase diagram, the thermodynamic properties of the phases, and diffusion constants of the

constituents is likely to be difficult.

In geological systems, where only the phase diagram is known at all, the difficulties presented are considerable. However, it was decided to attempt such a prediction, using the method of simulation, with the aid of a digital computer. The method is essentially simple, but the use of a stepwise process to simulate a continuous one involves loss of precision, unless the steps are made very small, in which case the computer time required becomes excessive.

The details of the method are given in Appendix E, but the principles involved, and details of the approximations and guesses made are given below. The object of the simulation model is to predict the diffusion behaviour of basic, ultrabasic and acid gneisses of the granulite facies.

Simulation model

The model depends on a simple variation of Fick's first law (equation (8), p. 80). It involves a cyclic series of steps:

(1) An initial composition profile is set up giving concentrations of each constituent in a series of layers (representing layers parallel to the contact).

(2) For each layer the bulk composition is recalculated into proportions and compositions of minerals.

(3) From the mineral constitution values of the activity of each constituent are calculated in each layer.

(4) The activity difference between each layer and the next, for each constituent, is calculated.

(5) An amount of each constituent is taken from each layer and added to the adjacent layer in the direction of decreasing activity. The amount

is proportional to the activity gradient at the point, and the diffusion coefficient L' ($= L'_{11}$) for that constituent.

(6) The compositions of the layers will not now, in general, total 100%, and they are adjusted to give this value (by changing their thicknesses, so that the total mass of each constituent remains unchanged). (For details, see Appendix E).

(7) The cycle is repeated a sufficient number of times to give a consistent profile.

Choice of components:

The 13 elements Si, Ti, Al, Fe, Mn, Mg, Ca, Na, K, Cr, Ni, H and O suffice to describe the compositions of all the major mineral phases and rocks seen at Scourie. It is difficult to deal mathematically with a 13-component system, and to keep the method simple enough to visualise it was decided to use as few components as could not be neglected. The five oxides SiO_2 , Al_2O_3 , FeO , MgO , and CaO define, with acceptable precision, all the phases present, except hornblende, potash feldspar, and the ore minerals. In view of the approximations presently to be made, the loss of any predictive value by neglecting the other constituents is irrelevant.

Recalculation into minerals:

In order to convert bulk compositions to granulite facies mineralogy, the following minerals were considered:

Quartz	S
Anorthite	CaSi_2
Kyanite	AS
Wollastonite	CS

Diopside	CMS_2	end-members
Aluminous diopside	$(\text{CMS}_2)_{0.94} \cdot \text{A}_{0.12}$	
Enstatite	MS	end-members
Aluminous enstatite	$(\text{MS})_{0.94} \cdot \text{A}_{0.06}$	
Pyrope	M_3AS_3	end-members
Calcic pyrope	$(\text{M}_3\text{AS}_3)_{0.86} \cdot (\text{C}_3\text{AS}_3)_{0.14}$	
Olivine	M_2S	
Spinel	MA	

Where C = CaO, A = Al_2O_3 , S = SiO_2 , M = (MgO, FeO)

The assemblages permitted are shown graphically in fig. 4-37.

Estimation of activities:

Attention was given to attempts to calculate values for free energy functions in natural minerals. The sources of information were the compilations of data by Kelley (1960), and Clark (1966). Methods are available for calculating some of the thermodynamic effects of simple solution (Thompson, 1967), and these were applied in an attempt to modify the data for the synthetic minerals, to apply to natural solid solutions.

It transpired from these attempts, that published thermochemical data are not sufficiently accurate for the calculation of free energies of silicates. This is because we are interested in the differences in free energies between a number of states, and this difference is often of the same order of magnitude as the errors in the thermochemical measurements. Even more important is that free energy calculations for high pressures require very accurate knowledge of the molar volumes at all pressures up to those being studied. This knowledge is not available.

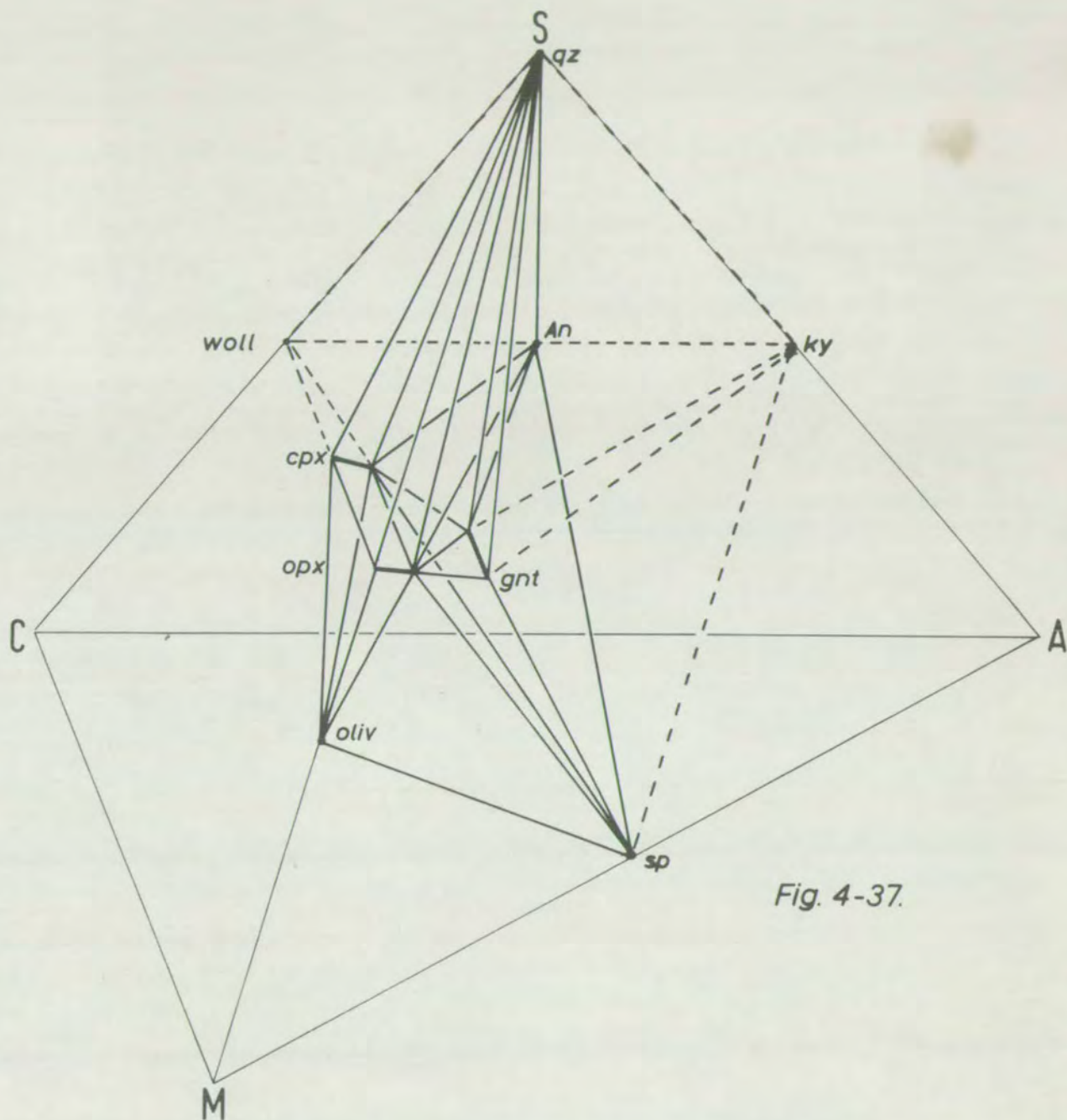


Fig. 4-37.

Mineral assemblages in the system C-M-A-S used in the simulation model.

These correspond to the observed assemblages (without ore or hornblende) in the Scourie rocks, except those shown in broken lines, which are hypothetical.

It is suggested that experiments on the lines of those by Morey and Hesselgesser (1950), in which compositions of vapour phases in equilibrium with high temperature, high pressure assemblages are measured, would be feasible ways of determining chemical potentials under such conditions.

The failure of these calculations means that any values of activities used in the simulation model were purely abstract. This removes any rigour from the predictions, and leaves them with only an illustrative significance.

The method adopted was as follows. When recalculation into a mineral constitution gave less than 5% (molecular) of a mineral, that mineral was assumed to be absent (in this way, three, two, and one phase assemblages can be generated by the model). Each pure mineral was allocated values of activity for each component and the activity of a component was the weighted average of the activity in the four phases defining the assemblage, the activity for each phase being weighted by a factor which was 1 for 'present' minerals, and varied from 0 to 1 for 'absent' (< 5%) minerals. E.g., in an assemblage consisting of 47% quartz, 50% anorthite, 2% wollastonite, and 1% aluminous diopside, in which the activities of SiO_2 are 0.5, 1.0, 0.5, and 0.47 respectively, the activity would be $(0.5 + 1.0 + 0.4 \times 0.5 + 0.2 \times 0.47)/2.6 = 0.69$.

Activities of FeO and MgO were derived by considering them as a single component, calculating an activity for this component, and multiplying it by $\text{Fe}/\text{Fe} + \text{Mg}$ and $\text{Mg}/\text{Fe} + \text{Mg}$ for the activities of FeO and MgO respectively.

In this way the requirements of the phase rule are met, and, further, the activity of every component is dependent on the bulk composition. Only one activity can be varied in four-phase regions (that of FeO or MgO), while in single-phase regions the local system is tetra-variant.

The approximation used, that activity = concentration, in a pure mineral, is probably far from the truth. The measurements of Morey and Hesselgesser (1950), suggest that the activity of SiO_2 in quartz is about 10 times as great as in the assemblage enstatite-forsterite at 600°C and 1 Kb. The assumption that activity = concentration would indicate that it is only 2.4 times as great. It was preferred to more 'realistic' guesses, as it does not contain a subjective element, and is unable to bias the results towards a preconceived hypothesis.

Diffusion coefficients:

From the metallurgical literature, it appears that the diffusion coefficient D is not composition dependent in large one-phase regions. The values of D measured at one composition can be applied to other compositions and accurately predict experimental results (Kirkaldy and Brown, 1963, p. 96). In such large single-phase regions of the phase diagram, the deviation from the approximate equality activity = concentration may not be great, so that the diffusion coefficient L' will also not be strongly composition dependent. For this reason, the diffusion coefficient L' was used in the simulation model as a constant for each constituent.

The computer programme written to perform the calculations outlined is given in Appendix E, together with some explanatory notes.

4.11 Application of Theory to the Contact Sequences

The mass balance

As outlined above, the requirement that mass shall be conserved is fundamental to a diffusion zone sequence, and graphical methods are available to test a given sequence to determine whether they obey this requirement. Planar

projections of the chemical data must show either straight lines, or curves crossing the straight lines, joining the terminal compositions. Plots of concentration versus distance for any constituent must obey the condition that the area under the initial and final curves be the same. Given a zoned sequence, and assuming that it has formed by diffusion between two end members similar to the existing end members, this requirement may be used to determine the apparent original position of the contact, for each constituent. If the positions as determined for each constituent are the same, then the requirements of the mass balance have been entirely fulfilled.

The plots of cation atomic percent against $Fe/Fe + Mg$ (fig. 4-19) are planar projections of chemical data, and on each is shown a straight line joining the average compositions of the ultrabasic, garnetiferous basic, and acid gneisses.

It is apparent from fig. 4-19 that many of the sequences from ultrabasic to garnetiferous basic gneiss plot on lines which either closely parallel, or cross the lines joining the compositions of these two types. The case of sequences from ultrabasic to acid gneisses, however, is different. Many of these plot on curves lying entirely to one side of the straight line joining the terminal compositions (as far as the average analyses represent the terminal compositions in each case). Only the two non-garnetiferous sequences analysed show more nearly linear variations.

These observations do suggest that, if there is a continuous sequence of diffusion zones from ultrabasic through garnetiferous basic to acid gneiss, then the mass balance has not been maintained. Table 4-5 gives the average analyses of the ultrabasic, garnetiferous basic, basic, and acid gneisses, and fig. 4-38 shows a simple variation diagram for these types.

Table 4-5

	1	2	3	A	B	C	D	E	F
SiO ₂	47.5	47.6	60.8	54.7	64.5	71.5	72.0	71.0	31.6
TiO ₂	0.3	0.9	0.7	0.0	0.0	1.5	3.5	3.5	11.4
Al ₂ O ₃	6.5	14.4	14.4	5.0	6.6	10.1	12.8	12.8	14.8
Fe ₂ O ₃	12.3	14.3	7.2	6.8	2.6	0.0	0.0	1.2	19.0
MgO	26.5	8.7	4.5	29.5	22.9	11.9	4.6	4.5	6.3
CaO	6.7	11.8	7.1	2.1	0.0	0.0	1.7	2.5	16.5
Na ₂ O	0.7	1.8	3.1	1.5	2.6	3.7	4.1	4.0	0.4
K ₂ O	0.15	0.5	0.9	0.4	0.8	1.2	1.3	1.2	0.0
Cr	2200	300	20	2500	1800	900	0	0	400
Ni	1470	160	30	1700	1400	700	170	150	0
x				-0.95	-0.70	-0.67	-0.86	-1.00	+0.53
y				1.64	0.75	0.32	0.11	0.10	0.24

1 Average ultrabasic gneiss (Table 4-1)

2 Average basic and garnetiferous basic gneiss (Table 4-3)

3 Average acid gneiss (Holland, 1965)

A to F are 'ichors', which it is necessary to add to or subtract

from a mixture of ultrabasic and acid gneisses (1 and 3), to make material of basic composition (2).

x = no. of weight units to be added to or subtracted from one weight unit of ultrabasic-acid mixture.

y = ratio of the weight of ultrabasic to the weight of acid gneiss in the appropriate mixture.

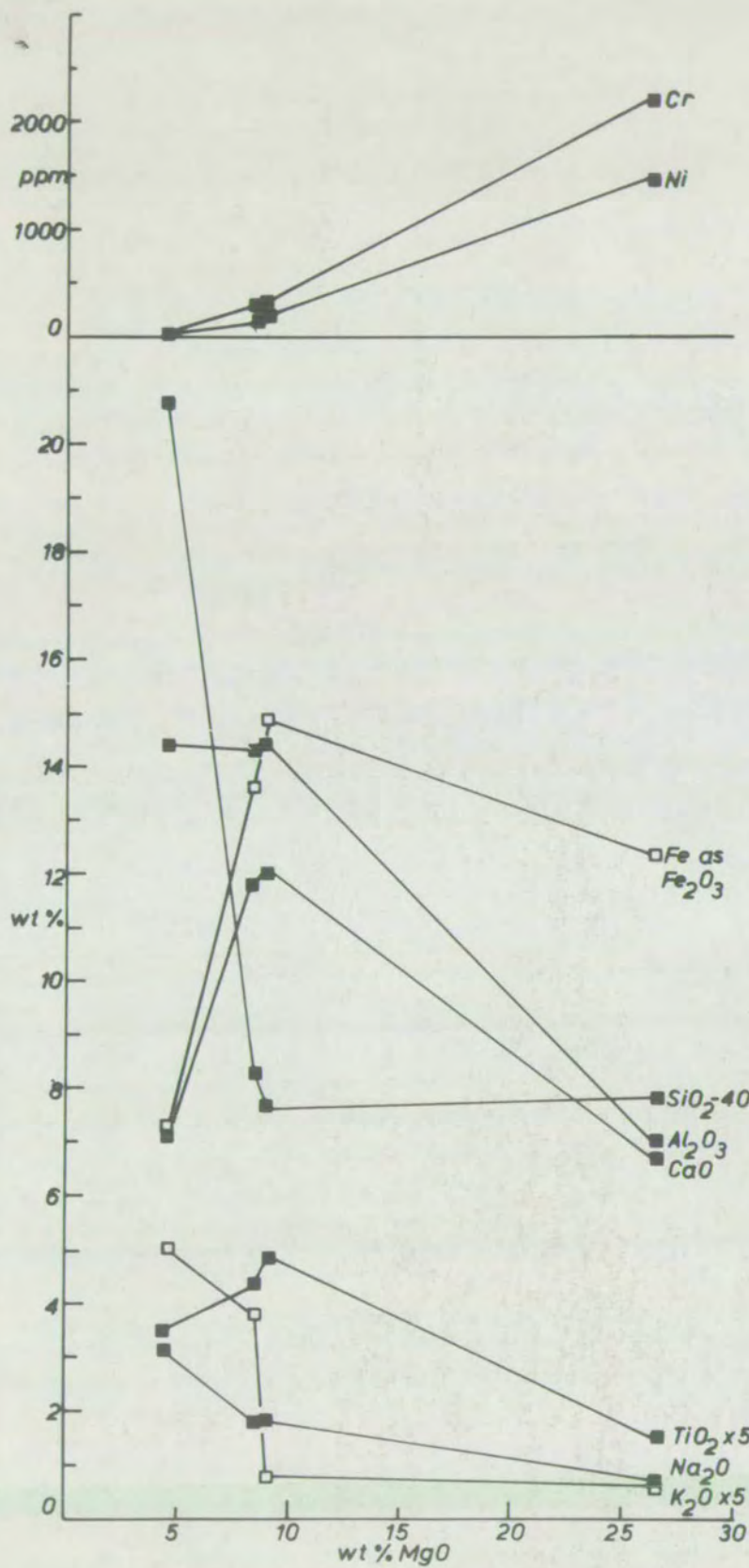


Fig. 4-38.

Variation diagram for the average analyses of acid, basic, ultra-basic, and garnetiferous basic gneisses from Table 4-5.

In terms of absolute masses, these four types form the overwhelming majority of the contact sequences. It is clear that the concentrations of TiO_2 , iron, and CaO are greater in the basic and garnetiferous basic gneisses, than in either the ultrabasic or acid gneisses. This fact need not, of itself, be a violation of the mass balance, but both the acid and ultrabasic gneisses have about 7% of CaO , and both the basic and garnetiferous basic gneisses have about 12% of CaO . This situation can only have arisen if there is a complementary zone of calcium depletion elsewhere. Such a zone is not evident from any of the observations made in this study or by O'Hara (1961).

Table 4-5 gives the calculated compositions of what may be termed 'ichors', which it is necessary to either add or subtract from a mixture of acid and ultrabasic gneisses to produce material, whose composition is the average of the basic and garnetiferous basic gneisses. Less extreme modification would be necessary, if it were possible for some constituents to pass in, and some out of the system. Nevertheless, it is evident that, in order to have produced rocks of this basic composition, a large quantity of material must have moved far enough through the acid gneisses for the effect of its enrichment or depletion to have gone unnoticed. Since diffusion of the same constituents has not obliterated the (presumably large) differences in chemical potential between the acid and ultrabasic gneisses, for the same constituents to have travelled so far down what must have been smaller chemical potential gradients within the acid gneiss requires either diffusion coefficients greater by some orders of magnitude, or transport by another mechanism entirely.

Applications of the requirements of the mass balance to the couple ultrabasic-garnetiferous basic gneiss by inspection of the plots of cation atomic

percent has been mentioned above. Graphs showing the variations in concentration with distance are shown in fig. 4-17. Where there are sufficient data available for the curves connecting the points to be drawn with some confidence, there is some agreement between the positions of the contact as determined for separate constituents. There is a disparity of three feet between the original contact positions as determined for Ca and Al in the Geodh'Eanruig upper contact, Z 718-Z 726.

Conclusions:

It has been shown that consideration of the mass balance does not support the conclusion that the basic and garnetiferous basic gneisses were formed, along with the contact gneisses, by a process of simple reaction between the ultrabasic and acid gneisses as they now exist. Any such reaction would require either gain or loss of considerable quantities of material from or into the surrounding rocks, or further. It has been postulated elsewhere (Ch. 2, & O'Hara, 1960) that the acid gneisses may have originated from a more normal rock series by partial melting with loss of the fluid phase. One of the possible 'ichors', which it would be necessary to subtract from a mixture of ultrabasic and acid gneisses to form a rock of basic composition (E of Table 4-5) is not unlike a granitic rock in composition, and it might have been lost in such a fluid phase. In this case, the original ultrabasic-acid gneiss contact would have been somewhere in the basic or garnetiferous basic gneiss, and not between the spinel-pyroxenite and contact gneiss, as suggested by O'Hara (1961).

Consideration of the mass balance does lend some support, within certain limits of error, to the postulate that the contact gneisses formed by reaction between the ultrabasic and basic or garnetiferous basic gneisses. This might

imply that the basic and garnetiferous basic gneisses represent a basic rock of earlier formation than the contact gneisses. It is not exclusive of the possibility that the contact gneisses also form part of a larger reaction sequence from ultrabasic to acid gneiss, provided that the above-mentioned restrictions on this process are met.

The simulation model

As already noted, the lack of precise thermochemical data for the minerals involved means that the simulation model described in Appendix E loses its precise predictive value, and can be used as an illustration. The model will allow free choice of the initial composition profile, and the five diffusion coefficients. For one initial pair of end members, the diffusion coefficients may be varied to give a whole series of results, and those which most closely match the observed sequences chosen.

Firstly, the diffusion couple ultrabasic-garnetiferous basic gneiss was simulated. As the mass balance shows, this couple can be treated approximately as an isolated couple within the contact sequences, even if it forms part of a larger diffusion system. The results are presented in fig. 4-39, and 'A-C-F' plots of the same data in fig. 4-40. The results, despite the wide variations in diffusion coefficients used, fall into a few well-defined groups. The results are summarised in Table 4-6.

A simple linear variation between the two end members produces mineralogical composition profile showing culminations and depressions, and this pattern is closely paralleled by several of the simulated diffusion results. In other cases, the results very closely resemble the Loch an Daish Mhor type of contact, with separate culminations in hypersthene, augite, and garnet.

TABLE 4-6

SUMMARY OF THE RESULTS OF THE SIMULATION MODEL FOR REACTION BETWEEN ULTRABASIC AND GARNETIFEROUS BASIC MATERIALS.

RUN NO.	DIFFUSION COEFFICIENTS					TYPE OF RESULT			
	<u>CaO</u>	<u>Al₂O₃</u>	<u>MgO</u>	<u>FeO</u>	<u>SiO₂</u>	<u>1</u>	<u>2</u>	<u>3</u>	<u>4</u>
1	-	-	-	-	-	X			
2	1	1	1	1	1	X			
3	0.01	1	1	1	1		X		
4	1	0.01	1	1	1	X			
5	1	1	0.01	1	1			X	
6	1	1	1	0.01	1	X			
7	1	1	1	1	0.01			X	
8	1	1	0.01	0.01	1			X	
9	1	0.01	0.01	0.01	1			X	
10	0.01	1	1	1	0.01		X		
11	0.01	0.01	0.01	0.01	1		X		
12	0.01	0.01	1	0.01	0.01		X		
13	0.01	0.01	1	0.01	1		X		
14	1	1	1	1	0.5				X
15	1	1	0.5	1	1				X

TYPES OF RESULT:

(1) Fall in olivine, with a gentle culmination in opx and cpx, followed by a sharp drop in opx, a culmination in garnet (in a nearly pure cpx-garnet zone), and a slow rise in plag.

(2) As (1), but olivine falls to zero before opx rises to a culmination.

(3) First olivine, then opx falls to zero, followed by sharp culminations, first in cpx, then in garnet. Slow rise in plag.

(4) Olivine falls to zero, with a concomitant sharp culmination in opx. This is followed by further marked culminations in cpx, and then garnet. Plag. rises slowly to a garnetiferous basic composition.

Run (1) is not the result of simulation, but the result of recalculating a series of compositions defining a linear variation between the two end members into mineral constitutions.

Two additional runs (16 and 17) were performed, identical to (14) and (15), but with a calcium-poor ultrabasic member. The results do not differ significantly because of this.

Fig. 4-39

Results of the simulation model for reaction between ultrabasic and garnetiferous basic materials.

The composition profiles are shown for each run after 15 cycles of the model. The abscissae are the numbers of the layers, the initial contact being at layer zero. Continuous curves have been drawn, through the points to facilitate the appreciation of the differences between the runs. Mineral proportions are shown in solid ornament where they exceed 5%.

The diffusion coefficients for the runs are given in Table 4-6.

Both oxides and mineral proportions are in molecular percent, the mineral molecule being considered as one oxide molecule.

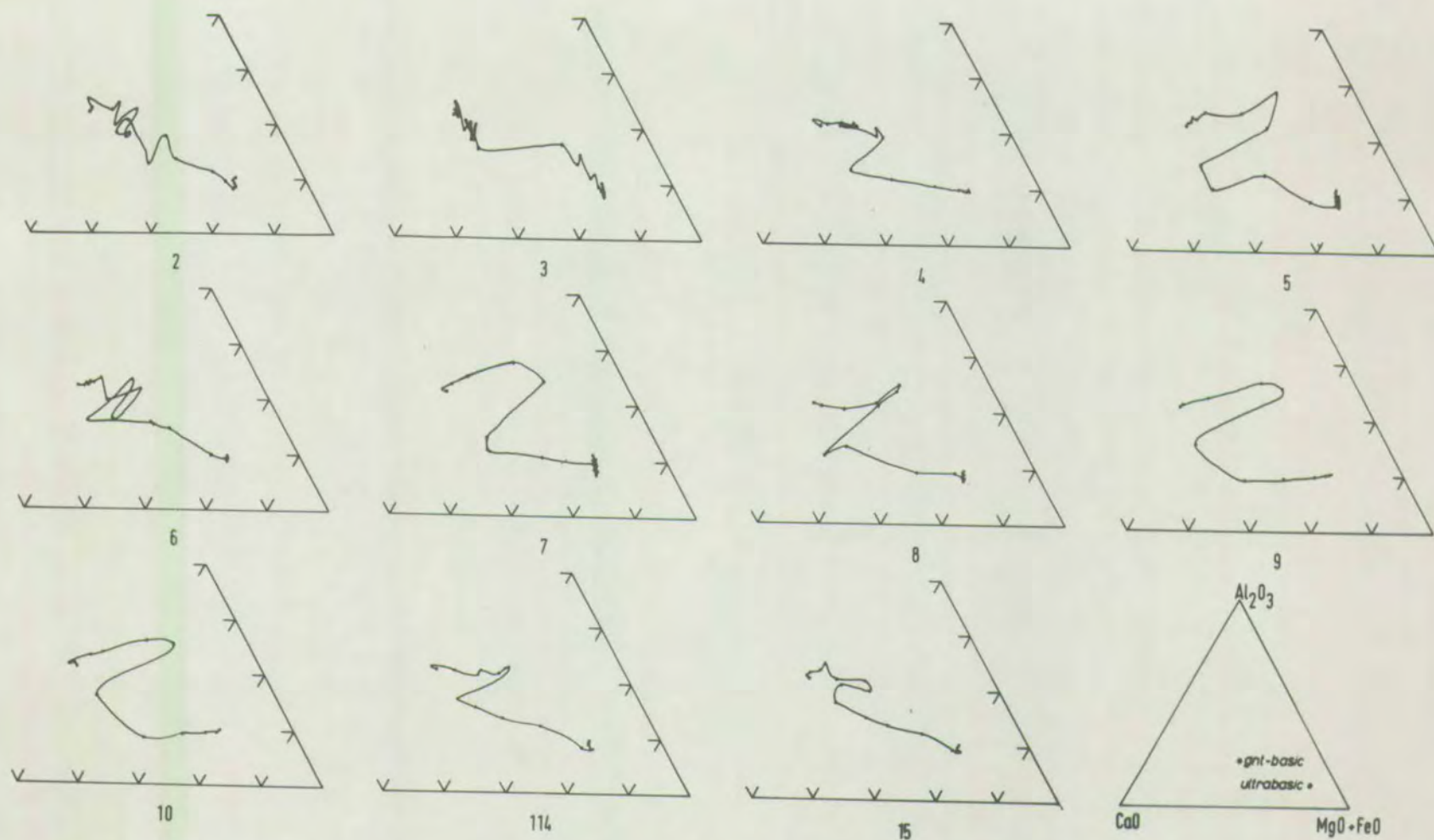
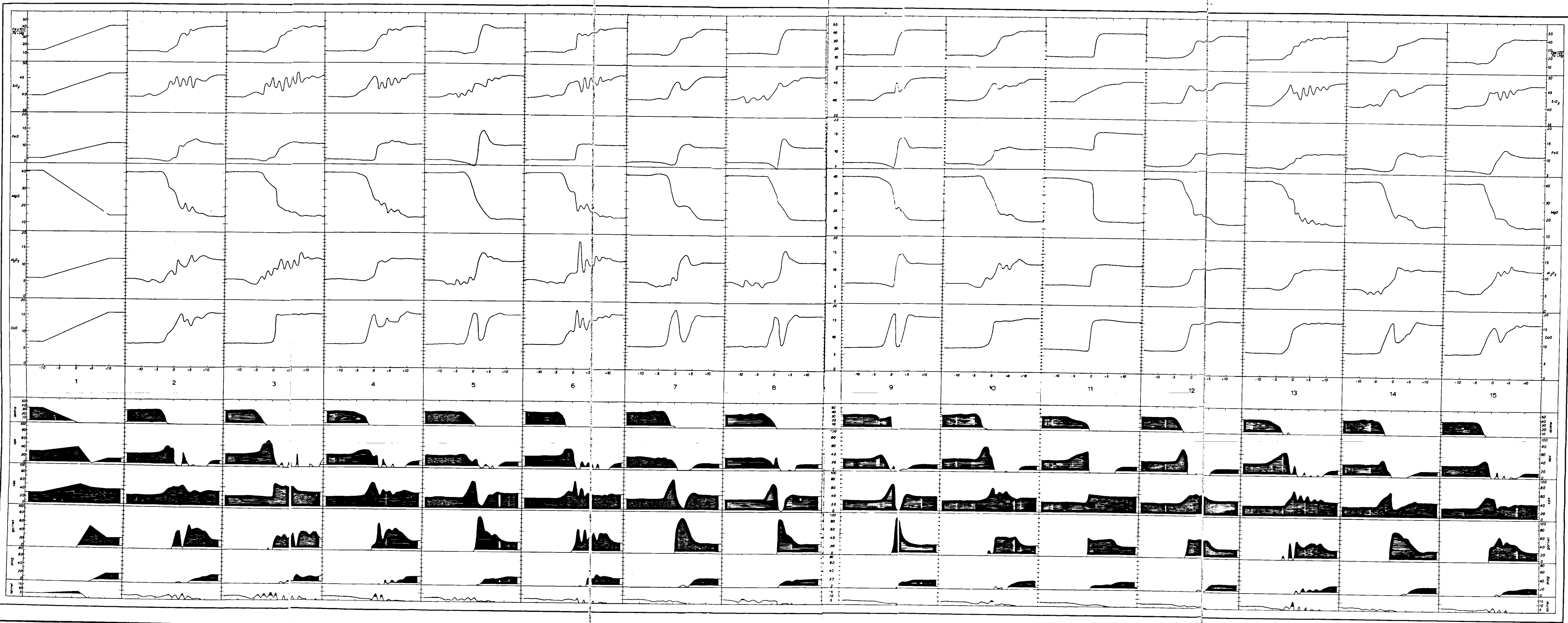
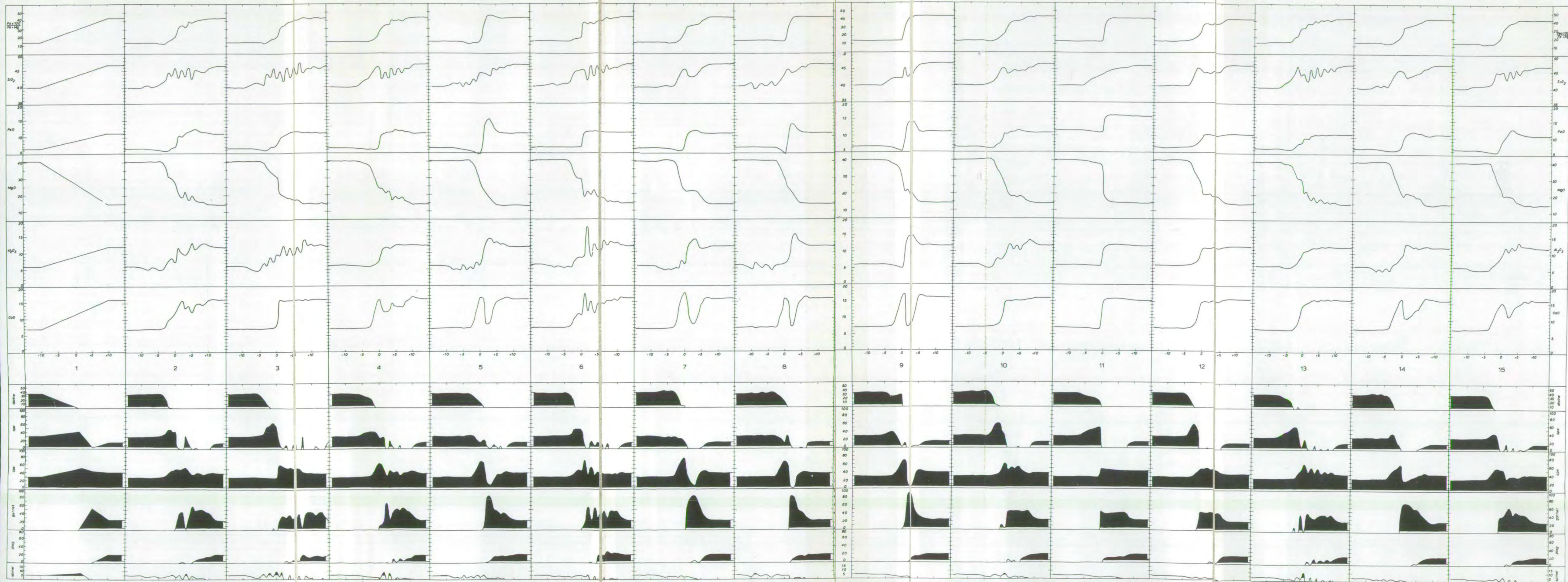


Fig. 4-40. A-C-F plots showing the results of the simulation model for reaction between ultrabasic and garnetiferous basic gneisses. Numbering as in Table 4-6. Runs 1, 11, 12, and 13 give linear plots and are omitted.





It appears that, for the development of diffusion zones with marked culminations and depressions, and a sigmoidal trend on the 'A-C-F' plot, there must be a contrast between the diffusion coefficients of MgO and SiO_2 , provided also that CaO also has a large diffusion coefficient. In results for which other conditions were used, a more nearly linear variation is produced, with a linear trend on the 'A-C-F' plot, and more gentle variations in mineral constitution.

Diffusion of these three oxides seems to control the resultant pattern. Those patterns most closely resembling the Loch an Daimh Mhor contact are nos. 14 and 15 (Table 4-6), in which all the diffusion coefficients are the same, except for those of SiO_2 and MgO respectively, with coefficients half those of the other oxides.

Wherever there is a sigmoidal trend on the 'A-C-F' diagram, it passes from the 'F' corner towards the 'C' corner, back towards the 'A-F' side, and then again towards the 'A-C' side. The only exception is result no. (3), where CaO is not an actively diffusing constituent. It would appear to be an inherent property of the system, as defined by the phase diagram and the activities used, to tend to produce trends of this type. Reduction of the CaO content of the ultrabasic member has no effect on the CaO enrichment of the contact gneisses predicted by the model.

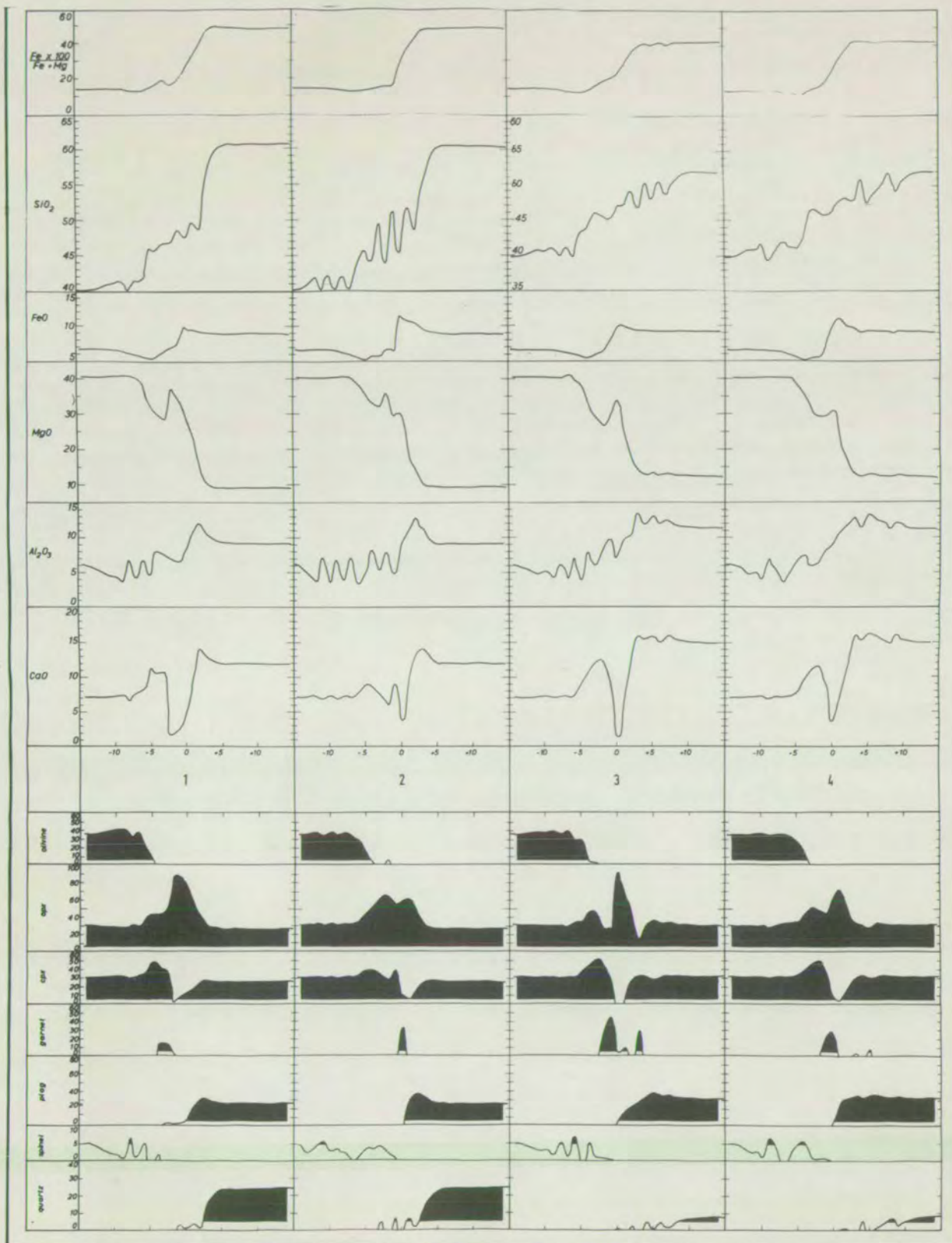
Using the values for diffusion coefficients which best simulate the Loch an Daimh Mhor sequence, simulation was attempted of the diffusion between both acid and quartz bearing basic, and ultrabasic gneisses. The results are shown in fig. 4-41, and 'A-C-F' plots of the results in fig. 4-42. The results do not resemble the contact sequences. There is first a culmination then a depression in augite content, the hypersthene shows a

Fig. 4-41

Results of the simulation model for the reaction between acid (1 and 2) and basic (3 and 4), and ultrabasic gneisses. Details as in fig. 4-39.

Diffusion coefficients

<u>RUN</u>	CaO	Al ₂ O ₃	MgO	FeO	SiO ₂
1	1	1	1	1	0.5
2	1	1	0.5	1	1
3	1	1	1	1	0.5
4	1	1	0.5	1	1



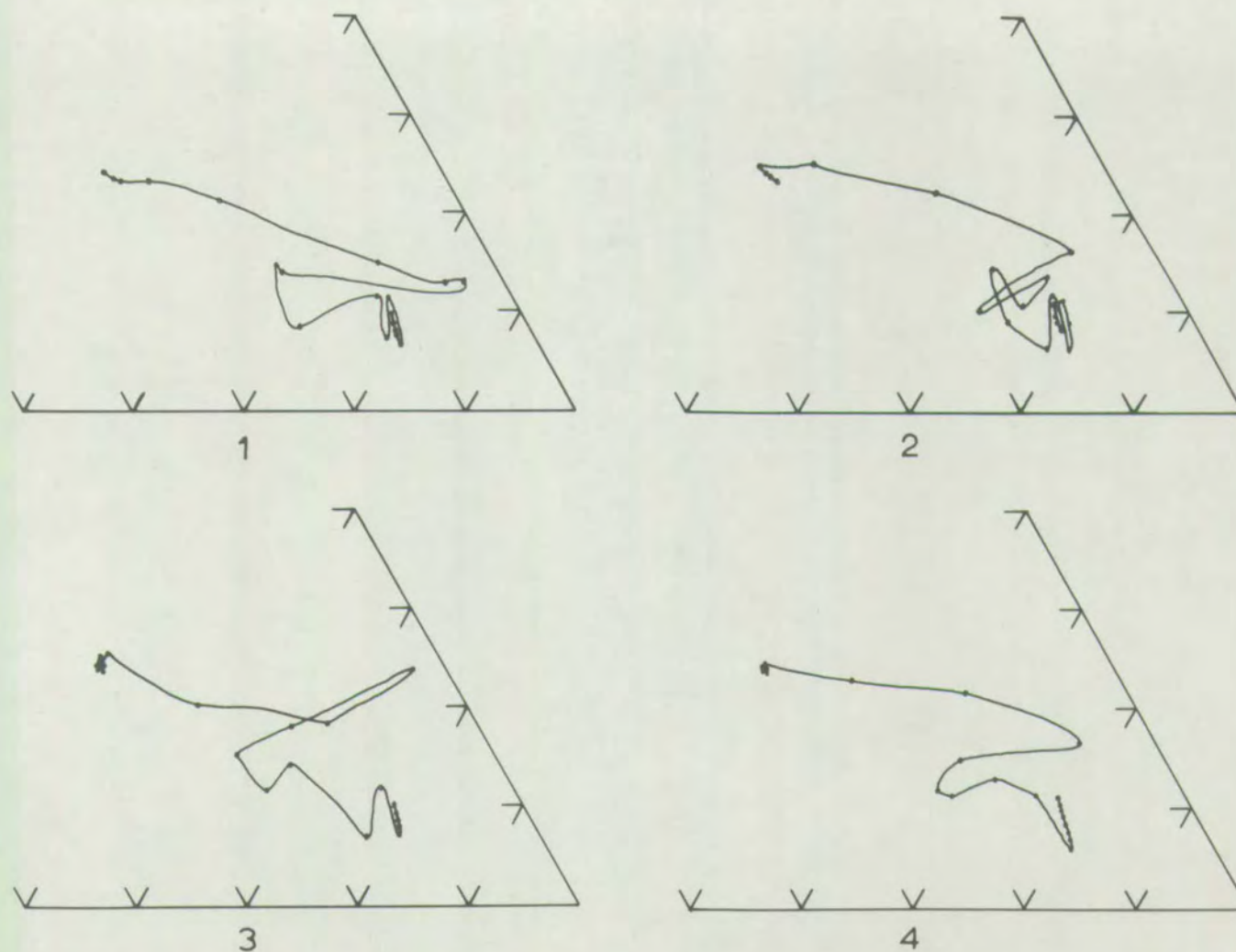


Fig. 4-42. A-C-F plots as in fig. 4-40 showing the results of the simulation model for reaction between acid and basic and ultrabasic gneisses. Captions as in fig. 4-41.

great culmination, and garnet appears as a minor phase in the same zone as the augite depletion. The association of garnet with abundant hypersthene and only minor augite is not seen in any rocks at Scourie or Ben Strome. The composition of the hypersthene rich zone is not dissimilar to that of the marginal pyroxene-hornblendites or to the contact described by Sørensen (1954), and if hornblende had been considered as a possible phase, with water as a component, such rocks might perhaps have been successfully simulated. Once again, all the sequences, as seen on 'A-C-F' diagrams (fig. 4-42) are sigmoidal, and in the same sense as those of figs. 4-40.

4.12 Summary

From structural and other field observations, it was concluded that the formation of the contact gneisses probably post-dated the juxtaposition of ultrabasic and basic or garnetiferous basic gneiss material.

From a consideration of the chemistry of the ultrabasic gneisses, it was concluded that the chemical variation, and hence the compositional layering in these rocks, may result from metasomatic introduction of country rock material into an originally homogeneous peridotite, or from their being hypersthene-olivine-amphibole cumulates in a layered intrusion. The chemistry of the basic and garnetiferous basic gneisses is not inconsistent with their being gabbroic liquids, but does not favour their being cumulates unless an amphibole was a major cumulus phase. A scheme of liquid evolution involving extensive olivine fractionation, followed by hornblende fractionation, was suggested. The garnetiferous and garnet-free basic assemblages occur in rocks of similar composition and may be explained by the two states being almost in equilibrium, the basic having formed from the earlier, and more chemically homogeneous, garnetiferous basic by a small

amount of metasomatic interchange with the acid gneisses.

The chemical variation in the contact sequences was summarised, and it appeared that the two extreme types of contact defined on field and petrographic features can be distinguished chemically, and further, that all intermediate types also occur. The occurrence of contact gneisses of Loch an Daish Mhor type with extreme chemical culminations and depressions, is associated with the existence of a great deal of garnetiferous basic gneiss; as the amount of basic rock decreases the chemical variation becomes more nearly linear, until the Geodh'Banruig Lower Contact type is reached, in which no basic material is present, and there is a simple chemical discontinuity between what appear to be modified ultrabasic and acid gneisses.

The mineral chemistry of the contact gneisses from Geodh'Banruig and Loch an Daish Mhor showed that in these rocks local equilibrium prevailed until a late stage, with a continuous variation in mineral composition across the contacts. At this late stage, a change in the stability of garnet resulted ⁱⁿ ~~and~~ its partial conversion to hypersthene + plagioclase + spinel, and this process caused chemical redistribution on the scale of single grains only.

The theory of diffusion between contrasted rock types was outlined, a simple test of mass balance to distinguish sequences which have originated by diffusion alone proposed, and a simple simulation model for diffusion outlined. The mass balance test showed that the contact sequence ^{from} ~~from~~ ultrabasic to garnetiferous basic gneiss could be regarded, within reason, as a diffusion sequence, but the same test showed that the entire sequence ultrabasic/garnetiferous basic/basic/acid gneiss cannot have originated by simple diffusion but that a large amount of much longer-distance mass transfer must have taken place.

The mathematical model can simulate with some accuracy the Loch an Daimh Mhor and Geodh'Eanruig upper contact types of sequence from ultrabasic to garnetiferous basic gneiss. When the values of diffusion coefficients which ^{give} the most satisfactory results for these sequences are used to simulate reaction between ultrabasic and acid gneisses, a chemical pattern which more nearly matches the Geodh'Eanruig lower contact type results, but which is not exactly similar to any observed rocks.

4.13 Discussion

All these observations lead towards the conclusion that the formation of the contact gneisses is a later feature than the formation of the basic and garnetiferous basic gneisses. It is very probable that these contact gneisses resulted from simple diffusion between the ultrabasic and garnetiferous basic gneisses, under conditions of the granulite facies.

The origin of the basic and garnetiferous basic gneisses is more obscure. The failure of the simulation model to produce rocks of this basic composition does not preclude the possibility that they originated by diffusion between the ultrabasic and acid gneisses; neither does it favour it. It is possible that they originated under lower grade metamorphic conditions by such diffusion processes. Under the conditions of the amphibolite facies, the basic rocks would consist of amphibolite. Such a rock type might have formed by diffusion between a serpentinite and an acid schist: the conditions of the mass balance still apply, and some long distance transport would be required. As suggested above, this could have been by the migration of material into or out of a paligenetic fluid, which would be subsequently lost.

The alternative possibility, that the basic rocks represent original basic igneous material, has been considered. None of the analyses of basaltic rock

presented in this chapter is of a rock from an orogenic basic-ultrabasic complex. Although Alpine ultrabasic rocks are very frequently associated with basic types (e.g. Nakayama, 1960; Miyashiro, 1965; Thayer, 1967), attention has usually been focussed almost exclusively on the ultrabasic members. The association has been regarded as the result of the basic rocks forming a favourable site for the intrusion of serpentinite (Jahns, 1967), but more usually has been interpreted as a magmatic association (Bailey and McCallien, 1960; Hess, 1968; Thayer, 1967). Miyashiro (1965) has observed that some Alpine serpentinites have compositions similar to some picritic lavas, and concluded that they may, in some cases, be derived from such lavas. The association of cherts with basic lavas and serpentinites ('The Steinman Trinity', of Bailey and McCallien, 1960) is very common. One rock which could be interpreted as representative of a chert has been observed at Scourie, and consists of a quartz-ore-pyroxene gneiss (with some garnet), forming a thin band in the basic mass at Pairc a'Cladaich (O'Hara, 1960, p. 43).

The lack of geochemical studies of Alpine basic-ultrabasic complexes means that a direct comparison of the compositions of the basic and garnetiferous basic gneisses with those of less metamorphosed igneous rocks from similar situations is not possible. The general similarity with the compositions of some igneous rocks, and the existence of some poorly defined geochemical trends do suggest the possibility of an origin as igneous liquids. Although the compositions have an unusual relation to the putative phase boundaries in the reduced system C-M-A-S, this has been shown to be a similar relation to that of the ocean floor tholeiites. Thus, whatever mechanism is postulated for the origin of this unusual relationship, it must have operated in a wide variety of places, and at different times.

The change in variation across the contacts appears to be related to the amount of garnetiferous basic gneiss between the ultrabasic and acid gneisses. This may be explicable by the influence of the acid gneiss in changing the assemblage of the garnetiferous basic to that of the basic gneisses. The chemical potential of silica in the basic member will thus be raised, and if this happens close to the ultrabasic contact, the diffusion of silica into the ultrabasic gneiss will have been increased. This effect could be paralleled in the simulation model by an increase in the diffusion coefficient of silica. If this were previously lower than that of MgO the results derived by the model would change to a nearly linear variation, instead of the erratic variation of the Loch an Daibh Mhor type. If the garnetiferous basic were entirely made over to basic gneiss, or there was no basic material present at all, then the results derived by the model would change to the hypersthene rich types of fig. 4-41. These to some extent resemble the contacts at Cleit Mhor and the Geodh'Eanruig lower contact, but the latter are hornblende rich and cannot be simulated by the model. The effect is shown diagrammatically in fig. 4-43.

Conclusions

From the data and arguments presented above, the following tentative conclusions may be drawn.

Ultrabasic gneisses

The ultrabasic gneisses may represent either a layered series of olivine-hypersthene-amphibole cumulates, in which the amphibole crystallising had about 2500 p.p.m. Cr, and Fe/Fe + Mg about 0.19 or an originally fairly homogeneous series of peridotites, whose compositions were similar to that of B 241, from Camas an Lochain, in which metasomatic introduction of country rock material

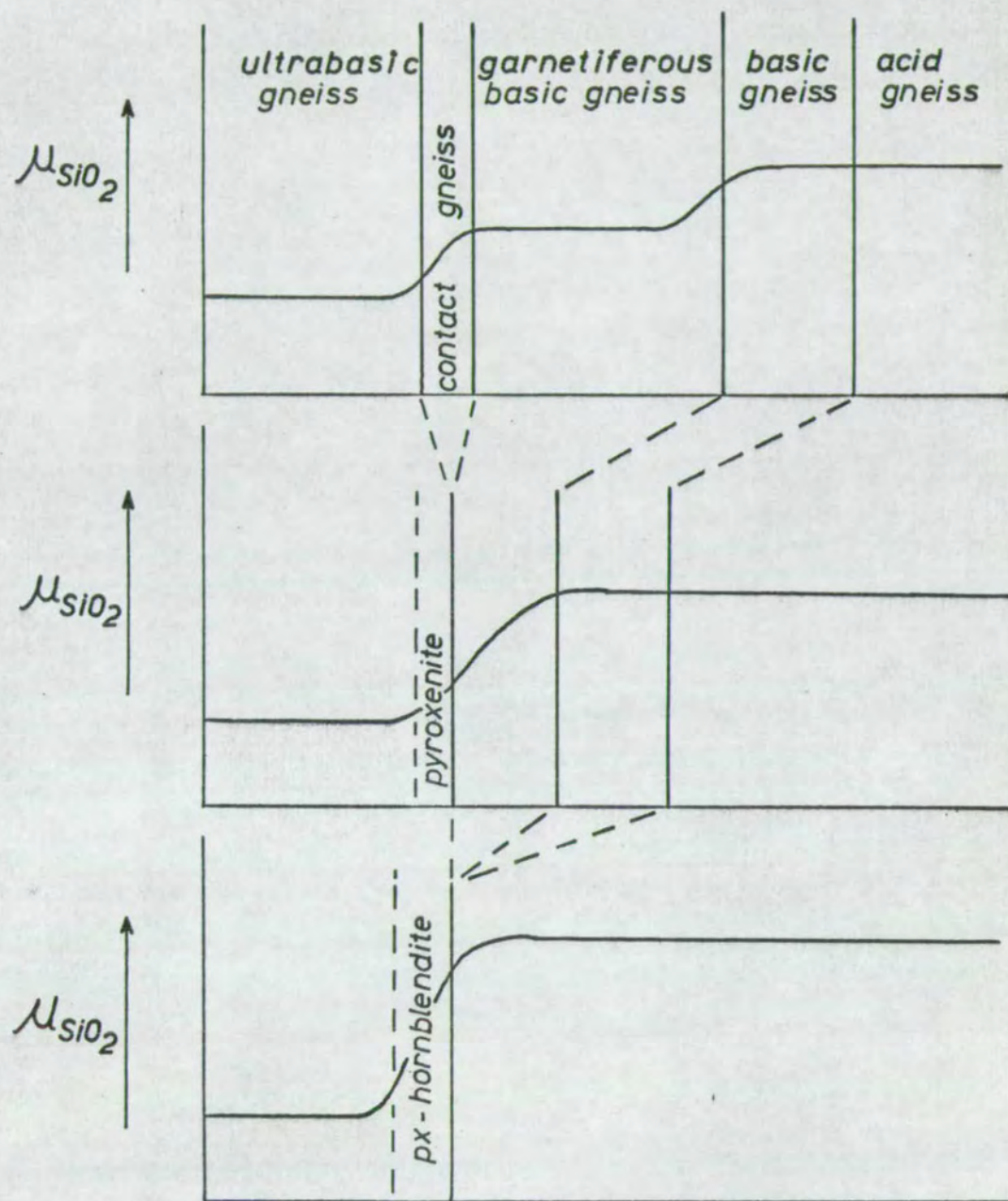


Fig. 4-43. Possible influence of μ_{SiO_2} on the diffusion of silica across ultrabasic contacts. For explanation, see text.

has produced compositional layering.

Basic and garnetiferous basic gneisses

The basic rocks may represent either a diffusion zone produced between the acid and ultrabasic gneisses at a relatively low metamorphic grade, from which a large amount of material was exchanged with a palingenetic fluid phase, now lost, or a series of basic igneous rocks. These igneous rocks could be either liquids produced by partial melting of garnet-peridotite at 30-40 Kb., followed by continuous fractionation of olivine at decreasing pressure to 10-15 Kb., with later fractionation possibly involving an amphibole, or a series of cumulates in which an amphibole was a major cumulus phase.

The two different mineral assemblages may be largely due to their representing two states almost in equilibrium, and that the acid gneiss caused a small amount of metasomatic transfer, sufficient to render the basic assemblage the stable state in the outer parts of the bodies.

Contact gneisses

The contact gneisses were probably formed by reaction between the ultrabasic and garnetiferous basic gneisses under granulite facies conditions. The proximity or otherwise of the acid gneiss may have caused the chemical profile across the contact to vary from nearly linear to extremely erratic. Where no basic rock was present, the hornblende rich type of contact developed.

A change in physical conditions at a relatively late stage caused magnesian garnet to become unstable, and its partial breakdown to hypersthene + plagioclase + spinel resulted in the reaction textures characteristic of these rocks.

These conclusions are summarised in fig. 4-44.

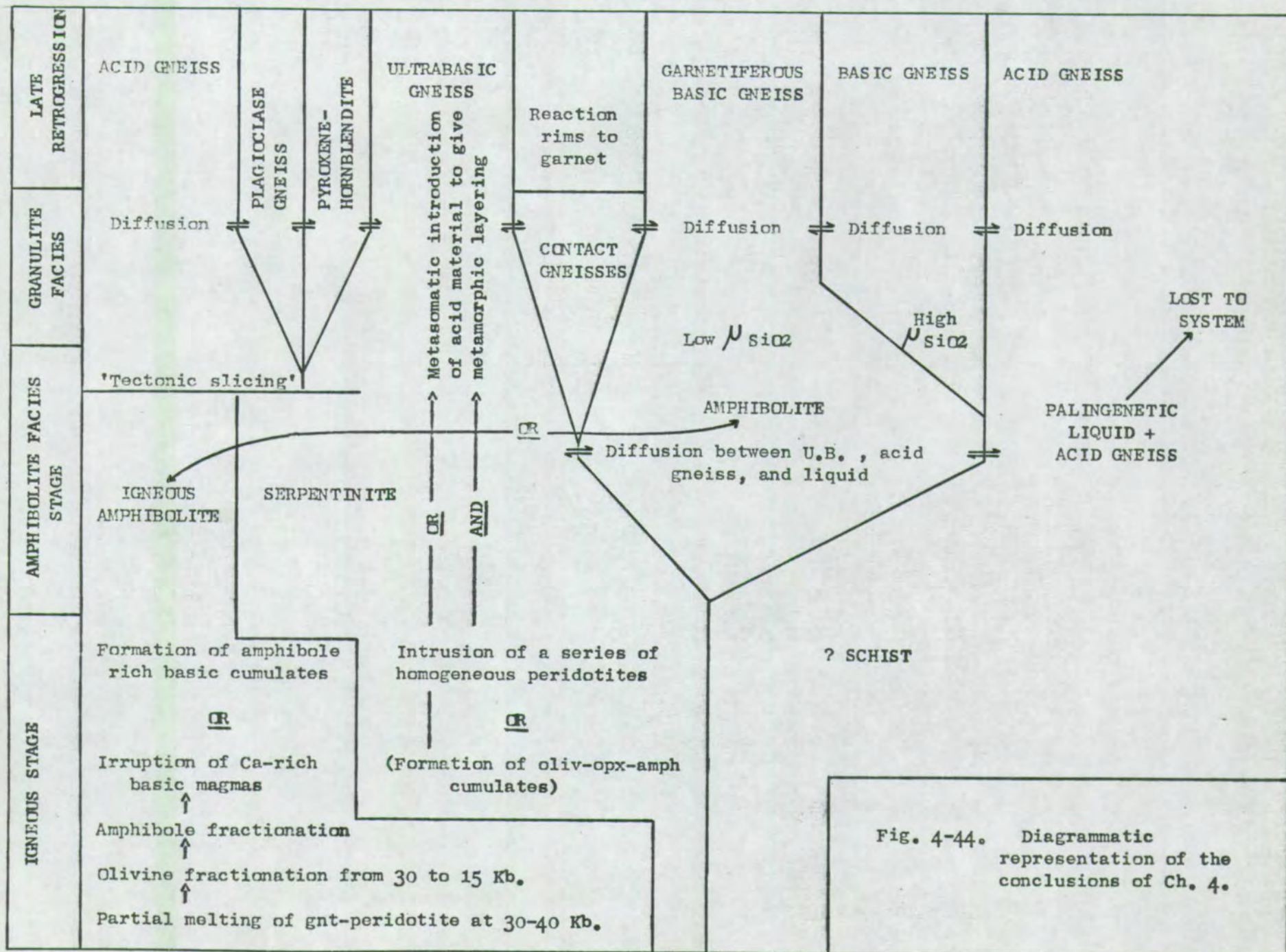


Fig. 4-44. Diagrammatic representation of the conclusions of Ch. 4.

CHAPTER 5THE POTASH RICH LEUCOCRATIC GNEISSES

These rocks, termed 'quartz-perthite gneisses' (O'Hara, 1960), and 'bands of unusually acid character' (Clough et al., 1907, p. 132), are almost unique amongst the Scourian gneisses, in that they often contain potash feldspar. They form a very minor part of the Complex, and are closely associated with the basic and ultrabasic gneisses. Several features of the group suggest that they may represent the products of partial melting at an early stage in the evolution of the Complex, and an argument will be advanced in support of this suggestion.

5.1 Petrography

The petrography of this group has been described by O'Hara (1960, pp. 38-40). The principal features may be summarised:

(1) Lenticular grains of quartz, often pale blue and opalescent, up to 1 cm. long and 2 mm. wide, define the foliation. In some cases, the quartz grains are equidimensional, and the rock is massive.

(2) The occurrence of primary bar-like perthitic intergrowths in the feldspar, which may be orthoclase-perthite, mesoperthite, or andesine-antiperthite. The exsolution lamellae are continuous across a whole grain, and are of a regular crystallographic orientation.

(3) The further exsolution of these perthitic feldspars into microcline and andesine or oligoclase. This process can be observed in all its stages, from the uniform bar-like perthites to discrete grains of the two feldspars (O'Hara, 1960, figs. 19-21).

(4) Small grains of accessory apatite, zircon, or rarely (B 235, Camas an Lochain) garnet.

(5) Sericite and carbonate, finely disseminated through the felspar, especially the plagioclase, as alteration products.

(6) Occasional development of a crude banding, either due to the occurrence of relatively mafic streaks, or layers relatively richer in quartz and felspar.

5.2 Chemistry

Analyses, norms, and modes of thirteen leucocratic gneisses, twelve of which contain free potash felspar, are given in Table 15. Some of the geochemical features of the group are shown in the following figures: figs. 5-1 to 5-4 show the element pairs K-Rb, Rb-Sr, Ba-Sr, and Y-Rb for the analysed rocks (figs. 5-1 to 5-3 also showing the same data for the Scourian acid gneisses from Holland (1965)). Figs. 5-5 and 5-6 are ternary diagrams of the normative felsic minerals (Ab-Or-An and (Ab + An) - Or-Qz diagrams), with the composition fields of the Scourian acid gneisses, the Laxfordian gneisses, and the Laxford Granites (Holland, 1965).

5.3 Field relations

The potash rich leucocratic gneisses occur almost exclusively associated with basic-ultrabasic masses (Clough et al., 1907, pp. 132 and 134). Where they form layers within such masses, they are always bordered by basic gneiss, although this may show evidence of having been garnetiferous (e.g. B 287, p. 38). The layers may extend beyond the margins of the basic mass. Such is the case at Pairc a'Cladaich (fig. 3-6) where the leucocratic gneiss layer extends for over 1000 feet north-eastwards beyond the basic and ultrabasic rocks (and beyond the edge of the map).

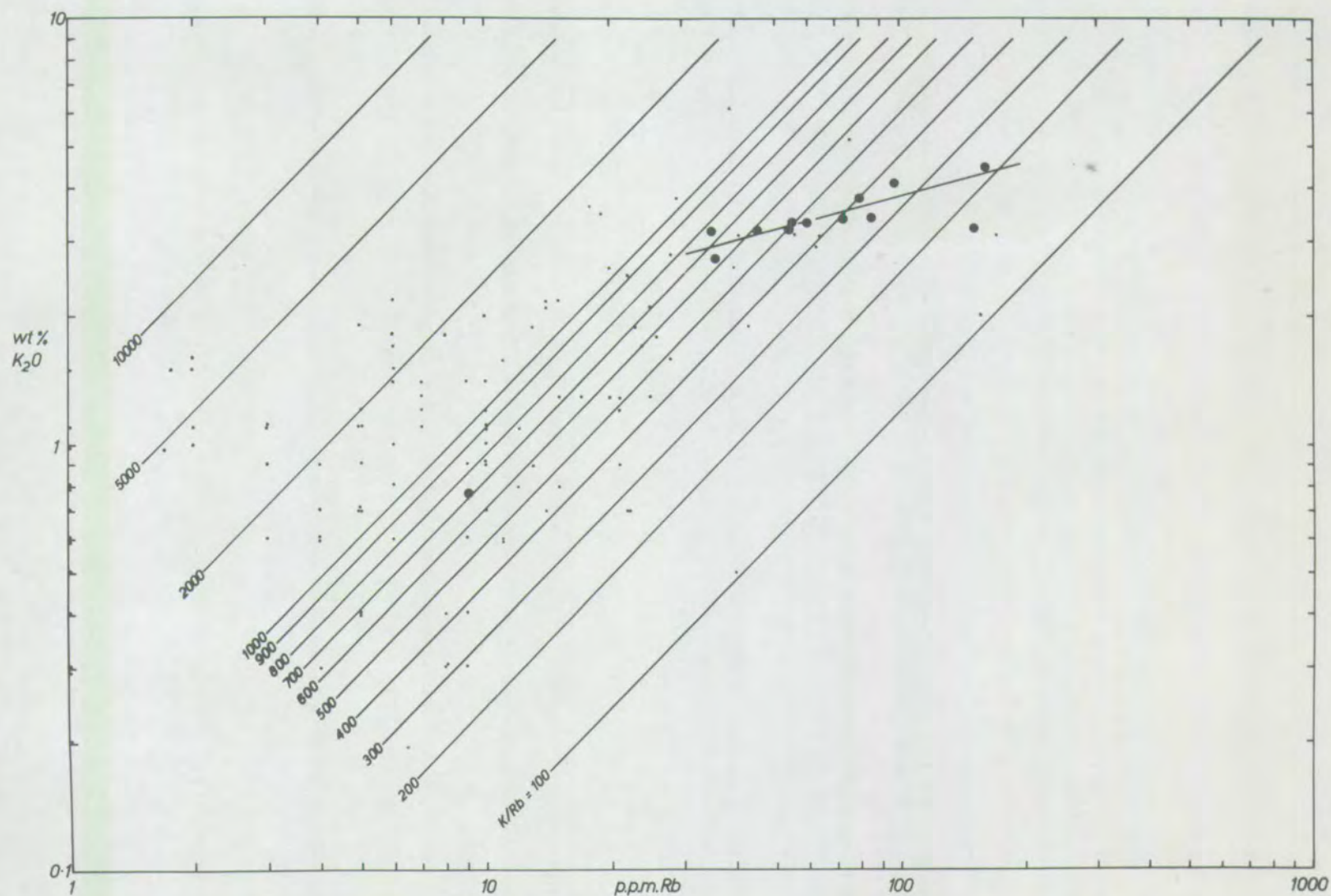
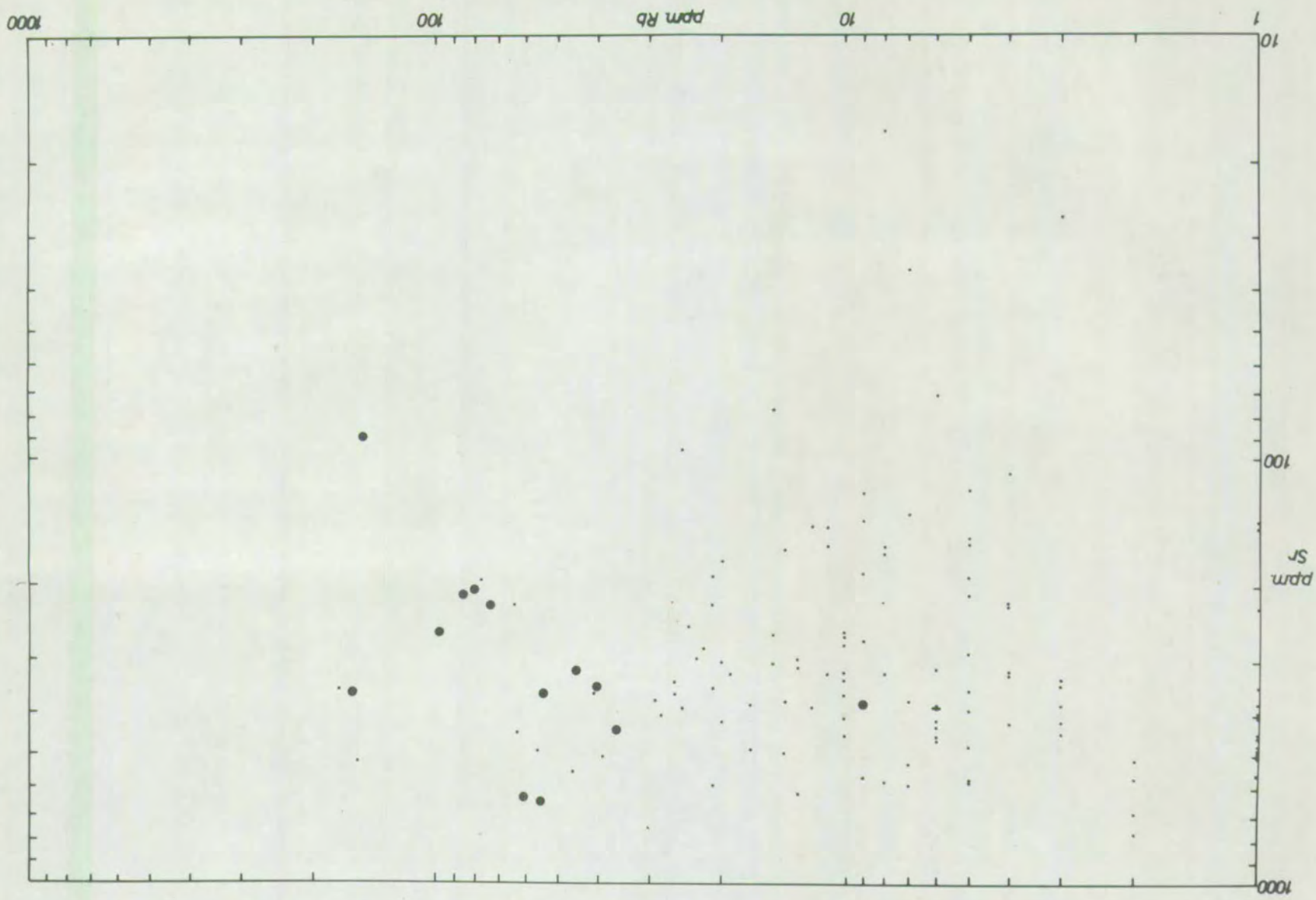


Fig. 5-1. Logarithmic plot of K (as K₂O) against Rb for the leucocratic gneisses (circles). Dots represent analyses of 'pyroxene granulites' (mostly acid gneisses) from Holland (1965). Parallel lines are of constant K/Rb ratio.

Fig. 5-2. Logarithmic plot of Rb against Sr for the leucocratic gneisses. Symbols as in fig. 5-1.



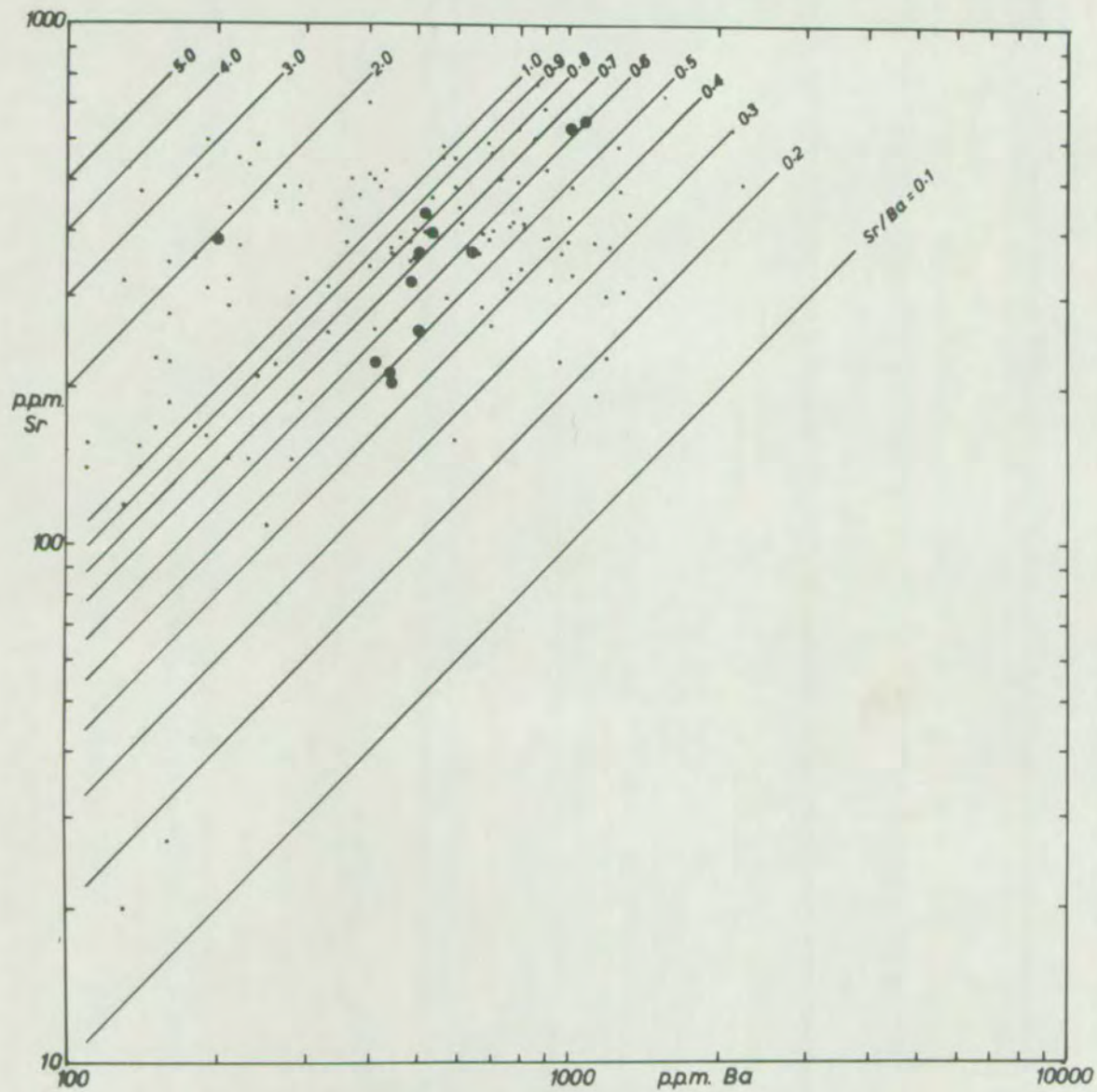


Fig. 5-3. Logarithmic plot of Ba against Sr for the leucocratic gneisses. Symbols as in fig. 5-1.

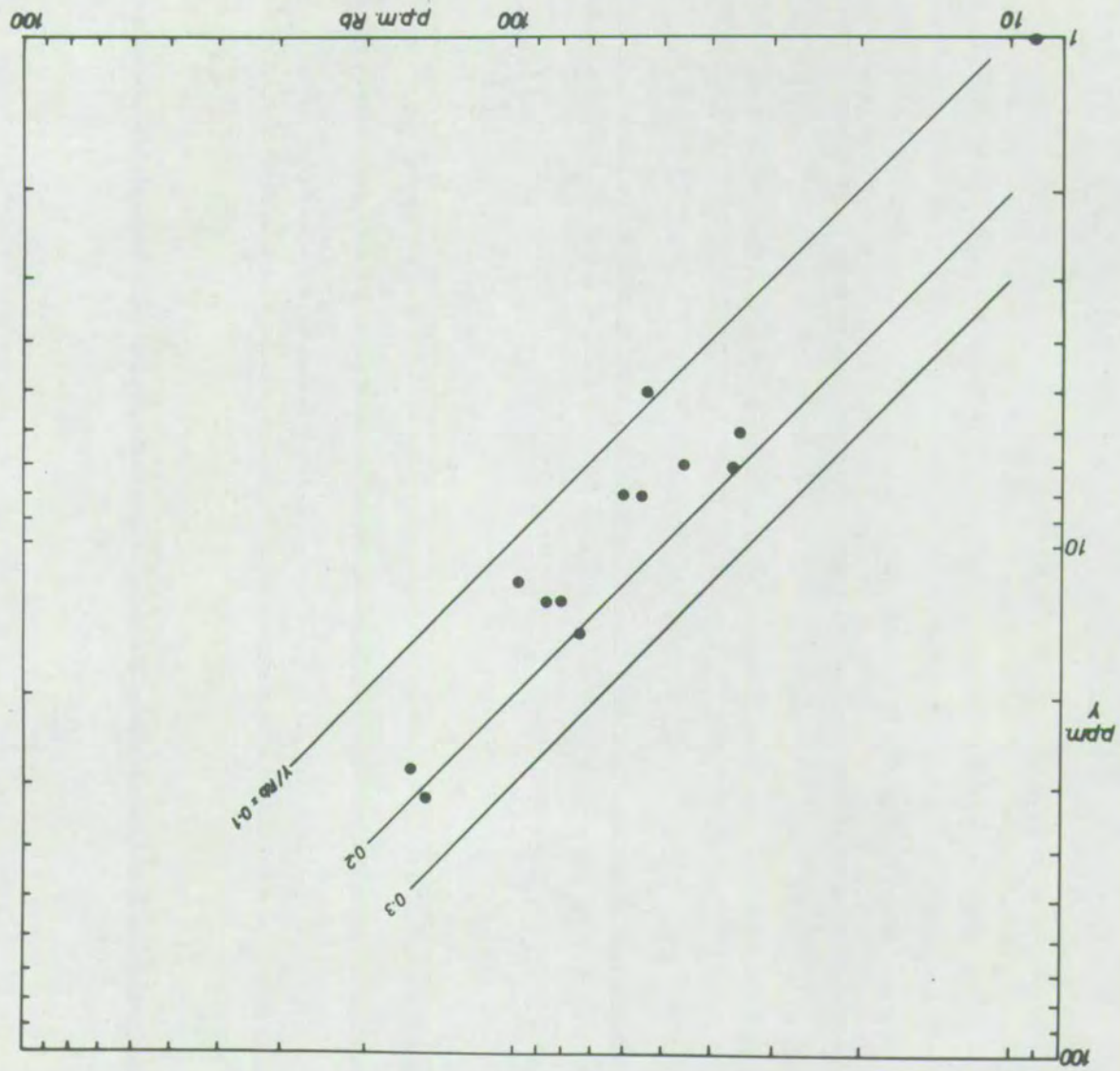


Fig 5-4. Logarithmic plot of Y against Rb
for the leucocratic gneisses.

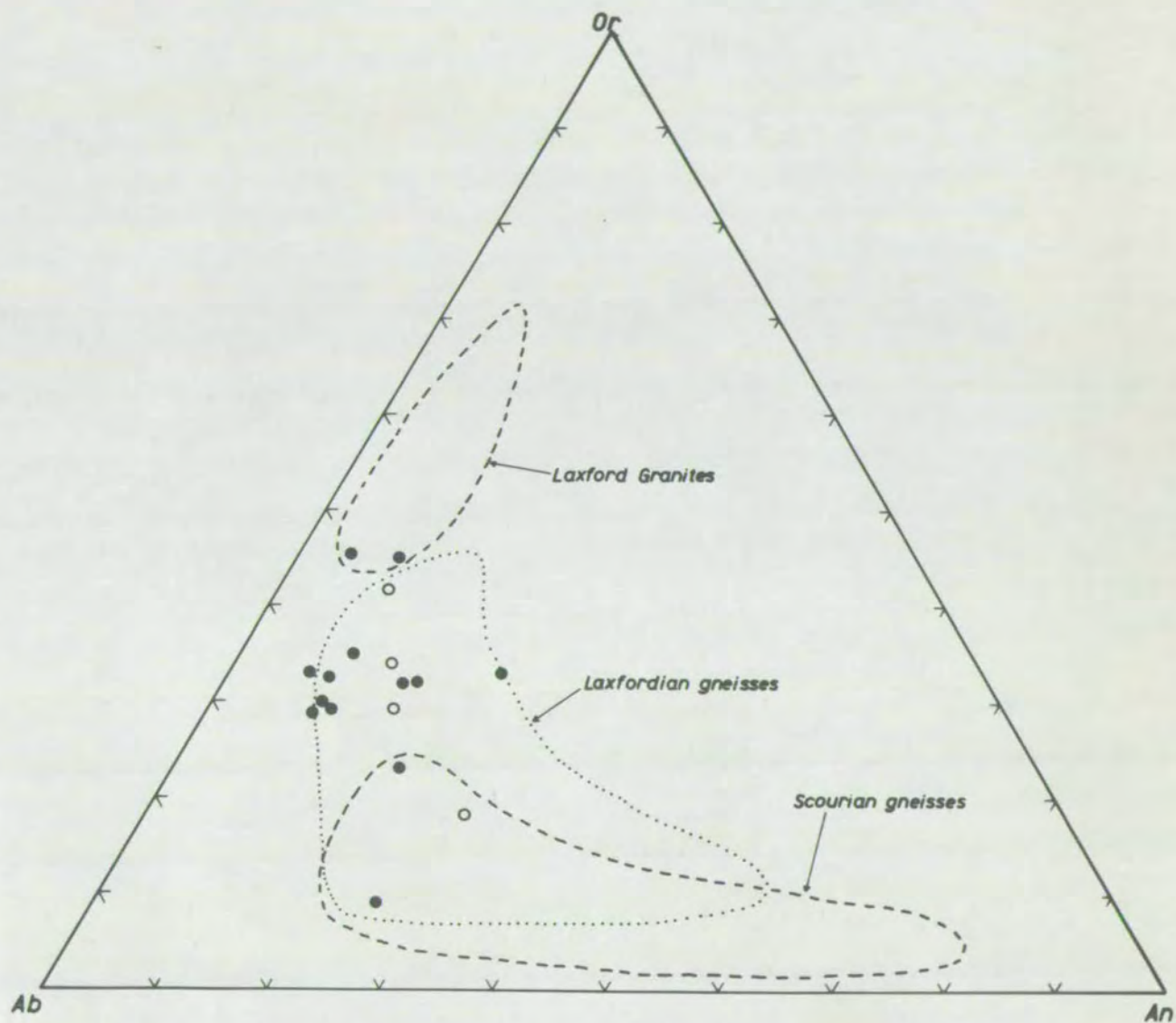


Fig. 5-5. Normative feldspar compositions (wt.%) of the leucocratic gneisses. The fields of other Lewisian acid rocks are taken from Holland (1965)

Solid circles - analyses from this study

Open circles - " " O'Hara (1960)

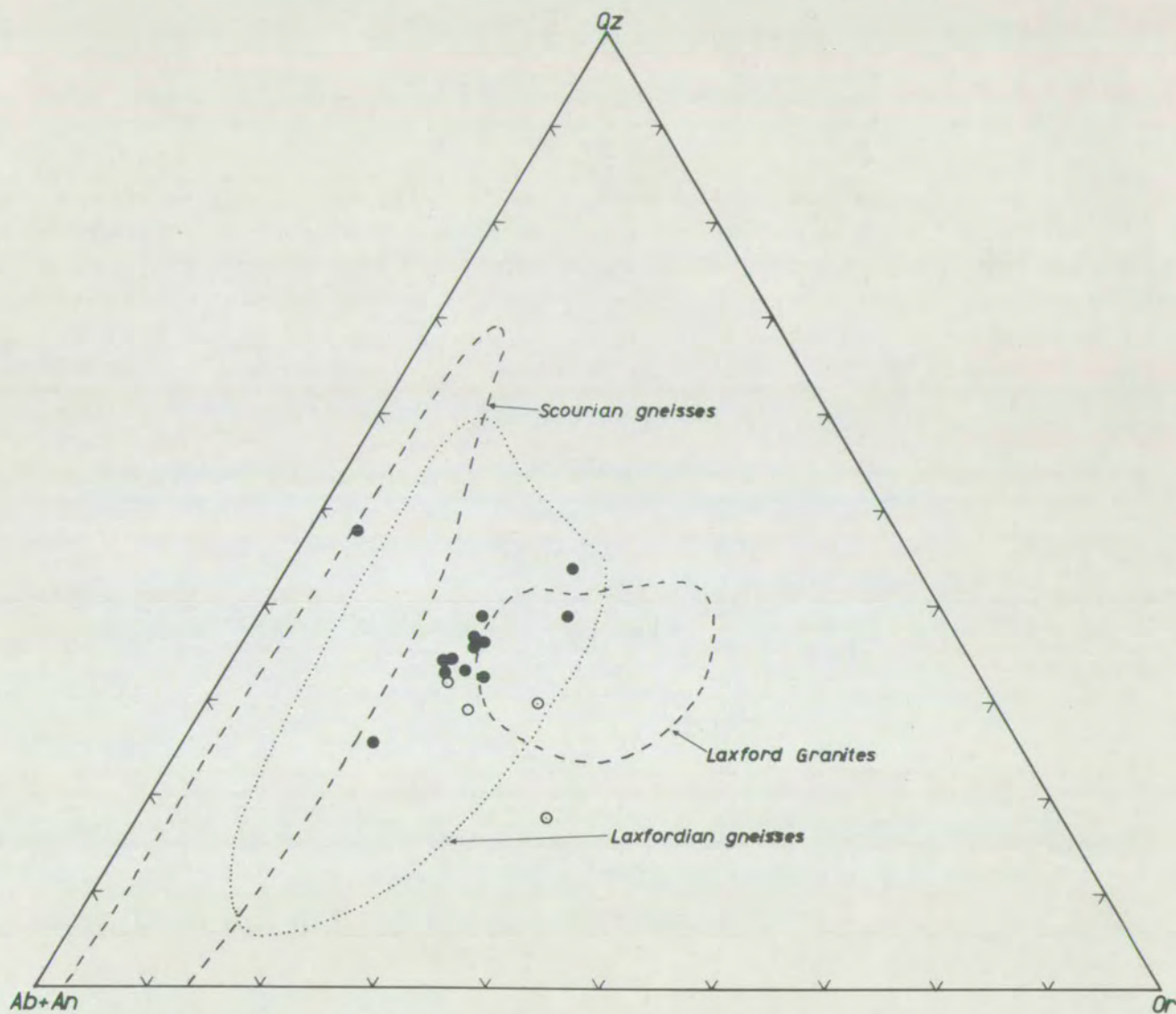


Fig. 5-6.

Compositions of the leucocratic gneisses in the residua system (wt. %). Sources of data as in fig. 5-5.

The occurrence of potash rich rocks at Scourie More (fig. 3-1) is different from the other localities mentioned in this study. The layer, where it is seen furthest inland, is indistinguishable from the adjacent acid gneisses, except by its salmon pink colour, the other rocks being greyish. As it is followed towards the shore, it becomes broader, and pegmatitic patches up to 2 feet across become common, in which the grain size coarsens and the banding is lost, forming up to 10% of the rock (fig. 5-7). Also, as the band becomes broader, layers of basic gneiss are observed on either side of the potash rich rocks, and separate them from normal acid gneisses.

The large masses of leucocratic gneiss within the basic and ultrabasic mass at Ben Stromie occur as layers between basic bands. They appear to have been mobile relative to the basic gneisses, and separate disrupted masses of the latter. At the core of the major F1 fold (see Appendix A), the poorly defined foliation and lineation in the leucocratic gneisses are axial plane and axial structures to the fold (p. A-3), indicating that these rocks were solid and susceptible to deformation at that time.

The overall concordance of the leucocratic gneiss layers is evident from a brief inspection of the occurrences. The layers are often multiple (the individual bands being too thin to be separately shown on the map), the bands frequently uniting and dividing. This phenomenon is shown at the Pairc A'Cladaich locality on a relatively large scale (fig. 3-5), and at other localities on the scale of individual exposures (fig. 5-8). The layer, in this case, is a zone of basic gneiss including a series of ramifying veins of potash rich leucocratic gneiss.

Fig. 5-7

Pegmatite patch in potash rich banded gneiss, on the coast at Scourie More (fig. 3-1). Banded gneiss of a normal appearance (left) passes along the strike into a coarse grained, massive rock.



Fig. 5-8

Leucocratic gneiss layer at the head of Camas near Buth (fig. 3-7).
The layer splits up and divides obviously separated masses of basic
gneiss.



Locally, the leucocratic gneiss layers show discordant contacts, both to the acid gneisses (fig. 5-9), and the basic gneisses (fig. 5-10). The discordance shown in fig. 5-10a is important in that, although the contact cuts the banding in the basic gneiss at angles up to 90° , the foliation in the leucocratic gneiss, defined by the lenticular quartz grains and a weak banding, is concordant with that in the basic gneiss. Thus, if the discordance is accepted as the result of the intrusion of a liquid, this liquid must have been largely solidified by the time of the main phase of deformation.

5.4 Petrogenesis

O'Hara (1960) regarded the leucocratic gneisses as of metasomatic origin, formed by the introduction of country rock material into the basic masses. The occurrence of identical rocks outside the basic-ultrabasic masses is not entirely consistent with such a conclusion. It is more consistent with an origin by segregation from the acid gneisses, by a process which does not require the basic gneiss as a recipient for metasomatism. Petrological opinion is increasingly favouring the mechanism of partial melting as a means of segregation in high grade metamorphic complexes. As this process has already been invoked (Chapter 2) for the evolution of the Scourian acid gneisses, it is relevant to consider the possible nature of liquids generated in this way, and to compare the postulated nature of these liquids with the compositions of the leucocratic gneisses, which, by their locally discordant contacts, show evidence, at least of mobility.

Data on melting relations in the system $\text{Ab-Or-An-SiO}_2\text{-H}_2\text{O}$ are not adequate to predict exactly the compositions of liquids generated by partial fusion of a given set of quartzofelspathic rocks. The following data were

Fig. 5-9

- (a) Discordant contact between leucocratic gneiss (above) and banded acid gneiss.

50 yards east of the road, North end of Loch an Daimh Mhor (fig. 3-1).

- (b) Discordant contact between leucocratic gneiss (above) and banded acid gneiss.

200 yards inland at Pairc a'Cladaich (fig. 3-6).



(a)



(b)

(q)



(p)

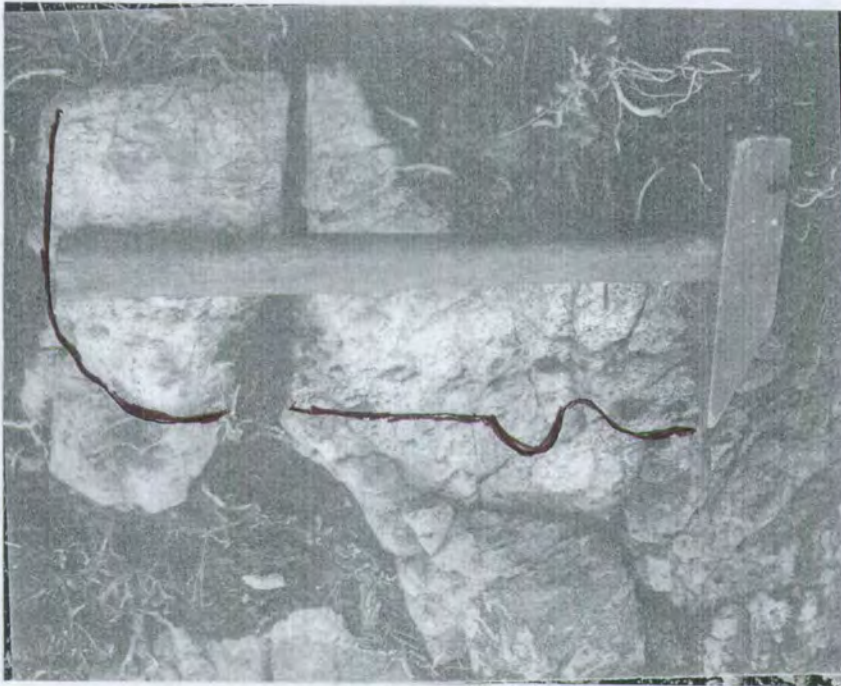


Fig. 5-10

Discordant contacts between leucocratic and basic gneisses, (a) at the head of Camas nam Buth, 40 yards inland (fig. 3-7), and (b) 50 yards east of the road, North end of Loch an Daimh Mhor.



(a)

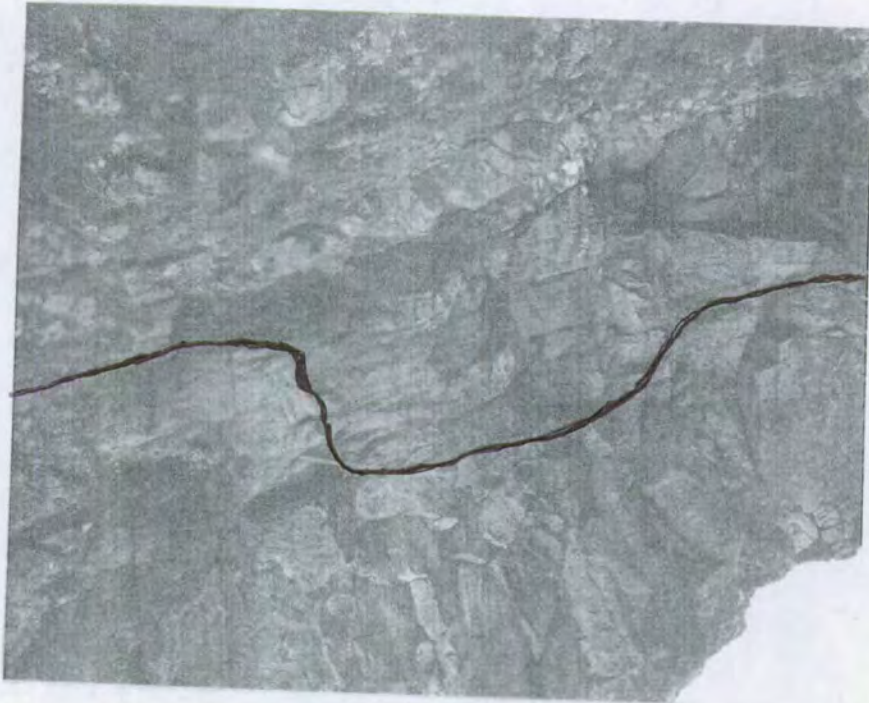


(b)

(q)



(p)



abstracted to construct tentative phase diagrams for relevant parts of the system. From the experimental data of Bowen and Tuttle (1958) and Luth et al. (1964) on the system $\text{Ab-Or-SiO}_2\text{-H}_2\text{O}$ the movement of the feldspar (potash feldspar or albite) + quartz + liquid + vapour cotectic towards the feldspar join with increasing $P_{\text{H}_2\text{O}}$ is well known. The quaternary invariant point (temperature minimum on the cotectic or five phase eutectic) moves towards the $\text{Ab-SiO}_2\text{-H}_2\text{O}$ face of the tetrahedron, also with increasing $P_{\text{H}_2\text{O}}$.

The work of Luth (1969) shows that the effect of pressure on the feldspar-quartz cotectic in the water-free system is very similar, so that at 10 Kb. the 'wet' and 'dry' cotectics are nearly coincident (when projected into the anhydrous system). The invariant point in the 'dry' system, however, lies close to the Or-SiO_2 join.

James and Hamilton (1969) and Von Platen (1965) present data on the movement of the cotectic towards the SiO_2 apex, and the quaternary eutectic towards the $\text{Or-SiO}_2\text{-H}_2\text{O}$ face with increasing anorthite content of the plagioclase at 1 and 2 Kb., water pressure. This data, combined with that cited above, and that of Stewart (1957) was used to construct fig. 5-11a, which gives the normative quartz contents of the plagioclase + quartz + liquid + vapour pseudoternary eutectic at various pressures. Fig. 5-11b represents the same data as a plot of normative quartz content of the 'eutectic' against anorthite content of the plagioclase.

The change in orientation of plagioclase-alkali feldspar tie-lines with temperature was predicted by Barth (1951). An experimental determination of tie-lines by Yoder et al. (1957) indicates that Barth's calculations

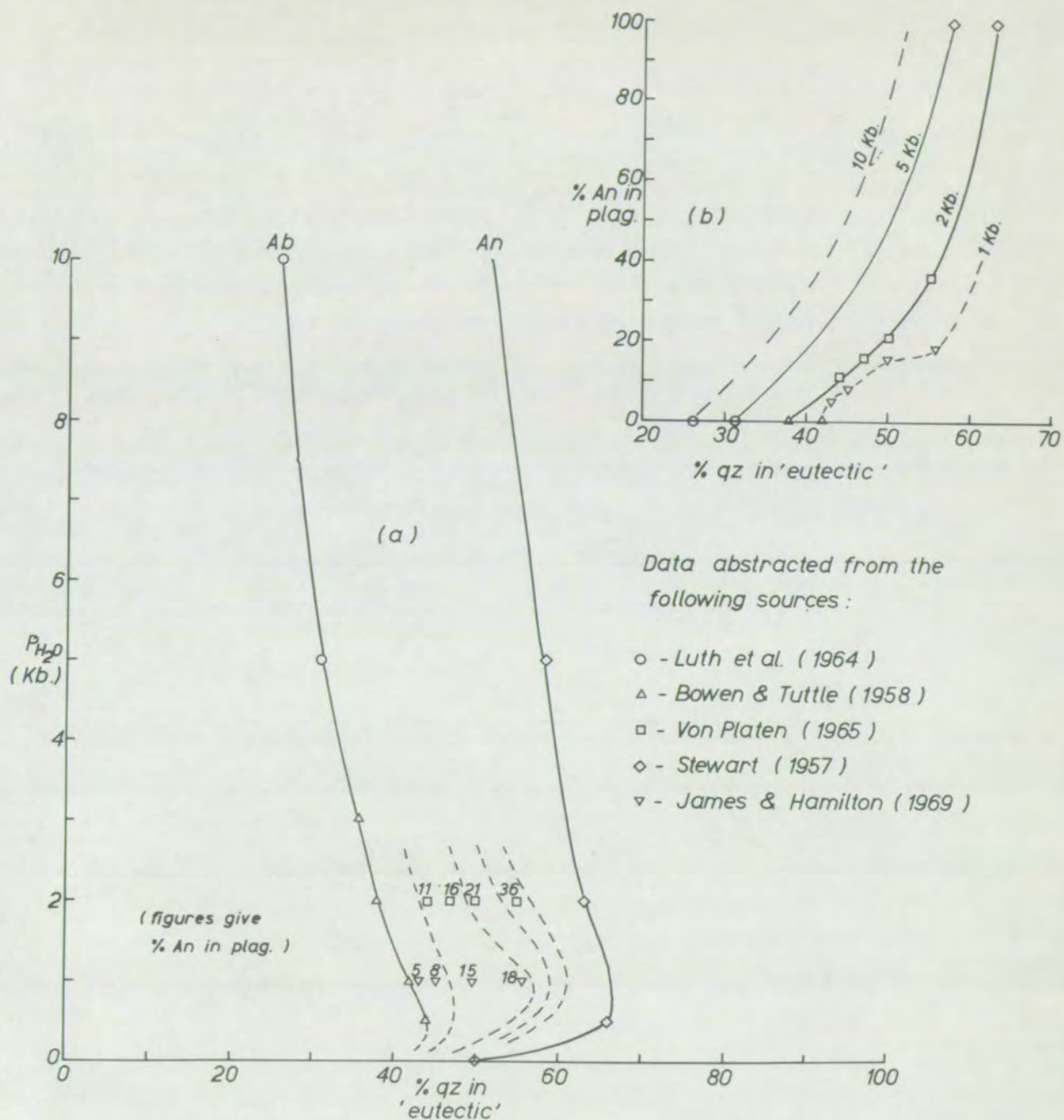


Fig. 5-11. Variation in composition of the qz.+plag.+liq.+vap. pseudoternary eutectic with (a) pressure at various plagioclase compositions, and (b) with plagioclase composition at various pressures.

give too low a temperature estimate for a given felspar pair. Fig. 5-12 gives tie-lines at 600-700°C, (calculated from the data of Yoder et al. (1957), on the assumption (Barth, 1951) that the ratio %Ab in alkali felspar/%Ab in plagioclase is constant at a given temperature) and 1000°C (extrapolation of the 700°C data assuming that the calculations of Barth (1951) correctly give the amount of change in tie-line orientation with temperature).

In general, the tetrahedron Ab-Or-An-H₂O (isothermal, isobaric projection from SiO₂ of the system Ab-Or-An-SiO₂-H₂O) at about 700°C will appear as in fig. 5-13. The field of liquid will expand with temperature, until, at about 850°C, it will intervene entirely between the H₂O apex and the anhydrous base of the tetrahedron. The melting of water deficient rocks can take place, the amount of melt produced being dependent on the water content. Tentative isothermal, isobaric projections of melting relations on to the anhydrous base of the tetrahedron for 650 and 675°C at 5 Kb. and 1000°C and 10 Kb. are given in fig. 5-14. The data used in the construction of these diagrams was obtained from the references cited above. Liquid compositions shown in heavy ink are in equilibrium with water rich vapour, while other liquid compositions are on the water deficient underside of the liquid volume in the tetrahedron Ab-Or-An-H₂O. The compositions of liquids likely to have been in equilibrium with the Scourian acid gneisses are shown in each case (i.e. the liquids from which the gneisses could have been the residua of partial melting). Fig. 5-15 shows the three liquid fields in comparison with the compositions of the leucocratic gneisses. All the compositions lie in or

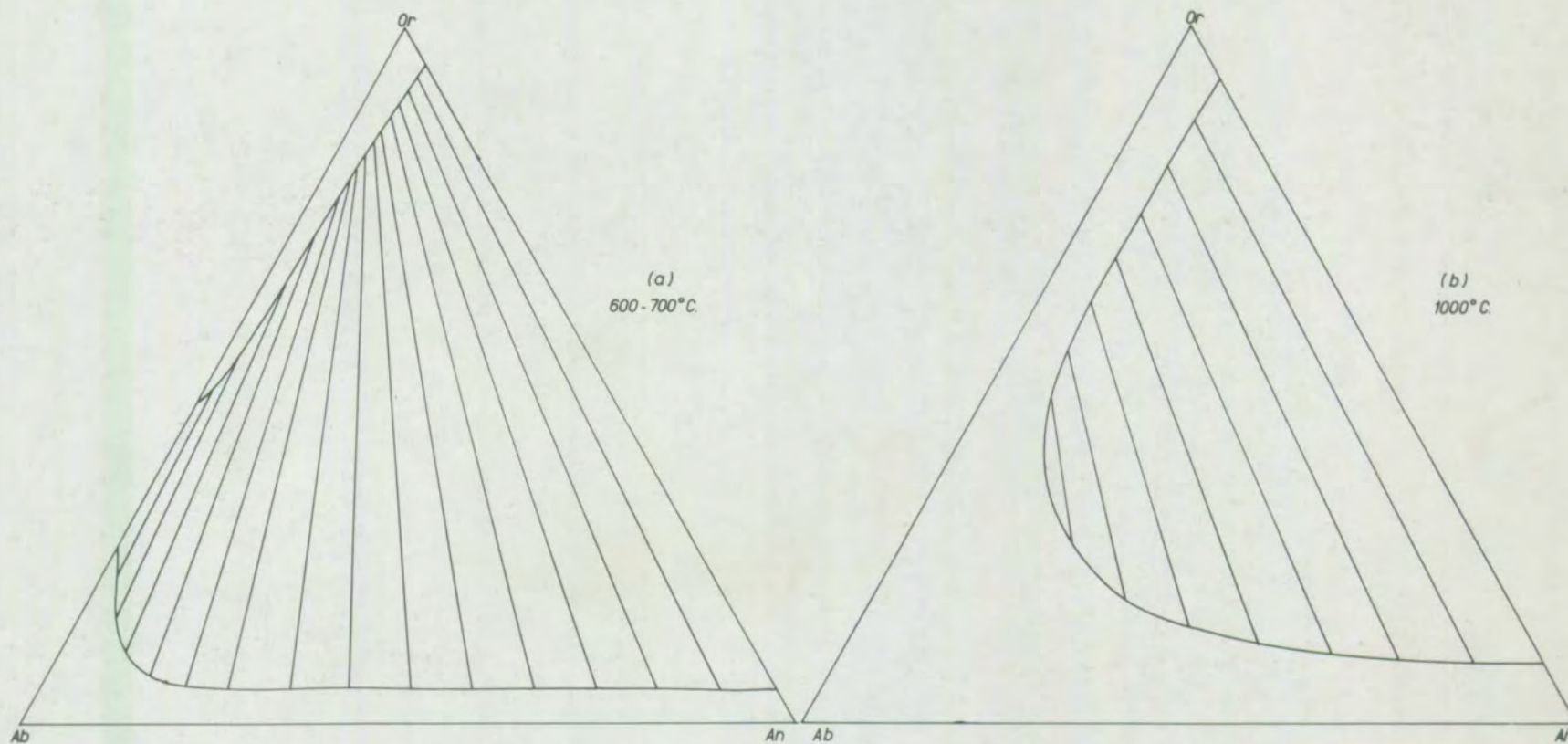


Fig. 5-12. Possible feldspar solvi and tie-lines. For derivation, see text. Diagrams in weight proportions.

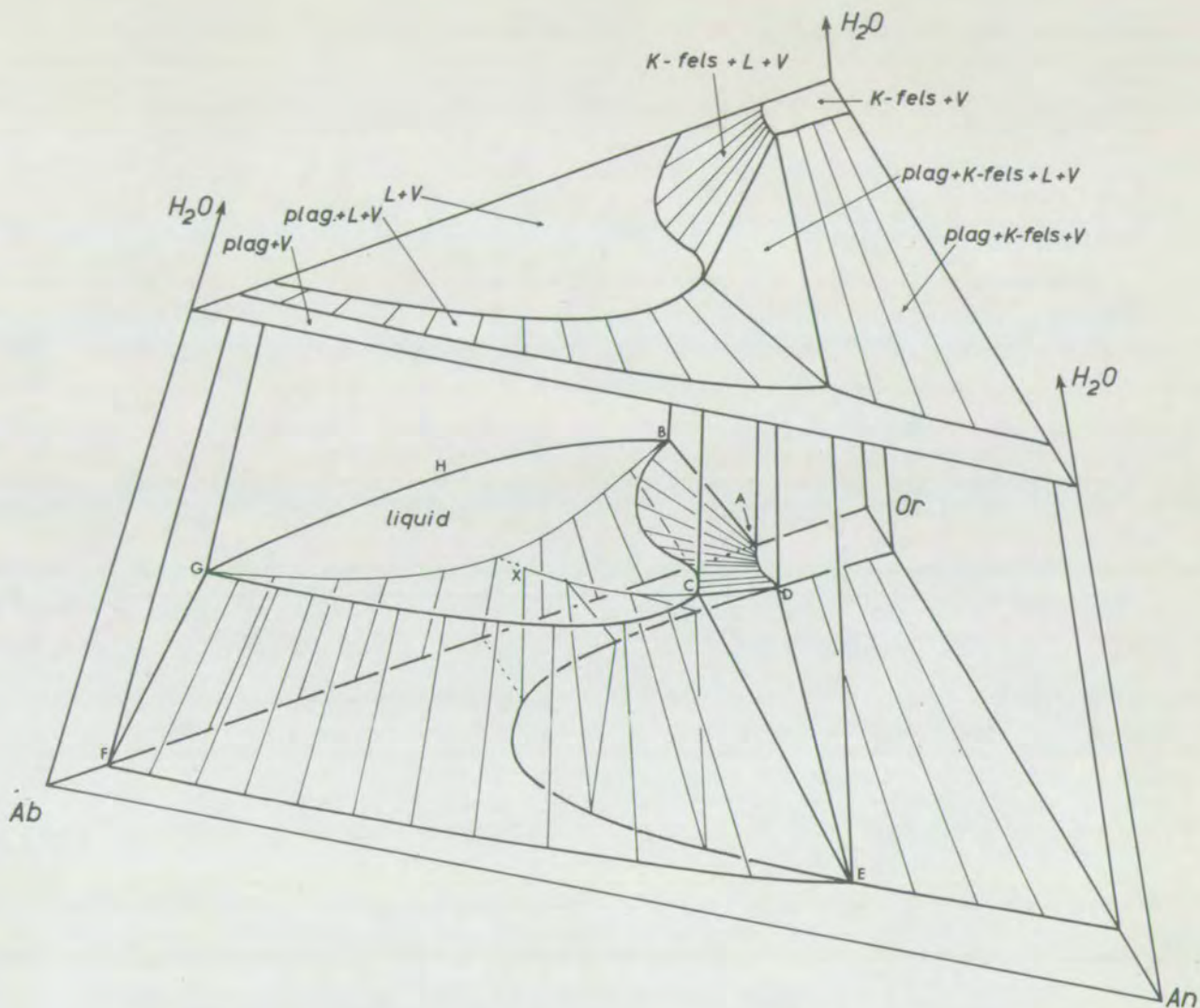


Fig. 5-13.

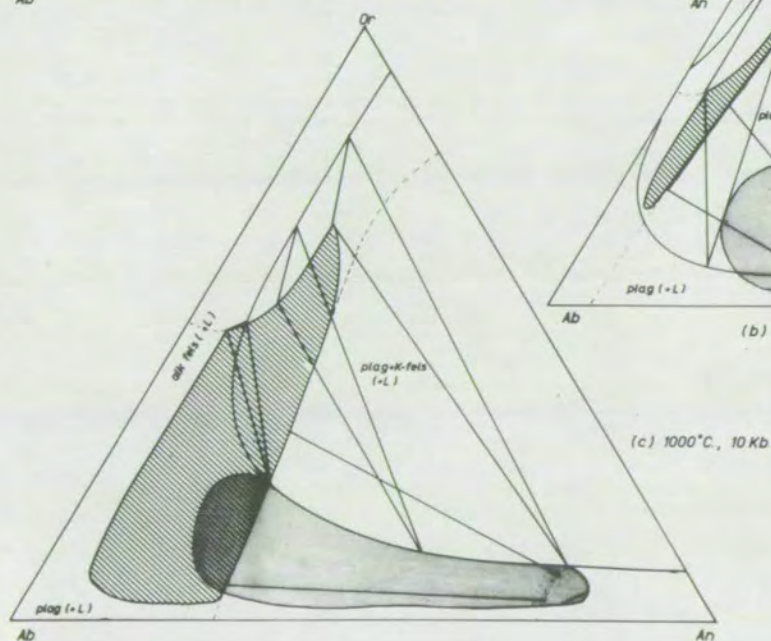
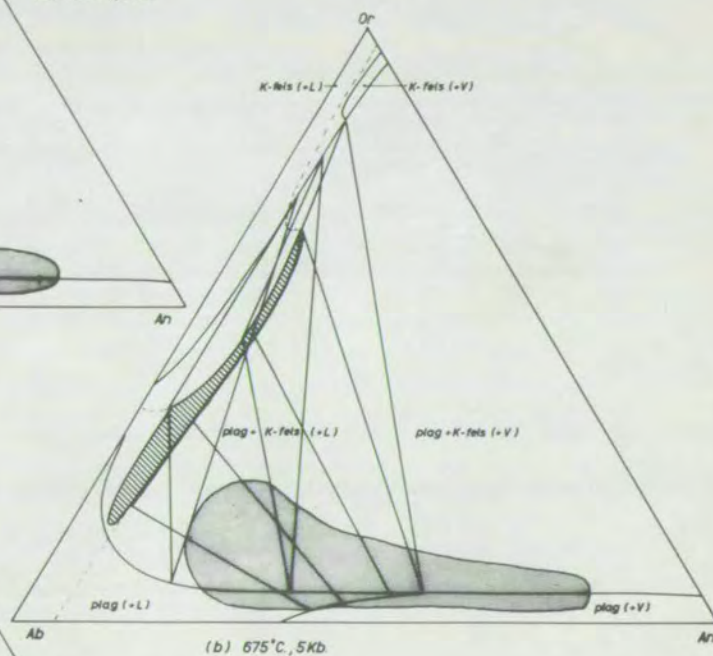
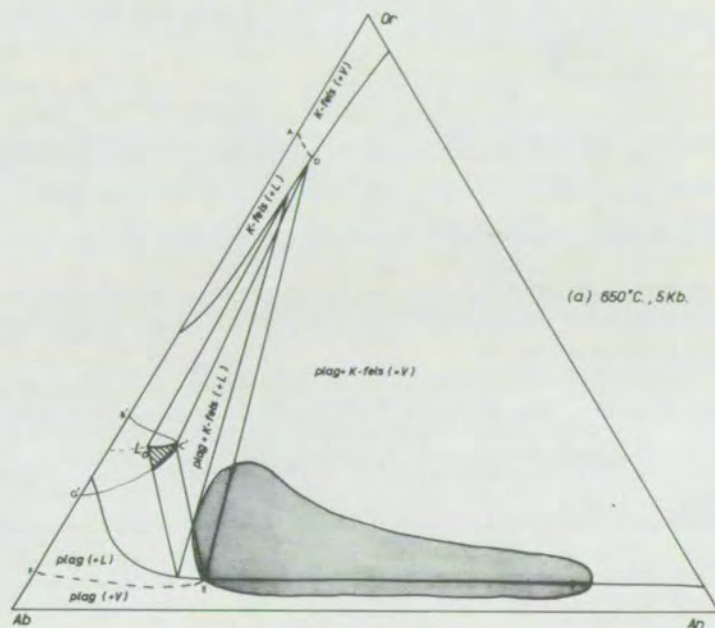
Schematic isothermal, isobaric (approx. 5 Kb. and 700°C.) projection from SiO_2 of phase relations in part of the system $\text{Or-Ab-An-SiO}_2\text{-H}_2\text{O}$. The surface A-B-C-D-E-F-G-H separates compositions in equilibrium with vapour from those which are undersaturated in water. The line A-D-E-F on the anhydrous base of the tetrahedron separates those felspar compositions which can produce a silicate-rich melt in the presence of water from those which cannot. The line C-X is a cotectic on the water-deficient side of the liquid volume.

Fig. 5-14

Projections from SiO_2 of the system Ab-Or-An- SiO_2 at various temperatures and pressures. The anhydrous phases are shown, and the phases listed in parentheses are those which will appear with the introduction of a little water. Tie-lines are shown between anhydrous compositions and the co-existing liquid compositions (where a liquid will appear with the introduction of a little water), projected from H_2O . The field of compositions of the Scourian gneisses, from fig. 5-5 (stippled), and the probable range of liquid compositions which would co-exist with them in a slightly hydrous environment are also shown (lined).

The points A, D, E, and F in (a) correspond to points on fig. 5-13, and B', C', and G' correspond to B, C, and G of fig. 5-13, projected from H_2O .

Sources of data as in fig. 5-11. Diagrams are plotted in weight proportions.



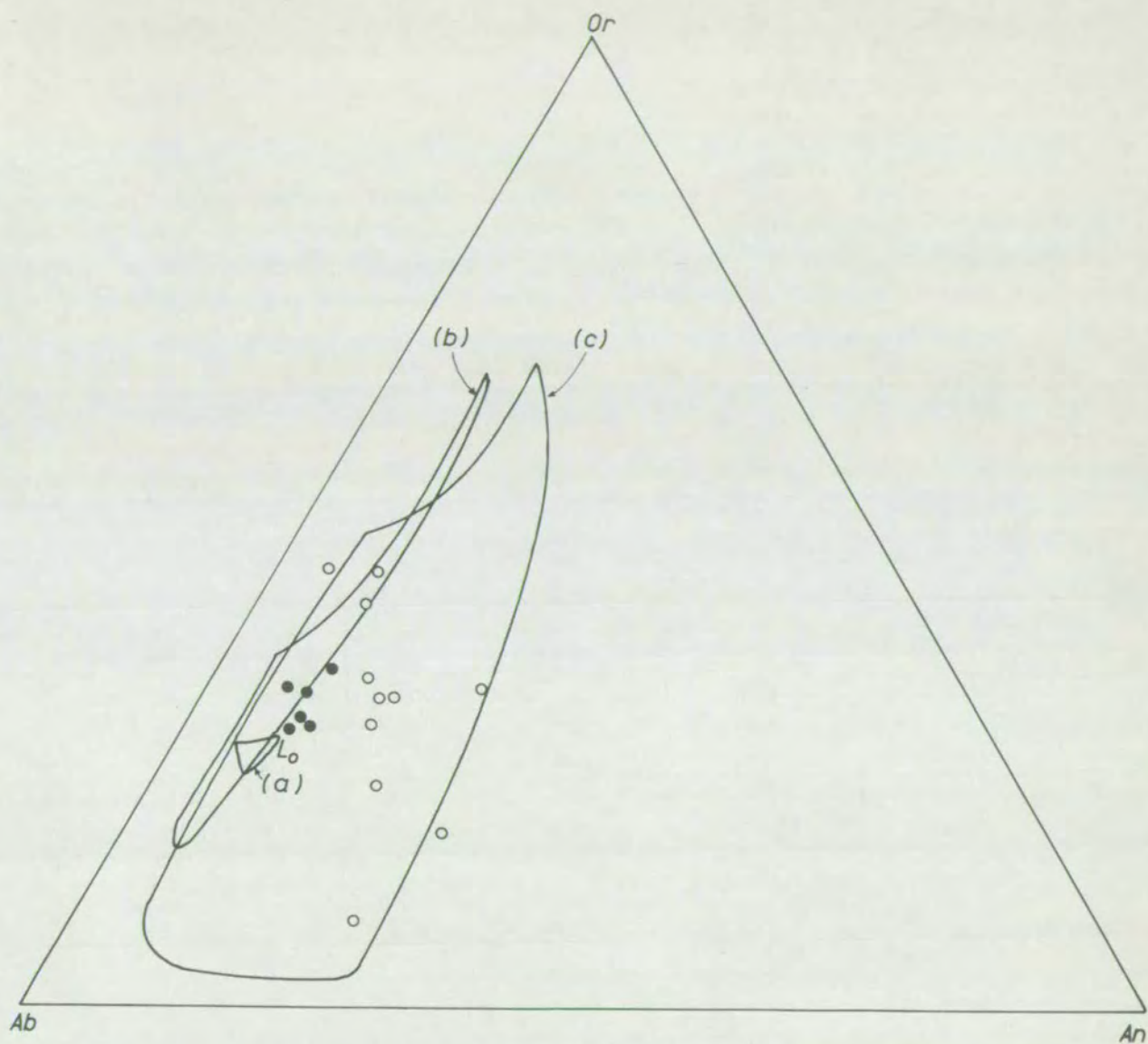


Fig. 5-15. Normative felspar compositions (wt.%) of the leucocratic gneisses from fig. 5-5 compared with the probable compositions of liquids which could coexist with the Scourian acid gneisses, from fig. 5-14.

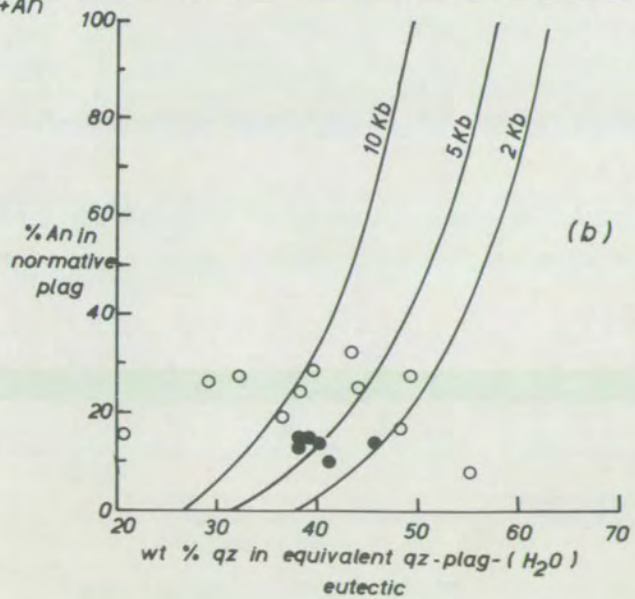
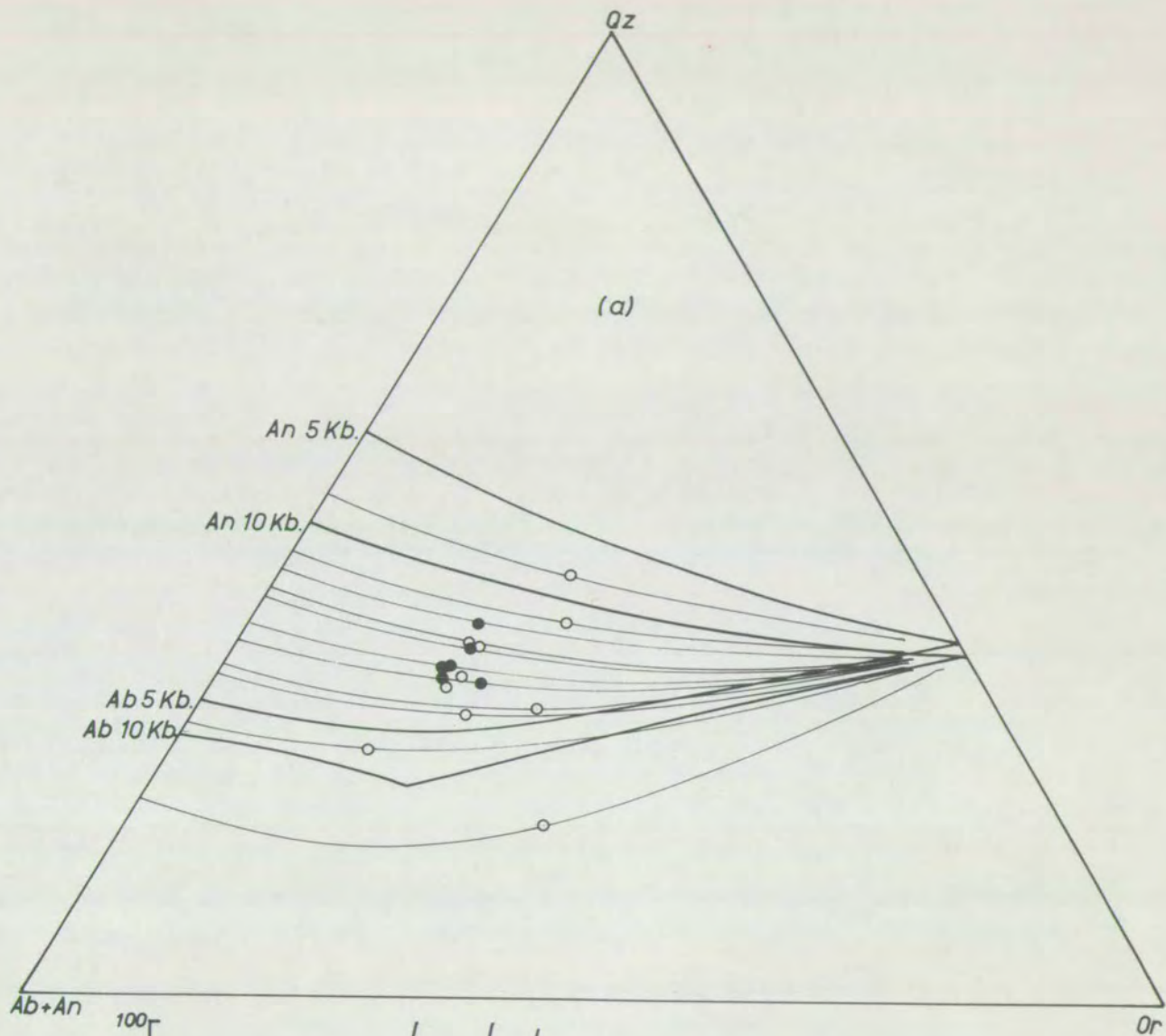
very close to the 1000°C field, and there is a distinct cluster of points about the first 650°C liquid L_0 .

The normative quartz contents of liquids generated by partial melting of quartz-felspathic rocks will be dependent on the physical conditions and on the normative plagioclase compositions. Data on these effects are available for water saturated systems (fig. 5-11). Insofar as these data are applicable to water deficient melts, they can be used to assess the likelihood of the generation of the leucocratic gneisses by partial melting. On fig. 5-16a are shown the 5 and 10 Kb. $\text{Ab-Or-SiO}_2\text{-H}_2\text{O}$ and $\text{An-Or-SiO}_2\text{-H}_2\text{O}$ cotectics (from the references cited above). As mentioned above, the 10 Kb. anhydrous Ab-Or-SiO_2 cotectic is nearly coincident with the $\text{Ab-Or-SiO}_2\text{-H}_2\text{O}$ cotectic. Through the point representing each leucocratic gneiss composition was drawn a curve of the same form as the experimentally determined cotectic, from the Or-SiO_2 side of the triangle near the 5 and 10 Kb. $\text{Or-SiO}_2\text{-H}_2\text{O}$ eutectics to the $(\text{Ab} + \text{An}) - \text{SiO}_2$ side of the triangle. On the assumption that each leucocratic gneiss represents a cotectic liquid, this construction will give an approximate value for the normative quartz content of the quartz-plagioclase 'eutectic', representing a terminal point on the relevant cotectic line.

The results obtained are plotted against the normative plagioclase compositions of the leucocratic gneisses in fig. 5-16b, together with the estimated curves of fig. 5-11b. All but ^{four} ~~two~~ of the points lie between the 2 Kb. and 10 Kb. curves for the water-saturated systems. It is noticeable that those analyses which cluster near the first liquid L_0 in the Or-Ab-An diagram of fig. 5-15, also lie close to the 5 Kb. curve in this new plot. In view of the fact that many of these gneisses show a

Fig. 5-16

- (a) Experimentally determined quartz-felspar- H_2O cotectics at 5 and 10 Kb. (data sources as in fig. 5-11). A line is drawn through each point representing the composition of a leucocratic gneiss, of roughly the same form as the 5 and 10 Kb. cotectics. The intersection of this line with the quartz-plagioclase join gives the normative quartz content of the equivalent quartz-plagioclase- H_2O pseudobinary eutectic, on the assumption that the rock represents a cotectic liquid (also on the assumption that the form of the water-deficient cotectics is similar to those of the water-saturated ones shown: see p. 109).
- (b) Part of fig. 5-11 (b) reproduced, with the normative plagioclase compositions of the leucocratic gneisses plotted against the normative quartz content of the equivalent quartz-plagioclase- H_2O 'eutectic' for each gneiss, taken from (a).



weak banding with quartz and feldspar rich layers, the scatter of points so that one analysis lies in the quartz field and ~~two~~^{three} in the feldspar field at any reasonable pressure, might be best explained by assuming relative segregation of quartz and feldspar from an original series of 5 Kb. cotectic liquids.

For the reasons outlined above, it is possible to consider the potash rich leucocratic gneisses as the partial melting products of acid gneiss material. In Chapter 2 it was postulated that the Scourian acid gneisses acquired their present compositions as the residue of partial melting. A scheme of evolution of the Complex can thus be put forward as follows:

(1) Widespread partial melting of (relatively) potassic gneisses, possibly consequent on the breakdown of hydrous phases (eg. Lundgren, 1966). The first liquids are likely to have been produced at about 5 Kb. and 650°C , and to have compositions close to L_0 (fig. 5-15). Later liquids (up to 675°C) will have a greater range of compositions.

(2) Removal of most of this liquid phase (Boettcher and Wyllie (1967) suggest that, even at moderate temperatures and pressures, liquids in the system $\text{Ab-SiO}_2\text{-H}_2\text{O}$ approach critical conditions. Although the same authors (1968) do not observe supercritical fluids in the granite-water system, the high water contents of water-saturated granitic magmas (approx. 10% at 5 Kb. and 20% at 10 Kb.) (Luth, 1969) suggest that a very fluid granitic magma could be generated in a metamorphic environment) containing most of the available water. The acid gneisses at this stage achieved nearly their present compositions. The liquid phase remained in the Complex only where it was enclosed, as in fissures in the basic-ultrabasic masses, and rarely elsewhere.

(3) At this stage (pre-F1 or syn-F1) the liquids are required to become largely solid in order to experience the deformation. Calculations on the molar volume of hornblende relative to the chemically equivalent but anhydrous assemblage in basic rocks suggest that this phase will be stabilised by increased pressure in this general pressure range. Thus, if the hornblende of the basic rocks had started to break down, it would tend to be restored by a rise in pressure, and water would diffuse from the hydrous liquid into the basic gneiss. The presence of any water would produce a small quantity of liquid in both leucocratic and normal acid gneisses, but if this were only interstitial, it would not prevent deformation and the development of foliation: the reverse might be expected.

(4) Further rise in temperature to about 1000°C would produce interstitial melts in the acid gneisses of a wide range of compositions. The general lack of water at this stage would probably prevent the production of large quantities of liquid.

If the hornblende of the basic gneisses continued to break down, available water in the region of the basic-ultrabasic masses might enable the production of larger volumes of liquid there, and the more calcium rich leucocratic gneisses might have originated in this way. Alternatively, since an interstitial liquid would be ubiquitous in all quartzo-feldspathic rocks of the Complex, it is likely that diffusion could take place through this liquid (enhanced by the low viscosity consequent on its high water content) so that the interstitial liquids in the leucocratic gneisses was made over towards that of the outside acid gneisses. As an interstitial liquid would continually equilibrate with the solid portion of the rock,

the effect would be to make over the bulk composition towards one more in equilibrium with that of the surrounding acid gneisses.

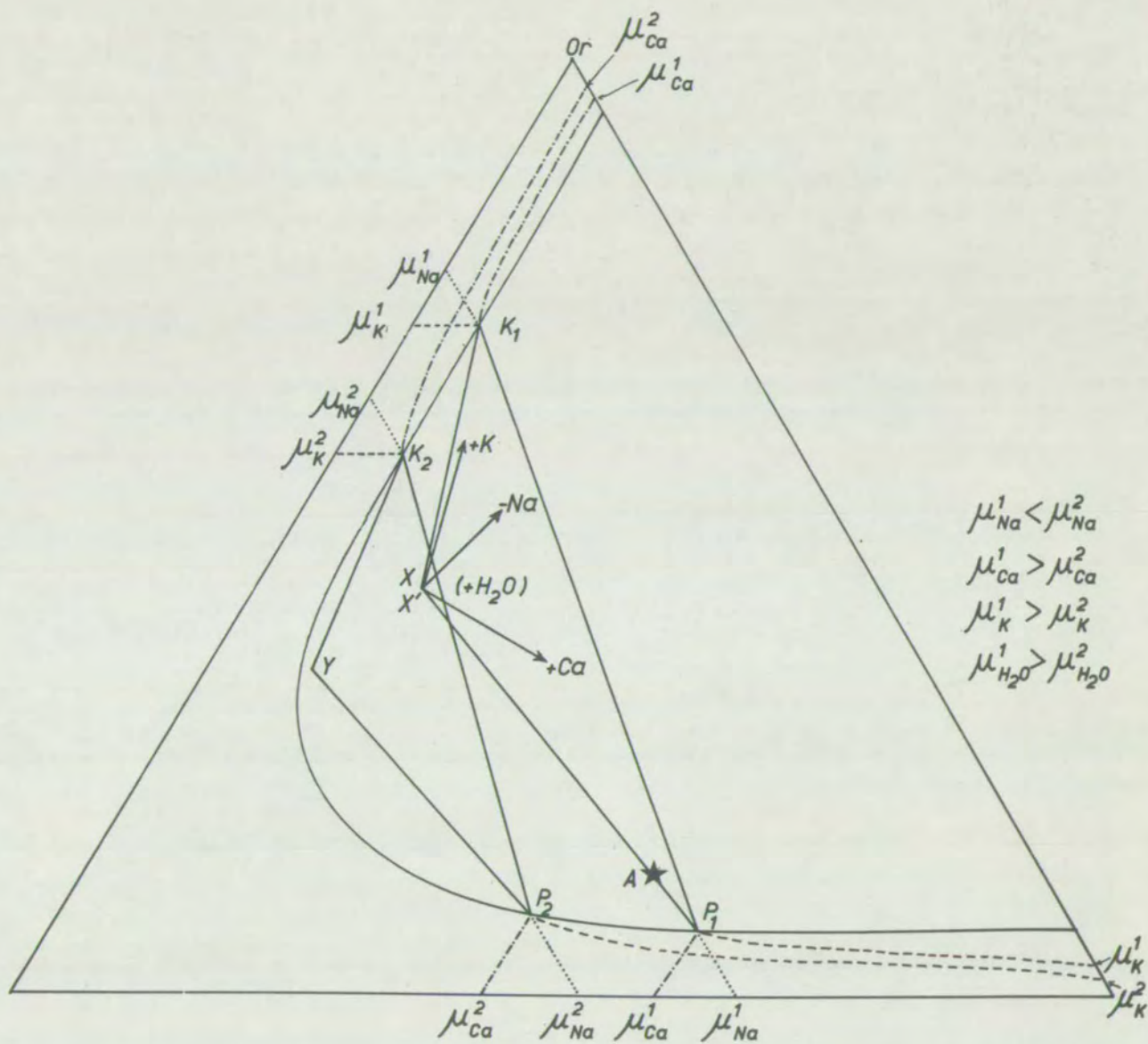
Although these surrounding acid gneisses were now potash-poor (after the departure of most of the liquid phase), the configuration of the feldspar tie-lines means that the activity of the potash feldspar molecule, as well as that of the anorthite molecule, might be higher in the calcium rich acid gneisses than in the leucocratic gneisses, now composed of one or two feldspars and a liquid phase (fig. 5-17). Dependent on the relative diffusion rates of potassium and calcium, the composition of the leucocratic gneisses could be enriched to varying degrees in either of these constituents, and depleted in sodium.

As a result of such a process of equilibration via an interstitial silicate liquid, the compositions of rocks representing early partial melts lying originally close to the Ab-Or join can be enriched in calcium, and still further in potassium, to achieve the relatively wide range of compositions now observed in the leucocratic gneisses. If such a metasomatic interchange has taken place, and the anorthite contents of the leucocratic gneisses have been raised, the normative quartz contents of the gneisses would be a relic of an early, anorthite-poor cotectic liquid. In this way, the scatter of points on fig. 5-16b could have been enhanced.

Schematic isothermal, isobaric projection from H_2O of the tetrahedron Ab-Or-An- H_2O (projection from SiO_2 of the system Ab-Or-An- SiO_2 - H_2O). The rock A gave rise to partial melt X and itself attained the refractory composition P_1 (composed largely of quartz and plagioclase). The liquid X has lost most of its water, and now has the water-poor composition X' . It consists of plagioclase P_2 , potash feldspar K_2 , a small proportion of liquid Y, and quartz (i.e. it is a potash rich leucocratic gneiss).

K_1 - P_1 -X and K_2 - P_2 -Y are three-phase triangles, and are thus isopleths of chemical potential. The intersections of the extensions of these isopleths with the anhydrous base of the tetrahedron are shown, with different symbols for the chemical potentials of $NaAlSi_3O_8$, $KAlSi_3O_8$, and $CaAl_2Si_2O_8$ (abbreviated as μ_{Na} , μ_K , and μ_{Ca} , on the assumption that ions of these elements will be the species whose diffusion is most significant). The relations of the chemical potentials in the acid gneiss assemblage P_1 -(K_1)-X (some interstitial liquid of composition close to X is presumed to be still present), and the leucocratic gneiss assemblage P_2 - K_2 -Y, are indicated. It is clear that the two rocks are no longer in equilibrium, although one was formed from the other. Diffusion can take place via the (presumably ubiquitous) interstitial liquid, which will continuously equilibrate with the solid phases present.

The leucocratic gneiss X' will be modified by the addition of K, Ca and H_2O , and subtraction of Na. The limits of the ^{irrec} ~~directions~~ in which its composition may change are shown by arrows. Total equilibration of X' with the acid gneiss P_1 will result in it consisting of unknown proportions of P_1 , K_1 , and liquid X.



CHAPTER 6

SUMMARY AND CONCLUSIONS6.1 Summary

In Chapter 2 the origin of the acid gneisses of the Scourian Complex was considered. The 'peculiar geochemistry', in particular the deficiency in potassium and the unusually high K/Rb ratios, the exceptionally low $\text{Sr}^{87}/\text{Sr}^{86}$ ratios, and the occurrence of possible sedimentary relics are the bases for any hypothesis of the origin of the Complex.

It was observed that intra-mantle and intra-crustal fractionation of rubidium relative to strontium must give rise to a spread of Rb/Sr ratios, and hence, in time, of $\text{Sr}^{87}/\text{Sr}^{86}$ ratios, so that parts of the mantle may quite possibly have higher $\text{Sr}^{87}/\text{Sr}^{86}$ ratios than parts of the crust. Low crustal ratios may not be conclusive evidence of mantle derivation. Furthermore, the number and variety of rocks whose origin is difficult to explain as other than sedimentary strongly suggests that a group of sediments was at least partly involved in the formation of the Scourian Complex.

It was postulated that rocks of the granulite facies may often be derived from water-rich, lower grade metamorphic rocks by a process of partial melting and loss of the fluid phase. Indeed, if partial melting ensues before the breakdown of hydrous minerals, this may be the only way of generating anhydrous rocks. Much of the potassium and most of the rubidium would be contained in the fluid phase, and this appears to be a feasible mechanism for the conversion of a 'normal' rock series into the chemically 'unusual' Scourian acid gneisses. It was concluded that the Scourian Complex consisted originally of intermediate volcanic rocks and/or sediments derived from them, with subordinate amounts of

basic and ultrabasic igneous rocks and some impure limestones, argillaceous rocks, and possibly quartzites.

The coincidence of the $\text{Sr}^{87}/\text{Sr}^{86}$ ratios of the Scourian and Laxfordian Complexes when extrapolated back to approximately the time of the Scourian metamorphism indicates a genetic relationship between them, but the chemical differences between the basic rocks of the two areas suggests that they are not parts of the same complex which have evolved differently. It was concluded, with Holland (1965) that the Laxfordian gneisses probably represent sediments derived largely from the Scourian Complex in immediately post-Scourian times.

In Chapter 5 the potash rich leucocratic gneisses were interpreted as the partial melting products of those rocks which became the acid gneisses. Their compositions, in relation to experimental studies in the system $\text{Ab-Or-An-SiO}_2\text{-H}_2\text{O}$, suggest that they may have been initially formed by partial melting of quartzo-felspathic rocks in the presence of excess water at about 5 Kb. and 650°C . They probably became entrapped in and near the basic masses during the regional loss of the palaeogenetic liquid, and subsequently became largely solid due to an increase of pressure, with consequent re-amphibolitisation of some of the basic rocks and removal of most of the available water.

It was suggested that the gneisses derived by the solidification of these early partial melts could have changed in composition by metasomatism as a result of this solidification. The small quantity of interstitial liquid which must have remained would have been depleted in calcium relative to the whole rock, and would thus be susceptible to metasomatism from the

interstitial liquid of the surrounding acid gneisses, which could, as the temperature rose to a maximum of 1000°C , be even more calcium rich (and also have a higher chemical potential of potassium). Continuous equilibration of the interstitial liquid with the solid part of the gneiss would change the bulk composition by enrichment in calcium and potassium.

In Chapter 3 it was shown that neither the description of the basic and ultrabasic masses as 'layered' nor as 'zoned' totally describe their field relations. Although they are often stratiform in their overall shape, the frequent repetition of the ultrabasic to basic sequence, the lack of asymmetry in these sequences, and the paucity of rocks intermediate in composition between basic and ultrabasic are not consistent with the conclusion that the masses are layered igneous intrusions, either simple or multiple.

On making a traverse from ultrabasic to acid gneiss a variety of different types of sequences of rocks may be encountered. On the one extreme, there is the Loch an Daibh Mhor contact, with the sequence: peridotite-spinel-pyroxenite/clinopyroxenite/garnet-augite gneiss (and arlegite)/garnetiferous basic gneiss/basic gneiss/acid gneiss. All intermediates between this type and the Cleit Mhor contact (peridotite/hornblende-pyroxenite/basic gneiss/acid gneiss) are found, and the Geodh'Eanraig lower contact represents another type: peridotite/pyroxene-hornblende/plagioclase gneiss/acid gneiss, basic material being absent. It appears that the most richly garnetiferous rocks are developed at contacts where a large thickness of material of basic composition (basic or garnetiferous basic gneiss) is developed between the ultrabasic and acid gneisses. This variation in type of sequence is not consistent with a simple series of diffusion zones formed by reaction between

two rock types.

In Chapter 4, it was shown, from the field observations, that the formation of the contact gneisses and the marginal pyroxene-hornblendites probably post-dated the juxtaposition of the basic and ultrabasic rocks (however this took place). The mineral facies and paragenesis were summarised, and it was found that the best estimate of the physical conditions at the climax of metamorphism was that of O'Hara (1967), of 1000°C and 17 Kb.

A discussion of the petrogenesis of the basic and ultrabasic rocks was then made, firstly in terms of probable igneous processes, and then in terms of diffusion processes.

The chemical variation due to the compositional layering in the ultrabasic gneisses is consistent with an origin as olivine-hypersthene-amphibole cumulates in a layered intrusion, provided, either that the Cr content and Fe/Fe + Mg ratio of the amphibole were close to those of the other two phases, or, that a fourth phase, rich in Cr and Fe relative to Mg varied in amount conversely with the amphibole. The variation is also not inconsistent with the metasomatic introduction of material from the country rocks into an originally homogeneous peridotite. The fact that the layering-free peridotites of Camas an Lochain have compositions close to that which defines the most basic possible end-member of the variation diagram for the ultrabasic gneisses supports the latter possibility. On the cumulate hypothesis, these rocks would be olivine-hypersthene cumulates, and might still be expected to show layering due to variations in the proportions of these two minerals.

There was found to be no great chemical variation amongst the basic and garnetiferous basic gneisses, and there is little compositional difference between the two groups. All the analysed rocks are tholeiitic, with both olivine and hypersthene in the norm. Comparison with a number of basic igneous rocks showed that they are somewhat lower in Na and higher in Ca than many otherwise similar rocks. Projection into the system C-M-A-S reveals that, along with most of the analysed ocean floor tholeiites, the compositions plot closer to the diopside projection than most 'normal' basaltic or gabbroic rocks. A scheme of evolution was proposed for magmas of this composition, similar to that of O'Hara (1968b) for the ocean floor tholeiites. It involves partial melting of garnet-peridotite at 30-40 Kb., and continuous fractionation of olivine at pressures, steadily decreasing to 10-15 Kb. Any reduction of pressure below this value could not have been accompanied by significant fractionation of anhydrous phases.

The fractionation of hornblende and little else remains a possibility for the generation of magmas of this composition. The major element variation within the basic group, although not great, indicates that this process may be responsible for the later evolution of these rocks, and the simultaneous increase in both Fe/Mg and Ab/An ratios strongly suggest that it has occurred, as the compositions never fall in a plagioclase field in the system C-M-A-S. The likelihood of the basic group representing a series of cumulates was examined, and found to be unlikely, unless hornblende was a major cumulus phase.

The compositions of the ultrabasic gneisses are not consistent with their being cumulates from magmas now represented by the basic and garnetiferous

basic gneisses. If the basic and ultrabasic groups are both series of cumulates from different parts of a layered intrusion, the absence of rocks representing cumulates of intermediate $Fe/Fe + Mg$ ratio remains to be explained.

The compositions of the basic and garnetiferous basic gneisses, recalculated into ideal granulite facies minerals, show that only part of the difference in modal composition can be explained by the chemical differences considered in the process of recalculation. Very slight changes in Fe/Mg and Na/Ca ratio could change the relative free energies of the two assemblages, which must have been nearly in equilibrium with each other, so that either became the stable state. If the garnetiferous basic gneiss represents original basic igneous rock, then it must have been slightly metasomatised by the acid gneiss so that it became basic gneiss, which is silica-saturated and is more nearly in equilibrium with the acid gneiss.

The variation in the sequence of petrographic types encountered on a traverse from ultrabasic to acid gneiss is substantiated chemically. Profiles of the concentration of elements across the contacts vary from extremely erratic in the sequence where contact gneisses are best developed (Loch an Daibh Mhor) to nearly linear where only basic gneiss is encountered (Cleit Mhor). Where there is no basic material present (Geodh'Eanruig lower contact), there is a simple chemical discontinuity from pyroxene-hornblende (modified peridotite) to plagioclase gneiss (modified acid gneiss).

The variation in mineral composition across the ultrabasic-garnetiferous basic gneiss contact is continuous, but has been modified at a late stage by the breakdown of magnesian garnet in the contact gneisses, with the

development of garnet reaction rims. This garnet has broken down into a more iron rich garnet, and a chemically equivalent assemblage of hypersthene, plagioclase, and spinel which is more magnesian. Where garnet is the dominant phase, in one of the zones at Loch an Daigh Mhor, an apparent discontinuity in the pyroxene compositions as they vary across the contact, results, but this is not the case at Geodh'Eanraig, where the augite compositions in the garnet-augite gneisses is apparently unmodified by the development of garnet reaction rims. The theoretically invariant assemblage garnet-hypersthene-plagioclase-spinel involves minerals of different Fe/Fe + Mg ratio at the two localities, and it probably has a variance resulting from slight differences in the ferrous/ferric ratio, and possibly the chromium and sodium content of the original garnet.

The theory of diffusion zone formation was outlined, and it was shown that an excellent test to distinguish a series of diffusion zones is the mass balance. The total mass of each element must remain constant at each stage of the process. The simulation model for diffusion was then briefly described.

The tests of mass balance, applied to the sequence ultrabasic gneiss/basic and garnetiferous basic gneiss/acid gneiss (the contact gneiss, forming a small part of the sequence, was ignored) show that the basic rocks contain, in particular, considerable excesses of TiO_2 , CaO , and Fe over any possible mixture of acid and ultrabasic gneisses. It is therefore evident either that this sequence is not a series of diffusion zones, or that some relatively long-distance mass transport occurred during its formation. The sequences peridotite/pyroxene-hornblende/plagioclase gneiss/acid gneiss, and ultrabasic gneiss/contact gneiss/garnetiferous

basic gneiss both conform approximately to the requirements of the mass balance.

The simulation model can predict surprisingly well the variation in chemistry and mineral composition of the sequence ultrabasic gneiss/contact gneiss/garnetiferous basic gneiss, as a result of reaction between the two end-members. The change from the extremely erratic to the more gentle type of chemical variation in the contact gneiss sequence can be produced by changing the diffusion coefficient of MgO or SiO_2 by a factor of two. It was suggested that, if diffusion were responsible for the formation of the contact gneisses, the proximity of acid gneiss, which would cause the garnetiferous basic gneiss to be converted to basic gneiss, with a considerable rise in the chemical potential of silica, would enhance the diffusion of silica into the ultrabasic gneiss, and thus effect the change from one type of sequence to the other. In this way, all the intermediate types of contact gneiss sequence could arise.

When the model was used to simulate reaction between ultrabasic and acid gneisses, the results in no way resembled the sequence ultrabasic gneiss/contact gneiss/garnetiferous basic gneiss/basic gneiss/acid gneiss. The predominance of orthopyroxene in the results resembles, if anything, the pyroxene-hornblende type of contact, which it is difficult to envisage as resulting from any process but reaction between ultrabasic and acid gneisses.

6.2 Conclusions

The following conclusions have been tentatively drawn from the data and arguments presented in this thesis:

Acid gneisses of the Scourian Complex

These probably represent a group of intermediate igneous rocks, and/or sediments derived from them, with minor intercalations of impure calcareous, pelitic, and possibly quartzitic sediments, and basic and ultrabasic igneous rocks. They were subjected to partial melting at about 5 Kb. and 650°C, and subsequently at temperatures up to 1000°C and pressures up to 17 Kb. The palingenetic liquid was removed at a relatively early stage, and with it much of the potassium, and most of the rubidium, lithium, and water.

The Laxfordian acid gneisses probably represent a group of sediments derived largely from the Scourian Complex in immediately post-Scourian times.

Leucocratic gneisses

These gneisses probably represent the early partial melting products of the acid gneisses, where they have remained in the Complex, trapped in and near the basic-ultrabasic masses. These liquids largely solidified to give the leucocratic gneisses, and these may have been modified at a later stage by metasomatism from the same acid gneisses which gave rise to them, via an interstitial, palingenetic liquid.

Ultrabasic gneisses

These are either a group of olivine-orthopyroxene-amphibole cumulates, in which the original layering is still preserved, or, more probably, originally homogeneous olivine-orthopyroxene peridotites, in which a compositional banding has been induced by the metasomatic introduction of acid gneiss material.

Basic and garnetiferous basic gneisses

These rocks are either a series of basic magmatic rocks generated by partial melting of garnet-peridotite at 30-40 Kb., which have evolved by

continuous fractionation of olivine at pressures decreasing to 10-15 Kb., and subsequently by a relatively small amount of hornblende fractionation, or original igneous amphibolites, (cumulates or magmatic liquids) (in either case the basic and ultrabasic rocks being associated in an igneous complex or series of complexes), or rocks produced as a diffusion zone by reaction between ultrabasic and acid gneisses during an early, amphibolite facies stage of the metamorphism, a considerable amount of their mass having been lost to the paligenetic liquid of the acid gneisses, which has now been lost.

The basic gneiss probably developed from the garnetiferous basic gneiss by a small metasomatic interchange with the acid gneisses, when the former were converted from amphibolite to the silica-undersaturated garnetiferous basic assemblage of the granulite facies.

Contact gneisses

These are a series of diffusion zones produced by reaction between the ultrabasic and garnetiferous basic gneisses at the granulite facies stage, when they were probably converted from serpentinite and amphibolite to the granulite facies assemblages. The petrology is somewhat complicated by the instability of magnesian garnet at a late stage, and the formation of garnet reaction rims.

Pyroxene-hornblendites

These are rocks which developed as a margin to the ultrabasic masses, at the granulite facies stage, following a postulated stage of 'tectonic slicing', which exposed the ultrabasic rocks to acid gneisses, from which it was previously separated by basic rocks (either igneous or formed by reaction at the amphibolite facies stage).

APPENDIX A

STRUCTURE OF THE LEWISIAN IN THE SCOURIE AND BEN STROME AREAS

During the course of mapping the basic and ultrabasic rocks, it was necessary to elucidate, as far as possible, the structural history of the whole area. Most of the results of this study do not bear directly on the petrogenesis of the basic and ultrabasic rocks, so the details are given in this appendix.

A.1 Structure of the Ben Strome area

Structural elements of the Scourian Complex

(1) Lithological layering. This comprises the gross alternation of acid, basic, and ultrabasic rocks. At some localities (e.g. near Loch Clach a'Chinn Dubh, fig. 3-9) layers of acid gneiss rich in saussurite lenticles (see Appendix B) form mappable horizons.

(2) Banding. The banding of the acid gneisses is due to variations in the proportions of mafic and felsic constituents. It is present in virtually all of the acid gneisses of the Complex. The ultrabasic, and to a lesser extent, the basic gneisses, also show a compositional banding.

(3) Lineation. Linear structures are not abundant in the Scourian rocks, but enough were found by diligent mapping to construct a lineation map. The lineation consists of a rough striation or crenulation which is seen on foliation surfaces. Where strike sections can be examined at the same exposure, the lineation can usually be seen to be the result of small scale, often intrafolial folds. Where lenticular quartz grains are well developed, the quartz lenticles are sometimes elongated parallel to the lineation. Minor fold axes, and the long axes of ellipsoidal ultramafic

Fig. A-2. Lineations (overlay of fig. A-1)

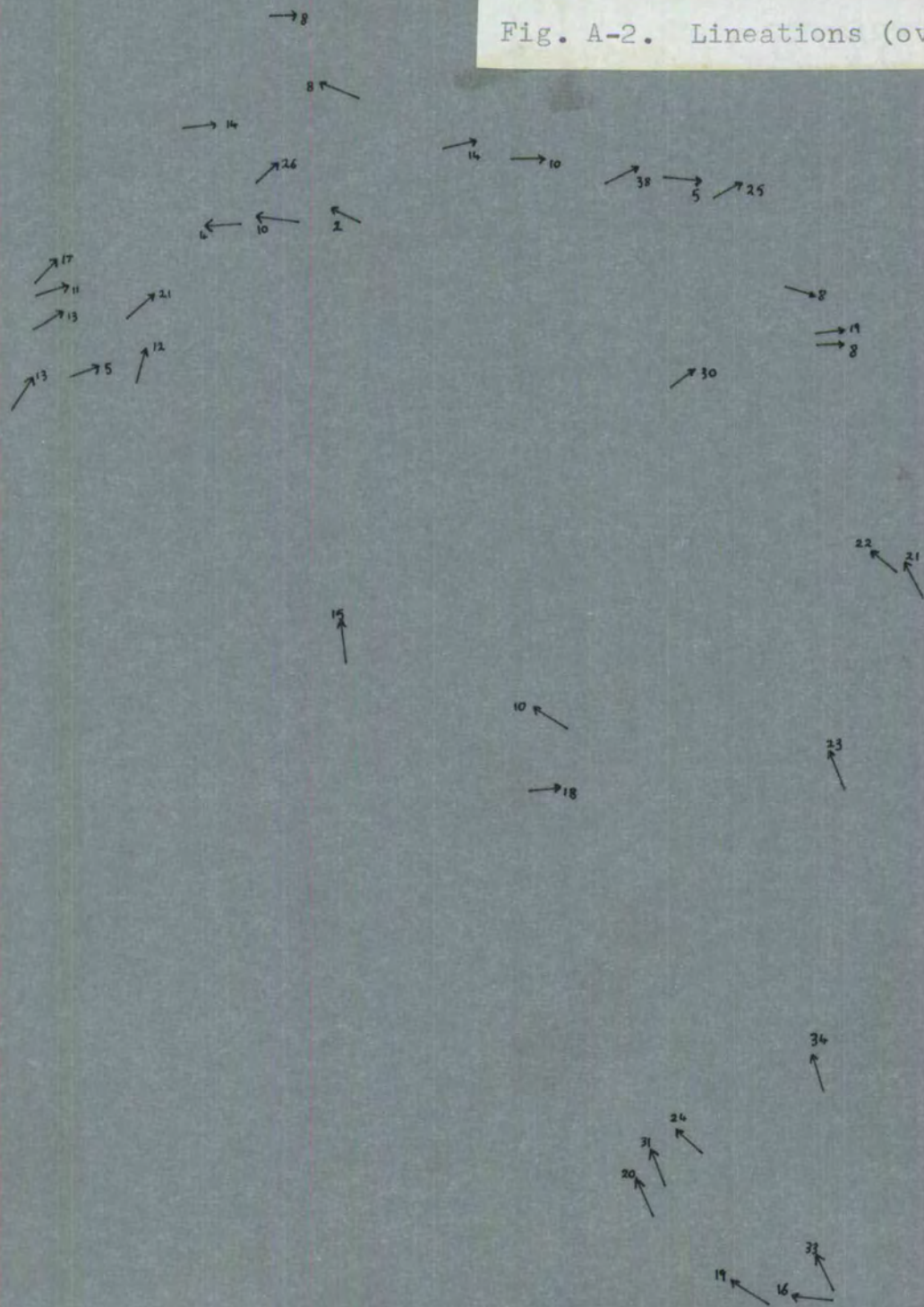


Fig. A-1.

MAP OF THE BEN STROME AREA, SHOWING DIP AND STRIKE.

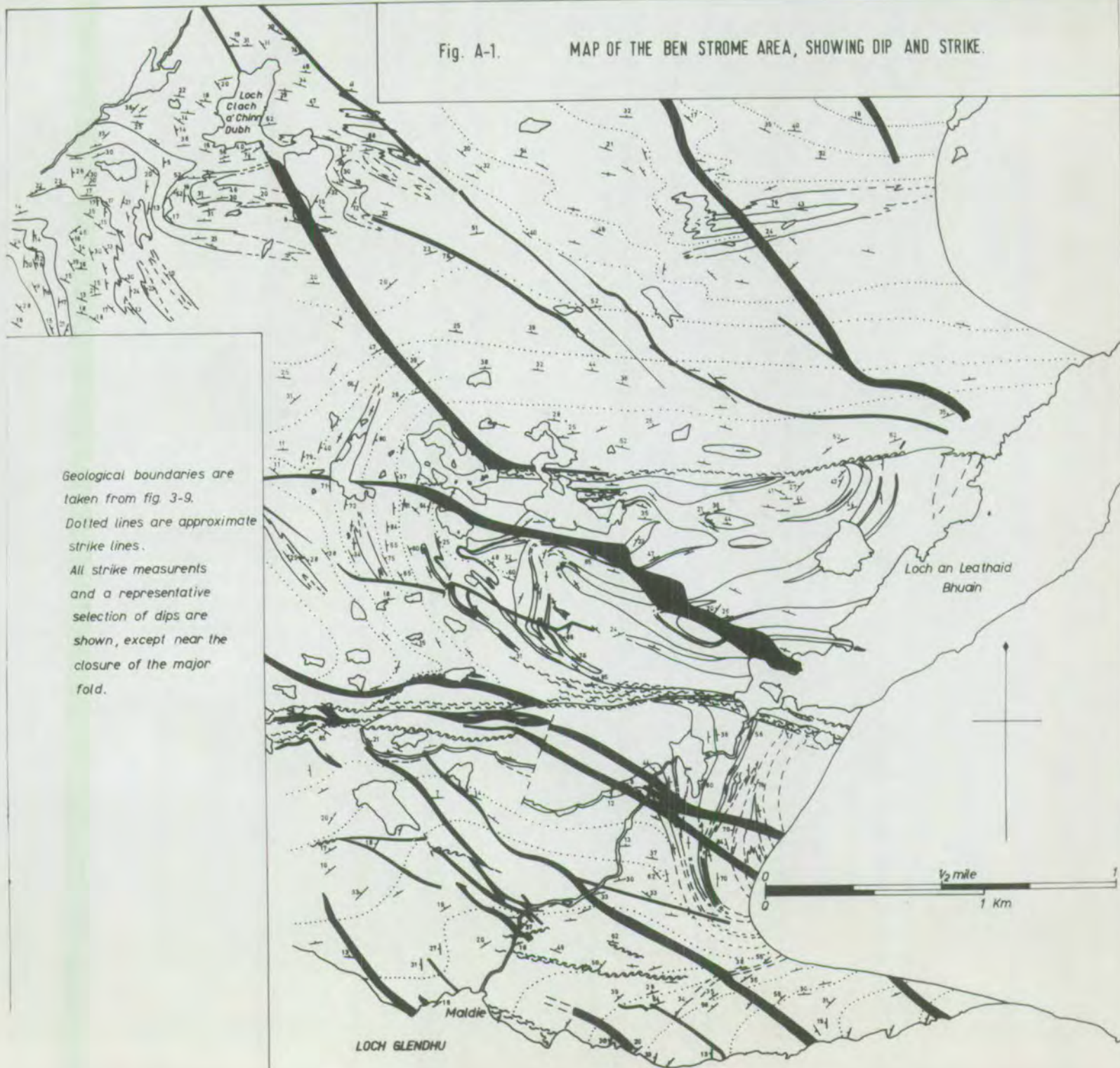
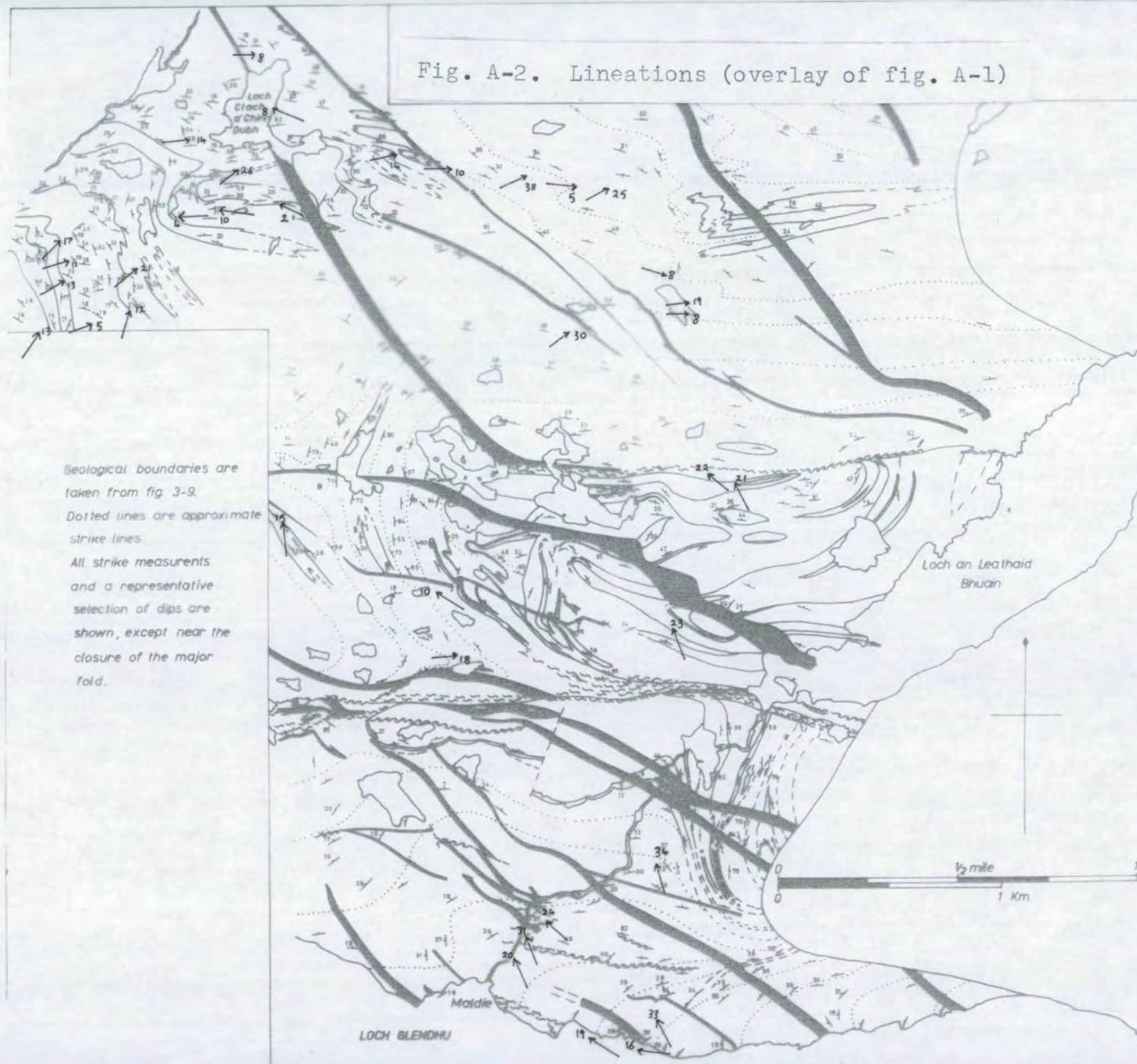


Fig. A-2. Lineations (overlay of fig. A-1)



lumps are, wherever they have been observed, parallel to the lineation.

Structural sequence

The following sequence of events will be postulated. Some of the events cannot be dated precisely with respect to the others: where this happens, a guess has been made of their position in the sequence, on the basis of the observation that the later folds in a single metamorphic episode tend to be more open, and of a more brittle style.

(1) Early isoclinal folding on a large scale (F1).

(2) Main phase of deformation, with the development of the present banding and lineation in the acid gneisses, and two phases of folding (F2 and F3).

(3) N.N.E.-S.S.W. trending monoclines (F4).

(4) N.W.-S.E. trending open warps (F5).

(5) Vertical, E.-W. fractures.

(6) Development of retrogressively metamorphosed, steeply dipping gneiss belts (in the case studied, with an arcuate but mainly N.W.-S.E. trend) and associated complex minor folds.

(7) Intrusion of generally N.W.-S.E. basic dykes.

(8) Development of E.-W. trending steep monoclines (potential shear belts?).

(9) E.-W. shear belts, with amphibolite facies retrograde metamorphism and simultaneous mylonite and pseudotachylite formation elsewhere.

A map of Ben Strome showing the lithological boundaries generalised from fig. 3-9, and foliation measurements is given in fig. A-1. Fig. A-2 is a similar map with the lineation measurements.

Early isoclines and main phase deformation

Fig. A-1 shows, quite distinctly, that there is a major isoclinal fold in the basic and ultrabasic gneisses on Ben Strom. Fig. A-3 shows a stereographic plot of the measurements of the banding in the basic and ultrabasic gneisses around this fold. Lineations and foliations from the band of leucocratic acid gneiss in the fold core show that these fabric elements are axial and axial plane structures respectively. At the fold nose, the banding in the acid gneisses outside the fold is discordant to the contact with the basic band.

Fig. A-2 shows that the lineations in the acid gneisses are curved in such a way as to parallel the fold in the basic body. A stereographic plot (fig. A-4) shows that the lineations form a complete girdle and could be expressed as the result of the intersection of a curved surface with a planar surface dipping north at about 30° (the present banding surface). The lineations of the acid gneisses within the major isocline also lie in the plane of this banding surface.

On the assumption that the two-dimensional parallelism of the lineations and the early isoclinal fold can be extended to three dimensions, the relations of the banding and lineation will be as shown in fig. A-5. On a single, north dipping banding surface, the lineation will be effectively constant in direction, because of the fact that the axis of the early fold (F1) lies in the plane of the banding (S_1). The lineation can thus be explained by the interference of an early folded surface (S_0), parallel to the fold in the basic band (F1), with the present nearly planar banding (S_1).

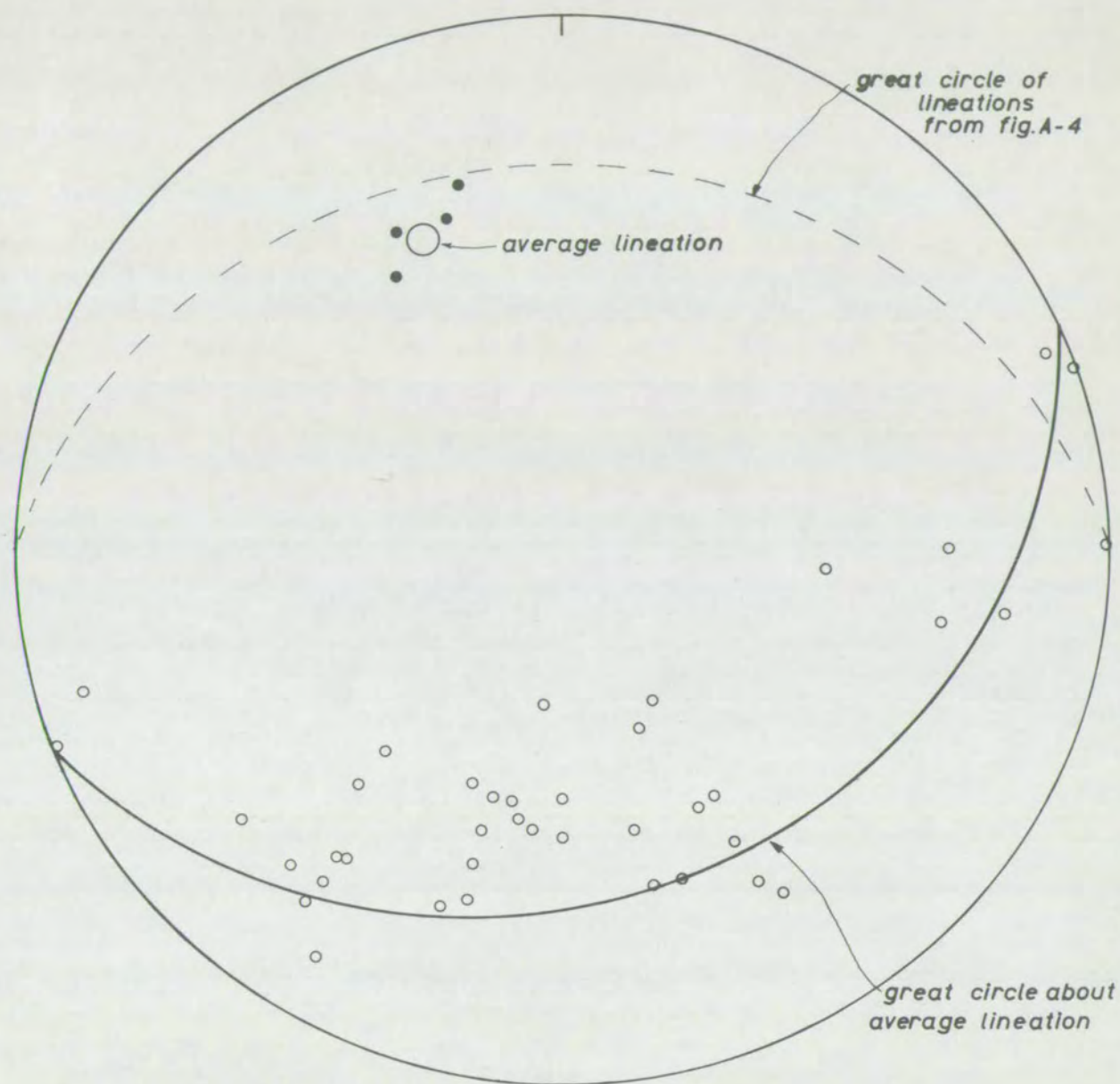


Fig. A-3. Poles to the banding in basic and ultrabasic rocks near the major fold at Ben Strome (open circles). Lineations from acid (leucocratic) gneiss within the fold (solid circles)

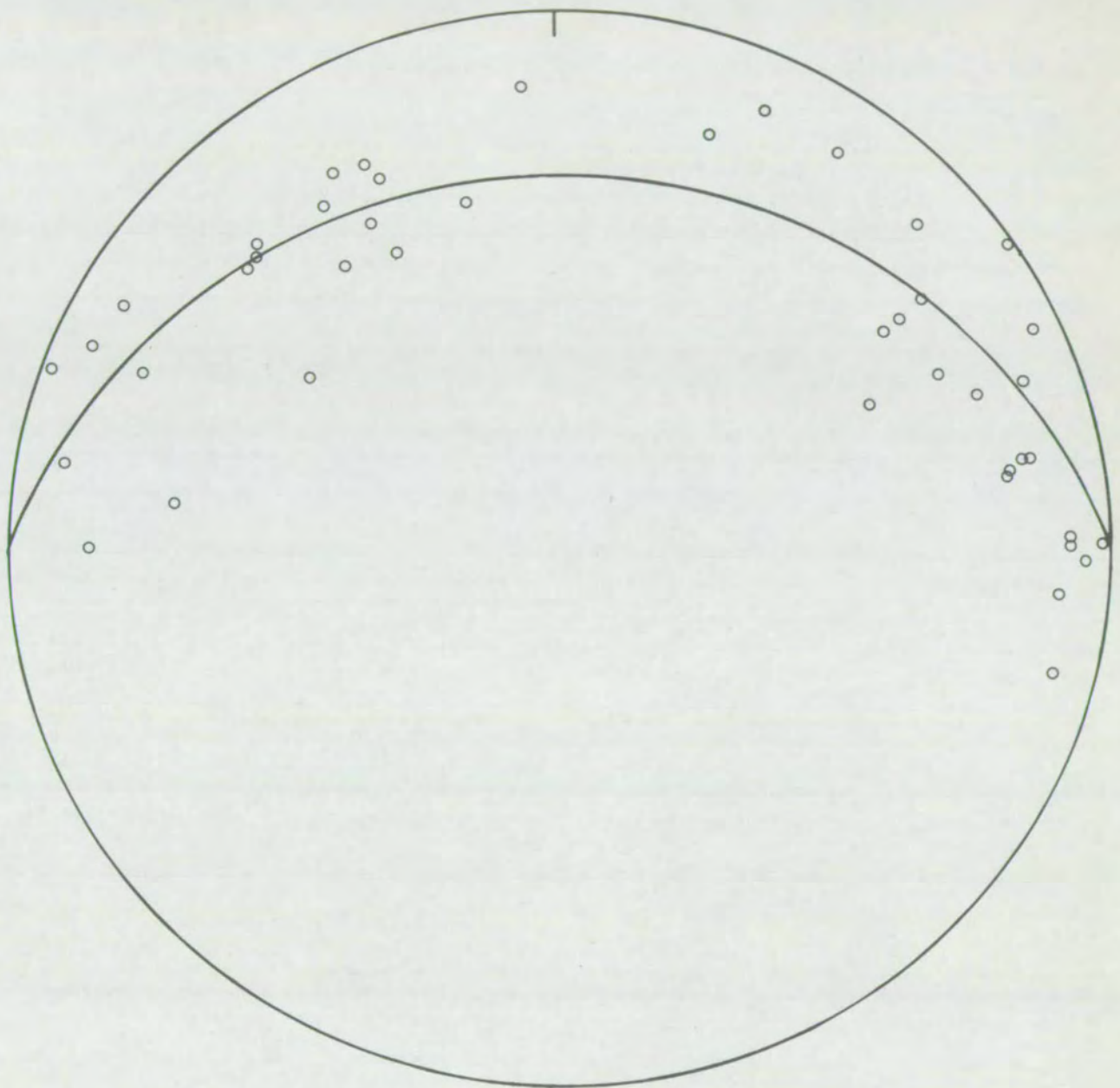
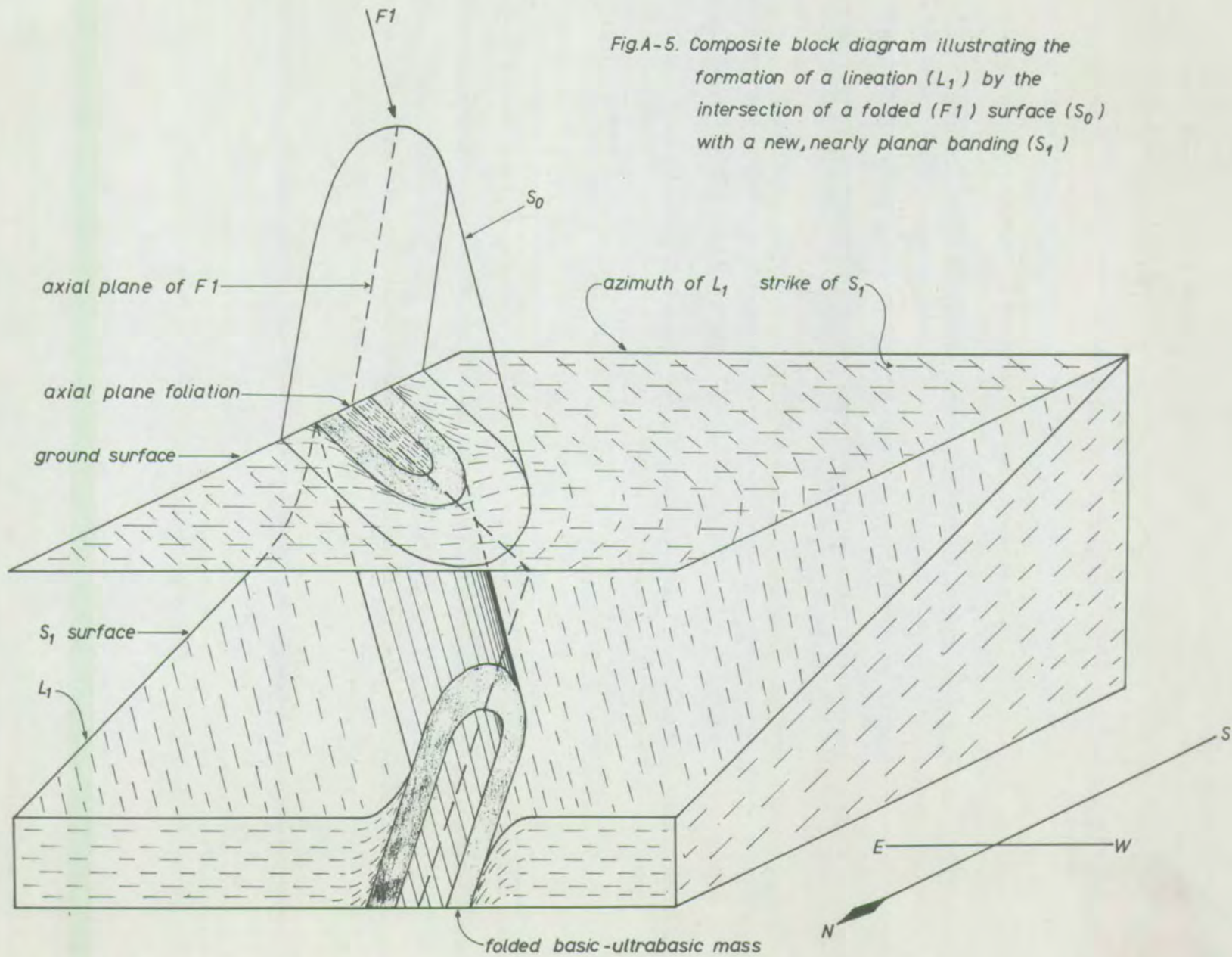


Fig.A-4. All lineations and linear structures from Ben Strome.



The main phase folds are not common, and they are best developed in the axial region of the postulated early fold, near Loch Clach A'Chinn Dubh. 400 yards south of the S.W. end of the loch there is an exposure illustrating two phases of folding (fig. A-6). An earlier, isoclinal fold in basic gneisses has a quartz-plagioclase vein developed along its axial plane, and this axial plane is folded by smaller scale, somewhat more open folds. The axes of both fold sets plunge at a few degrees to the east, and are coincident with the lineation in the area. It is therefore likely that the main phase of deformation included two stages of folding, which may be called F2 and F3. The relatively large scale, open folds in the adjacent area (fig. A-1) may be presumed to belong to F3. Another example of a small scale F3 fold is shown in fig. A-7. In this case, the lenticular quartz grains are clearly seen to define an axial plane foliation.

The N.N.E.-S.S.W. trending monocline

A major fold belonging to this group is seen near the Maldie Burn (fig. A-1). Small scale folds of the same style are observed in the same area (fig. A-8), and their axial and axial plane directions are nearly coincident with those of the major fold (fig. A-9). In the minor fold illustrated in fig. A-8, the lenticular quartz grains in quartz-plagioclase bands in the basic gneiss have been flattened into an axial plane orientation. As they still preserve the pale blue colour characteristic of the quartz of the Scourian rocks, granulite facies conditions may be presumed to have still prevailed.

Near Scourie, folds of the same style and orientation often have potash pegmatites intruded along their steep limbs. These pegmatites

Fig. A-6

Photographs illustrating the two phases of folding at Ben Strome, 400 yards south of Loch Clach a'Chinn Dubh. An earlier, F2, isocline is folded by F3 folds with axial planes dipping north at $30-50^{\circ}$. Photographs both taken looking east.



Fig. A-7

Small scale F3 fold showing axial plane orientation of lenticular quartz grains. Rudha Clach an Eorna (fig. 3-8).

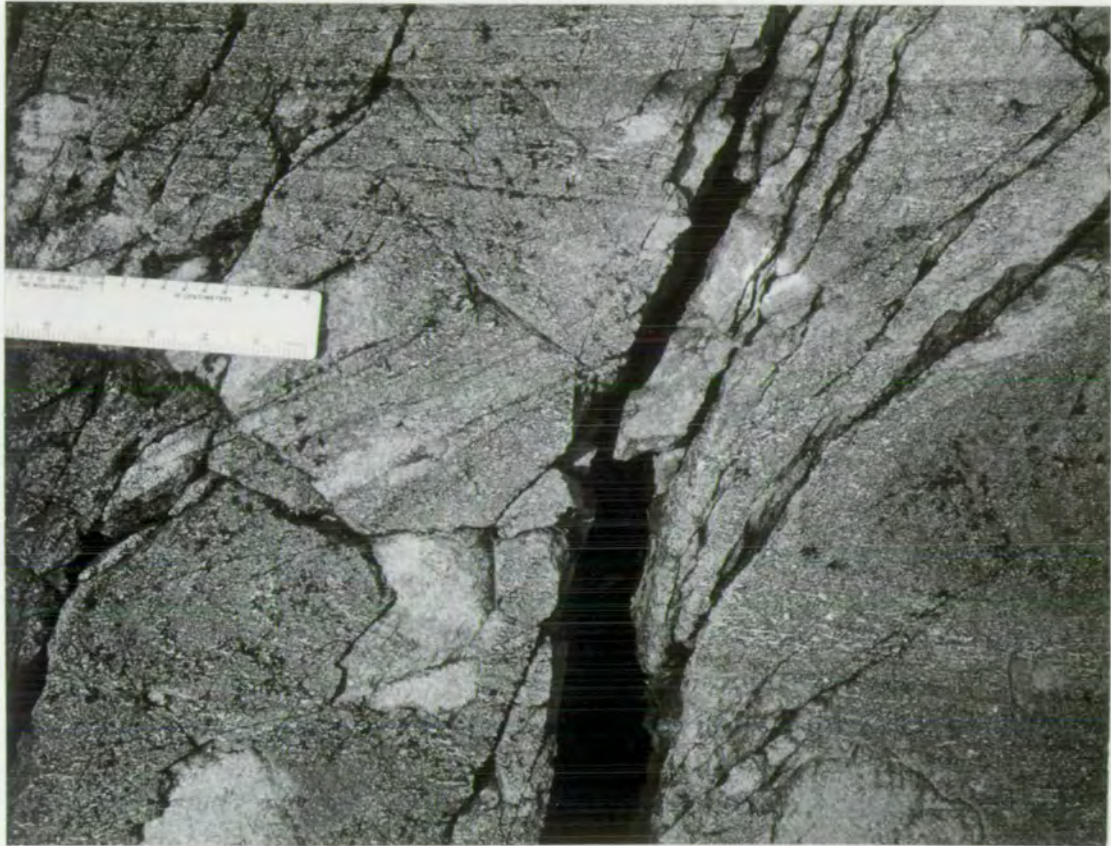


Fig. A-8

Gently N.W.E. plunging monocline (F4) in basic gneisses, by the path west of the Maldie Burn (figs. 3-9 and A-1).



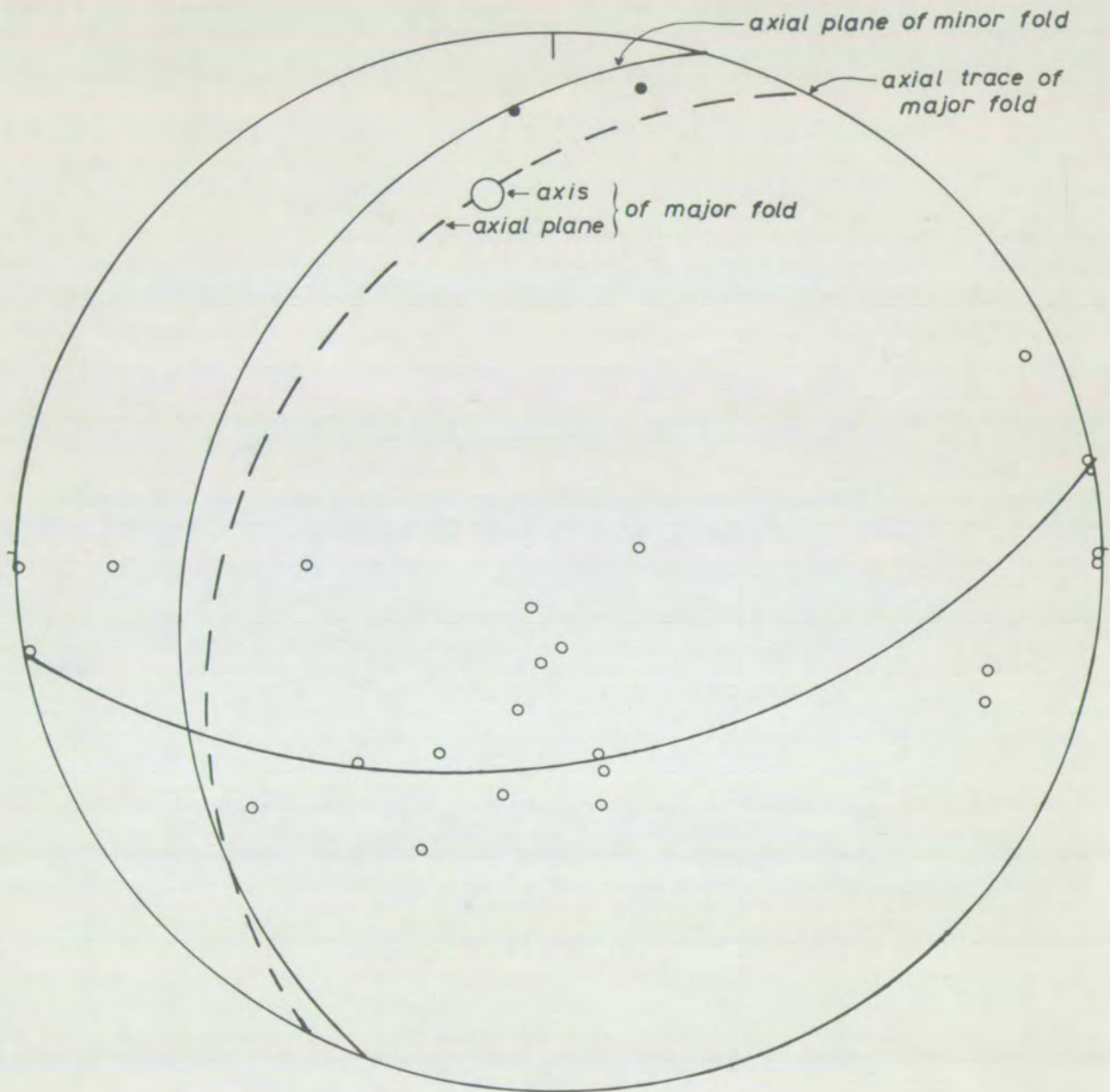


Fig.A-9. Poles to foliation in the major N.N.E.-S.S.W. monocline near the Maldie Burn (open circles). Also axes (solid circles) and axial plane of minor folds of the same style.

can sometimes be seen to terminate downwards, fingering out into quartz and felspar rich layers in the acid gneiss. This phenomenon is also described by Khoury (1968a).

The N.W.-S.E. trending open warps

Only one example of such a fold has been encountered in the area. It occurs west of the Maldie Burn (fig. A-1). This fold appears to be of the same type, and may be of the same age as the 'Kylesku Fold' of Khoury (1968a), which is a large scale N.W.-S.E. trending antiform. A small scale example from the hinge region of the major fold is illustrated in fig. A-10.

E.-W. vertical fracture

The major basic dyke which cuts the Ben Strome basic mass turns from its usual N.W.-S.E. direction on meeting the E.-W. Laxfordian shear belt which forms the northern margin of the mass. It runs due west for 1½ miles, and in this part of its course is only 10-20 yards wide, as opposed to its normal width of up to 140 yards, the widest dyke in the area (Clough et al., 1907, p. 139).

Clough et al. (1907, p. 150) suggest that, as other dykes are displaced only for short distances by the same shear belt further west, this dyke was originally intruded for part of its length along a pre-existing E.-W. fracture. A specimen from the centre of the dyke where it runs E.-W. was found, in thin section, to consist of a fine grained meta-dolerite with ophitic texture. As the same dyke is very coarse grained elsewhere, it may be presumed that the interpretation of Clough et al. (1907) is correct, and that the dyke was intruded as an originally thin body, along a pre-existing fracture, which subsequently became the site of

Fig. A-10

Small scale open warp (F5), $\frac{1}{2}$ mile N.W. of Maldie (fig. A-1). Photo-
graph taken looking north. Axis of the fold runs N.W.



a Laxfordian shear belt, and has not been tectonically thinned.

Steeply dipping gneiss belts

To the west of the major isocline on Ben Strone, there is a curved belt of steeply dipping, amphibolite facies gneisses. These have acquired a foliation of hornblende crystals, but have not been sheared, and still preserve a coarse grain size. Within the belt are some basic and ultrabasic bands, which have suffered partial retrograde metamorphism in their central parts, and have been completely reconstituted at their margins. The belt is of similar type to the N.W.-S.E. monoclinial folds of Khoury (1968b), but it differs from these in that it has not been the site of intrusion of a basic dyke. On the contrary, two basic dykes cross it; one (the E.-W. dyke described above) cuts the belt at right angles.

Complex folds, indicating multi-phase deformation are developed just to the south of the southern basic (metadolerite) dyke which cuts the steep belt. Unlike those described by Khoury (1968b) from Duartbeg, they appear to be folds of concentric type. They, and the steep banding of the gneisses adjacent to them, indubitably pre-date the basic dyke, and may be tentatively correlated with the Inverian metamorphic event (Evans, 1964). No detailed structural analysis of the complex folds was attempted. Some of the structures are shown in fig. A-11.

Basic dykes

Several basic dykes occur in the area. They consist either of metadolerite or massive epidiorite (the former preserving the igneous pyroxenes in an altered state, and the latter consisting largely of amphibolite). The metadolerite dykes are thinner than the epidiorites, the difference in

Fig. A-11

Folds in the N.W.-S.E. belt of steeply dipping, retrograde gneisses at Ben Strome (see figs. 3-9 and A-1).

Photographs all taken looking N.W.



metamorphic alteration being possibly a result of the different heat contents of the dykes, and their capacity to effect auto-metamorphism (O'Hara, 1961b). An alternative explanation of the phenomenon has been advanced by Tarney (1963), working in the Assynt region, who finds metadolerite dykes cutting broader dykes of epidiorite. Both types were supposed to have been intruded into a slowly cooling metamorphic complex, the metadolerites at a later stage, when the environment was less hot.

Barooah (1967, fig. 5-11) finds two N.W.-S.E. metadolerite dykes apparently cutting an E.-W. Laxfordian shear belt, which, a short distance to the west, displaces two epidiorite dykes sinistrally by about 50 yards. Both dyke types are converted into hornblende schist near the shear belt, the epidiorite dykes being foliated parallel to the E.-W. shear belt, but the metadolerite dykes foliated parallel to their margins. Similar metadolerite dykes elsewhere cut a N.W.-S.E. steep gneiss belt (of assumed Inverian age), but are themselves displaced by another E.-W. (Laxfordian) shear belt (Barooah, 1967, fig. 5-12). Barooah concludes that the metadolerite dykes are of intra-Laxfordian age.

Laxfordian shear belts

The E.-W. shear belts which are common in the area are accepted by all workers to the present as being of Laxfordian age. Barooah's (1967) observations on the metadolerite dykes (cited above) require two phases of movement on the shear belts (one pre- and one post-metadolerite). Just east of Maldie, independent evidence of two phases of movement has been found, although, unfortunately, no dykes are present to date either as Laxfordian.

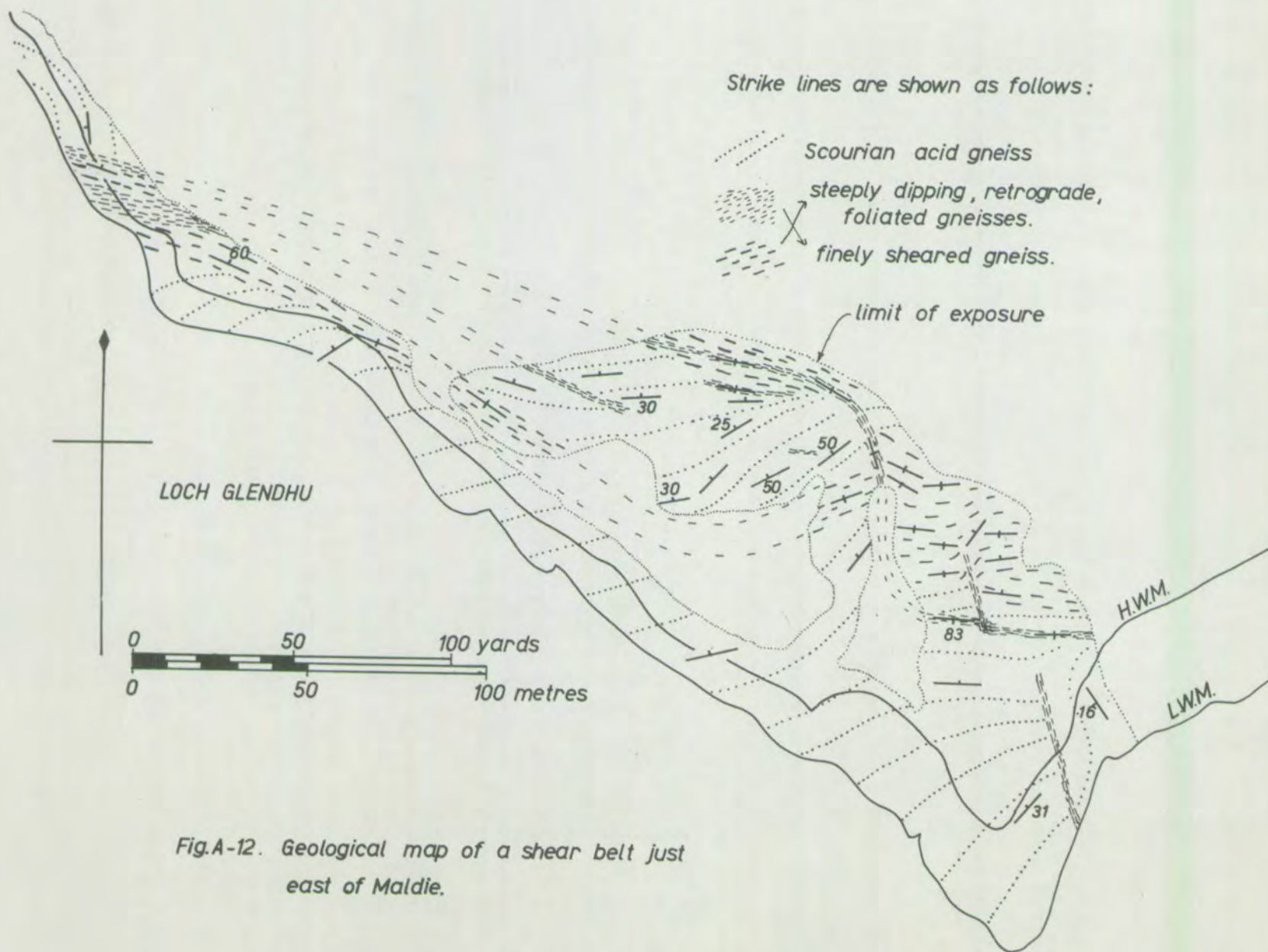


Fig.A-12. Geological map of a shear belt just east of Maldie.

Fig. A-12 is a map of the area. An E.-W. belt of steeply dipping, retrogressively metamorphosed gneiss cuts across the gently dipping Scourian banding. A narrower belt of finely sheared gneiss is coincident with the steep belt in the west, but diverges from it, and, in the east, clearly cuts it at a steep angle. At this point, the finely granulitised shear belt consists of three small shears, arranged en echelon.

The more northerly of the two major shear belts which run across Ben Strome consists, in its eastern part, of finely sheared gneiss, and, where a dyke intersects it, of hornblende schist. Further west, no such rock types are observed, but instead there are a number of narrow veins of mylonite and pseudotachylite, occurring mostly near the southern margin of the E.-W. basic dyke. Similar features are seen in the southern major shear belt, which, in its western part, splits up into a number of separate shears, which consist of finely crushed, epidote bearing gneiss, and enclose lenses of unaltered gneiss and dyke rock.

Summary

The structural sequence described above is summarised in Table A-1.

A.2 Some regional observations

Some controversy has arisen with regard to the nature of the 'middle belt' of Clough et al. (1907) (i.e. the Claisfearn and Foindle zones of Sutton and Watson (1950)). Clough, Sutton and Watson regard the steeply dipping foliation in these areas as the product of a single episode of deformation (i.e. the Laxfordian Orogeny). Sutton and Watson (1950, 1962) make the distinction between two types of deformation: that which

gave rise to steeply dipping foliated but coarse gneisses; and that which gave rise to finely granulated shear belts. These two types of deformation were referred to by Ghose (1958) as 'flattening' and 'shearing'. These terms will be used subsequently in this section.

Holland (1965) concludes that two metamorphic episodes are represented in the area: the Inverian which gave rise to the whole steeply dipping middle belt; and the Laxfordian, which modified the structural pattern in localised shear belts to the south of, and regionally to the north of the 'Ben Stack line', which runs N.W.-S.E. from Laxford to Achfary. Many of Holland's (1965) conclusions depend on the existence of the 'Skerricha Synform', an overturned fold whose hinge lies at Skerricha, 2 miles north of Laxford. As there is no detectable synform at Skerricha (Chowdhary, 1969, and personal communication) it may be wise to regard Holland's (1965) conclusions with reserve, and look for other evidence.

(Barcoah, 1967, fig. 5-10) finds, at a locality about 3 miles E.N.E. of Scourie, an epidiorite dyke which has locally departed from its N.W.-S.E. trend and runs N.N.E.-S.S.W. Here it is unfoliated, and cuts W.N.W.-S.S.E. striking, steeply dipping gneisses at right angles. The same dyke is displaced and foliated by shear belts which strike parallel to the W.N.W.-E.S.E. steeply dipping gneisses. The flattening which produced the steep gneisses must pre-date the dyke, while the shearing post-dates it. They may belong to the Inverian and Laxfordian episodes respectively.

In the course of this study, evidence was found which supports Barcoah's (1967) conclusions. 300 yards W.N.W. of the rubbish tip to the north of Achfary (NC 29154035) a basic dyke which forms a prominent ridge on the

S.E. side of Ben Stack sends an offshoot into the gneiss. The dyke as a whole strikes virtually parallel to the amphibolite facies gneisses, which dip at high angles to the S.W., but at this point it is evidently discordant (fig. A-13). The dyke is of partially amphibolitised dolerite: in the small offshoot pyroxene is still abundant and there is no sign of foliation. Either an intra-Laxfordian age for the dyke or an Inverian age for the flattening deformation which produced the steeply dipping gneisses is required. Neither conforms to the picture of Sutton and Watson (1950, 1962), which is seen to require certain qualifications or modifications.

If an Inverian age for the flattening deformation is accepted, the conclusions become consistent with those of Barcoah (1967), cited above. Schematic profiles across the Scourian-Laxfordian boundary according to Sutton and Watson (1962) (a), and the conclusions outlined above (b and c) are given in fig. A-14. The observation of Sutton and Watson (1962, p.) that the dykes are always steeper than the banding, from which it was concluded that no inversion had taken place, can be as satisfactorily explained by the sequence: deformation of the gneisses, resulting in their vertical attitude; intrusion of N.E. dipping dykes; further deformation and slight overturning. The fact that the Laxfordian gneisses dip under the (modified) Scourian gneisses is more satisfactorily explained by assuming that they have been thrust or folded under the Scourian Complex, particularly in view of the conclusion (Holland, 1965, and Chapter 2, above) that the Laxfordian Complex represents post-Scourian sedimentary material.

FIG. A-13

Sketch, traced from a series of photographs, showing discordant relations between a large basic dyke, and steeply dipping, N.W.-S.E. striking acid gneisses. The locality is $\frac{1}{4}$ mile north of Achfary (exact location given on p. A-9), and the view is looking south-eastwards towards Loch More and the Cambrian escarpment.

The basic dyke consists of patches of metadolerite in epidiorite (amphibolite), the two types grading into each other. The thin off-shoots are of metadolerite. The margin of the dyke consists of hornblende schist for a width of about one foot in the foreground, and for a considerable width in the middle distance.

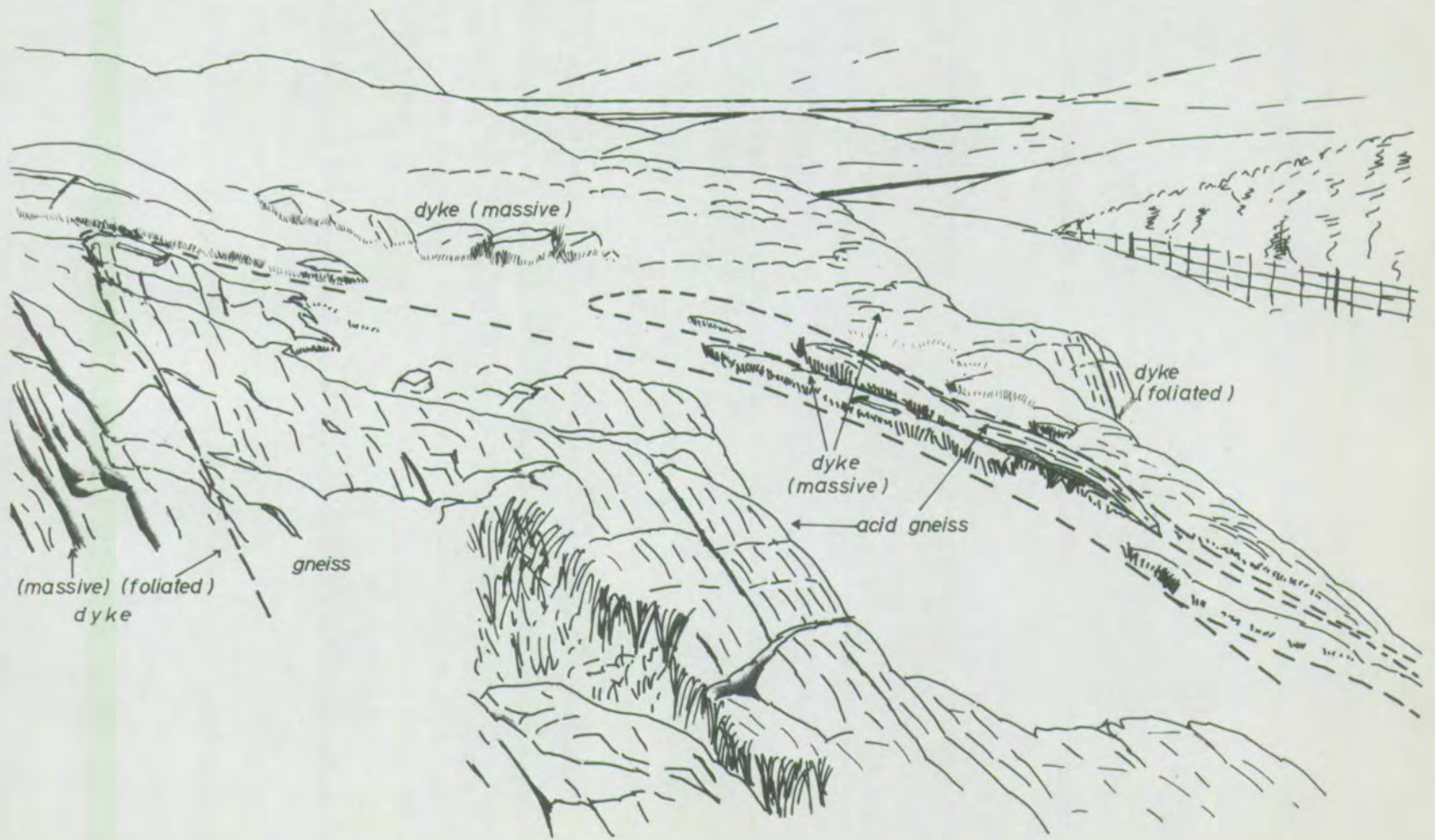
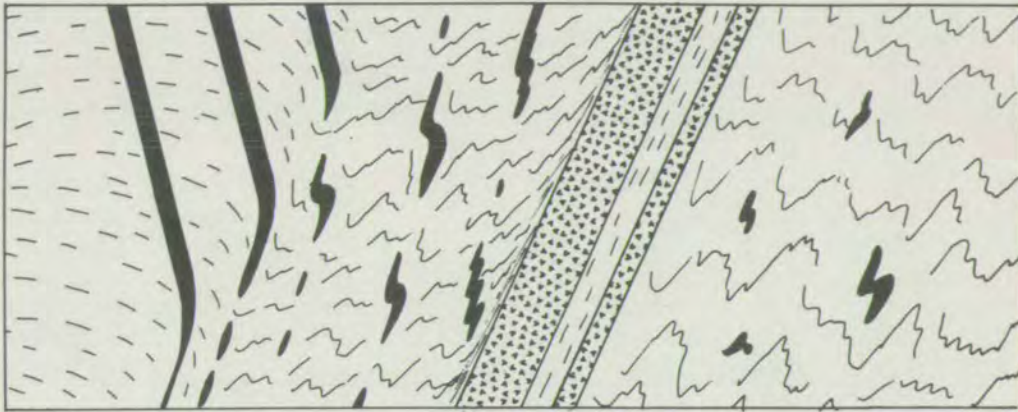


Fig. A-14

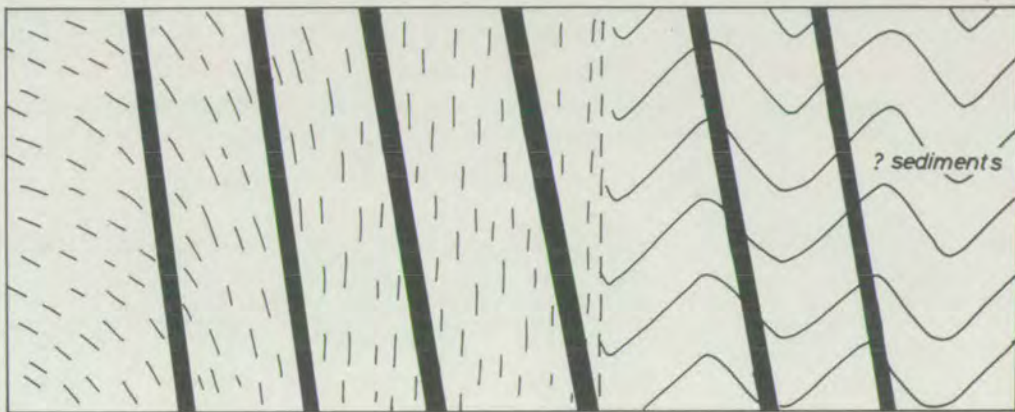
A series of schematic sections across the Scourian-Laxfordian contact. (a) is slightly simplified from Sutton and Watson (1962, fig. 6). (b) and (c) are according to the conclusions of the present study, and express essentially the same sequence of events as was postulated by Holland (1965).



S.W.

(a) Post-Laxfordian

N.E.



S.W.

(b) Post-Inverian

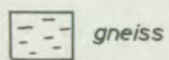
N.E.



S.W.

(c) Post-Laxfordian

N.E.



gneiss



dykes



shear belt



granite

TABLE A-1

TENTATIVE CHRONOLOGY OF THE LEWISIAN FOR THE SCOURIE AND BEN STROME AREAS

LAXFORDIAN	Various folds (not analysed)
	Mylonitisation and pseudotachylite formation partly
	Shearing to form shear belts contemporaneous
	Steeply dipping E.-W. gneiss belts
?INVERIAN	Basic dyke intrusion and autometamorphism
	Steeply dipping N.W.-S.E. gneiss belts and complex folds with flat axial planes
	E.-W. vertical fractures
SCOURIAN	N.W.-S.E. trending open warps (F5)
	N.N.E.-S.S.W. monoclinial folds (F4) with axial plane foliation of quartz grains at Ben Strome, and with potash pegmatites at Scourie
	Main phase folds. Isoclines (F2) and monoclines (F3)
	Axial plane foliation of quartz grains. Lineation (L1)
	Earliest isoclines (F1). Formation of banding (S1), probably as an axial plane structure
	Formation of the complex with an early planar structure (S0)
	?sedimentation and vulcanism

APPENDIX B

POSSIBLE TRACES OF SEDIMENTARY ROCKS IN THE LEWISIAN NEAR SCOURIE

The group of rocks described in this section, although accounting for only a very small proportion of the Complex, give important evidence about its origin. Together with possible traces of sediments described by other workers in the area (p. 11), they strongly suggest the presence of a group of sediments in the Complex.

The types to be described are:

- (1) Saussurite lenticles.
- (2) Diopside-apatite-scapolite-sphene-orthoclase rock.
- (3) Garnet-biotite-titanomagnetite rock.
- (4) Limestone.
- (5) Garnet-biotite schist.

Saussurite

As mentioned in Chapter 2 (p.12) lenticular bodies of pale green rock, made of saussuritised plagioclase, have been noted by Clough (Geol. Survey of Scotland, 6-inch sheet, Sutherland 39), and described by O'Hara (1960 p. 146). They are of common occurrence, and can be found in many areas between Scourie and Kylesku. The rocks can be examined in the following areas, where they are abundant:

(a) In road cuttings between Unapool and Kylesku, especially 50-100 yards north of the school at Unapool.

(b) On the north shore of Loch Glendhu, 400 yards east of Maldie (O'Hara, 1960, p. 146 and fig. 3-9).

(c) South and east of Loch Clach a'Chinn Dubh (fig. 3-9).

The rocks occur as lenticular bodies in the gneiss, whose banding sweeps around them. The largest individual body found was 6 feet long and 3 feet broad. They are generally pale green in colour, but a few are white, and the centres of the larger lenticles may be pale pink in colour. All are white on a weathered surface.

The rocks consist of a coarse granoblastic aggregate of plagioclase, now pseudomorphed by a fine-grained mass of albite (and possibly potash feldspar), clinozoisite, and sericite. On occasions, the albite twinning of the original plagioclase can be distinguished. One section shows unaltered plagioclase, and a determination by the Michel-Levy method gave a maximum extinction angle of 56° (An_{98}).

Garnet occurs in some lenticles. O'Hara (1960, p. 147) determined a garnet refractive index as greater than 1.830, indicating a grossular rich composition. One specimen (B 61) is fairly rich in pale brown garnet with B.I. = 1.778 and $a_o = 11.561 \text{ \AA}$, giving a composition $alm_{52} pyr_{31} gross_{17}$.

Some sections have accessory apatite in anhedral grains, and well rounded grains of zircon. Poikiloblasts of green hornblende enclosing small grains of quartz occurs in aggregates as patches or bands, which may form a margin to the lenticle. Clusters of green biotite may also occur. One specimen (S1) contains a few grains of scapolite.

Four analyses are given in Table B-1. The norms all contain nepheline, corundum, and olivine (except B 191, which contains nepheline and wollastonite) in small quantities. The potash rich character of the rocks is not consistent with the assumption that they consist only

of altered anorthite or bytownite. It is, however, possible that potash enrichment occurred during the saussuritisation.

If most of the original plagioclase were bytownite or a calcic labradorite (and the anorthite which has been mentioned above represents an exceptionally calcic portion which has not been susceptible to saussuritisation by virtue of its homogeneous crystal structure) this would probably be more readily saussuritised during the retrograde stages of metamorphism than the more sodic plagioclase of the acid gneiss. (Bown and Gay (1958) show that the spacing of the postulated anti-phase domains in intermediate plagioclases increases from 40 Å in oligoclase to 100 Å in bytownite; this increase in domain size would probably facilitate breakdown to albite + epidote or zoisite). If albite were formed in the saussurite lenticles, it would be susceptible to increase in potassium and calcium, and loss of sodium by metasomatism from the more calcic plagioclase of the acid gneiss (cf. p. 114). In this way, potassium enrichment of an originally potassium poor calc-silicate rock might have occurred.

Diopside-apatite-scapolite-sphene-orthoclase rock

This rock has been described by O'Hara (1960, p. 45). It forms irregular lenticles and strips between the acid gneiss and plagioclase gneiss on the east side of the basic mass at Geodh'Eanruig, and smaller masses on both sides of the mass at Pairc a'Cladaich.

A petrographic description is given by O'Hara (1960, specimen X 812) of the Geodh'Eanruig rock. An analysis of a similar specimen is given in Table B-1. This specimen differs from that described by O'Hara in that the scapolite is entirely altered to a fine grained epidotic aggregate,

and no optical properties could be determined for it. The low chlorine content indicates that the scapolite must be poor in the marialite component.

Garnet-biotite-titanomagnetite rock

This rock forms a band about 2 cm. thick on the west side of Geodh¹ Eanruig, where it is exposed for a length of about 10 feet. It is bordered on the lower side by normal acid gneiss, and on the upper by a 4 inch thick layer of basic gneiss. In hand specimen it is a brownish schistose rock with prominent red garnets around which the schistosity sweeps.

In thin section it is seen to consist of a coarse aggregate of red-brown biotite, pink garnet, ore, and minor plagioclase. The biotite flakes have a strong preferred orientation, but are often bent and kinked. The ore consists of large subhedral grains of magnetite with very coarse lamellae of ilmenite. The garnet has $R.I. = 1.784$, and $a_0 = 11.585 \text{ \AA}$. Analyses of the garnet and biotite are given in Table 20.

Some small anhedral apatite crystals occur, and there are numerous rounded grains of zircon.

The basic gneiss for 2 cm. adjacent to the band consists of a granoblastic aggregate of augite, hypersthene, plagioclase, ore and biotite. The pyroxenes are rimmed by a thin mantle of green hornblende.

Analyses of the garnet-biotite-titanomagnetite rock and four samples of the adjacent basic gneiss are given in Table B-2. The garnet-biotite-titanomagnetite rock is corundum-normative, a feature which is very uncommon amongst Scourian rocks, and may be suggestive of a pelitic origin. The basic gneiss adjacent to it is very poor in normative diopside, while

that more than 2 cm. away is of normal basic gneiss composition.

Limestone

Two occurrences of limestone have been noted. One, mentioned by Clough et al. (1907, p. 148) occurs as an elongated, vertical lens in a shear belt about 1½ miles S.E. of Geisgil. It is a relatively large body, about 400 yards long, and up to 25 yards wide. The other occurrence consists of a number of small lenticles in a shear belt on Bilean Garbh, in Badcall Bay. The largest of these masses is only 2 feet long.

The Geisgil occurrence consists of a coarse granular calcite rock. Thin bands and wisps rich in green hornblende, with considerable amounts of apatite and green biotite define a foliation which is parallel to that of the adjacent sheared gneiss. The Bilean Garbh limestone is somewhat finer grained, although still coarse, and consists of about equal proportions of calcite and dolomite. Magnetite occurs, finely disseminated throughout, and there are thin bands of green biotite with a strong preferred orientation. Analyses of a specimen from each locality are given in Table B-1.

As these limestone masses both occur in shear belts, it may be doubted whether they represent parts of the Scourian Complex. The low Cr and Ni contents do not suggest an origin from ultrabasic material: introduction of CO₂ along the shear belts is a possibility for their formation.

Garnet-biotite schist

Clough et al. (1907, p. 153) refer briefly to "bands of yellow weathering pyritous gneiss, often with small red garnets" which occur "in the north-eastern part of the middle belt", i.e. close to the S.W. margin

of the Laxford granites. One such band, up to 200 yards wide, was said to form a prominent gulley half way up the N.E. side of Ben Stack, and could be followed along the strike, to the coast near Tarbet (Clough et al., 1907, p. 154).

This band was briefly examined at Ben Stack. It is very poorly exposed, owing to its ease of weathering. Where exposures could be found, about 500 yards S.W. of Loch Stack Lodge, it consisted of a schistose rock, rich in small rounded garnets, and biotite, with pale greenish plagioclase and quartz. In thin section it is seen to consist of bands alternately rich in plagioclase (An_{55}) and quartz, and garnet and biotite. The quartz occurs in nearly strain free, elongated grains, with abundant needle like inclusions (rutile?) which have a strong preferred orientation, parallel to the elongation of the grains and to the foliation. The biotite is reddish brown, and the garnet pink and isotropic. Apatite, rounded grains of zircon, and some orthite occur as accessory minerals.

TABLE B-1

	S 1	B 57	B 61	B 191	B 171	B 198	B 301
SiO ₂	48.85	46.05	50.2	48.3	48.85	3.95	8.65
TiO ₂	0.18	0.07	0.10	0.03	1.32	0.52	0.07
Al ₂ O ₃	28.7	29.6	27.2	28.4	7.75	0.4	3.6
Fe ₂ O ₃	1.55	0.7	0.7	0.8	1.85	3.85	0.55
FeO	0.8	1.05	1.35	0.41	4.9	7.8	3.55
MnO	0.04	0.03	0.05	0.01	0.23	0.31	0.43
MgO	0.9	1.05	1.35	0.95	7.9	15.35	4.9
CaO	8.05	10.9	7.55	13.95	18.6	30.7	42.9
Na ₂ O	2.18	1.60	3.49	3.21	1.23	0.07	0.23
K ₂ O	5.04	4.36	3.60	1.03	1.97	0.07	0.64
H ₂ O	3.53	3.80	2.58	2.24	n.d.	0.08	0.62
P ₂ O ₅	0.1	0.1	0.1	0.1	2.29	0.1	0.25
CO ₂	0.21	0.09	0.2	0.00	0.21	n.d.	n.d.
S	-	-	n.d.	n.d.	0.11	n.d.	n.d.
total	99.8 100.1	99.44	98.45	99.4	97.2	-	-

Trace elements, p.p.m.

Cr	35	20	40	50	100	870	20
Ni	10	30	20	14	140	140	60
Rb	37	29	32	13	-	-	5
Sr	485	520	490	370	350	970	435
Ba	930	1150	930	340	980	230	420

C.I.P.W. norms

Qz	-	-	-	-	1.4
Cor	6.0	3.0	4.8	-	-
Or	30.8	27.0	22.2	6.3	11.0
Ab	18.7	5.4	29.5	20.0	10.7
An	39.3	55.3	36.9	61.8	10.1
Ne	0.2	4.8	0.7	4.3	-
Di	-	-	-	5.3	54.3
Ol	1.6	2.9	3.9	-	-
Woll	-	-	-	0.8	-
Mt	2.2	1.1	1.1	1.3	2.0
Hm	0.1	-	-	-	-
Il	0.4	0.1	0.2	0.1	2.6
Ap	0.2	0.2	0.2	0.2	5.6

TABLE B-2

	GE 13	GE14A-1	GE14A-2	GE14B-1	GE14B-2
SiO ₂	46.3	54.8	52.1	47.5	48.4
TiO ₂	1.62	1.40	0.96	0.77	0.93
Al ₂ O ₃	21.05	19.25	16.15	13.8	13.8
Fe ₂ O ₃	2.8	1.7	3.4	5.05	5.05
FeO	11.25	6.9	9.65	9.25	8.85
MnO	0.18	0.20	0.33	0.29	0.25
MgO	3.75	4.35	7.4	8.55	9.05
CaO	6.7	5.92	5.75	10.6	11.2
Na ₂ O	3.00	4.84	3.92	2.54	2.38
K ₂ O	1.80	0.84	0.39	0.39	0.49
H ₂ O	0.62	0.46	0.23	0.36	0.40
total	99.1	100.7	99.9 100.3	99.1	100.8

Trace elements, p.p.m.

Cr	25	130	220	140	80
Ni	160	210	160	200	170
Rb	19	-	-	4	-
Sr	340	350	245	130	115

C.I.P.W. norms

Qz	-	0.2	3.3	-	-
Cor	2.0	-	-	-	-
Or	10.8	4.9	2.4	2.3	2.9
Ab	25.8	40.8	33.9	21.8	20.1
An	33.7	28.2	27.0	25.4	25.4
Di	-	0.9	2.3	22.7	24.2
Hy	4.6	19.7	24.0	8.6	9.6
Ol	15.8	-	-	10.3	8.7
Mt	4.1	2.5	5.1	7.4	7.3
Il	3.1	2.7	1.9	1.5	1.8

APPENDIX C

CHEMICAL ANALYSES OF ROCKS

In this Appendix the majority of the whole rock chemical analyses made during the course of this study are presented. They are all expressed in weight percentages of oxides, with trace element concentrations in parts per million. The totals do not include trace element values, ~~except for the ultrabasic rocks, where the Cr and Ni concentrations have been converted to oxides and added to the totals. For these rock types, these are major elements, in that they often exceed TiO_2 , MnO , Na_2O , and K_2O .~~

Where a value for an element or oxide is not quoted, this is indicated either by n.d. (not determined), or by a dash, which indicates that the concentration was below the lower level of sensitivity of X-ray fluorescence analysis. This level is about 10 p.p.m. for Sr, 5 p.p.m. for Rb in basic rocks and 10 p.p.m. in ultrabasic rocks (but only about 2 p.p.m. in acid rocks, where the matrix composition is closely similar to that of the synthetic standards used), and 2 p.p.m. for Pb.

The analyses are also given recalculated, on a water- and CO_2 -free basis, to cation atomic percentages. For the ultrabasic contact sequences in Tables 4 to 14, the reduced compositional parameters of O'Hara (1968a) are also given. These are:

$$'CaO' = CaO + 2Na_2O + 2K_2O - P_2O_5/3$$

$$'Al_2O_3' = Al_2O_3 + TiO_2 + Fe_2O_3 + Cr_2O_3 + Na_2O + K_2O$$

$$'MgO' = MgO + FeO + MnO + NiO - TiO_2$$

$$'SiO_2' = SiO_2 - 2Na_2O - 2K_2O$$

All are in molecular proportions of oxides, and the reduced parameters are also quoted in molecular percentages.

The analyses were recalculated to proportions of idealised granulite facies minerals. This was achieved by using part of the computer programme in Appendix E, and the reduced parameters referred to above. These minerals are also quoted in molecular percentages, the 'molecule' being one oxide molecule for each mineral, e.g. anorthite would be $(\text{CaO})_{\frac{1}{2}} \cdot (\text{Al}_2\text{O}_3)_{\frac{1}{2}} \cdot (\text{SiO}_2)_{\frac{1}{2}}$ on this basis.

The methods of analysis are given in Appendix G, together with the accuracy with which it is believed possible to quote the analyses.

TABLE 1

Analyses of ultrabasic gneisses

Geodh nam Cliabh:

Specimens collected from adjacent bands in the northern part of the main ultrabasic layer (fig. 3-4).

(5) Hornblende-rich olivine-pyroxenite from massive, coarse grained 4-inch thick layer, overlain by

(6) Pyroxene-rich layer with some olivine, 2 inches thick, overlain by

(7) Olivine-rich peridotite layer, 8 inches thick, overlain by

(8) Pyroxene-rich, peridotite, distinctly more massive.

(9) Hypersthene-rich layer, with little olivine or spinel, 1 ft. above (8).

(11) Olivine-pyroxenite, from approximately the same horizon as (7), 20 ft. N.W. along the outcrop.

Ben Strome: (for specimen localities, see fig. 3-9)

Specimens from outlet of loch on the Maldie Burn:

B 3. Coarse hornblende-rich olivine-pyroxenite, overlain by

B 4. Somewhat serpentinitised peridotite gneiss.

Specimens from a thin ultrabasic layer in basic gneiss, west of the summit of Ben Strome:

B 177. 1-inch layer of granular pyroxenite, poor in spinel and hornblende, overlain by

B 178. 1-inch layer of peridotite gneiss.

Specimens from the thick ultrabasic layer, west of the Maldie Burn:

B 63A. Peridotite gneiss, with a particularly pale green hornblende, overlain by

B 63B(1). 3-inch layer of olivine-pyroxenite, with a normal green hornblende, and spinel, overlain by

B 63B(2). 4-inch layer of hornblende-pyroxenite, without spinel or olivine.

The analysis of (7) is not complete, as the entire sample was inadvertently used for mineral separation before the determination of FeO , Na_2O , and H_2O .

Modes are quoted only for the Geodh nam Cliabh specimens, as these samples were small chips, of which one or two thin sections were representative. The Ben Strome specimens were larger, so that each analysis represents an average of a number of bands of different mineral constitution, and a modal analysis with only one or two thin sections was not feasible.

TABLE 1

	5	6	7	8	9	11	B 3	B 4	B 177	B 178	B 63A	B 63B-1	B 63B-2
SiO ₂	45.8	49.9	44.9	45.5	51.0	46.6	45.65	45.2	49.9	43.7	43.7	44.55	47.65
TiO ₂	0.44	0.26	0.27	0.33	0.23	0.28	0.35	0.32	0.25	0.31	0.21	0.25	0.31
Al ₂ O ₃	8.3	6.4	5.2	5.5	5.45	6.05	7.15	6.15	5.75	5.2	5.85	5.8	7.5
Fe ₂ O ₃	5.15	3.55	4.6	4.6	n.d.	4.25	4.45	4.65	1.7	5.55	4.4	4.3	2.9
FeO	7.1	7.3	7.8	8.15	11.25	6.6	6.05	6.35	8.4	6.65	5.8	6.2	6.65
MnO	0.22	0.23	0.18	0.20	0.20	0.19	0.18	0.18	0.18	0.16	0.16	0.17	0.17
MgO	22.6	26.4	27.8	27.5	25.6	26.4	23.4	25.4	24.7	25.1	26.1	27.2	24.6
CaO	6.8	4.35	5.95	5.9	6.9	7.75	7.6	6.5	6.65	7.3	6.6	5.5	6.25
Na ₂ O	1.31	1.06	0.42	0.55	n.d.	0.80	0.80	0.45	0.41	0.48	0.72	0.28	0.99
K ₂ O	0.27	0.13	0.10	0.14	0.25	0.16	0.12	0.07	0.06	0.07	0.16	0.16	0.30
S	0.03	-	0.03	0.03	-	-	0.08	0.02	0.04	0.00	0.07	0.05	0.06
CO ₂	n.d.	n.d.	n.d.	n.d.	n.d.	n.d.	0.17	0.08	0.02	0.13	0.23	0.07	0.07
H ₂ O	2.65	0.94	3.21	2.82	n.d.	1.62	3.17	4.19	0.75	4.59	4.89	4.58	1.73
total	100.7	100.6	100.4	100.2	-	100.7	99.2	99.6	98.8	99.2	98.9	99.1	99.2

Trace elements, p.p.m.

Cr	1800	1900	1700	2200	1600	1900	2300	2400	2200	2400	2400	2500	2350
Ni	980	1260	1980	2000	1100	1610	1120	1460	1180	1710	1420	1540	1120
Ba	210	170	200	160	n.d.	190	200	240	230	330	330	460	610
Sr	95	70	50	60	50	75	60	50	n.d.	35	n.d.	n.d.	n.d.

Cation atomic percent

Si	41.6	44.1	40.6	40.7	-	41.4	42.2	40.4	44.6	41.0	41.1	41.3	43.0
Ti	0.30	0.17	0.18	0.22	-	0.19	0.24	0.22	0.17	0.22	0.15	0.17	0.21
Al	8.9	6.7	5.5	5.8	-	6.3	7.8	6.8	6.2	5.8	6.5	6.3	8.0
Fe ⁺⁺⁺	3.5	2.4	3.1	3.1	-	2.8	3.1	3.3	1.2	3.9	3.1	3.0	2.0
Fe ⁺⁺	5.4	5.4	5.9	6.1	-	4.9	4.7	5.0	6.4	5.2	4.6	4.8	5.0
Mn	0.17	0.17	0.14	0.15	-	0.14	0.14	0.14	0.14	0.13	0.13	0.13	0.13
Mg	30.6	34.8	37.5	36.7	-	35.0	32.2	35.4	33.6	35.1	36.6	37.6	33.1
Ca	6.6	4.1	5.8	5.7	-	7.4	7.5	7.6	6.5	7.3	6.6	5.5	6.1
Na	2.3	1.8	0.7	1.0	-	1.4	1.4	0.8	0.7	0.9	0.5	0.5	1.7
K	0.31	0.15	0.12	0.16	-	0.18	0.14	0.08	0.07	0.08	0.19	0.19	0.35
S	0.05	0.00	0.05	0.05	-	0.00	0.14	0.04	0.07	0.00	0.12	0.09	0.10
Cr	0.19	0.20	0.18	0.23	-	0.20	0.25	0.26	0.27	0.24	0.26	0.27	0.24
Ni	0.09	0.11	0.18	0.18	-	0.14	0.10	0.14	0.11	0.17	0.14	0.15	0.10

$\frac{\text{Fe}}{\text{Fe}+\text{Mg}}$	22.6	18.3	19.4	20.0	18.2	18.1	19.5	18.9	18.4	20.7	17.3	17.2	17.4
---	------	------	------	------	------	------	------	------	------	------	------	------	------

Modes, volume percent

oliv.	8	1	24	9	3	6
opx	19	38	23	36	33	26
cpx	19	32	25	32	46	37
Amph.	52	29	22	18	19	32
sp/ore	3	1	5	3	tr.	4

TABLE 2

Analyses of garnetiferous basic gneisses

Specimens B 214 to 234, B 2, B 11, and B 203 are from Ben Strome.
Localities are shown on fig. 3-9.

Specimens Z 718 and B 285 are from Geodh'Eanruig (see also Table 4).

Specimens SH 15-16 are from Scourie House (see also Table 14).

These specimens are petrographically similar, and no descriptions are given. The modal analyses are all from one or two thin sections and probably do not give the proportion of garnet with any accuracy. They may be satisfactory for the relative proportions of the other minerals.

TABLE 2

	B 214	B 215	B 216	B 217	B 218	B 219	B 220	B 224	B 231	B 232	B 233	B 234	B 203	B 2	B 11	Z 718	B 285	SH 15	SH 16
SiO ₂	47.1	45.8	47.6	47.0	44.2	47.6	46.5	46.65	46.45	46.8	45.5	49.1	45.5	50.25	46.15	45.78	47.05	48.5	48.0
TiO ₂	1.03	1.07	0.89	1.10	1.31	0.88	1.12	0.56	0.97	1.00	1.16	0.95	1.07	0.91	1.05	0.96	0.99	0.80	0.81
Al ₂ O ₃	15.4	14.4	14.2	14.25	13.0	13.95	12.85	12.7	14.55	13.45	12.9	13.2	15.05	17.35	15.25	15.26	15.8	14.95	15.65
Fe ₂ O ₃	1.65	5.3	2.9	1.65	3.8	1.8	1.95	3.1	2.1	2.4	1.85	1.35	3.7	0.65	2.3	3.58	2.7	2.05	1.85
FeO	10.65	9.0	10.6	13.15	14.25	12.2	11.7	9.95	12.2	12.85	14.75	12.1	9.65	10.4	9.6	11.39	11.55	10.15	9.4
MnO	0.20	0.22	0.22	0.27	0.30	0.23	0.23	0.20	0.25	0.24	0.29	0.20	0.21	0.17	0.16	0.26	0.22	0.20	0.23
MgO	8.0	9.25	8.2	7.05	8.9	8.6	11.95	12.5	8.8	8.65	7.7	8.35	9.85	8.1	9.7	8.28	7.5	7.3	7.35
CaO	11.9	11.55	13.0	12.4	12.3	12.25	11.4	11.7	12.05	12.3	12.2	11.75	13.45	10.6	12.5	12.73	11.95	12.2	13.45
Na ₂ O	1.96	2.66	1.95	1.60	1.62	1.74	1.35	1.44	1.52	1.62	1.30	1.97	1.53	1.77	1.64	1.71	2.00	2.55	2.22
K ₂ O	0.21	0.07	0.07	0.06	0.15	0.08	0.19	0.54	0.06	0.05	0.28	0.07	0.09	0.25	0.16	0.05	0.02	0.12	0.26
H ₂ O	1.12	1.09	0.74	1.30	0.82	0.60	0.86	0.75	0.93	0.85	0.98	1.04	0.63	0.44	0.89	0.30	0.51	0.36	0.35
total	99.2	100.4	100.4	99.8	100.6	99.9	99.9 100.1	100.1	99.9	100.2	99.1 98.9	100.1	100.7	100.9	99.4	100.3	100.3	99.5	99.7
Trace elements, p.p.m.																			
Cr	320	190	150	140	120	250	370	810	310	220	150	n.d.	n.d.	n.d.	360	250	130	210	270
Ni	200	140	120	180	85	130	280	260	170	140	200	120	230	120	260	160	90	280	200
Ba	130	190	80	60	90	100	80	70	70	40	120	60	90	70	70	60	40	80	100
Zr	60	60	35	50	70	40	25	25	55	50	50	40	50	55	35	40	30	65	70
Y	29	24	16	29	32	22	23	15	26	28	32	23	17	18	22	27	26	21	26
Sr	105	345	115	110	35	190	65	100	100	115	80	90	135	70	105	80	75	150	140
Rb	-	-	-	-	-	-	-	-	-	-	8	-	-	-	-	6	-	-	-
Zn	85	120	90	105	140	120	120	95	130	125	125	110	90	115	90	110	100	110	85
Cu	85	30	60	125	40	80	50	60	85	80	205	195	110	65	110	310	155	180	45
Cation atomic percent																			
Si	44.8	42.9	44.8	45.1	42.0	44.9	43.5	44.5	44.1	45.4	44.2	46.5	42.4	46.6	43.5	43.1	44.3	45.7	45.0
Ti	0.7	0.8	0.6	0.8	0.9	0.6	0.23	0.38	0.7	0.7	0.9	0.7	0.8	0.6	0.7	0.7	0.7	0.6	0.6
Al	17.3	15.9	15.7	16.1	14.5	15.5	14.2	13.6	16.3	14.7	14.8	14.7	16.5	19.0	16.9	16.9	17.5	16.6	17.3
Fe'''	1.2	3.7	2.1	1.2	2.7	1.3	1.4	2.1	1.5	1.7	1.4	1.0	2.6	0.46	1.7	2.5	1.9	1.5	1.3
Fe''	8.5	7.1	8.3	10.6	11.3	9.6	9.1	7.6	9.7	10.0	12.0	9.6	7.5	8.1	7.6	9.0	9.1	8.0	7.4
Mn	0.16	0.17	0.18	0.22	0.24	0.18	0.18	0.15	0.20	0.19	0.24	0.16	0.17	0.13	0.13	0.21	0.18	0.16	0.18
Mg	11.3	12.9	11.5	10.1	12.6	12.1	16.7	17.0	12.4	12.0	11.1	11.8	13.7	11.2	13.6	11.6	10.5	10.2	10.3
Ca	12.1	11.6	13.1	12.8	12.6	12.4	11.4	11.4	12.2	12.3	12.7	11.9	13.4	10.5	12.6	12.8	12.1	12.3	13.5
Na	3.6	4.8	3.6	3.0	2.9	3.2	2.5	2.5	2.8	2.9	2.5	3.6	2.8	3.2	3.0	3.1	3.7	4.7	4.0
K	0.25	0.08	0.08	0.07	0.18	0.10	0.23	0.6	0.07	0.06	0.35	0.08	0.11	0.30	0.19	0.06	0.02	0.14	0.31

TABLE 2(a)

	B 214	B 215	B 216	B 217	B 218	B 219	B 220	B 224	B 231	B 232	B 233	B 234	B 203	B 2	B 11	Z 718	B 285	SH 15	SH 16
C.I.P.W. norms																			
Or	1.3	0.4	0.4	0.4	0.9	0.5	1.1	3.2	0.4	0.3	1.7	0.4	0.5	1.5	1.0	0.3	0.1	0.7	1.6
Ab	16.9	20.9	16.6	13.7	13.5	14.8	11.5	12.2	13.0	13.8	11.2	16.8	12.9	14.9	14.1	14.5	17.0	21.8	18.9
An	33.2	27.4	29.9	32.0	27.9	30.2	28.6	26.7	33.0	29.5	29.1	27.2	33.9	38.5	34.3	33.8	34.1	29.3	32.2
Di	22.2	24.6	28.6	25.3	27.6	25.5	23.1	25.5	22.6	26.4	27.2	26.1	26.6	11.4	23.0	24.1	20.9	26.4	28.7
Hy	9.3	-	7.9	15.6	0.06	12.5	12.7	7.2	13.2	12.0	11.5	18.4	2.2	29.1	6.9	5.7	10.7	5.1	0.7
Ol	12.7	16.0	10.7	8.4	22.1	12.1	17.9	19.4	12.9	12.6	14.2	7.2	16.5	1.9	15.2	14.6	11.4	12.1	13.5
Mt	2.5	7.8	4.3	2.1	5.5	2.6	2.8	4.5	3.0	3.5	2.8	2.0	5.3	1.0	3.4	5.2	3.9	3.0	2.7
Il	2.0	2.0	1.7	2.1	2.5	1.7	2.1	1.1	1.9	1.9	2.3	1.8	2.0	1.7	2.0	1.8	1.9	1.5	1.6
Ne	-	0.9	-	-	-	-	-	-	-	-	-	-	-	-	-	-	-	-	-
Reduced compositional parameters																			
'CaO'	18.2	19.0	18.9	17.8	17.6	17.5	15.7	16.5	17.0	17.4	17.3	17.4	18.5	15.9	17.9	18.2	17.9	19.5	20.3
'Al ₂ O ₃ '	13.5	15.0	12.8	12.4	12.5	12.0	11.0	11.2	12.4	11.9	11.5	11.6	13.3	13.7	13.2	13.6	14.0	13.7	13.7
'MgO'	21.9	22.3	21.9	22.6	26.2	23.9	28.0	27.6	24.3	23.5	25.1	23.3	23.4	21.3	23.3	22.9	21.8	20.3	20.0
'SiO ₂ '	46.5	43.7	46.4	47.3	43.7	46.6	45.3	44.7	46.3	46.2	46.1	47.7	44.8	49.0	45.6	45.3	46.3	46.5	46.3
$\frac{\text{Fe}}{\text{Fe}+\text{Mg}}$	46.0	45.5	47.5	53.8	52.6	47.4	38.7	36.4	47.3	49.4	54.5	47.2	42.5	43.2	40.4	48.9	51.1	51.5	46.3
$\frac{\text{Fe}^{++}}{\text{Fe}^{++}+\text{Mg}}$	42.9	35.5	41.9	51.2	47.3	44.2	35.3	30.9	43.9	45.5	51.9	44.9	35.4	42.0	35.8	43.6	46.4	43.9	41.8
Modes, volume percent																			
opx	0.3	2	1	0.3	1	0.3	0.3	3	tr.	0.2	tr.	0.3	2	5	tr.	6	2	3	1
cpx	43	42	34	37	49	47	35	31	38	56	46	60	48	42	33	47	34	37	51
garnet	42	3	5	15	30	11	28	33	42	23	39	16	16	18	35	17	24	8	21
plag	10	39	50	48	15	39	7	20	16	20	13	21	22	31	20	20	34	52	26
amph	2	14	9	tr.	3	2	30	13	2	tr.	tr.	0.3	11	2	12	1	4	-	0.5
ore	2	-	1	0.3	2	0.3	-	1	2	1	2	2	-	0.5	-	9	2	-	-

TABLE 3

Analyses of basic gneisses

Specimens B 286-7 are from Geodh'Eanruig and petrographic summaries are given on p. 38. The other specimens are very similar petrographically.

B 522. Basic gneiss from the exposure at the south end of the Scourie House mass (C on fig. 3-5).

B 523. Very poorly garnetiferous basic gneiss from the eastern side of the western part of the Pairc a'Cladaich basic mass. Approximately 20' below Z 706 (Table 9), and 8' from the acid gneiss contact (fig. 3-6).

B 526. Very poorly garnetiferous basic gneiss from the Camas nam Buth basic mass (fig. 3-8).

B 527. Basic gneiss. A composite specimen from the basic band west of the summit of Ben Strome (fig. 3-9).

TABLE 3

	B 286	B 287	B 522	B 523	B 526	B 527
SiO ₂	47.5	46.55	48.9	48.5	48.5	49.9
TiO ₂	1.01	0.85	0.24	1.22	1.11	0.82
Al ₂ O ₃	14.25	14.1	15.8	14.4	12.6	14.45
Fe ₂ O ₃	1.75	4.4	1.7	2.7	2.65	2.75
FeO	11.75	9.85	5.95	10.75	10.65	9.6
MnO	0.22	0.23	0.19	0.21	0.22	0.21
MgO	8.0	9.7	10.9	7.0	8.3	6.45
CaO	12.15	11.25	11.6	11.3	12.15	10.2
Na ₂ O	1.74	1.72	1.01	1.99	1.85	2.33
K ₂ O	0.06	0.48	1.85	0.89	0.16	1.04
H ₂ O	0.63	0.74	0.95	0.62	1.23	1.31
total	99.1	99.91	99.1	99.6	99.4	99.1

Trace elements, p.p.m.

Cr	170	190	740	180	340	260
Ni	120	150	150	140	160	130
Ba	80	200	700	300	120	420
Zr	45	45	20	100	50	60
Y	32	26	12	40	19	22
Sr	140	165	180	45	115	180
Rb	-	10	20	10	-	12
Zn	110	110	55	180	110	130
Cu	260	50	20	130	65	160

Cation atomic percent

Si	45.3	43.9	45.6	46.2	46.4	47.9
Ti	0.7	0.6	0.17	0.9	0.8	0.6
Al	16.0	15.7	17.4	16.2	14.2	16.3
Fe'''	1.3	3.1	1.2	2.0	1.9	2.0
Fe''	9.4	7.8	4.6	8.6	8.5	7.7
Mn	0.19	0.18	0.16	0.16	0.16	0.16
Mg	11.4	13.6	15.2	9.9	11.9	9.2
Ca	12.4	11.4	11.6	11.5	12.4	10.5
Na	3.2	3.1	1.8	3.7	3.4	4.3
K	0.07	0.6	2.2	1.0	0.20	1.3

TABLE 3(a)

	B 286	B 287	B 522	B 523	B 526	B 527
C.I.P.W. norms						
Or	0.4	2.9	11.1	5.0	1.0	6.3
Ab	15.0	14.7	8.7	17.0	15.9	20.2
An	31.4	29.6	33.8	28.2	26.1	26.5
Di	24.6	21.5	20.0	23.6	28.9	26.9
Hy	15.5	11.9	12.3	14.2	19.1	19.6
Ol	8.6	11.4	11.1	5.7	3.0	0.9
Mt	2.6	6.4	2.5	4.0	3.9	4.1
Il	2.0	1.6	0.5	2.3	2.2	1.6
Reduced compositional parameters						
'CaO'	17.7	17.1	17.7	18.5	18.0	18.1
'Al ₂ O ₃ '	12.4	13.5	12.9	14.0	12.0	14.4
'MgO'	22.7	23.8	22.4	20.2	22.1	18.9
'SiO ₂ '	47.2	45.6	47.0	47.3	47.9	48.3
$\frac{\text{Fe}}{\text{Fe}+\text{Mg}}$	48.2	44.3	27.8	51.5	46.7	51.3
$\frac{\text{Fe}^{2+}}{\text{Fe}^{2+}+\text{Mg}}$	45.2	36.3	23.2	46.5	41.7	45.6

TABLE 4

Analyses of rocks, Upper Contact, Geodh'Eanruig

Petrographic summaries of these rocks are given on pp. 38-41. The specimens were collected in a downward sequence, as follows:

B 285. Garnetiferous basic gneiss

20' to

Z 718. Garnetiferous basic gneiss

4' 6" to

Z 720. Garnet-augite gneiss

2' 0" to

Z 721. Garnet-augite gneiss

5" to

Z 722. Garnet-augite gneiss, transitional

continuous

Z 723. to clinopyroxenite

sample,

Z 724.

9" long

1' 0" to

Z 725. Hornblende-spinel-pyroxenite

5" to

Z 726. Olivine-pyroxenite

2' 6" to

Z 727. Peridotite (not analysed owing to loss of specimen)

TABLE 4

	Z 726	Z 725	Z 724	Z 723	Z 722	Z 721	Z 720	Z 718	B 285
SiO ₂	45.46	45.66	48.81	47.97	48.15	46.38	47.46	45.78	47.05
TiO ₂	0.36	0.41	0.44	0.46	0.42	0.50	0.62	0.96	0.99
Al ₂ O ₃	7.65	8.42	8.23	9.71	9.21	11.94	11.25	15.26	15.8
Fe ₂ O ₃	5.10	5.19	2.38	2.05	2.82	2.67	2.44	3.58	2.71
FeO	7.25	7.56	9.28	9.06	10.36	10.03	11.40	11.39	11.55
MnO	0.21	0.23	0.22	0.14	0.19	0.23	0.24	0.26	0.22
MgO	23.87	20.19	15.06	13.86	15.34	13.05	12.66	8.28	7.5
CaO	8.11	9.38	13.80	15.04	11.99	13.32	12.73	12.73	11.95
Na ₂ O	0.57	0.78	0.81	0.95	0.71	0.91	1.03	1.71	2.00
K ₂ O	0.11	0.15	0.28	0.20	0.28	0.22	0.10	0.05	0.02
H ₂ O	1.16	0.72	0.61	0.46	0.72	0.61	0.40	0.30	0.51
S	0.03	0.04	0.00	0.06	0.14	0.06	0.07	0.00	n.d.

total	99.88	99.18 98.73	99.912	99.96	100. 47 33	99.92	100.40	100.30	100.3
-------	-------	---------------------------	--------	-------	--------------------------	-------	--------	--------	-------

Trace Elements, p.p.m.

Cr	2600	2500	990	900	790	800	600	250	130
Ni	1300	860	200	260	280	280	230	160	90
Sr	95	95	70	70	65	85	65	80	75

Cation Atomic Percent.

Si	41.02	41.85	45.24	44.37	44.46	43.17	44.05	43.05	44.30
Ti	0.24	0.28	0.31	0.32	0.29	0.35	0.43	0.68	0.70
Al	8.14	9.10	8.99	10.59	10.02	13.10	12.31	16.92	17.53
Fe ⁺⁺⁺	3.46	3.58	1.66	1.43	2.00	1.87	1.70	2.53	1.92
Fe ⁺⁺	5.47	5.80	7.19	7.01	8.00	7.81	8.85	8.96	9.09
Mn	0.16	0.18	0.17	0.11	0.15	0.18	0.19	0.21	0.18
Mg	32.10	27.58	20.80	19.11	21.11	18.10	17.51	11.60	10.52
Ca	7.84	9.65	13.71	14.91	11.86	13.29	12.66	12.83	12.06
Na	1.00	1.39	1.46	1.70	1.41	1.64	1.85	3.12	3.65
K	0.13	0.18	0.33	0.24	0.33	0.26	0.24	0.06	0.02
Cr	0.27	0.27	0.10	0.10	0.09	0.09	0.07	0.03	0.01
Ni	0.12	0.08	0.02	0.02	0.03	0.03	0.02	0.02	0.01
S	0.05	0.07	0.02	0.10	0.24	0.10	0.12	0.00	-

$\frac{\text{Fe}}{\text{Fe}+\text{Mg}}$	21.8	25.4	29.8	30.6	32.1	34.8	37.6	48.9	51.1
$\frac{\text{Fe}^{++}}{\text{Fe}^{++}+\text{Mg}}$	14.6	17.4	25.7	26.8	27.5	30.1	33.6	43.6	46.4

TABLE 4(a)

	Z 726	Z 725	Z 724	Z 723	Z 722	Z 721	Z 720	Z 718	B 285
Reduced compositional parameters									
'CaO'	9.6	12.1	16.6	18.2	14.7	16.7	16.1	18.2	17.9
'Al ₂ O ₃ '	7.2	8.2	7.0	7.9	7.8	9.7	9.3	13.6	14.0
'MgO'	40.3	36.1	29.9	28.0	31.3	28.3	28.6	22.9	21.8
'SiO ₂ '	42.8	43.6	46.5	45.9	41.2	45.3	45.9	45.3	46.3
Recalculated mineral constitution									
plag	-	-	0.3	-	0.4	2.0	4.5	22.0	26.9
cpx	40.9	51.7	67.2	72.5	56.7	59.1	56.2	46.6	39.1
opx	39.9	37.3	20.4	7.3	21.6	-	9.1	-	-
garnet	-	-	12.2	19.4	21.3	38.6	30.3	28.8	33.7
olivine	14.4	5.4	-	-	-	-	-	-	-
spinel	4.8	5.7	-	0.8	-	0.4	-	2.5	0.3
Modes, volume percent									
olivine	1	-	-	-	-	-	-	-	-
opx	32	30	29	13	8	3	5	6	2
cpx	24	34	71	82	55	45	33	47	34
garnet	-	-	-	-	-	-	28	17	24
garnet'	-	-	-	-	31	51	30	-	-
plag	-	-	0.4	4	-	0.4	2	20	34
amph	35	28	-	0.2	6	0.2	2	1	4
spinel	6	7	7	-	-	-	-	-	-
ore	1	1	-	-	0.8	-	-	9	2

(garnet'=garnet reaction rim)

TABLE 5

Analyses of rocks, Inland Contact, Geodh'Eanruig

Specimens were collected in a downward (eastward) sequence from ultra-basic to garnetiferous basic gneiss, over a distance of about 4 feet:

10719 Hornblende-spinel-pyroxenite, with very minor olivine.

10720 Very coarse garnet-augite gneiss. Exsolution of hypersthene, ore, and plagioclase from the large augite grains (O'Hara, 1961a, fig. 7), which are often surrounded by a matrix of finer grained pyroxenes without exsolution phenomena. The garnets are surrounded by thin reaction rims, around which are concentrations of grass-green hornblende and ore.

10721 Garnet-augite gneiss transitional to garnetiferous basic gneiss.

10722 There are thin reaction rims to the garnets, and plagioclase is a minor constituent. Generally similar to Z 720 (p. 39).

X646, from O'Hara (1961a) is from the same band as 10720.

TABLE 5

	10719	10720	10721	10722	x 646
SiO ₂	45.58	44.10	45.33	45.08	41.38
TiO ₂	0.45	0.52	0.79	0.61	0.76
Al ₂ O ₃	8.38	12.90	13.38	13.49	15.24
Fe ₂ O ₃	5.47	5.00	2.49	2.15	3.68
FeO	7.06	16.01	12.29	12.06	16.25
MnO	0.19	0.43	0.26	0.24	0.44
MgO	20.26	9.99	11.10	11.79	8.67
CaO	10.77	11.35	12.85	12.49	10.67
Na ₂ O	0.79	0.70	1.04	0.84	1.12
K ₂ O	0.14	0.12	0.15	0.34	0.18 0.91
H ₂ O	0.75	0.45	0.36	0.62	3.29 0.72
total	99.84	101.57	100.04	99.71	99.70 99.84

Trace elements, p.p.m.

Cr	2590	140	380	190	65
Ni	910	100	280	330	55
Sr	105	55	65	80	125

Cation atomic percent.

Si	41.49	41.64	42.50	42.29	40.02
Ti	0.31	0.37	0.56	0.43	0.55
Al	8.99	14.36	14.79	14.92	17.37
Fe'''	3.75	3.55	1.76	1.52	2.68
Fe''	5.37	12.64	9.64	9.46	13.14
Mn	0.15	0.34	0.21	0.19	0.36
Mg	27.48	14.06	15.51	16.49	12.49
Ca	10.50	11.48	12.91	12.56	11.06
Na	1.39	1.28	1.89	1.53	2.10
K	0.16	0.14	0.18	0.41	0.22
Cr	0.27	0.01	0.02	0.04	0.01
Ni	0.09	0.01	0.03	0.03	0.01

<u>Fe</u>	31.9	53.5	42.4	40.0	52.1
Fe+Mg					
<u>Fe''</u>	16.3	47.3	38.3	36.5	51.3
Fe''+Mg					

TABLE 5(a)

	10719	10720	10721	10722
Reduced compositional parameters				
'CaO'	13.1	14.4	16.6	16.1
'Al ₂ O ₃ '	8.2	11.2	11.0	10.7
'MgO'	35.5	29.7	27.6	28.5
'SiO ₂ '	43.2	44.8	44.9	44.7
Recalculated mineral constitution				
pag	-	3.7	6.0	3.5
cpx	55.6	44.0	54.7	54.2
OPX	31.4	-	-	-
garnet	-	51.7	37.5	40.7
OLIVINE	7.0	-	-	-
spinel	6.0	0.6	1.7	1.6
Modes, volume percent				
olivine	2	-	-	-
opx	36	3	4	3
cpx	26	53	43	40
garnet	-	29	36	29
garnet'	-	7	16	15
plag	-	2	1	2
amph	27	5	-	11
spinel	6	-	-	-
ore	2	1	-	-

(garnet'=garnet reaction rim)

TABLE 6

Analyses of rocks, Lower Contact, Geodh'Eanruig

(D on fig. 3-2)

Specimens were collected in an eastward sequence from peridotite to basic gneiss.

B 165 Peridotite. Granoblastic aggregate of olivine (entirely serpentinised), hypersthene, augite, and pale green hornblende. Minor spinel.

4' 0" to

B 166 Olivine-pyroxenite. Very similar to B 165, but with less olivine.

1' 0" to

B 167 Hornblende-spinel-pyroxenite. Granoblastic aggregate of hypersthene, augite and very pale green hornblende, with relatively abundant green spinel, and magnetite.

Adjacent to

B 168 Basic gneiss. Hypersthene, augite, plagioclase, and abundant small grains of ore. Green hornblende forms poikiloblasts about pyroxenes and especially ore. A few garnets in hand specimen, but none were seen in thin section. Instead, the plagioclase tends to be concentrated in circular areas which appear to be garnet pseudomorphs.

GE4 and GE5 Plagioclase gneisses (see p. 41) were collected about 5 feet and 10 feet respectively from the contact with basic gneiss on a line about 15 feet south of the above rocks (i.e. between A and D on fig. 3-2).

TABLE 6

	B 165	B 166	B 167	B 168	GE 4	GE 5
SiO ₂	44.4	45.0	48.85	48.4	67.4	60.9
TiO ₂	0.31	0.34	0.38	0.69	0.41	0.54
Al ₂ O ₃	6.2	6.5	7.1	14.6	15.7	17.4
Fe ₂ O ₃	5.45	5.1	2.45	2.25	1.35	1.75
FeO	7.05	6.85	8.0	10.1	2.0	2.65
MnO	0.20	0.19	0.16	0.19	0.04	0.04
MgO	24.3	24.2	21.8	10.0	1.7	2.4
CaO	7.15	8.5	8.35	8.8	4.65	6.15
Na ₂ O	0.69	0.73	0.93	1.56	4.90	5.30
K ₂ O	0.09	0.08	0.12	1.60	0.87	0.99
H ₂ O	3.08	2.56	1.09	1.46	0.58	0.72
total	98.9	100.1	99.2	99.87	99.6	98.8

Trace elements, p.p.m.

Cr	2280	2310	2480	170	50	60
Ni	1300	1180	920	260	30	25
Sr	25	40	45	200	560	620

Cation atomic percent

Si	41.2	41.0	44.4	45.7	62.7	56.9
Ti	0.22	0.23	0.26	0.49	0.29	0.38
Al	6.8	7.0	7.6	16.2	17.3	19.2
Fe'''	3.8	3.5	1.7	1.6	0.9	1.2
Fe''	5.5	5.2	6.1	8.0	1.6	2.1
Mn	0.16	0.15	0.12	0.15	0.03	0.03
Mg	33.6	32.9	29.5	14.1	2.4	3.3
Ca	7.1	8.3	8.1	8.9	4.6	6.1
Na	1.2	1.3	1.6	2.9	8.9	9.6
K	0.11	0.09	0.14	1.9	1.0	1.2
Cr	0.24	0.24	0.26	0.02	0.00	0.00
Ni	0.13	0.11	0.09	0.02	0.00	0.00

<u>Fe</u>	21.9	21.3	21.1	40.9	51.5	50.0
<u>Fe+Mg</u>						
<u>Fe'''</u>	14.0	13.7	17.1	36.2	39.7	38.5
<u>Fe''' + Mg</u>						

TABLE 6(a)

	B 165	B 166	B 167	B 168	GE 4	GE 5
Reduced compositional parameters						
'CaO'	9.0	10.3	10.5	15.5	17.0	20.1
'Al ₂ O ₃ '	6.7	6.7	6.3	13.4	16.8	19.0
'MgO'	41.8	40.7	37.8	24.7	4.3	6.0
'SiO ₂ '	42.5	42.3	45.3	46.4	61.9	54.8

Recalculated mineral constitution						
quartz	-	-	-	-	24.5	10.7
plag	-	-	-	24.7	64.4	71.7
cpx	38.4	44.0	44.9	31.2	3.9	9.4
opx	38.9	32.0	46.8	10.7	7.2	8.1
garnet	-	-	-	33.3	-	-
olivine	18.6	19.7	6.7	-	-	-
spinel	4.2	4.3	1.6	-	-	-

Modes, volume percent						
olivine	23	-	-	-	-	-
opx	36	54	13	-	-	-
cpx	36	34	20	-	-	-
garnet'	-	-	25	-	-	-
plag	-	-	25	72	77	-
amph	1	10	17	-	-	-
spinel	2	2	-	-	-	-
quartz	-	-	-	18	7	-
mafics	-	-	-	10	16	-

(garnet'=plagioclase-rich garnet pseudomorphs)

(mafics=hornblende, pyroxenes, ore, and biotite, generally closely associated in fine grained clusters)

TABLE 7

Analyses of rocks, Lower Contact, Geodh'Eanruig

(A on fig. 3-2)

Specimens collected in an eastward sequence.

Brief petrographic descriptions on p. 41.

Distance (perpendicular to foliation)

0	<u>GE 1A</u>	Pyroxene-hornblendite
5"	<u>GE 1C</u>	Pyroxene-hornblendite
7"	<u>GE 1D(1)</u>	Pyroxene-hornblendite
8"	<u>GE 1D (2)</u>	Hypersthene-rich contact to plagioclase vein
9"	<u>GE 1D(3)</u>	Coarse plagioclase vein
12"	<u>GE 1E</u>	Pyroxene-hornblendite
16"	<u>GE 1F</u>	Pyroxene-hornblendite
22"	<u>GE 1J</u>	Plagioclase gneiss
	2' gap to	
	<u>GE 2</u>	Plagioclase gneiss

TABLE 7(a)

GE 1A GE 1C GE 1D-1 GE 1D-2 GE 1D-3 GE 1E GE 1F GE 1J GE 2

Reduced compositional parameters

'CaO'	15.4	8.7	9.8	10.0	22.4	9.6	10.5	20.8	20.8
'Al ₂ O ₃ '	10.5	6.9	6.9	9.7	18.8	6.9	7.4	19.3	16.2
'MgO'	33.5	39.7	38.1	33.2	9.7	38.5	38.4	12.0	12.8
'SiO ₂ '	40.6	44.7	45.2	47.1	49.2	45.1	43.6	47.8	50.2

Recalculated mineral constitution

quartz	-	-	-	-	0.4	-	-	-	2.9
plag	-	-	-	15.7	67.3	-	-	60.5	54.7
cpx	65.4	37.0	41.9	23.6	23.5	40.8	44.8	19.2	30.5
opx	15.3	53.3	51.0	52.1	8.8	51.6	41.4	12.0	12.0
garnet	-	-	-	8.7	-	-	-	19.9	-
olivine	7.9	6.8	4.6	-	-	5.0	9.3	-	-
spinel	11.4	3.0	2.6	-	-	2.7	4.5	0.4	-

Modes, volume percent

opx	35					53	36	4	-
cpx	7					7	8	7	27
amph	56					40	56	5	8
plag	-					-	-	77	60
biotite	-					-	-	6	4
ore	1					-	-	1	1

Modal composition of GE 1D

Layer	1	2	3	4	5	6	7	8	9
opx	57	52	43	62	48	54	25	13	10
cpx	18	19	36	15	-	-	-	-	-
amph	25	29	20	23	36	10	13	6	3
plag	-	-	-	-	16	36	62	81	87

(each layer is approx. 3.75 mm. wide, except 8 and 9, which are 5 mm. wide.
Total width of the section, measured normal to the strike, is about 3.6 cm.)

TABLE 8

Analyses of rocks, Cleit Mhor (F on fig. 3-2)

Specimens were collected outwards (in an easterly direction) from the peridotite core of a small ultrabasic mass in acid gneiss.

GE 22 Peridotite. Hypersthene, olivine (partly serpentinised), augite, and brownish-green hornblende in that order of abundance. Green spinel, full of inclusions of magnetite and almost opaque. The olivine grains are often concave against hypersthene.

22" to

GE 34 Pyroxene-hornblendite. Green hornblende, augite, and hypersthene in granoblastic aggregate. No spinel or ore. Very small proportion of plagioclase in extremely small grains. Very similar to GE 1A (p. 41).

7" to

GE 31 Hornblende-rich basic gneiss. Green hornblende, hypersthene, augite and plagioclase in roughly equal proportions form a granoblastic mass. No ore is present.

11" to

GE 25 Basic gneiss. Plagioclase-rich rock with augite, hypersthene, and ore. Blue-green hornblende forms thin fringes around the pyroxenes, and red-brown biotite grows around the ore grains. This specimen passes, with a sharp contact, to normal acid gneiss.

TABLE 8

	GE 22	GE 34	GE 31	GE 25
SiO ₂	42.2	47.7	49.0	49.55
TiO ₂	0.18	0.39	0.60	0.95
Al ₂ O ₃	4.6	7.65	10.4	14.15
Fe ₂ O ₃	4.5	2.75	2.35	3.45
FeO	7.45	10.05	10.9	8.3
MnO	0.19	0.18	0.24	0.22
MgO	31.25	18.15	13.7	7.9
CaO	4.65	9.1	9.4	10.5
Na ₂ O	0.17	2.02	1.48	2.90
K ₂ O	0.02	0.63	0.06	0.48
H ₂ O	3.33	1.60	0.97	0.58
total	98.6	100.2	99.1	99.0

Trace elements, p.p.m.

Cr	3350	2110	1090	250
Ni	1800	800	380	150
Sr	-	25	60	240

Cation atomic percent

Si	38.4	43.6	46.1	46.8
Ti	0.12	0.27	0.42	0.7
Al	4.9	8.2	11.5	15.7
Fe'''	3.1	1.9	1.7	2.5
Fe''	5.7	7.7	8.5	6.6
Mn	0.15	0.14	0.19	0.18
Mg	42.3	24.7	19.2	11.1
Ca	4.5	8.9	9.5	10.6
Na	0.30	3.6	2.7	5.3
K	0.02	0.7	0.07	0.6
Cr	0.35	0.22	0.12	0.00
Ni	0.17	0.07	0.04	0.00

<u>Fe</u>	17.1	27.9	34.7	44.8
<u>Fe+Mg</u>				
<u>Fe'''</u>	11.8	23.7	30.8	37.1
<u>Fe''' + Mg</u>				

TABLE 8(a)

	GE 22	GE 34	GE 31	GE 25
Reduced compositional parameters				
'CaO'	5.1	14.3	13.4	18.9
'Al ₂ O ₃ '	4.7	8.2	9.3	14.6
'MgO'	50.4	35.0	30.1	19.7
'SiO ₂ '	39.8	42.5	47.3	46.8
Recalculated mineral constitution				
plag	-	-	15.3	32.8
cpx	21.6	60.9	39.6	38.2
opx	32.7	22.0	40.9	0.3
garnet	-	-	4.3	28.6
olivine	42.9	10.7	-	-
spinel	2.8	6.5	-	-
Modes, volume percent				
olivine	36	-	-	-
opx	44	37	21	20
cpx	13	15	20	31
plag	-	tr.	24	46
amph	4	47	34	-
spinel	2	-	-	-
ore	2	-	-	3

TABLE 9

Analyses of rocks from ultrabasic contact, Pairc a'Cladaich

Specimens were collected in a downward (eastward) sequence from ultrabasic to basic gneiss, from the eastern margin of the ultrabasic band in the western part of the mass.

Z 701 Peridotite gneiss. Olivine, hypersthene, hornblende, and spinel are all abundant and all exceed augite.

6" to

Z 702A Hornblende-spinel-pyroxenite. The specimen passes almost directly to garnetiferous basic gneiss, but there is a very thin zone (about 1 cm.) of contact gneiss.

Z 702B First there is about $\frac{1}{2}$ cm. of nearly pure clinopyroxenite, which has a sharp contact to the hornblende-spinel-pyroxenite. This passes to a 1 mm. zone of fine-grained plagioclase, with some granular hypersthene and a little spinel, then at the outer margin of this zone garnet appears, growing along the hypersthene-plagioclase boundaries. Some of the garnet tongues contain vermicules of spinel. Next is a zone about 3 mm. thick of garnet-augite gneiss, very fine grained in comparison with the more common occurrence of the rock in larger quantities. There is little sign of any reaction rim to the garnets, and the texture is granoblastic. Plagioclase comes in over a distance of about 1 mm., so that the sequence finishes in garnetiferous basic gneiss. It is clear that this contact duplicates virtually all the features of the Geodh'Eanruig Upper Contact, on about one hundredth of the scale. The shape of the specimen is such that the analysis very largely represents the garnet-augite gneiss.

6" gap to

Z 703 Garnetiferous basic gneiss. The rock consists of granoblastic plagioclase and augite, with no hypersthene or hornblende. Rounded garnets up to 1 cm. across are surrounded by an unusually wide rim of plagioclase grains, up to their own diameter in width.

4" to

Z 704 Garnetiferous basic gneiss. This rock is very similar to Z 703 in thin section, but the plagioclase rims about garnet are virtually absent.

1' 0" to

Z 705 Garnetiferous basic, transitional to basic gneiss. The rock is similar to Z 704, but garnet is somewhat scarcer. The section contains a prominent patch rich in large and dendritic grains of ore, some of which contain granules of green spinel. The ore is mantled by garnet where it borders on to plagioclase.

2' 3" to

Z 706 Basic gneiss. This rock consists almost entirely of a granoblastic aggregate of plagioclase and augite. Ore occurs as occasional specks, and there are traces of garnet. The calcium rich character of the rock is reflected by the trace of wollastonite in the recalculated mineral constitution.

TABLE 9

	Z 701	Z 702A	Z 702B	Z 703	Z 704	Z 705	Z 706
SiO ₂	44.8	48.6	44.8	48.4	45.4	47.0	47.8
TiO ₂	0.29	0.30	1.42	0.97	1.02	0.81	0.74
Al ₂ O ₃	8.3	7.5	15.95	13.7	14.25	14.95	15.55
Fe ₂ O ₃	3.7	2.1	2.3	2.35	2.5	2.4	3.9
FeO	9.15	9.95	10.6	10.15	11.55	9.6	7.15
MnO	0.21	0.21	0.39	0.27	0.32	0.25	0.23
MgO	24.8	19.9	9.7	8.1	7.95	7.05	5.75
CaO	6.45	9.7	11.0	14.1	13.65	14.5	14.7
Na ₂ O	0.63	0.77	1.47	1.88	1.62	1.97	2.36
K ₂ O	0.10	0.30	1.00	0.23	0.18	0.20	0.74
H ₂ O	0.57	0.53	0.62	0.71	0.69	0.48	0.63
S	0.02	0.22	0.03	0.10	0.10	0.08	0.09
total	99.0	100.0	99.2	101.0	99.2	99.3	99.7

Trace elements, p.p.m.

Cr	2760	2290	300	260	260	230	230
Ni	1160	980	220	180	150	170	160
Sr	55	60	145	115	100	100	265

Cation atomic percent

Si	40.3	44.0	42.3	45.3	43.3	44.5	45.1
Ti	0.20	0.20	1.0	0.7	0.7	0.6	0.5
Al	8.8	8.0	17.7	15.1	16.0	16.7	17.3
Fe ⁺⁺⁺	2.5	1.4	1.6	1.7	1.8	1.7	2.8
Fe ⁺⁺	6.9	7.5	8.3	8.0	9.2	7.6	5.6
Mn	0.16	0.17	0.31	0.21	0.26	0.20	0.18
Mg	33.3	26.9	13.6	11.3	11.3	10.0	8.1
Ca	6.2	9.4	11.1	14.1	13.9	14.7	14.9
Na	1.1	1.3	2.7	3.4	3.0	3.6	4.3
K	0.11	0.35	1.2	0.27	0.22	0.24	0.9
S	0.03	0.37	0.05	0.15	0.18	0.14	0.16
Cr	0.28	0.24	0.03	0.03	0.03	0.02	0.02
Ni	0.11	0.09	0.02	0.02	0.02	0.02	0.02

<u>Fe</u>	22.0	25.0	42.2	46.0	49.4	48.3	51.0
<u>Fe+Mg</u>							
<u>Fe⁺⁺</u>	17.1	21.9	38.0	41.3	44.9	43.3	41.1
<u>Fe⁺⁺+Mg</u>							

TABLE 9(a)

	Z 701	Z 702A	Z 702B	Z 703	Z 704	Z 705	Z 706
Reduced compositional parameters							
'CaO'	7.9	11.8	17.2	20.0	19.4	21.1	23.2
'Al ₂ O ₃ '	7.1	6.3	14.5	12.3	12.7	13.3	15.2
'MgO'	43.1	36.7	24.4	21.1	22.6	19.5	15.5
'SiO ₂ '	41.9	45.2	43.9	46.7	45.3	46.1	46.1
Recalculated mineral constitution							
plag	-	-	19.5	22.9	19.1	27.1	38.5
cpx	33.8	50.4	44.6	55.2	56.7	57.7	56.4
opx	41.3	40.2	-	-	-	-	-
garnet	-	-	30.8	21.6	21.1	12.7	-
olivine	19.8	7.8	-	-	-	-	-
spinel	5.1	1.7	5.2	0.3	3.1	2.5	4.5
woll	-	-	-	-	-	-	0.7
Modes, volume percent							
olivine	24	-	-	-	-	-	-
opx	25	40	8	1	2	-	-
cpx	26	40	30	63	42	43	53
garnet	-	-	28	2	22	19	0.3
garnet'	-	-	-	-	-	4	-
plag	-	-	31	33	33	31	45
amph	24	-	-	-	-	-	-
spinel	7	-	-	-	-	-	-
ore	0.7	-	-	0.5	1	2	2

(garnet'=garnet growing as fringes on large ore grains)

TABLE 10

Analyses of rocks from the ultrabasic contact, Loch an Daimh Mhor

A specimen from this locality has been described by O'Hara (1961a, specimen UA). The contact rocks form a single hand specimen 19 cm. long, which was divided into 12 slices (UA 1-12) for the purposes of analysis. UA 1 is peridotite, and UA 12 is ariegite (garnet-spinel-hornblende-pyroxene rock), which passes, within about 3 feet, to garnetiferous basic gneiss. The sequence of rock types is as follows:

0 to 1 cm. UA 1 Peridotite. Rich in hypersthene, and virtually free of spinel and hornblende.

1 to 2 cm. UA 2 'Lherzolite' (O'Hara, 1961a, fig. 3), i.e. olivine-poor, and hypersthene-rich, and transitional from peridotite to spinel-pyroxenite.

2 to 3 cm. UA 3 Spinel-pyroxenite. Hypersthene predominates over augite. Minor hornblende and spinel. Augite increases rapidly at the margin of

3 to 4 cm. UA 4 Clinopyroxenite. Granoblastic augite and little else. An irregular zone consisting largely of green-brown hornblende occurs at the outer margin of this zone, and is represented in the analysis of this and the next specimen.

4 to 6 cm. UA 5, 6 to 8 cm. UA 6, 8 to 9 cm. UA 7, and 9 to 10 cm. UA 8 are all rather similar petrographically. They consist essentially of a single mass of garnet, within which are set grains of hypersthene, hornblende, blue-green spinel, and minor augite (in UA 5 and 6 only). All these specimens were termed ariegite by O'Hara (1961a, fig. 3).

11 to 13 cm. UA 10, and 15 to 17 cm. UA 12 are very similar to the previous four specimens, except that the blue-green spinel is crowded with inclusions of magnetite, and the ore minerals ilmenite, pyrrhotite, pyrite, and chalcopyrite become abundant (O'Hara, 1961a, fig. 3). Augite is also present in these specimens.

The electron probe analyses of minerals from this specimen in the present study were performed on sections cut from the thin slices which remained. The only difference between these slices and the rest of the specimen was the presence of a small ($\frac{1}{2}$ cm.) patch of clinopyroxenite at 6 cm. (i.e. on the margin between UA 5 and 6).

EXTRA STRONG

TABLE 10

	UA 1	UA 2	UA 3	UA 4	UA 5	UA 6	UA 7	UA 8	UA 10	UA 12
SiO ₂	44.1	50.2	50.3	46.8	42.6	41.7	38.3	34.3	32.3	32.2
TiO ₂	0.20	0.34	0.36	0.86	1.00	0.96	0.21	0.81	0.48	0.17
Al ₂ O ₃	2.5	3.8	3.9	7.9	16.2	18.6	20.3	20.9	20.4	20.0
Fe ₂ O ₃	5.0	2.4	2.1	2.1	3.6	2.9	5.4	5.3	7.7	10.2
FeO	4.1	6.4	6.1	5.3	7.3	10.2	11.6	11.9	15.7	14.7
MnO	0.15	0.16	0.17	0.18	0.28	0.35	0.46	0.38	0.49	0.53
MgO	32.8	27.4	24.2	15.1	16.1	14.4	14.4	15.1	13.6	13.0
CaO	2.3	5.5	9.3	18.0	9.7	7.4	5.4	5.2	4.6	4.2
Na ₂ O	0.92	0.36	0.87	0.23	0.12	0.61	0.32	1.20	0.32	0.15
K ₂ O	0.70	0.01	0.35	0.33	0.01	0.31	0.05	0.76	0.17	0.05
P ₂ O ₅	0.03	0.01	0.01	0.03	0.04	0.05	0.06	0.07	0.11	0.12
H ₂ O	6.6	2.2	0.75	1.6	0.7	0.7	0.35	0.85	1.4	2.3
S	0.12	0.32	0.28	0.34	0.13	0.09	0.19	0.67	1.54	1.19
CO ₂	0.16	0.41	0.65	0.70	1.10	1.40	2.20	1.90	1.60	1.40
total	99.6	99.4	99.2	99.2	98.8	99.6	99.2	99.0	99.6	99.6

Trace elements, p.p.m.

Cr	1300	1110	600	280	110	80	70	180	240	210
Ni	2420	1470	1020	460	320	300	290	590	420	470
Sr	50	80	90	200	290	220	130	165	90	60

Cation atomic percent

Si	40.5	45.5	45.5	44.1	40.0	40.0	36.5	32.2	30.8	31.3
Ti	0.14	0.23	0.24	0.6	0.7	0.7	0.15	0.6	0.34	0.12
Al	2.7	4.1	4.1	8.8	17.9	21.0	22.8	23.1	22.9	22.9
Fe ^{'''}	3.5	1.6	1.4	1.5	2.5	2.1	3.9	3.8	5.5	7.5
Fe ^{''}	3.1	4.9	4.6	4.2	5.7	8.2	9.2	9.3	12.5	12.0
Mn	0.12	0.13	0.13	0.14	0.22	0.28	0.37	0.30	0.39	0.44
Mg	44.9	37.0	32.6	21.2	22.5	20.6	20.5	21.1	19.3	18.8
Ca	2.3	5.4	9.0	18.2	9.8	7.6	5.5	5.2	4.7	4.4
Na	1.6	0.6	1.5	0.42	0.22	1.1	0.6	2.2	0.6	0.28
K	0.8	0.01	0.40	0.40	0.01	0.38	0.06	0.9	0.21	0.06
P	0.02	0.01	0.01	0.02	0.03	0.04	0.04	0.06	0.09	0.10
S	0.20	0.5	0.47	0.6	0.23	0.16	0.34	1.2	2.8	2.2
Cr	0.13	0.11	0.06	0.03	0.01	0.01	0.01	0.02	0.02	0.02
Ni	0.25	0.15	0.10	0.05	0.03	0.03	0.03	0.06	0.04	0.05

[illegible]

TABLE 10(a)

	UA 1	UA 2	UA 3	UA 4	UA 5	UA 6	UA 7	UA 8	UA 10	UA 12
Reduced compositional parameters										
'CaO'	4.9	6.2	11.4	20.3	11.3	10.2	7.1	9.9	6.5	5.5
'Al ₂ O ₃ '	4.7	3.6	4.2	6.6	12.5	14.6	16.1	18.7	18.2	18.9
'MgO'	50.5	43.6	38.9	26.7	31.4	31.9	35.0	36.4	38.8	37.9
'SiO ₂ '	39.8	46.6	45.5	46.4	44.9	43.3	41.8	35.0	36.5	37.7
Recalculated mineral constitution										
plag	-	-	-	-	8.5	8.7	6.2	-	-	1.6
cpx	20.9	26.6	48.6	86.4	23.5	15.2	0.8	33.5	14.0	-
opx	33.7	63.8	37.0	12.2	7.9	-	-	10.1	14.7	-
garnet	-	-	-	0.02	60.2	73.9	89.1	33.8	53.4	85.7
olivine	42.5	9.6	14.4	-	-	-	-	-	-	-
spinel	2.9	-	-	1.4	-	2.2	3.8	22.7	17.9	12.6

TABLE 11

Analyses of rocks from ultrabasic contact, Camas an Lochain

(A on fig. 3-7)

The specimens were collected from the upper contact of a thin (2 ft.) ultrabasic band just below the thick ultrabasic layer shown on the map. The two are separated by 2 ft. of garnetiferous basic gneiss. The thin band does not extend far laterally, and is only exposed for a length of about 15 ft. All the specimens are contiguous, and together they cover a thickness of 10 cm. (B 241 is 4 cm. thick, B 242-1 and 2 are 1 cm. each, and B 242-3 and 4 are 2 cm. each).

B 241 Peridotite. The rock is totally serpentised, and no fresh olivine is present. Serpentine accounts for over half the rock, a feature which is rare in any of the other masses studied, but is normal at Camas an Lochain. Spinel is abundant. Most of the pyroxene is hypersthene, which occurs as small grains disseminated through the serpentine, and as lenticular clusters of about a dozen grains, which often show a preferred orientation of their long dimensions. These features give the strong foliation, which replaces the normally ubiquitous banding. Hypersthene also occurs as larger grains without preferred orientation. Augite and hornblende are very minor constituents, the former occurring in a similar situation to the hypersthene. The hornblende is very pale brown, and pleochroic to nearly colourless, and is of even weaker colour at the margins of the grains. It occurs as large grains without preferred orientation, which are often bent and broken.

B 242-1 Spinel-pyroxenite. This consists entirely of a granoblastic aggregate of pale coloured hypersthene, with a little brown spinel. The hypersthene shows no sign of preferred orientation, either of dimensional or crystallographic features.

B 242-2 Garnet-pyroxene gneiss. This is a relatively fine-grained granoblastic aggregate of garnet, augite, and hypersthene, in that order of abundance. The garnet is not noticeably larger in grain size than the pyroxenes. At the contact with B 242-1, there is a zone, about 3 mm. wide, in which the garnets are progressively more corroded, and are replaced by radiating intergrowths of hypersthene and plagioclase. Spinel is present as rare independent grains.

Hypersthene is rather too abundant for the term 'garnet-augite gneiss' to be applied. The specimen passes suddenly into a garnet-free zone of granoblastic plagioclase with small grains of hypersthene and augite, about 5 mm. wide. This forms the margin of

B 242-3 and 4 Garnetiferous basic gneiss. These two specimens are petrographically identical. They consist of alternate bands rich in plagioclase, and augite, hypersthene and garnet. There is no tendency for plagioclase to rim the garnet. Ore occurs as small, usually independent grains of magnetite and ilmenite, the two being occasionally intergrown. Garnets tend to enclose the ore grains where the latter are abundant or large.

The features which distinguish this contact from the others studied are: the poverty in augite of the two ultrabasic specimens; the absence of even a trace of the clinopyroxenite zone, and the relative abundance of

hypersthene in the garnet-pyroxene gneiss. These features may all be attributable to the calcium-poor character of the peridotite member.

TABLE 11

	B 241	B 242-1	B 242-2	B 242-3	B 242-4
SiO ₂	38.5	49.15	45.7	49.0	48.0
TiO ₂	0.21	0.32	1.27	1.83	1.89
Al ₂ O ₃	3.8	5.0	9.65	12.4	12.35
Fe ₂ O ₃	8.2	4.1	3.05	2.85	3.9
FeO	7.5	12.15	14.45	11.3	13.65
MnO	0.16	0.23	0.35	0.30	0.29
MgO	29.6	24.2	15.6	7.1	6.0
CaO	3.05	1.	8.05	11.5	10.8
Na ₂ O	0.11	0.12	0.25	2.40	2.21
K ₂ O	0.03	0.04	0.11	0.56 0.18	0.18
H ₂ O	7.90	2.56	1.44	0.56	0.52
total	99.1	99.6	99.9	99.4	98.8 99.8

Trace elements, p.p.m.

Cr	3400	4700	360	30	40
Ni	1700	570	510	120	80
Sr	-	-	-	160	100

Cation atomic percent

Si	37.1	45.7	43.4	46.8	46.3
Ti	0.15	0.22	0.9	1.3	1.4
Al	4.3	5.5	10.8	14.0	14.0
Fe'''	5.9	2.9	2.2	2.0	2.9
Fe''	6.1	9.4	11.5	9.0	11.0
Mn	0.13	0.18	0.28	0.24	0.24
Mg	42.5	33.6	22.1	10.1	8.6
Ca	3.1	1.7	8.2	11.8	11.2
Na	0.21	0.22	0.46	4.5	4.1
K	0.04	0.05	0.13	0.22	0.22
Cr	0.38	0.51	0.04	0.00	0.00
Ni	0.16	0.05	0.05	0.01	0.01

<u>Fe</u>	22.0	26.9	38.2	52.2	61.6
Fe+Mg					
<u>Fe''</u>	12.5	22.0	34.2	47.2	56.1
Fe''+Mg					

TABLE 11(a)

B 241 B 242-1 B 242-2 B 242-3 B 242-4

Reduced compositional parameters

'CaO'	3.6	2.1	9.5	18.6	17.6
'Al ₂ O ₃ '	5.9	5.0	8.4	13.2	13.6
'MgO'	51.5	45.2	35.8	20.5	21.1
'SiO ₂ '	39.0	47.7	46.4	47.7	47.7

Recalculated mineral constitution

quartz	-	0.5	-	-	-
plag	-	-	4.4	34.6	35.9
cpx	15.3	8.8	31.1	40.5	34.3
opx	39.0	90.7	45.9	17.3	19.8
garnet	-	-	18.7	7.7	9.9
spinel	5.3	-	-	-	-

TABLE 12

Analyses of rocks from the ultrabasic contact in the Maldie Burn

(F on fig. 3-9)

The specimens were collected in an upward (northward) sequence from the east bank of the Burn.

B 204 Olivine-pyroxenite. A coarse granoblastic aggregate of hypersthene with minor olivine, augite, spinel, magnetite, and pale green hornblende.

2' 0" to

B 205 Olivine-pyroxenite. Similar to B 204, but richer in olivine and much richer in the same pale green hornblende.

2" to

B 206-1 Hornblende-spinel-pyroxenite. Granoblastic hypersthene with a little green spinel. Large grains of pale brown hornblende, dusted with submicroscopic, opaque inclusions. This is a 1 cm. thick layer on the edge of the specimen (i.e. it is presumed to continue downwards), and is transitional through 2 cm. of spinel-free pyroxenite, to

B 206-4 Clinopyroxenite. Also a 1 cm. layer on the edge of the specimen. Consists entirely of granoblastic pale green augite.

3" to

B 211 Garnet-augite gneiss. Some areas of granoblastic augite, as B 206-4, but with occasional small grains of plagioclase. Remainder of the specimen is the same, with rounded garnets, surrounded by thin rims of plagioclase grains, in which small granules of ore occur. No reaction rims

developed.

1' 3" to

B 210 Garnet-augite gneiss transitional to garnetiferous basic gneiss.

Very similar to B 211, but plagioclase is slightly more abundant, and occurs as slightly larger grains.

TABLE 12

	B 204	B 205	B 206-1	B 206-4	B 211	B 210
SiO ₂	45.95	46.0	46.9	48.2	43.3	44.55
TiO ₂	0.37	0.46	1.16	1.10	1.37	0.95
Al ₂ O ₃	7.05	7.95	8.2	7.25	14.1	14.05
Fe ₂ O ₃	4.7	4.1	1.1	3.15	3.0	2.95
FeO	6.6	8.05	10.05	9.35	13.95	13.25
MnO	0.17	0.13	0.14	0.20	0.37	0.32
MgO	25.0	22.8	17.6	12.8	8.35	8.0
CaO	7.05	7.0	11.05	15.3	12.4	12.8
Na ₂ O	0.63	1.01	1.20	0.55	0.93	1.12
K ₂ O	0.05	0.08	0.16	0.36	0.21	0.06
H ₂ O	1.93	1.19	1.00	1.31	1.03	0.98
total	99.5	98.8	98.6	99.6	99.0	99.0

Trace elements, p.p.m.

Cr	2200	2320	860	350	230	190
Ni	1280	1080	690	900	280	150
Sr	70	50	75	25	60	45

Cation atomic percent

Si	41.7	42.0	43.6	45.9	42.0	43.1
Ti	0.25	0.32	0.8	0.8	1.0	0.7
Al	7.5	8.5	9.0	8.1	16.2	16.0
Fe'''	3.2	2.8	0.8	2.3	2.2	2.1
Fe''	5.0	6.1	7.8	7.5	11.3	10.7
Mn	0.13	0.10	0.11	0.16	0.30	0.26
Mg	33.8	31.0	24.4	18.2	12.7	11.5
Ca	6.9	6.8	11.0	15.6	12.9	13.3
Na	1.1	1.8	2.2	0.9	1.7	2.1
K	0.06	0.09	0.19	0.44	0.26	0.07
Cr	0.23	0.25	0.10	0.04	0.02	0.02
Ni	0.12	0.10	0.07	0.08	0.03	0.02

Fe	19.5	22.4	26.1	34.9	52.8	52.7
Fe+Mg						
Fe'''	12.9	16.6	24.3	29.1	47.1	48.2
Fe''' + Mg						

TABLE 12(a)

	B 204	B 205	B 206-1	B 206-4	B 211	B 210
Reduced compositional parameters						
'CaO'	8.6	9.4	14.4	18.2	16.8	17.3
'Al ₂ O ₃ '	6.7	7.6	7.5	7.2	12.6	12.2
'MgO'	41.4	39.9	33.9	26.9	25.6	24.5
'SiO ₂ '	43.3	43.2	44.3	47.8	45.1	45.9
Recalculated mineral constitution						
quartz	-	-	-	1.1	-	-
plag	-	-	-	6.4	14.4	16.6
cpx	36.4	40.0	61.3	70.6	46.7	46.9
opx	45.2	51.8	28.8	22.0	-	-
garnet	-	-	-	-	37.1	36.3
olivine	14.7	6.1	5.8	-	-	-
spinel	3.7	4.2	4.1	-	1.9	0.2
Modes, volume percent						
olivine	3	2	-	-	-	-
opx	62	34	62	tr.	-	-
cpx	29	14	13	98	65	46
garnet	-	-	-	-	22	27
garnet*	-	-	-	-	11	13
plag	-	-	-	-	1	12
amph	2	49	24	8	0.3	1
spinel	3	1	-	-	-	-
ore	1	-	-	-	1	1

(garnet*=garnet rims, mostly of plagioclase and ore)

TABLE 13

Analyses of rocks from the ultrabasic contact on the south
slopes of Ben Strone (G on fig. 3-9)

This contact is the same one as that sampled at the Maldie Burn (Table 12), from which it differs in the degree of development of the garnet reaction rims, which are very spectacular at this locality. Exposure is less adequate also, so that some rock types may have been omitted. The specimens were collected in an upward sequence.

B 226 Olivine-pyroxenite. Very similar to B 205 (Table 12). Hornblende is slightly less abundant.

8' 0" to

B 227 Pyroxenite. Section shows granoblastic, pale green augite, with subordinate amounts of hypersthene. Plagioclase and brownish hornblende from occasional very small grains. The analysis indicates that hypersthene is more abundant in the whole specimen than the thin section would suggest, and it appears likely that the analysis corresponds to B 206-1 and B 206-4 bulked together.

6" to

B 229 Garnet-augite gneiss. The specimen consists of granoblastic augite, with abundant, brown hornblende, and some plagioclase, in which are set large rounded garnets. These garnets are almost entirely made over to reaction rims, exactly like those described on p. 39, but wider and more vermiform than any encountered elsewhere. Apatite is locally abundant as an accessory.

2' 0" to

B 230 Garnet-augite gneiss transitional to garnetiferous basic gneiss. Apart from the slightly greater proportion of plagioclase and the absence of apatite, this rock is virtually identical to B 229. The garnet reaction rims are just as well developed, and constitute the principal petrographic feature of the rock.

TABLE 13

	B 226	B 227	B 229	B 230
SiO ₂	41.75	51.95	45.5	45.5
TiO ₂	0.12	0.13	0.73	0.85
Al ₂ O ₃	5.65	5.1	15.9	14.0
Fe ₂ O ₃	5.0	1.35	1.8	2.95
FeO	6.15	8.9	9.4	9.8
MnO	0.18	0.16	0.19	0.21
MgO	29.8	21.7	11.7	13.0
CaO	3.85	9.4	11.0	11.8
Na ₂ O	0.48	0.64	1.87	1.38
K ₂ O	0.05	0.01	0.09	0.06
H ₂ O	5.75	0.52	0.87	0.90
total	98.8	99.9	99.0	100.4

Trace elements, p.p.m.

Cr	3190	1440	260	560
Ni	1720	1160	260	350
Sr	35	-	120	100

Cation atomic percent

Si	38.8	46.9	42.5	42.1
Ti	0.08	0.09	0.5	0.6
Al	6.2	5.4	17.5	15.3
Fe'''	3.5	0.9	1.2	2.1
Fe''	4.8	6.8	7.3	7.6
Mn	0.14	0.12	0.15	0.16
Mg	41.3	29.2	16.3	17.9
Ca	3.8	9.1	11.0	11.7
Na	0.9	1.1	3.4	2.5
K	0.06	0.01	0.11	0.07
Cr	0.35	0.15	0.03	0.06
Ni	0.16	0.11	0.02	0.03

<u>Fe</u>	16.7	20.8	34.5	35.0
Fe+Mg				
<u>Fe''</u>	10.4	18.8	31.0	29.8
Fe''+Mg				

TABLE 13(a)

	B 226	B 227	B 229	B 230
Reduced compositional parameters				
'CaO'	5.0	10.7	16.4	15.9
'Al ₂ O ₃ '	5.9	4.1	13.2	11.8
'MgO'	49.0	37.6	26.3	28.1
'SiO ₂ '	40.1	47.7	44.1	44.2

Recalculated mineral constitution				
plag	-	-	13.1	6.5
cpx	21.5	45.3	46.5	50.6
opx	39.0	53.0	-	-
garnet	-	-	36.5	39.9
olivine	35.0	1.7	-	-
spinel	4.5	-	3.9	3.0

Modes, volume percent				
opx		63	3	13
cpx		37	16	34
garnet		-	13	8
garnet*		-	33	26
plag		tr.	20	tr.
amph		tr.	15	15
ore		-	0.3	2

(garnet*=garnet reaction rim)

TABLE 14

Analyses of rocks, Scourie House mass (A on fig. 3-5)

This contact is poorly exposed, but it appears from the map to be transgressive to the banding in both ultrabasic and garnetiferous basic gneisses. The three middle specimens were collected in a line along the strike, probably to within one foot of the same horizon, while the sequence as a whole is an upward one.

SH 12 Pyroxene-hornblendite. Green hornblende, augite, and hypersthene in a granoblastic aggregate. Very good foliation defined by orientation of the minerals, particularly hornblende. Hornblende cleavages are prominent on a foliation surface. A few grains of magnetite are seen in this section.

8' across the strike to

SH 13 Peridotite. Olivine very abundant, and only slightly serpentinised, with hypersthene, augite, and brownish-green hornblende. Magnetite abundant, but very little spinel. Hypersthene rims between hornblende and olivine (O'Hara, 1961a, fig. 2) are very well developed.

6' along the strike (S.W.) to

SH 14 Pyroxenite. Granoblastic hypersthene and augite with minor brownish-green hornblende. No ore or spinel.

12' along the strike to

SH 15 Garnetiferous basic gneiss. Augite-plagioclase (and minor hypersthene) matrix, with large garnets. Garnets have granular plagioclase rims, around which hypersthene tends to be concentrated in small

grains. A small amount of ore is present, often with narrow rims of blue-green hornblende, and occasionally of garnet.

3' across the strike to

SH 16 Garnetiferous basic gneiss. Identical to SH 15.

TABLE 14

	SH 12	SH 13	SH 14	SH 15	SH16
SiO ₂	48.1	42.7	50.1	48.5	48.0
TiO ₂	0.49	0.31	0.36	0.80	0.81
Al ₂ O ₃	7.7	4.85	5.3	14.95	15.65
Fe ₂ O ₃	2.65	4.95	2.05	2.05	1.85
FeO	10.25	9.0	11.1	10.15	9.4
MnO	0.21	0.23	0.22	0.20	0.23
MgO	19.05	27.5	19.85	7.3	7.35
CaO	9.3	6.0	8.8	12.2	13.45
Na ₂ O	1.27	0.48	0.71	2.55	2.22
K ₂ O	0.44	0.20	0.11	0.12	0.26
H ₂ O	0.71	2.51	0.51	0.36	0.35
S	0.08	0.05	0.02	0.26	0.09
total	100.2	98.8	99.1	99.4	99.7

Trace elements, p.p.m.

Cr	2440	3070	1890	210	270
Ni	780	1400	920	280	200
Sr	75	50	50	150	140

Cation atomic percent

Si	43.7	39.1	46.2	45.7	45.0
Ti	0.33	0.21	0.25	0.6	0.6
Al	8.2	5.2	5.7	16.6	17.3
Fe'''	1.8	3.4	1.4	1.5	1.3
Fe''	7.8	6.9	8.5	8.0	7.4
Mn	0.16	0.18	0.17	0.16	0.18
Mg	25.8	37.5	27.3	10.2	10.3
Ca	9.0	5.9	8.7	12.3	13.5
Na	2.2	0.9	1.3	4.7	4.0
K	0.5	0.23	0.13	0.14	0.31
S	0.14	0.09	0.03	0.08	0.16
Cr	0.26	0.33	0.20	0.02	0.03
Ni	0.07	0.13	0.09	0.02	0.02

Fe	27.4	21.8	27.1	51.5	46.3
Fe+Mg					
Fe'''	23.2	15.5	23.9	43.9	41.8
Fe''+Mg					

TABLE 14(a)

	SH 12	SH 13	SH 14	SH 15	SH 16
Reduced compositional parameters					
'CaO'	12.7	7.4	10.6	19.5	20.3
'Al ₂ O ₃ '	7.4	5.5	4.9	13.7	13.7
'MgO'	36.0	47.0	37.6	20.3	20.0
'SiO ₂ '	44.0	40.1	47.0	46.5	46.3
Recalculated mineral constitution					
plag	-	-	-	28.1	28.7
cpx	54.0	31.4	45.1	46.8	51.4
opx	34.2	27.8	51.3	-	-
garnet	-	-	-	24.3	18.1
olivine	7.7	36.8	3.6	-	-
spinel	4.2	3.9	-	0.8	1.9
Modes, volume percent					
olivine	-	39	-	-	-
opx	27	30	52	3	1
cpx	20	11	37	37	51
garnet	-	-	-	8	21
plag	-	-	-	52	26
amph	53	16	11	-	0.5
sp/ore	-	4	-	-	-

TABLE 15

Analyses of leucocratic gneisses

The petrographic features of these rocks have been summarised on pp. 105-6. As they are all petrographically similar, no further information will be presented. The specimen localities are as follows:

Leucocratic layers in the Pairc a'Cladaich basic mass (fig. 3-6). All specimens from within 50 feet of the shore: B 160, B 265, 10734, 10735, 10736.

Leucocratic gneiss masses within the Camas an Lochain basic mass (fig. 3-7): B 235 from the eastern, and B 236 from the western of the two leucocratic gneiss occurrences on the shore at the N.W. headland of Camas nam Buth.

Leucocratic gneiss occurrence at Geodh'Eanruig (fig. 3-2): B 288.

Leucocratic gneiss occurrence at the N. end of Loch an Daimh Mhor (fig. 3-1): MD 7.

Scurie More (fig. 3-1): SM 9, SM 11.

Ben Strome (fig. 3-9): B 19, 55/38B.

TABLE 15

	B 160	B 265	B 235	B 236	B 288	MD 7	SM 9	SM 11	10734	10735	10736	B 19	55/38B
SiO ₂	74.7	74.8	74.0	75.8	77.8	76.5	71.4	73.1	75.9	75.4	75.4 70.2	70.4	74.7
TiO ₂	0.06	0.03	0.13	0.06	0.04	0.04	0.25	0.17	0.08	0.09	0.12	0.35	0.06
Al ₂ O ₃	14.4	14.2	14.25	13.95	12.6	13.45	15.1	14.4	13.9	14.25	15.9	14.55	14.65
Fe ₂ O ₃	0.2	0.09	0.45	0.09	0.35	0.25	0.8	0.8	0.4	0.01	0.1	0.4	0.04
FeO	0.3	0.4	0.7	0.1	0.5	0.3	1.0	0.6	0.45	0.8	1.4	2.2	0.3
MnO	0.01	0.00	0.01	0.00	0.02	0.00	0.02	0.02	0.02	0.02	0.04	0.05	0.00
MgO	0.05	0.4	0.4	0.25	0.5	0.1	0.8	0.4	0.35	0.35	0.7	1.5	0.05
CaO	1.4	2.1	1.4	1.05	2.6	0.5	2.25	1.35	0.85	1.45	2.8	2.85	3.1 1.1
Na ₂ O	4.52	3.66	4.23	4.08	3.92	3.13	3.81	4.56	4.42	4.47	4.75	2.85	3.12
K ₂ O	3.20	3.30	3.78	3.23	0.77	4.09	3.33	3.14	3.41	3.14	2.73	3.20	4.45
H ₂ O	0.32	0.33	0.37	0.26	0.56	0.38	0.61	0.53	0.24	0.27	0.41	0.63	0.30
P ₂ O ₅	0.10	0.00	0.10	0.00	0.00	0.00	0.20	0.10	-	-	-	0.10	0.00
total	99.13	99.73	99.8	99.0 98.9	99.7	99.8 98.7	99.46	99.42	100.0	100.3	99.1	98.9	98.8
Trace elements, p.p.m.													
Rb	54	60	80	85	9	97	55	35	73	45	36	150	160
Sr	365	640	205	215	385	260	655	400	225	320	440	90	365
Y	5	8	13	13	1	12	8	6	15	7	7	32	28
Zr	31	38	85	73	93	170	77	90	53	53	36	177	32
Ba	50	1010	440	440	200	500	1070	530	410	480	510	500	640
Pb	4	3	22	3	-	15	3	3	6	6	-	9	30
Cu	28	31	12	16	2	39	12	20	10	10	31	2	16
Nb	60	-	60	42	48	24	9	21	48	40	18	51	36
Ni	4	6	8	70	6	15	16	6	10	6	15	25	10
C.I.P.W. norms													
Qz	33.6	35.9	31.5	37.6	45.8	42.0	31.0	31.7	34.7	33.1	24.4	67.1	37.5
Cor	1.21	0.80	0.90	1.86	0.60	3.01	1.63	1.30	1.37	0.85	0.08	1.48	2.74
Or	19.1	19.7	22.5	19.4	4.6	24.6	19.9	18.8	20.2	18.6	16.4	19.2	26.7
Ab	38.7	31.3	36.0	35.0	33.5	26.9	32.6	39.1	37.5	37.8	40.7	24.5	26.8
An	6.4	10.5	6.3	5.3	13.0	2.5	9.95	6.1	4.2	7.2	14.0	13.7	5.5
Hy	0.43	1.64	1.63	0.64	1.91	0.55	2.82	1.24	1.30	2.20	4.11	7.09	0.59
Mt	0.26	0.13	0.69	0.13	0.53	0.38	1.17	1.19	0.54	0.01	0.15	0.59	0.06
Il	0.12	0.06	0.25	0.12	0.08	0.08	0.48	0.33	0.15	0.17	0.15	0.68	0.12
Ap	0.24	-	0.24	-	-	-	0.48	0.24	-	-	0.23	0.24	-

APPENDIX D

MINERALOGICAL DATA

In this Appendix chemical analyses of minerals and some X-ray diffraction data and refractive indices are presented. None of the mineral analyses include determinations of H_2O , as in only a few cases was sufficient sample available. The major elements in the augite analyses of Table 19, and those of the garnet and augite of B 521 in Table 20 were determined using a Phillips PW 1212 automatic X-ray spectrometer. Neither Na_2O nor H_2O were determined in these analyses.

Unit cell parameters for the minerals were determined with a Phillips PW 1051 diffractometer, using $CuK\alpha$ radiation. Six scans were made at $\frac{1}{2}^\circ$ per minute, and the unknown peaks were measured relative to the (3,1,1) peak of a silicon internal standard.

The hypersthene compositions given in Table 21 were estimated from measurements of $d(10,3,1)$ and $d(0,6,0)$. Values for the Al_2O_3 content and the $Fe/Fe + Mg$ ratio were obtained from charts by Hancock (1964, figs. 79-81). This method gave satisfactory results for ultrabasic hypersthene but not for those of any other rock type.

The garnet compositions given in Table 22 were estimated from determinations of the refractive indices, using the oil immersion method and a Leitz-Jelley refractometer, and of the unit cell edge, from measurements of $d(6,4,0)$ and $d(6,4,2)$. The analysed garnets of O'Hara (1961a) and the garnet of B 521 (Table 20) were used to construct a chart showing variation of the refractive index and a_0 against the $Fe/Fe + Mg$ ratio and the molecular proportion of grossular.

All the analysed augites and hornblendes were run on the diffractometer, but no systematic variation of the d-spacings was found which could have been easily applicable to estimation of the compositions of the same minerals in other rocks.

TABLE 16

Analyses of clinopyroxenes from ultrabasic gneisses,
Geodh nam Cliabh (the rocks of Table 1).

ROCK NO.	5	6	7	8	9	11
SiO ₂	52.55	52.75	51.65	51.6	52.8	52.1
TiO ₂	0.15	0.21	0.26	0.23	0.14	0.19
Al ₂ O ₃	4.7	4.7	4.7	4.3	4.25	4.4
Fe ₂ O ₃	1.5	1.45	1.4	1.4	1.25	1.75
Cr ₂ O ₃	0.22	0.22	0.19	0.20	0.17	0.15
FeO	4.2	3.5	3.0	3.1	3.75	3.15
MnO	0.14	0.11	0.10	0.10	0.12	0.11
NiO	0.06	0.07	0.09	0.07	0.07	0.06
MgO	16.5	16.05	15.95	15.55	16.65	16.7
CaO	20.55	21.5	20.85	22.3	20.75	21.55
Na ₂ O	0.13	0.86	0.24	1.44	0.43	0.50
K ₂ O	0.03	0.01	0.50	0.00	0.03	0.00
total	100.47	101.24	98.79	100.93	100.24	100.57

Formulae on the basis of 6 oxygens

Si	1.899	1.895	1.898	1.886	1.913	1.868
Al[4]	0.101	0.105	0.102	0.114	0.087	0.132
Al[6]	0.099	0.095	0.103	0.071	0.096	0.155
Ti	0.004	0.006	0.007	0.007	0.004	0.005
Cr	0.006	0.006	0.006	0.006	0.005	0.004
Fe ⁺⁺⁺	0.041	0.039	0.039	0.039	0.034	0.047
Fe ⁺⁺	0.126	0.105	0.093	0.094	0.114	0.094
Mn	0.004	0.003	0.003	0.003	0.004	0.003
Ni	0.002	0.002	0.002	0.002	0.002	0.002
Mg	0.889	0.860	0.875	0.846	0.898	0.893
Ca	0.796	0.829	0.822	0.874	0.805	0.829
Na	0.009	0.060	0.017	0.102	0.030	0.035
K	0.001	0.000	0.023	0.000	0.001	0.000
X	0.81	0.89	0.86	0.98	0.84	0.86
Y	1.17	1.12	1.13	1.07	1.16	1.20
Z	2.00	2.00	2.00	2.00	2.00	2.00

TABLE 17

Analyses of hornblendes from ultrabasic gneisses, Geodh nam Cliabh
(the rocks of Table 1).

ROCK NO.	5	6	8	9	11
SiO ₂	43.1	43.6	44.9	43.5	43.25
TiO ₂	0.94	1.07	0.99	0.88	0.77
Al ₂ O ₃	13.75	13.9	12.3	13.65	12.75
Fe ₂ O ₃	2.6	2.05	2.5	2.15	2.45
Cr ₂ O ₃	0.33	0.48	0.39	0.53	0.39
FeO	5.95	5.2	4.9	5.15	4.8
MnO	0.09	0.06	0.11	0.08	0.09
NiO	0.13	0.18	0.18	0.16	0.16
MgO	17.15	17.3	18.3	17.1	18.65
CaO	11.2	12.0	11.8	11.8	11.6
Na ₂ O	3.26	3.16	2.51	2.95	2.51
K ₂ O	0.62	0.62	0.62	1.14	0.57
H ₂ O	1.72	1.52	1.62	1.63	1.66
total	100.8	101.1	101.1	100.7	99.7

Formulae on the basis of 24 (O,OH) ions.

Si	6.18	6.23	6.20	6.24	6.24
Al[4]	1.82	1.77	1.80	1.76	1.76
Al[6]	0.51	0.57	0.20	0.55	0.41
Ti	0.10	0.12	0.10	0.09	0.08
Cr	0.04	0.05	0.04	0.06	0.05
Fe ⁺⁺⁺	0.28	0.22	0.26	0.23	0.27
Fe ⁺⁺	0.71	0.62	0.57	0.62	0.58
Mn	0.01	0.01	0.01	0.01	0.01
Ni	0.02	0.02	0.02	0.02	0.02
Mg	3.67	3.69	3.77	3.66	4.02
Ca	1.72	1.84	1.75	1.82	1.80
Na	0.91	0.88	0.67	0.82	0.70
K	0.11	0.12	0.11	0.21	0.11
OH	1.65	1.45	1.49	1.56	1.69
X	2.74	2.84	2.53	2.85	2.61
Y	5.34	5.30	4.97	5.24	5.44
Z	8.00	8.00	8.00	8.00	8.00
OH	1.65	1.45	1.49	1.56	1.69

TABLE 18

Trace elemnts in minerals from ultrabasic gneisses,
Geodh nam Cliabh

<u>ROCK No.</u>	<u>Ni in</u>			<u>Cr in</u>		
	<u>opx</u>	<u>cpx</u>	<u>amph</u>	<u>opx</u>	<u>cpx</u>	<u>amph</u>
5	720	480	1030	1040	1490	2270
6	1040	520	1420	1680	1490	3270
7	1360	530	1640	1030	1330	1980
8	1370	670	1450	1270	1350	2640
9	960	530	1280	1230	1140	3610
11	1090	450	1220	1260	1010	2700

Trace elements in mineral concentrates (95 percent purity,
approx.) from garnetiferous basic gneisses.

	<u>Ba</u>	<u>Zr</u>	<u>Y</u>	<u>Sr</u>	<u>Rb</u>	<u>Zn</u>	<u>Cu</u>	<u>Ni</u>
<u>Garnets</u>								
B 217	50	20	93	-	-	65	25	90
B 219	60	20	64	-	-	75	10	70
B 224	60	15	40	-	-	70	15	235
<u>Augites</u>								
B 217	90	95	18	25	-	125	55	190
B 219	40	75	8	30	-	145	15	160
B 224	80	75	18	30	-	65	-	200
<u>Plagioclases</u>								
B 217	90	-	-	510	15	35	140	n.d.
B 219	80	-	-	730	-	10	20	n.d.
B 224	90	-	4	445	30	5	15	n.d.
<u>Hornblende</u> B224	35	75	28	65	20	20	20	360
<u>opx</u> B 224	60	10	-	-	-	300	80	350
<u>Rocks</u>								
B 217	60	50	29	110	-	105	125	180
B 219	100	40	22	190	-	120	80	130
B 224	70	25	15	100	-	95	60	260

TABLE 19

Analyses of clinopyroxenes,
Upper Contact, Geodh'Eanruig.

ROCK NO.	Z 718	Z 720	Z 721	Z 722	Z 723	Z 724	Z 725	Z 726
SiO ₂	50.4	50.45	48.8	50.45	50.15	50.6	52.05	52.0
TiO ₂	0.76	0.79	0.67	0.67	0.60	0.68	0.26	0.39
Al ₂ O ₃	6.96	6.83	7.73	6.78	6.37	6.42	4.83	4.36
Fe ₂ O ₃	2.15	2.0	2.1	2.0	1.9	2.35	2.0	1.8
FeO	8.0	6.65	6.65	5.95	6.1	5.7	3.05	2.8
MnO	0.18	0.18	0.17	0.17	0.16	0.17	0.11	0.10
MgO	11.8	12.0	12.2	12.6	13.0	13.25	14.75	16.05
CaO	17.9	17.65	17.1	18.4	17.65	18.05	19.55	18.9
K ₂ O	0.00	0.00	0.02	0.03	0.00	0.00	0.00	0.00
total	97.9 98.2	96.16	95.14	96.8 97.1	95.89	97.02	96.16	96.14

Owing to the apparently inferior quality of these analyses,
structural formulae have not been calculated

TABLE 20

	B 521		GE 13 (see Table B-2)			
	cpx	garnet	garnet	biot.	ore	plag.
SiO ₂	49.4	40.0	37.6	37.6	-	-
TiO ₂	0.12	0.04	0.34	4.35	18.4	-
Al ₂ O ₃	8.4	22.7	20.95	15.95	2.5	-
Fe ₂ O ₃	2.15	1.3	3.7	0.45	<14.9	-
FeO	4.45	15.75	24.2	14.7	>30.9	-
MnO	0.10	0.43	0.66	0.04	0.24	-
MgO	13.7	13.4	5.5	12.8	-	-
CaO	17.9	5.15	6.45	0.5	-	-
Na ₂ O	-	-	-	0.7	-	-
K ₂ O	0.03	0.02	0.04	9.0	-	-
total	96.2	98.8	99.7	96.1	-	-

Trace elements, p.p.m.

Cr	910	390	430	100	910	-
Ni	400	120	400	70	350	-
Sr	-	-	-	30	-	850
Rb	-	-	-	100	-	*

Garnet formulae on the basis of 12 oxygens

Si	2.987	2.952
Al[4]	0.002	0.048
Al[6]	1.996	1.891
Ti	0.002	0.020
Fe'''	0.073	0.219
Fe''	0.984	1.589
Mn	0.027	0.044
Mg	1.491	0.643
Ca	0.412	0.543
X	0.41	0.54
Y	4.57	4.41
Z	3.00	3.00

Note: * indicates below the level of sensitivity
 - indicates the element not determined

TABLE 21

X-RAY DIFFRACTION DATA FOR HYPERSTHENES.

	<u>5</u>	<u>6</u>	<u>7</u>	<u>8</u>	<u>9</u>	<u>11</u>
$d_{(0,6,0)}$	1.4710	1.4714	1.4700	1.4721	1.4714	1.4698
$d_{(10,3,1)}$	1.4865	1.4865	1.4856	1.4865	1.4865	1.4854
$Al^{(6)}$	0.033	0.028	0.035	0.018	0.028	0.035
Al_2O_3	3.0	2.8	3.1	2.2	2.8	3.1
$\frac{Fe_{100}}{Fe-Mg}$	14	14	10	13	13	9

d-spacings in Å. Al_2O_3 contents in weight percent.

Sample numbers refer to the rocks of Table 1.

Chemical parameters were deduced from charts provided by Hancock (1964), as follows;

$Al^{(6)}$ contents - Hancock (1964, fig. 80)

Al_2O_3 contents - " (" , fig. 81)

Fe/Mg ratios - " (" , fig. 79)

TABLE 22

UNIT CELL EDGES AND REFRACTIVE INDICES OF GARNETS.

	R.I.	a_o^o (Å)	$\frac{Fe_{x100}}{Fe-Mg}$	mol. gross.
Z 718	1.773	11.581	57	22
Z 720	1.763	11.567	49	20
Z 721	1.757	-	45	-
Z 722	1.768	11.565	53	19
Z 723	1.769	-	54	-
Z 724	1.767	-	52	-
Z 703	1.778	11.588	61	24
Z 704	1.786	11.590	66	23
Z 705	1.781	11.591	63	24
Z 706	1.780	11.611	62	29
SH 15	1.779	11.581	61	21
SH 16	1.779	11.590	61	24
10720	1.777	11.579	59	21
10721	1.772	11.571	56	20
10722	1.767	11.574	52	21
B 521	1.751	11.546	41(42)	20(19)
GE 13	1.784	11.586	65(74)	21(18)
B 61	1.778	11.561	61	17

For derivation of Fe/Mg ratio and grossular content, see text.

Values in parentheses are those calculated from chemical analyses.

APPENDIX E

A SIMULATION MODEL FOR DIFFUSION

In the following pages the computer programme used to simulate diffusion between contrasted rocks under granulite facies conditions is presented. A sufficient number of comment statements have been inserted to enable the interested reader to follow the course of the calculations, after reading the outline of the method on pp. 89-93.

The programme is written in Atlas Autocode, and was prepared using an iso-coded 8-hole tape punch (Teletype). It was run on an English Electric KDF 9 Computer.

The routine EQN SOLVE K (x,y,n,det) may be peculiar to the Edinburgh compiler. X is an nxn matrix, and y is an n vector. The routine solves the equation $ax = y$, and puts the answers a into the array y.

```

%BEGIN
%INTEGER L1,L2,I,J,T,TIME,LLIM,ULIM
%ARRAY A,C,K(1:6,-100:100),B(1:6,1:13),L,KD(1:6)

%ROUTINESPEC GRADIENT
%ROUTINESPEC REDISTRIBUTE
%ROUTINESPEC MINERAL

%CYCLE J=1,1,6;      !J=OXIDE
->1 %IF J=4 %OR J=5
%CYCLE I=1,1,13;     !I=MINERAL
READ(B(J,I));        !ACTIVITY IN PURE MINERAL
%REPEAT
1:%REPEAT

%CYCLE I=1,1,4
  READ(KD(I));        !DISTRIBUTION COEFFICIENT OF FE TO MG
%REPEAT

2:%CYCLE I=1,1,6;    !I=OXIDE FROM HERE ON
  READ(L(I));         !DIFFUSION COEFFICIENTS
%REPEAT

READ(TIME);          !NUMBER OF STEPS
READ(LLIM);          !LOWER LIMIT TO NUMBER OF LAYERS
READ(ULIM);          !UPPER LIMIT TO NUMBER OF LAYERS

%COMMENT START READING IN INITIAL COMPOSITION PROFILE

L1=-100
3:READ(L2);          !UPPER LIMIT TO LAYERS OF THIS COMPOSITION
J=L1;               !J=NO. OF LAYER FROM HERE ON
%CYCLE I=1,1,6
  K(I,J)=0;          !K(I,J)=CONC. OF OXIDE I IN JTH LAYER
->4 %IF I=4
  READ(C(I,J));      !C(I,J)=DITTO, C IS USED IN MOST STAGES
4:%REPEAT

C(4,J)=C(3,J)*(1-C(5,J)); !CONC. OF MGO [C(3,J)=FEO+MGO]
C(5,J)=C(3,J)*C(5,J); !CONC. OF FEO [C(5,J)] READ AS FE/FE+MG

->9 %IF L2=L1;        !ONLY 1 LAYER OF THIS COMPOSITION
%CYCLE J=L1,1,L2-1
%CYCLE I=1,1,6
  C(I,J+1)=C(I,J)
  K(I,J+1)=0
%REPEAT
%REPEAT

```


9:L1=L2+1; !LOWER LIMIT FOR LAYERS OF THE NEXT COMP.
->3 %UNLESS L2=100

%COMMENT INITIAL COMPOSITION PROFILE READ IN

READ(L1); !INITIAL LOWER LIMIT TO NO. OF LAYERS
READ(L2); !INITIAL UPPER LIMIT TO NO. OF LAYERS
T=0
REDISTRIBUTE; !TO PRINT OUT INITIAL COMP. PROFILE

%CYCLE T=1,1,TIME; !T=NUMBER OF THE STEP
%CYCLE J=L1,1,L2; !J=NUMBER OF THE LAYER
MINERAL; !CALCULATES ANAL. AS MINERAL CONSTITUTION
%REPEAT
GRADIENT; !DIFFUSION TAKES PLACE ACC. TO ACT. GRADS.
REDISTRIBUTE; !READJUSTS COMP. OF LAYERS TO 100% TOTAL
L1=L1-1 %UNLESS L1=LLIM
L2=L2+1 %UNLESS L2=ULIM
%REPEAT

%ROUTINE GRADIENT

%REAL GRAD,FLUX

NEWLINES(5)
%CAPTION ACTIVITIES~~~ CAO AL2O3 MGO FEO%C
SIO2~
%CYCLE J=L1,1,L2
NEWLINE;PRINT(J,2,0);SPACES(5)
%CYCLE I=1,1,6
->8 %IF I=3
PRINT(A(I,J),4,2); !PRINTING OUT ACTIVITIES
8:%REPEAT
%REPEAT

NEWLINES(5)

%CAPTION ACTIVITY GRADIENTS~~~ CAO AL2O3%C
MGO FEO SIO2~
%CYCLE J=L1+3,1,L2-3
NEWLINE
PRINT(J,2,0);SPACES(5)
%CYCLE I=1,1,6
->1%IF I=3
GRAD=A(I,J)-A(I,J+1);!GRAD=NEGATIVE ACTIVITY GRADIENT

```
PRINT(('-GRAD'),4,2); !+VE ACT. GRAD. IN CONVENTIONAL SENSE
FLUX=- (GRAD*L(I)); !DIFF. FLUX FROM LAYER J+1 TO LAYER J
->1 %IF GRAD=0
```

```
%COMMENT START TO DIFFUSE IN DIR. OF NEG. ACT. GRADIENT
```

```
C(I,J)=C(I,J)+FLUX
C(I,J-1)=C(I,J-1)+FLUX/2
C(I,J-2)=C(I,J-2)+FLUX/4
C(I,J+1)=C(I,J+1)-FLUX
C(I,J+2)=C(I,J+2)-FLUX/2
C(I,J+3)=C(I,J+3)-FLUX/4
```

```
%COMMENT DIFFUSION COMPLETE FOR THIS LAYER
```

```
1:%REPEAT
%REPEAT
```

```
%CYCLE J=L1,1,L2
C(3,J)=C(4,J)+C(5,J); !OXIDE 3 IS MGO+FE0
%REPEAT
```

```
%END
```

```
%ROUTINE REDISTRIBUTE
%INTEGER X,P,TT
%REAL RESERVE,VACANCY
```

```
TT=0
NEWPAGE
%CAPTION _____ STEP_NUMBER;PRINT((T+1),1,0)
%CAPTION: _____ MOL_PERCENT_COMPOSITION_PROFILE
6:%CAPTION~~ _____ CAO _____ AL2O3 _____ MGO _____ FEO%C
_____ SIO2 TOTAL
->98 %IF TT=0
%CAPTION FE/FE+MG
98:NEWLINE
```

```
%CYCLE J=L1,1,L2
NEWLINE;PRINT(J,2,0);SPACES(5)
%CYCLE I=1,1,6
->9 %IF I=3
PRINT(C(I,J),4,2); !PRINTS OUT NEW COMPOSITION PROFILE
9:%REPEAT
PRINT((C(1,J)+C(2,J)+C(3,J)+C(6,J)),4,2);!TOTAL AFTER DIFFUSION
->97 %IF TT=0
PRINT(C(5,J)/C(3,J),6,2)
97:%REPEAT
->7 %IF TT=1 %OR T=0
```

```
! ADJUSTMENT STARTS AT LOWER LIMIT, AND MOVES THROUGH LYRS.
```



```

J=L1;      !J=NO. OF LAYER AFTER ADJUSTMENT
X=L1;      !X=NO. OF LAYER BEFORE ADJUSTMENT
VACANCY=1

1:RESERVE=(C(1,X)+C(2,X)+C(3,X)+C(6,X))/100
->4 %IF RESERVE>VACANCY
%CYCLE I=1,1,6
K(I,J)=K(I,J)+C(I,X); !OXIDE CONCS. GO INTO K AFTER ADJUSTMENT
%REPEAT

VACANCY=VACANCY-RESERVE
->3 %UNLESS VACANCY=0

2:J=J+1
VACANCY=1

3:X=X+1
->5 %IF X=L2+1
->1

4:%CYCLE I=1,1,6
  K(I,J)=K(I,J)+C(I,X)*(VACANCY/RESERVE)
  C(I,X)=C(I,X)*(1-(VACANCY/RESERVE))
%REPEAT

RESERVE=RESERVE-VACANCY
J=J+1
VACANCY=1
->4 %IF RESERVE>VACANCY

%CYCLE I=1,1,6
K(I,J)=C(I,X)
%REPEAT

VACANCY=VACANCY-RESERVE
->3 %UNLESS VACANCY=0
->2

5:%CYCLE J=L1,1,L2
%CYCLE I=1,1,6
  C(I,J)=K(I,J)
  K(I,J)=0
%REPEAT
%REPEAT

%COMMENT READJUSTMENT FINISHED, OXIDE CONCS. INTO C

%CAPTION~~MOL _PERCENT _COMPOSITION _PROFILE _ADJUSTED _TO%C
 _100 _PERCENT

TT=1; ->6
7:NEWLINES(5)
%CAPTIONMINERAL COMPOSITIONS~~~QZ AN%C
  CPX OPX GNT OLIV SPINEL KY WOLL%C
  CA-TSCH AL2O3 INPX GRINGNT

%END

```

%ROUTINE MINERAL

%INTEGER POSITIVE PHASES,N,P

%ROUTINESPEC FOURPHASE(%INTEGER VARIABLE PHASES,M1,M2,M3,M4)

%COMMENT TETRAHEDRON C-A-M-S DIVIDED INTO SUB-TETRAHEDRA, EACH
!DEFINED BY 4 MINERALS [M1 TO M4]. COMPOSITION TESTED TO FIND
!WHICH SUB-TETRAHEDRON IT LIES IN. WHEN FOUND, GO ON TO WORK
!OUT ACTIVITIES. PHASES OF VARIABLE COMPOSITION ARE OPX, CPX, &
!GARNET. VARIABLEPHASES STATES NO. OF MINERALS DEFINING THE
!SUB-TETRAHEDRON WHICH ARE OF THIS TYPE. IF VARIABLEPHASES=4
!FIRST 2 MINERALS ARE END-MEMBERS OF SAME PHASE. IF VARIABLE
!PHASES=5, DITTO, AND 3RD MINERAL IS ALSO A VARIABLE PHASE.
!IF VARIABLEPHASES=6, FIRST 3 MINERALS ARE ALL PYROXENE
!END-MEMBERS.

->3 %IF C(6,J)<50

2:FOURPHASE(1,6,2,4,1); ->1 %IF POSITIVE PHASES=4

FOURPHASE(2,6,8,2,1); ->1 %IF POSITIVE PHASES=4

FOURPHASE(2,8,10,2,1); ->1 %IF POSITIVE PHASES=4

FOURPHASE(1,10,3,2,1); ->1 %IF POSITIVE PHASES=4

FOURPHASE(4,5,6,4,1); ->1 %IF POSITIVE PHASES=4

FOURPHASE(6,5,6,7,1); ->1 %IF POSITIVE PHASES=4

FOURPHASE(6,7,8,6,1); ->1 %IF POSITIVE PHASES=4

FOURPHASE(5,9,10,8,1); ->1 %IF POSITIVE PHASES=4

FOURPHASE(4,9,10,3,1); ->1 %IF POSITIVE PHASES=4

->3 %UNLESS C(6,J)<50

%CAPTION~COMPOSITION UNLIKELY;%STOP

3:FOURPHASE(3,6,8,10,2); ->1 %IF POSITIVE PHASES=4

FOURPHASE(2,6,8,11,12); ->1 %IF POSITIVE PHASES=4

FOURPHASE(3,6,8,10,12); ->1 %IF POSITIVE PHASES=4

FOURPHASE(2,6,10,2,12); ->1 %IF POSITIVE PHASES=4

FOURPHASE(1,10,2,3,12); ->1 %IF POSITIVE PHASES=4

FOURPHASE(5,9,10,8,12); ->1 %IF POSITIVE PHASES=4

FOURPHASE(4,9,10,3,12); ->1 %IF POSITIVE PHASES=4

FOURPHASE(6,5,6,7,11); ->1 %IF POSITIVE PHASES=4

FOURPHASE(6,7,8,6,11); ->1 %IF POSITIVE PHASES=4

FOURPHASE(1,6,4,13,2); ->1 %IF POSITIVE PHASES=4

FOURPHASE(2,6,10,12,13); ->1 %IF POSITIVE PHASES=4

FOURPHASE(1,10,12,13,2); ->1 %IF POSITIVE PHASES=4

FOURPHASE(4,5,6,4,11); ->1 %IF POSITIVE PHASES=4

FOURPHASE(1,6,4,11,13); ->1 %IF POSITIVE PHASES=4

->2 %IF C(6,J)<50

%CAPTION~__COMPOSITION__ UNLIKELY;%STOP

%ROUTINE FOURPHASE(%INTEGER VARIABLEPHASES,M1,M2,M3,M4)

%INTEGER L,S,D,START

%INTEGERARRAY M(1:4)

%REAL DET,OPX,CPX,GNT,OLIV,SP,FE

%ARRAY Y,F(1:4),X,Z(1:4,1:4),W(1:4,1:4,1:4),XX(1:13)

%ROUTINESPEC APEX(%INTEGER M1,M2,M3,M4)

POSITIVE PHASES=0

APEX(M1,M2,M3,M4); !SET THE 4 MINERAL COMPS DEFINING THIS
!SUB-TETRAHEDRON INTO ARRAY X

%CYCLE N=1,1,3

Y(N)=C(N,J)

%REPEAT

Y(4)=C(6,J)

EQN SOLVE K(X,Y,4,DET); !RECALCULATES INTO MINERAL PROPORTIONS

%CYCLE N=1,1,4

Y(N)=Y(N)*100; !Y(N) NOW THE MOL PROP OF NTH MINERAL IN MOL%.

POSITIVE PHASES=POSITIVE PHASES+1 %IF Y(N)>0

%REPEAT

%RETURN %UNLESS POSITIVE PHASES=4

%COMMENT BULK COMP. LIES IN THIS SUB-TETRAHEDRON

%CYCLE L=1,1,4

%CYCLE S=1,1,4

%CYCLE D=1,1,4

W(L,S,D)=0

%REPEAT

Z(L,S)=0

%REPEAT

%REPEAT

%CYCLE L=1,1,4

%CYCLE S=1,1,4

->1 %IF S=L

Z(L,S)=Z(L,S)+(Y(S)/(100-Y(L)))*100; !% OF MIN S WHEN PROJ FROM L

%CYCLE D=1,1,4

->2 %IF D=L %OR D=S

W(L,S,D)=W(L,S,D)+(Z(L,D)/(100-Z(L,S)))*100

!% OF MINERAL D, WHEN PROJECTED FROM L AND S

2:%REPEAT

1:%REPEAT

%REPEAT

START=1

%COMMENT F(L) IS FACTOR FOR WEIGHTING THE ACTIVITIES

```
->4 %UNLESS Y(1)>=95; !1-PHASE REGION, MINERAL 1
%CYCLE L=2,1,4
F(L)=Y(L)/5
%REPEAT
```

```
->31
```

```
4:->9 %UNLESS VARIABLE PHASES=1
```

```
%CYCLE N=2,1,4
->5 %IF Z(N,1)>=95; !2-PHASE REGION, MINERALS N & 1
%REPEAT
```

```
->6
```

```
5:%CYCLE L=2,1,4
F(L)=Z(N,L)/5
%REPEAT
```

```
->31
```

```
6:%CYCLE N=2,1,4
%CYCLE P=2,1,4
->7 %IF W(N,P,1)>=95; !3-PHASE REGION, MINERALS N, P, & 1
%REPEAT
%REPEAT
```

```
->8; !4-PHASE REGION
```

```
7:%CYCLE L=2,1,4
F(L)=W(N,P,L)/5
%REPEAT
```

```
F(N)=1
F(P)=1
```

```
->31
```

```
8:F(2)=1
F(3)=1
F(4)=1
```

```
->31
```

```
9:->10 %UNLESS Y(2)>=95; !1-PHASE REGION, MINERAL 2
START=2
%CYCLE L=1,1,4
F(L)=Y(L)/5
%REPEAT
```

```
->31
```

```
10:->11%UNLESS (Y(1)+Y(2))>=95;!1- OR 2-PHASE REGION, MINS 1&2
START=1
```


F(2)=1
F(3)=Y(3)/5
F(4)=Y(4)/5

->31

11:->19 %IF VARIABLE PHASES=3 %OR VARIABLE PHASES>4

%CYCLE N=3,1,4

->12 %IF Z(N,1)>=95; !2-PHASE REGION, MINERALS N & 1

->13 %IF Z(N,2)>=95; !2-PHASE REGION, MINERALS N & 2

->14 %IF (Z(N,1)+Z(N,2))>=95; !3-PHASE REGION, MINERALS N,1,&2

%REPEAT

->15

12:START=1

%CYCLE L=2,1,4

F(L)=Z(N,L)/5

%REPEAT

F(N)=1

->31

13:START=2

%CYCLE L=1,1,4

F(L)=Z(N,L)/5

%REPEAT

F(N)=1

->31

14:START=1

%CYCLE L=3,1,4

F(L)=Z(N,L)/5

%REPEAT

F(2)=1

F(N)=1

->31

15:->16 %IF W(3,4,1)>=95; !3-PHASE REGION, MINS 1, 3, & 4

->17 %IF W(3,4,2)>=95; !3-PHASE REGION, MINS 2, 3, & 4

->18; !4-PHASE REGION

16:START=1

F(2)=W(3,4,2)/5

F(3)=1

F(4)=1

->31

17:START=2

$F(1) = W(3,4,1)/5$

$F(3) = 1$

$F(4) = 1$

->31

18:START=1

$F(2) = 1$

$F(3) = 1$

$F(4) = 1$

->31

19:->20 %UNLESS $Y(3) \geq 95$; !1-PHASE REGION, MINERAL 3

START=3

%CYCLE L=1,1,4

$F(L) = Y(L)/5$

%REPEAT

->31

20:->21 %UNLESS $(Y(1)+Y(3)) \geq 95$; !2-PHASE, MINS 1 & 3

START=1

$F(2) = Y(2)/5$

$F(4) = Y(4)/5$

$F(3) = 1$

->31

21:->22 %UNLESS $(Y(2)+Y(3)) \geq 95$; !2-PHASE, MINS 2 & 3

START=2

$F(1) = Y(1)/5$

$F(3) = 1$

$F(4) = Y(4)/5$

->31

22:->23 %UNLESS $(Y(1)+Y(2)+Y(3)) \geq 95$; !3-PHASE, MINS 1, 2, & 3

START=1

$F(2) = 1$

$F(3) = 1$

$F(4) = Y(4)/5$

->31


```

23:->24 %IF Z(4,1)>=95;      !2-PHASE REGION, MINERALS 4&1
->25 %IF Z(4,2)>=95;      !2-PHASE REGION, MINERALS 4&2
->26 %IF Z(4,3)>=95;      !2-PHASE REGION, MINERALS 4&3
->27 %IF (Z(4,1)+Z(4,2))>=95; !3-PHASE, MINERALS 1, 2, & 4
->28 %IF (Z(4,2)+Z(4,3))>=95; !3-PHASE, MINERALS 2, 3, & 4
->29 %IF (Z(4,1)+Z(4,3))>=95; !3-PHASE, MINERALS 1, 3, & 4
->30;      !4-PHASE REGION

```

```
24:START=1
```

```

F(2)=Z(4,2)/5
F(3)=Z(4,3)/52
F(4)=1

```

```
->31
```

```
25:START=2
```

```

F(1)=Z(4,1)/5
F(3)=Z(4,3)/5
F(4)=1

```

```
->31
```

```
26:START=3
```

```

F(1)=Z(4,1)/5
F(2)=Z(4,2)/5
F(4)=1

```

```
->31
```

```
27:START=1
```

```

F(2)=1
F(3)=Z(4,3)/5
F(4)=1

```

```
->31
```

```
28:START=2
```

```

F(1)=Z(4,1)/5
F(3)=1
F(4)=1

```

```
->31
```

```
29:START=3
```

```

F(1)=1
F(2)=Z(4,2)/5
F(4)=1

```

```
->31
```

30:START=1

F(2)=1

F(3)=1

F(4)=1

31:%CYCLE I=1,1,6

A(I,J)=0; !SETS ACTIVITIES TO ZERO

%REPEAT

M(1)=M1

M(2)=M2

M(3)=M3

M(4)=M4

%CYCLE I=1,1,6

A(I,J)=B(I,M(START)); !SETS ACTIVITIES TO THOSE OF FIRST MIN

%REPEAT

->32 %IF VARIABLE PHASES<4

F(2)=2*Y(2)/(Y(1)+Y(2)) %IF START=1

F(1)=2*Y(1)/(Y(1)+Y(2)) %IF START=2

%COMMENT F IS CHANGED TO ALLOW FOR 2 MINS BEING SAME PHASE

32:%CYCLE I=1,1,6

->34 %IF I=4 %OR I=5

%CYCLE L=1,1,4

->33 %IF L=START

A(I,J)=((A(I,J)*(2-F(L)))+(B(I,M(L))*F(L)))/2

%COMMENT ACTIVITIES BEING WEIGHTED BY F FACTORS FOR EACH MIN

33:%REPEAT

34:%REPEAT

%CYCLE I=1,1,13

XX(I)=0

%REPEAT

%COMMENT XX(I)= PROPORTION OF MINERAL I

%CYCLE I=1,1,13

XX(I)=XX(I)+Y(1) %IF M1=I

XX(I)=XX(I)+Y(2) %IF M2=I

XX(I)=XX(I)+Y(3) %IF M3=I

XX(I)=XX(I)+Y(4) %IF M4=I

%REPEAT


```

OPX=XX(7)+XX(8)
CPX=XX(5)+XX(6)
GNT=XX(9)+XX(10)
OLIV=XX(11)
SP=XX(12)

```

```

FE=(C(5,J)/C(3,J))*(OPX+CPX+GNT+OLIV+SP)/(CPX*KD(1)+OPX%C
+GNT*KD(2)+SP*KD(3)+OLIV*KD(4))

```

```

%COMMENT FE=FE/FE+MG RATIO IN THE OPX

```

```

A(4,J)=A(3,J)/(1+FE)
A(5,J)=A(3,J)*FE/(1+FE)

```

```

NEWLINE; PRINT(J,2,0); SPACES(5)
PRINT(XX(1),4,2)
PRINT(XX(2),4,2)
PRINT((XX(5)+XX(6)),4,2)
PRINT((XX(7)+XX(8)),4,2)
PRINT((XX(9)+XX(10)),4,2)
PRINT(XX(11),4,2)
PRINT(XX(12),4,2)
PRINT(XX(3),4,2)
PRINT(XX(4),4,2)
PRINT(XX(13),4,2)
->38 %IF XX(5)+XX(6)+XX(7)+XX(8)=0
PRINT((((XX(6)+XX(8))/(XX(5)+XX(6)+XX(7)+XX(8)))*6),6,1)
->39
38:SPACES(9)
39:->36 %IF XX(9)+XX(10)=0
PRINT(((XX(10)/(XX(9)+XX(10)))*14.1414),4,1);->37
36:SPACES(7)

```

```

%ROUTINE APEX(%INTEGER M1,M2,M3,M4)
%ROUTINESPEC COMP(%INTEGER M,N)

```

```

COMP(M1,1)
COMP(M2,2)
COMP(M3,3)
COMP(M4,4)

```

%ROUTINE COMP(%INTEGER M,N)

%COMMENT SETS X TO COMPOSITION OF MINERAL N

%ROUTINESPEC IN(%REAL D,E,F)

%SWITCH MIN(1:13)

-->MIN(M)

MIN(1):IN(0,0,0);%RETURN;!QUARTZ

MIN(2):IN(25,25,0);%RETURN;!ANORTHITE

MIN(3):IN(0,50,0);%RETURN;!KYANITE

MIN(4):IN(50,0,0);%RETURN;!WOLLASTONITE

MIN(5):IN(25,0,25);%RETURN;!DIOPSIDE

MIN(6):IN(23.5,6,23.5);%RETURN;!DIOPSIDE+6%AL2O3

MIN(7):IN(0,0,50);%RETURN;!ENSTATITE

MIN(8):IN(0,6,47);%RETURN;!ENSTATITE+6%AL2O3

MIN(9):IN(0,14.141,42.857);%RETURN;!PYROPE

MIN(10):IN(6,14.141,36.857);%RETURN;!PYROPE+14%GROSSULAR

MIN(11):IN(0,0,66.667);%RETURN;!FORSTERITE

MIN(12):IN(0,50,50);%RETURN;!SPINEL

MIN(13):IN(33.3333,33.3333,0);!CA-TSCHERMAK'S

%ROUTINE IN(%REAL D,E,F)

X(1,N)=D

X(2,N)=E

X(3,N)=F

X(4,N)=100-D-E-F

%END

%END

%END

%END

1:%END

-->2

%ENDOFPROGRAM

APPENDIX F

THE INTERPRETATION OF FREE ENERGY-COMPOSITION DIAGRAMS

Diagrams representing the variation in molar free energy against molar composition have appeared in the Geological literature in papers by Khorzhinskii (1966, fig. 1), and Weill and Fyfe (1967, fig. 1). These diagrams give a simple graphical method of relating free energy to chemical potential. This may be used to extract chemical potentials from free energy data, and could provide a means for those not familiar with the manipulation of thermodynamic equations to visualise the significance of the chemical potential.

This Appendix derives the equation relating molar free energy and chemical potential, and illustrates the use of the free energy-composition diagram with an elementary example.

The relation between molar free energy and chemical potential

Consider 1 mole of a system composed of n_1, n_j, \dots moles of constituents i, j , etc. The mole fractions of these constituents are $x_i, x_j, \dots (= n_i, n_j, \dots)$. If the number of moles n_i of constituent i is increased by dn_i , at constant P and T , the system becomes one of $1 + dn_i$ moles. The mole fractions are no longer equal to the numbers of moles:

$$x_i + dx_i = \frac{n_i + dn_i}{1 + dn_i}$$

whence $n_i + dn_i = (1 + dn_i)(x + dx_i)$

and $dn_i(1 - x_i) = dx_i(1 + dn_i)$ since $x_i = n_i$

Thus $\frac{dx_i}{dn_i} = \frac{(1 - x_i)}{(1 + dn_i)}$ (1)

Similarly, $G + dG = (1 + dn_i)(\bar{G} + d\bar{G})$

and $\frac{dG}{dn_i} = \bar{G} + \frac{d\bar{G}}{dn_i} \cdot (1 + dn_i)$ since $G = \bar{G}$

and, substituting (1),

$$\frac{dG}{dn_i} = \bar{G} + (1 - x_i) \frac{d\bar{G}}{dx_i} \text{ (2)}$$

Since P, T , and n_j have all been kept constant, equation (2) gives the expression for chemical potential of constituent i . Thus a plot of the molar free energy against mole fraction of i will give the chemical potential of i as the intercept of the tangent to the curve at any point on the free energy axis at $x_i = 1$ (fig. F-1).

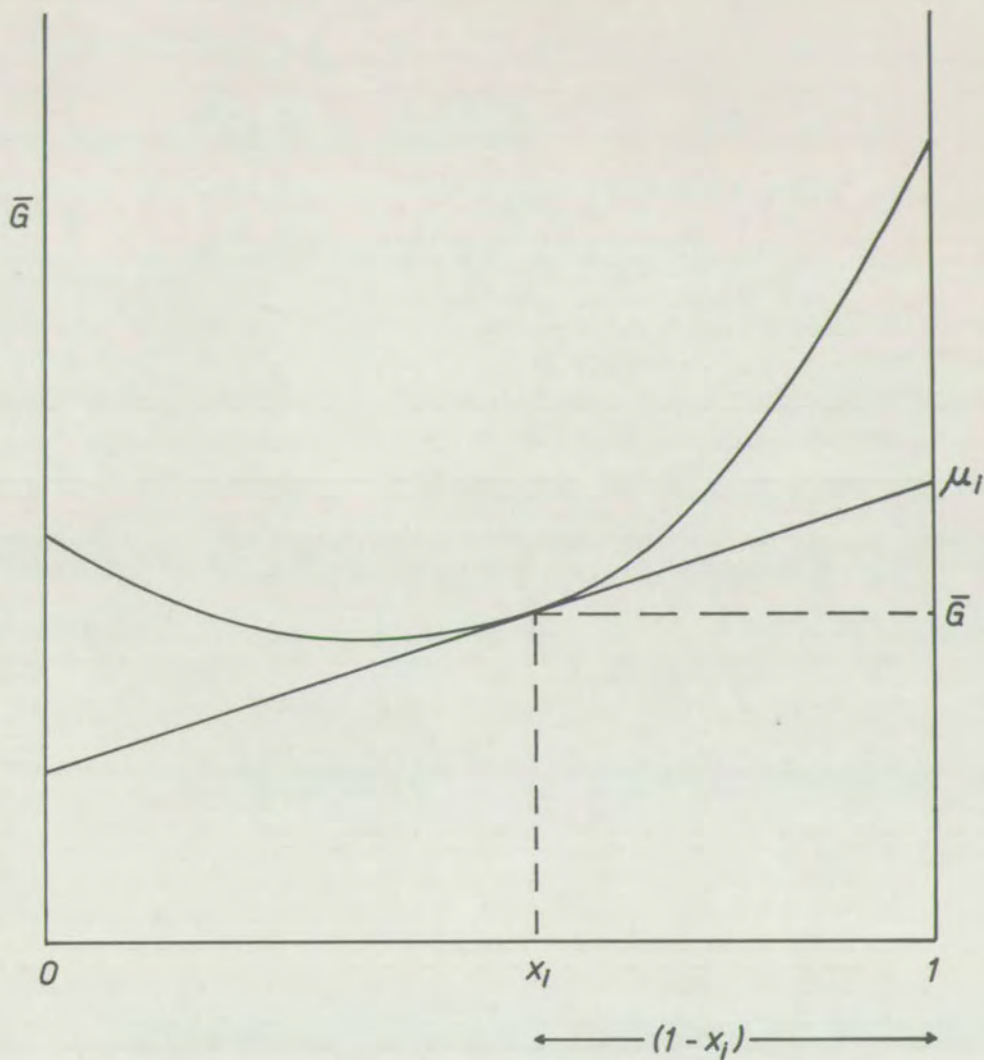


Fig. F-1.

The graphical interpretation of the equation relating molar free energy, mole fraction, and chemical potential;

$$\mu_i = \bar{G} + \frac{\partial \bar{G}}{\partial x_i} (1 - x_i)$$

It follows that the chemical potential of component i is given by the intercept of the tangent to the \bar{G} - x_i curve on the \bar{G} axis at $x_i=1$.

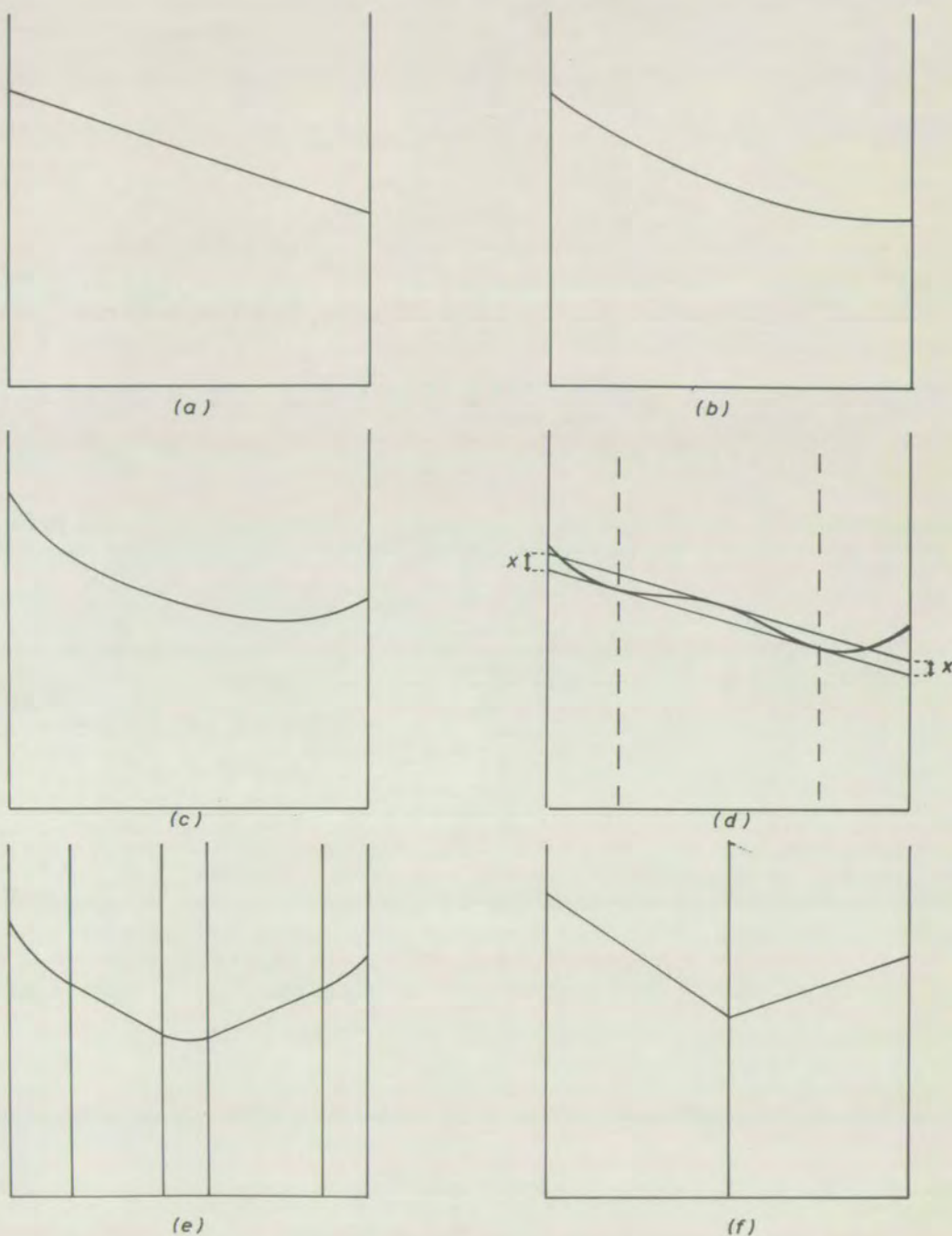


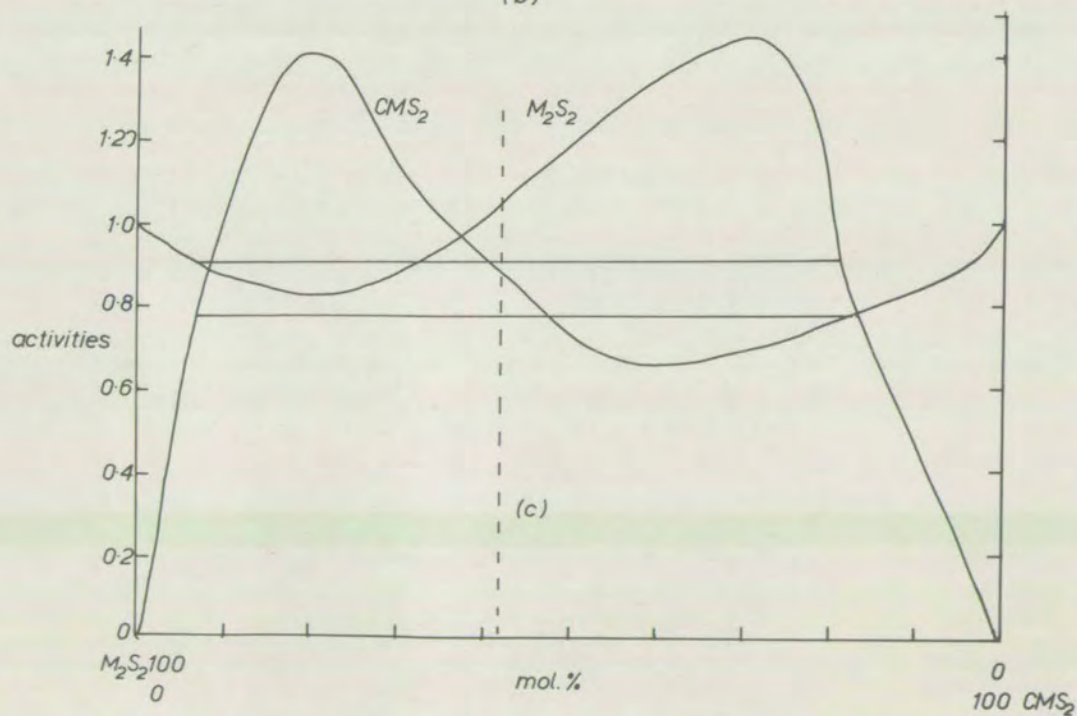
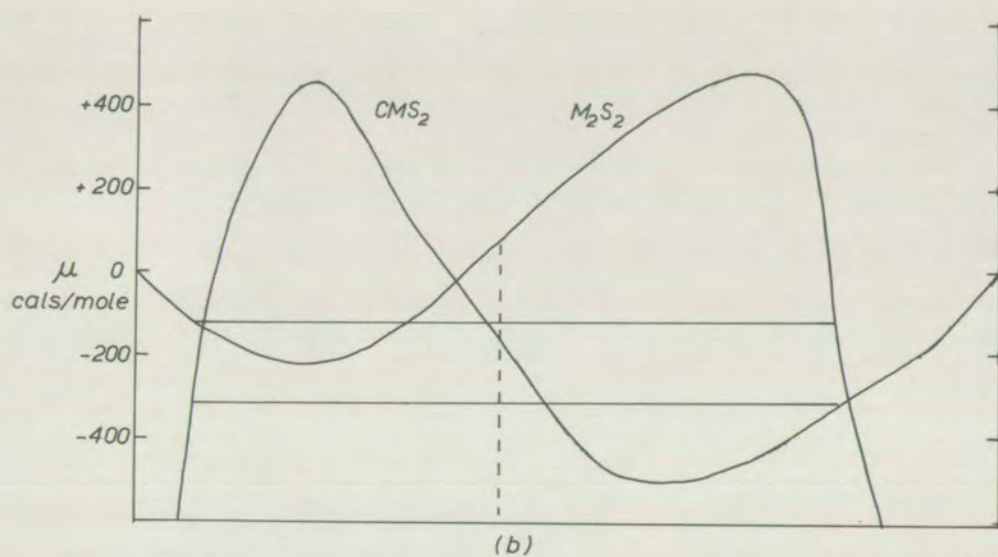
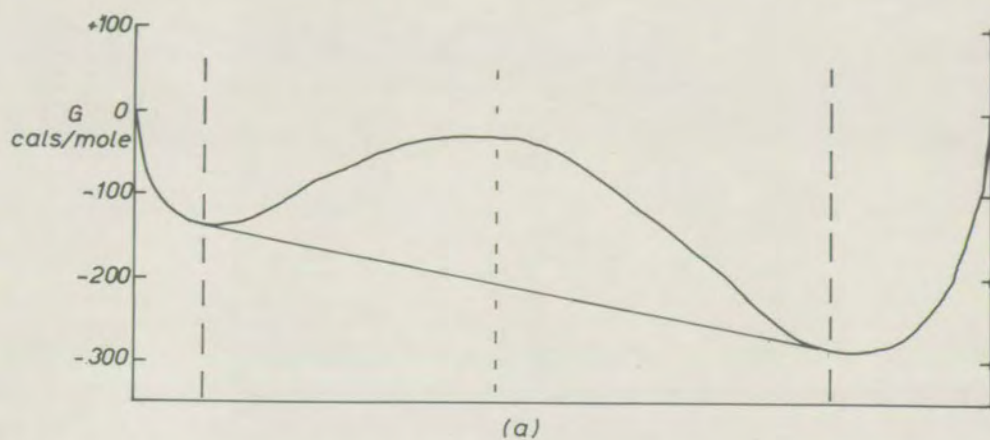
Fig. F-2 The form of the free energy-composition diagram for the system A-B in various situations.

- | | |
|---------------------------------------|--------------------------------------|
| (a) No solid solution | (b) Ideal solution |
| (c) Non-ideal solution | (d) Non-ideal solution with a solvus |
| (e) Compound AB with limited solution | (f) Compound AB with no solution |

The quantity x in (d) is the maximum free energy difference between a metastable solution and the equivalent stable state. It is also the difference in μ_A and μ_B between the two states.

Fig. F-3

- (a) Free energies of solid solutions in the system diopside-enstatite at 1 bar and 1300°K . For derivation, see text. The two broken lines indicate the solvus boundaries, and the central broken line is the composition of maximum free energy difference between stable and metastable states. The standard state is diopside + enstatite at the same P and T.
- (b) Chemical potentials derived from (a) by drawing tangents to the curve.
- (c) Activities derived from (b).



An illustration of the interpretation of free energy-composition diagrams is in the study of the breakdown of solid solutions with the intervention of a solvus. One has already been used to illustrate the breakdown of garnet (fig. 4-28). Fig. F-2 shows the form of the diagram for various types of two-component system (no solid solution, ideal solid solution, non-ideal solid solution with or without a solvus, and intermediate compound formation).

Fig. F-3(a) shows a free energy-composition diagram for the system diopside-enstatite at 1 bar and 1300°K. The free energies were calculated from the solvus data of Boyd and Schairer (The system $MS-CMS_2$. Carnegie Inst. Wash. Y.B. 61, 68-75, 1962), assuming simple solid solution and using equations presented by Thompson (1967). Fig. F-3(b) and (c) show the chemical potentials and activities of M_2S_2 and CMS_2 derived from (a) by the method outlined above.

There is a composition $(M_2S_2)_{58}(CMS_2)_{42}$ where the activities are 0.92 and 1.04, as opposed to 0.78 and 0.90 in the stably coexisting phases representing the same composition. The corresponding chemical potentials are -130, + 60, - 310, and -120 cal./mole respectively. These differences are small compared with differences between metastable phases just inside the solvus and the stable phases.

The minimum difference between the chemical potentials of both end-member species in a single metastable phase and the stable phases is equal to the free energy difference between the two states (fig. F-2d), while compositions closer to the margin of the solvus can have very much larger differences of chemical potential between the two states, although the

free energy difference will be less. Because the breakdown of a metastable phase involves the diffusion of material into and out of the lattice, it follows, as a qualitative conclusion, that there are compositions, in any series of solid solutions of this type, which may break down less readily into the stable phases than most other metastable compositions.

If a tholeiitic magma were subjected to hypersolvus crystallisation of pyroxenes (to use a term from granite petrology), and the single (presumably pigeonitic) pyroxene phase to crystallise had a composition close to that of minimum chemical potential differences referred to above, such a pyroxene could perhaps be preserved metastably for some time. If the same magma, after fractionation to a more iron-rich composition, were subject to subsolvus pyroxene crystallisation, it would produce (say) a sub-calcic augite and a relatively calcium rich clinohypersthene. These phases would, from the argument outlined above, more readily exsolve to the equilibrium phases than the early pigeonite.

It must be emphasised that the above argument is not intended to be rigorous, or even to accurately describe any existing situation. It is presented merely as an illustration of one sort of reasoning which could follow from a familiarity with the concept of chemical potential, a familiarity which it is by no means difficult to acquire, to an elementary degree.

APPENDIX G

ANALYTICAL METHODS

Sample Preparation

Rock samples were first washed, and then reduced to small pieces with a hydraulic splitter. They were then further reduced to chips less than 1 cm. in size with a tungsten carbide mortar and pestle. 'Manchester' rollers were used to crush these chips to about 15 mesh, and the sample was then divided by 'cone and quartering' and about 150 grams ground to -100 mesh in an automatic agate mortar. The rock powder was dried at 110°C before analysis.

Wet chemical analysis

12 rocks from Geodh'Eanruig (Z 718-Z 726 and 10719-10722) were analysed completely (except for TiO_2 and MnO) by wet methods. SiO_2 , R_2O_3 , CaO , and MgO were determined gravimetrically, using a version of the 'classical' methods (Peck, 1964).

Total Fe was determined by fusion of the rock powder in Na_2CO_3 , and passing a solution of the residue through a silver reductor in the presence of CO_2 . The ferrous iron was then determined by titration with standard $\text{K}_2\text{Cr}_2\text{O}_7$ solution (Mercy and Saunders, 1966).

FeO was determined by the cold-solution method of Wilson (1955).

Al_2O_3 was determined by digestion of the rock powder in HF , HNO_3 and H_2SO_4 , igniting the residue, then dissolving in water, filtering and acidifying. Iron was removed by extraction with a solution of cupferron in chloroform. Aluminium was then determined by addition of standard DCTA solution, which was back-titrated with standard lead

nitrate solution (Mercy and Saunders, 1966).

Na_2O and K_2O were determined with an Eel Flame Photometer on solutions prepared in the same way as for Al_2O_3 .

H_2O was determined by direct weighing of the condensate from ignition of rock powder with a lead oxide-lead chromate flux in a Pyrex test tube, the water being condensed at the mouth of the tube and absorbed on filter paper.

Ni and Cr were determined spectrophotometrically on specimens Z 718, Z 720, Z 725, Z 726, GE 22, and UA 1. For Ni, the dimethyl glyoxime method was used, and Cr was measured as chromate (in the ultrabasic rocks) and as a diphenylcarbazide compound (in the basic rocks). The methods were as given by Sandell (1959).

All the other rocks, and the minerals were analysed by X-ray fluorescence. FeO , Na_2O , and H_2O (and also K_2O for the 1966 batch of specimens) were determined as outlined above.

X-ray fluorescence analysis

The X-ray fluorescence analyses were performed in four batches, in the years 1966, 1967, 1968, and 1969 respectively. The specimens analysed in each batch were as follows:

1966: The rocks of Tables 7, 9, 14 and B-2, the Geodh nam Cliabh specimens 5 to 11 of Table 1, and specimens 10734-6 of Table 15 were analysed for all major elements, and TiO_2 and MnO were determined for the rocks of Tables 4 and 5.

1967: All other whole rock analyses except those of Table 3. Repeat of about half the 1966 analyses, and trace element determinations on all

of them.

1968: The mineral analyses of Tables 16, 17, and 18, and those of minerals from GE 13 in Table 20.

1969: The rocks of Table 3, and the minerals of Table 19, and those from B 521 in Table 20. Trace elements on the rocks of Tables 2 and 3.

For the first three years all analysis was performed on a Phillips PW 1540 X-ray spectrometer, but in 1969 a PW 1212 was used for all the elements except Cr and Ni.

The methods adopted have been in use in Edinburgh for some years and are well established. Sample preparation was as follows for major element analysis:

(1) Fusion of the rock powder, with La_2O_3 as a heavy absorber, and $\text{Li}_2\text{B}_4\text{O}_7$ as a diluent, in the proportions 1:1:8 (i.e. the method of Rose et al. (1962), but with different proportions).

(2) The mixture was fused in graphite crucibles at 1050°C for 20 minutes.

(3) The resultant beads were brought back to their original weight of 7.5 g. by addition of boric acid.

(4) The bead and boric acid were ground for 40 minutes in a tungsten carbide ball mill. The resultant powder was not sifted as this was thought to involve the risk of contamination and/or hydration of the glass (the powders were sifted for the first batch of analyses, half of which gave unsatisfactory totals and had to be repeated).

(5) The powder was dried at 110°C , and

(6) pressed into a disc at 5 tons pressure, against a polished steel surface.

(7) The disc was backed with boric acid and again pressed to form a durable mount, about 5 mm. thick.

(8) The discs were stored in a cabinet at 40°C to delay hydration.

For trace and minor element determinations, the 100 mesh rock powder was used, supported on a mylar film. In the 1967 batch of analyses, the rock powders were mixed with 5% of boric acid as a binding agent, and pressed into briquettes. These were used for determinations of P_2O_5 and S, as well as the trace elements.

Standards:

The Geodh'Eanruig rocks which were analysed by wet methods were used as standards throughout. In addition, the following widely circulated standards were used:

U.S.G.S. standards G-1 and W-1, using the values of Fleischer and Stevens (1962). These were available in 1966 only.

U.S.G.S. standards G-2, GSP-1, AGV-1, BCR-1, PCC-1, and DTS-1 (Flanagan, 1967). Used for major elements in the 1969 batch only, and for trace elements in the 1967 and 1969 batches.

U.S.N.B.S. standards - 102 silica brick

91 opal glass

76, 77 burnt refractories

1a argillaceous limestone

For measurement of trace elements on the leucocratic gneisses, synthetic standards of approximately granitic composition were used. The six rocks analysed spectrophotometrically for Cr and Ni were used as standards for these elements, and together with two other ultrabasic

rocks analysed in Edinburgh by the same methods, gave excellent results.

In all cases, the samples were analysed in batches of 4, one of which was an internal standard, selected as being as rich in the element under analysis as any of the unknowns, and which remained in place throughout the session to allow correction for machine drift.

Operating conditions:

The conditions were set each day when using the PW 1540, and are set out in Table 23, together with the (standard) conditions used on the PW 1212. Where more than one set of conditions is tabulated for a batch of analyses, this refers to a duplicate run.

Although the PE crystal was used and gave tolerable results in 1966, the silica determinations in 1967 were totally unsatisfactory due to excessive drift during the long sessions involved in making 90 analyses, and they were all repeated using a gypsum crystal, which gave excellent stability and count rates only marginally lower.

Accuracy:

The accuracy and precision of the X-ray fluorescence methods used have already been investigated (e.g. Westoll, 1968), and found to be good. It was felt that to quote values of the oxides in an analysis to the nearest 0.01% would be to exaggerate the accuracy of the methods, however. For this reason, SiO_2 , Al_2O_3 , Fe_2O_3 , FeO , MgO and CaO are given to the nearest 0.05% in the X-ray analyses. TiO_2 , MnO , and K_2O (where this was determined by X-ray fluorescence) are given to the nearest 0.01%. Na_2O , K_2O , and H_2O , determined by wet methods are also quoted to 0.01%. Na_2O in Tables 16 and 17 was determined by X-ray fluorescence and is quoted to 0.1%.

Electron probe analyses

The electron probe analyses of minerals, the results of which are presented in some of the diagrams of Chapter 4, were performed on the Mk. I electron probe in the Department of Mineralogy and Petrology, University of Cambridge, under the supervision of Dr. J.V.P. Long. The elements Si, Al, Fe, Mg, and Ca were determined on a total of about 300 points. Single standards were used for each element. The correction procedure was performed manually on the Geodh'Eanruig samples, using average correction factors for each mineral, calculated from an average mineral analysis. The Loch an Daimh Mhor analyses were processed by Dr. Long using a computer programme to correct each analysis individually. The two methods gave similar results when applied to the same data. 9% of the pyroxene, olivine, garnet and spinel analyses gave totals outside the range 96%-104%, when recalculated to oxides (with Fe as FeO).

Modal Analysis

The modes quoted are only semi-quantitative. They were derived by counting 300 to 400 points on a 4 mm. grid, from a whole thin section projected on to a screen.

Reference

ROSE, H.J., A. ADLER, and F.J. FLANAGAN, 1962. X-ray fluorescence analysis of the light elements in rocks and minerals. Appl. Spectrosc. 17, 81-85.

Element	Year of analysis	Method (peak only, peak minus back-ground, peak/background ratio)	Peak measured	Tube	KV	mA	crystal	Counter (gas flow or scintillation)	Lower level	Channel width	Attenuation	Discriminator	Collimator (coarse or fine)	Counter E.H.T.	Vacuum (*) or no vacuum (-)	Total counting time, sedonds (where two times are given, first is peak, second is background)	Sample preparation (fusion disc, briquette, or powder on mylar film)	Notes
SiO ₂	66	P	K _α	Cr	50	20	PE	F	24 ¹⁶	24	25		c	1.80	*	120	disc	
	67	P	K _α	Cr	50	20	PE	F	6	16	25		c	1.71	*	60	disc	
	67	P	K _α	Cr	45	20	PE	F	7	18	25		c	1.71	*	60	disc	
	67	P	K _α	Cr	50	20	PE	F	5	16	25		c	1.72	*	100	disc	
	67	P	K _α	Cr	50	20	exps.	F	15	20	25		c	1.78	*	180	disc	
	68	P	K _α	Cr	60	20	exps.	F	6	11	25		c	1.72	*	120	disc	
TiO ₂	66	P	K _α	Cr	40	20	LiF	F	16	30	26		f	1.80	*	120	disc	
	67	P	K _α	Cr	40	20	LiF	F	6	20	25		f	1.62	*	40	disc	
	68	P	K _α	Cr	40	20	LiF	F	18	16	25		f	1.70	*	40	disc	
Al ₂ O ₃	66	P	K _α	Cr	45	32	PE	F	12	30	26		c	1.78	*	200	disc	
	66	P	K _α	Cr	45	32	PE	F	12	28	26		c	1.77	*	200	disc	
	66	P	K _α	Cr	45	32	PE	F	12	28	26		c	1.86	*	200	disc	
	67	P	K _α	Cr	45	32	PE	F	18	26	23		c	1.68	*	300	disc	
	67	P	K _α	Cr	45	32	PE	F	4	12	23		c	1.57	*	300	disc	
	67	P	K _α	Cr	45	32	PE	F	18	18	23		c	1.61	*	300	disc	
	68	P	K _α	Cr	45	32	PE	F	6	14	23		c	1.61	*	400	disc	
Fe (total)	66	P	K _α	W	40	20	LiF	S	2	24	24		f	0.95	-	120	disc	
	67	P	K _α	W	40	20	LiF	S	2	17	24		f	0.90	-	40	disc	
	68	P	K _α	W	40	20	LiF	S	8	24	21		f	0.75	-	40	disc	
MnO	66	P-B	K _α	W	40	28	LiF	S	8	34	22		f	0.86	-	120	disc	
	67	P-B	K _α	W	40	28	LiF	S	2	12	24		f	0.89	-	100	disc	
	68	P-B	K _α	W	40	20	LiF	S	8	24	21		f	0.75	-	100	disc	
MgO	66	P	K _α	Cr	50	28	ADP	F	14	13	25		c	1.80	*	400	disc	
	67	P	K _α	Cr	50	28	ADP	F	9	11	25		c	1.77	*	400	disc	
	67	P	K _α	Cr	50	28	ADP	F	13	17	25		c	1.80	*	400	disc	
	67	P	K _α	Cr	50	28	ADP	F	11	16	25		c	1.80	*	400	disc	
	67	P	K _α	Cr	55	28	ADP	F	6	14	25		c	1.77	*	400	disc	
CaO	66	P	K _α	Cr	40	20	LiF	F	8	24	26		c	1.79	*	80	disc	
	67	P	K _α	Cr	40	20	LiF	F	2	26	26		c	1.73	*	40	disc	
	68	P	K _α	Cr	40	20	LiF	F	12	16	25		c	1.71	*	40	disc	
Na ₂ O	68	P-B	K _α	Cr	55	28	exps.	F	14	20	24		c	1.76	*	1600	disc	
K ₂ O	67	P	K _α	Cr	45	20	LiF	F	4	14	23		c	1.50	*	400	disc	
	68	P	K _α	Cr	45	20	LiF	F	6	11	23		c	1.50	*	60	disc	
P ₂ O ₅	67	P-B	K _α	Cr	50	20	ADP	F	22	36	23		f	1.68	*	200	disc	
S	67	P-B	K _α	Cr	50	20	ADP	F	12	23	23		c	1.61	*	60	brig.	
Cr	67	P	K _α	W	50	20	topaz	F	6	12	24		f	1.52	*	72	brig.	U.B. only
	67	P/B	K _α	W	50	20	topaz	F	thr	-	24		f	1.55	*	60/120	brig.	others
	68	P/B	K _α	W	50	20	topaz	F	26	18	21		f	1.61	*	60/120	mylar	
	69	P/B	K _α	W	50	20	LiF(220)	F	28	20	21		f	1.61	*	40/80	mylar	

TABLE 23

OPERATING CONDITIONS FOR X-RAY SPECTROMETERS

Element	Year of analysis	Method (peak only, peak minus background, peak/background ratio)	Peak measured	Tube	kV	mA	crystal	Counter (gas flow or scintillation)	Lower level	Channel width	Attenuation	Discriminator	Collimator (coarse or fine)	Counter E.H.T.	Vacuum (*) or no vacuum (-)	Total counting time, seconds (where two times are given, first is peak, second is background)	Sample preparation (fusion disc, briquette, or powder on mylar film)	Notes
Ni	67	P/B	K _α	W	50	20	LIF	S	2	24	2 ³	f	0.83	-	-	80	brig.	
	67	P/B	K _α	W	50	20	LIF	S	2	30	2 ³	f	0.70	-	-	60	brig.	
	68	P/B	K _α	W	50	20	LIF	S	12	30	2 ¹	f	0.75	-	-	40/80	mylar	
	69	P/B	K _α	W	50	20	LIF	S	10	28	2 ¹	f	0.75	-	-	100/200	mylar	
Rb, Sr	66	P/B	K _α , K _β	W	40	20	LIF	S	8	18	2 ⁵	f	0.95	-	-	100	mylar various stds	
	67	P/B	K _α , K _β	W	50	20	LIF	S	2	20	2 ⁴	f	0.87	-	-	200	mylar USGS stds	
	67	P/B	K _α , K _β	W	50	20	LIF	S	4	22	2 ⁴	f	0.86	-	-	100	brig. synth stds	
Rb, Sr, Y, Zr	67	P/B	K _α (afl)	W	40	20	topaz	S	12	18	2 ³	f	0.80	-	-	100	brig. synth stds	
Ba	67	P/B	K _α	W	57	20	topaz	S	2	9	2 ⁴	f	0.72	-	-	100	brig.	
Nb	67	P/B	K _α	W	45	20	topaz	S	12	16	2 ⁴	f.	0.85	-	-	200	brig.	
Pb	67	P/B	L _α	W	50	20	topaz	S	8	22	2 ³	f	0.83	-	-	200	brig.	
Cu	67	P/B	K _α	W	45	20	topaz	S	8	23	2 ⁴	f	0.93	-	-	200	brig.	
OPERATING CONDITIONS FOR PW 1212																		
S102		P	K _α		60	24	PE					c				60		
TiO ₂		P	K _α		60	24	LIF					c				30		
Al ₂ O ₃		P	K _α		60	24	PE					c				60		
Fe	69	P	K _α	Cr	60	24	LIF	F	4.75	5.0	2 ²	f	1.80	*		30	disc	
MgO		P-B	K _α		40	32	ADP					c				300		
CaO		P	K _α		60	24	PE					f				30		
K ₂ O		P	K _α		60	24	PE					f				30		
trace 69 elements (Ba, Zr, Sr, Y, Zn, Cu)																		
		P-B	K _α	W	80	24	LIF	S	4.75	5.0	2 ¹	f	0.97	-	-	60	mylar	

REFERENCES

- BAILEY, E.B., 1951. Scourie Dykes and Laxfordian metamorphism. Geol. Mag. 88, 153-165.
- , and J. W. McCALLIEN, 1960. Some aspects of the Steinmann Trinity, mainly chemical. Q. Jl. Geol. Soc. Lond. 116, 365-395.
- BAROOAH, B. C., 1967. Ph.D. Thesis, Univ. of Glasgow.
- BARTH, T. F. W., 1951. The feldspar geologic thermometer. Neues Jb. Miner. 82, 143-154.
- BEST, M. G., and E. L. P. MERCY, 1967. Composition and crystallisation of mafic minerals in the Guadalupe Igneous Complex, California. Am. Miner. 52, 436-474.
- BOETCHER, A. L., and P. J. WYLLIE, 1967. Hydrothermal melting curves in silicate-water systems at pressures greater than 10 kilobars. Nature 216, 572.
- , and ———, 1968. Melting of granite with excess water to 30 Kb. pressure. J. Geol. 76, 235-244.
- BOLTZMANN, L., 1894. Zur integration der diffusionsgleichung bei variablen diffusionscoefficienten. Annln. Phys. u. Chem. 53, 959-964.
- BOWEN, N. L., and O. F. TUTTLE, 1958. Origin of granite in the light of experimental studies. Geol. Soc. Am. Mem. 74, 153 pp.
- BOWES, D. R., and T. S. GHALY, 1964. Age relations of Lewisian

basic rocks, south of Gairloch, Ross-shire. Geol. Mag. 101, 150-160.

BOWES, D. R., and S. G. KHOURY, 1965. Successive periods of basic dyke emplacement in the Lewisian Complex, south of Scourie, Sutherland. Scott. J. Geol. 1, 295-299.

———, A. E. WRIGHT, and R. G. PARK, 1961. Field relations of rocks containing coexisting pyroxenes. Geol. Mag. 98, 530-531.

———, ———, and ———, 1964. Layered Intrusive rocks in the Lewisian of the North-West Highlands of Scotland. Q. Jl. Geol. Soc. Lond. 120, 153-192.

———, ———, and ———, 1966. Origin of ultrabasic and basic masses in the Lewisian. Geol. Mag. 103, 280-284.

BOWN, M. G., and P. GAY, 1958. The reciprocal lattice structures of the plagioclase feldspars. Zeit. Kristallogr. 111, 1-13.

BOYD, F. R., 1959. Hydrothermal investigations in amphiboles. In Researches in Geochemistry (pp. 377-396), ed. P. H. Abelson. Wiley, N. Y. 511 pp.

———, and J. L. ENGLAND, 1962. Effect of pressure on the melting of pyrope. Carnegie Inst. Wash. Y. B. 61, 109-112.

BROWN, G. M., 1956. The layered ultrabasic rocks of Rhum, Inner Hebrides. Phil. Trans Roy. Soc. Ser. B. 240, 1-53.

- BURNS, D. J., 1956. D. I. C. Thesis, Imperial College, London.
- , 1966. Chemical and mineralogical changes associated with the Laxford Metamorphism of dolerite dykes in the Scourie-Loch Laxford area, Sutherland, Scotland. Geol. Mag. 103, 19-35.
- CHIDESTER, A. H., 1962. Petrology and geochemistry of selected talc-bearing ultramafic rocks and adjacent country rocks in North-Central Vermont. U. S. Geol. Surv. Prof. Pap. 345, 207 pp.
- CHOWDHARY, P. K., 1969. Ph.D. Thesis, Univ. of Glasgow.
- CLARK, J. B., and F. N. RHINES, 1958. Diffusion layer formation in the ternary system Aluminium-Magnesium-Zinc. Trans. Am. Soc. Metals 51, 199-221.
- CLARK, S. P., 1966. Handbook of physical constants. Geol. Soc. Am. Mem. 97, 587 pp.
- CLOUGH, C. T., B. N. PEACH, J. HORNE, W. GUNN, L. W. HINXMAN, J. J. H. TEALL, and A. GEIKIE, 1907. The geological structure of the North-West Highlands of Scotland. Mem. Geol. Surv. G. B., 668 pp.
- DASH, B., 1967. Ph.D. Thesis, Univ. of Glasgow.
- DAVIDSON, C. F., 1943. The Archaean rocks of the Rodil district, South Harris, Outer Hebrides. Trans. Roy. Soc. Edin. 61, 71-112.
- DEARNLEY, R., 1963. The Lewisian Complex of South Harris, with some observations on the metamorphosed basic dykes of the Outer Hebrides. Q. Jl. Geol. Soc. Lond. 119 243-313.

- DEARNLEY, R., and F. W. DUNNING, 1967. Metamorphosed and deformed pegmatites and basic dykes in the Lewisian complex of the Outer Hebrides, and their geological significance. Q. Jl. Geol. Soc. Lond. 123, 335-378.
- DEER, W. A., R. A. HOWIE, and J. ZUSSMANN, 1963. Rock-forming minerals, Vol. 2. Chain silicates. Longmans, London, 379 pp.
- De WAARD, D., 1965. The occurrence of garnet in the granulite-facies terrane of the Adirondack Highlands. J. Petrol. 6, 165-191.
- ESKOLA, P., 1921. The mineral facies of rocks. Norsk. Geol. Tidsskr. 6, 143-194.
- EVANS, C. R., 1963. D. Phil. Thesis, Univ. of Oxford.
- , 1964. Dating of the Lewisian Basement near Loch-inver, Sutherland. Adv. Sci. 20, 446.
- , and J. TARNEY, 1964. Isotopic ages of Assynt dykes. Nature 204, 638-641.
- FLANAGAN, F. J., 1967. U.S. Geological Survey silicate rock standards. Geochim. Cosmochim. Acta. 31, 289-308.
- FLEISCHER, M., and R. E. STEVENS, 1962. Summary of new data on rock samples G-1 and W-1. Geochim. Cosmochim. Acta 26, 525-543.
- GASS, I. G., 1958. Ultrabasic pillow lavas from Cyprus. Geol. Mag. 95, 241-251.
- GHOSE, C., 1958. Ph.D. Thesis, Univ. of Bristol.
- GILETTI, B. J., S. MOORBATH, and R. St. J. LAMBERT, 1961. A geo-

chronological study of the metamorphic complexes of the Scottish Highlands. Q. Jl. Geol. Soc. Lond. 117, 233-272.

GILL, K. R., 1965. Ph.D. Thesis, Univ. of Cambridge.

GOLDSCHMIDT, V. M., 1911. Die Kontaktmetamorphose im Kristiania-gebiet. Oslo Vidensk. Skr., I, Math. Naturv. Kl. 11, 405 pp.

GREEN, D. H., and A. E. RINGWOOD, 1967. The stability fields of aluminous pyroxene peridotite and garnet peridotite, and their relevance in upper mantle structure. Earth Planet. Sci. Lett. 3, 151-160.

HANCOCK, W. G., 1964. Ph.D. Thesis, Univ. of Durham.

HARKER, A., 1939. Metamorphism. Cambridge U.P., 326 pp.

HESS, H. H., 1968. Review of 'Ultramafic and related rocks', ed. P. J. Wyllie. Geotimes 13, pt. 6, 34-36.

HOLLAND, J. G., 1965. D.Phil. Thesis, Univ. of Oxford.

HURLEY, P. M., and G. FAURE, 1963. The isotopic composition of Strontium in oceanic and continental basalts; application to the origin of igneous rocks. J. Petrol. 4, 31-50.

INGLIS, J. W., 1966. Ph.D. Thesis, Univ. of Keele.

JAHNS, R. H., 1967. Serpentinities in the Roxbury district, Vermont. In Ultramafic and related rocks (pp. 137-172), ed. P. J. Wyllie. Wiley. N.Y., 464 pp.

JAMES, R., and D. L. HAMILTON, 1969. Phase relations in the system $\text{NaAlSi}_3\text{O}_8$ - KAlSi_3O_8 - $\text{CaAl}_2\text{Si}_2\text{O}_8$ - SiO_2 at 1

kilobar water pressure. Contrib. Mineral. Petrol. 21, 111-141.

KELLEY, K. K., 1960. Contributions to theoretical metallurgy, 3. High-temperature heat content and heat capacity data for the elements and inorganic compounds. U.S. Bur. Mines Bull. 584.

KENDALL, M. G., 1968. A course in multivariate analysis. Griffin and Co., London.

LIVINGSTONE, A., 1967. A garnet-peridotite and garnet-amphibole pyroxenite from South Harris, Outer Hebrides, and their bearing on the South Harris eclogite facies status. Min. Mag. 36, 380-388.

KHORZHINSKII, D. S., 1950. Phase rule and geochemical mobility of elements. Rep. 18th. session, Int. Geol. Cong. G.B., Pt. II, 50-65.

———, 1966. On thermodynamics of open systems and the phase rule (A reply to D. F. Weill and W. S. Fyfe). Geochim. Cosmochim. Acta 30, 829-835.

KHOURY, S. G., 1968a. The structural geometry and geological history of the Lewisian rocks between Kylesku and Geisgil, Sutherland, Scotland. Krystalinikum 6, 41-78.

———, 1968b. Structural analysis of complex fold belts in the Lewisian north of Kylesku, Sutherland, Scotland. Scott. J. Geol. 4, 109-120.

KIRKALDY, J. S., and L. C. BROWN, 1963. Diffusion behaviour in ternary, multiphase systems. Can. Metall. Quart. 2, 89-115.

- KUSHIRO, I., and H. S. YODER, 1966. Anorthite-forsterite and anorthite-enstatite reactions and their bearing on the basalt-eclogite transformation. J. Petrol. 7, 337-362.
- LUNDGREN, L. W., 1966. Muscovite reactions and partial melting in South-eastern Connecticut. J. Petrol. 7, 421-453.
- LUTH, W. C., 1969. The systems $\text{NaAlSi}_3\text{O}_8\text{-SiO}_2$ and $\text{KAlSi}_3\text{O}_8\text{-SiO}_2$ to 20 Kb. and the relationship between H_2O content, $P_{\text{H}_2\text{O}}$, and P_{total} in granitic magmas. Am. J. Sci. Schairer Vol. 267A 325-341.
- , R. H. JAHNS, and O. F. TUTTLE, 1964. The granite system at pressures of 4 to 10 kilobars. J. Geophys. Research 69 759-773.
- MACDONALD, G. A., 1949. The Hawaiian petrographic province. Bull. Geol. Soc. Amer. 60, 1541-1596.
- MacGREGOR, I. D., 1964. The reaction $4\text{Enstatite} - \text{Spinel} = \text{Forsterite-Pyrope}$. Carnegie Inst. Wash. Y.B. 63, 157.
- MANSON, V., 1967. Geochemistry of basaltic rocks: major elements. In Basalts (pp. 215-270), ed. H. H. Hess and A. Poldervaart. Wiley, N.Y., 862 pp.
- MATTHEWS, D. W., 1967. Zoned ultrabasic bodies in the Lewisian of the Moine Nappe in Skye. Scott. J. Geol. 3, 17-33.
- MEIJERING, J. L., 1958. Discussion after Clark and Rhines (1958). Trans. Am. Soc. Metals 51, 218-220.

- MERCY, E. L. P., and M. J. SAUNDERS, 1966. Precision and accuracy in the chemical determination of Fe and Al in silicate rocks. Earth Planet. Sci. Lett. 1, 169-182.
- MIYASHIRO, A., 1965. Some aspects of peridotite and serpentinite in orogenic belts. Jap. J. Geol. Geog. 38, 45-61.
- MOREY, G. W., and J. M. HESSELGESSER, 1950. The solubility of some minerals in superheated steam at high pressures. Econ. Geol. 46, 821-835.
- MUIR, I. D., and C. E. TILLEY, 1964. Basalts from the northern part of the rift zone of the Mid-Atlantic Ridge. J. Petrol. 5, 409-434.
- , and ———, 1966. Basalts from the northern part of the Mid-Atlantic Ridge, II The 'Atlantis' collections near 30° N. J. Petrol. 7, 193-201.
- NAKAYAMA, I., 1960. The tectonic movement and rock structure of the Sambagawa metamorphic zone, Japan. Monogr. Assoc. Geol. Collabor. Jap. 10. English translation in Int. Geol. Rev. 4, 817-862 (1962).
- NICHOLLS, G. D., 1965. Basalts from the deep ocean floor. Min. Mag. 34, 373-388.
- , A. J. NALWALK, and E. E. HAYS, 1964. The nature and composition of samples dredged from the Mid-Atlantic Ridge between 22° N. and 52° N. Marine Geol. 1 333-343.

- NOCKOLDS, S. R., 1954. Average compositions of some igneous rocks. Bull. Geol. Soc. Am. 65, 1007-1032.
- , and R. ALLEN, 1956. The geochemistry of some igneous rock series, III. Geochim. Cosmochim. Acta 2, 34-77.
- O'HARA, M. J., 1960. Ph. D. Thesis, Univ. of Cambridge.
- , 1961a*. Zoned ultrabasic and basic gneiss masses in the Early Lewisian Complex at Scourie, Sutherland. J. Petrol. 2, 248-276.
- , 1961b. Petrology of the Scourie Dyke, Sutherland. Min. Mag. 32, 848-865.
- , 1962. Some intrusions in the Lewisian Complex near Badcall, Sutherland. Trans. Edin. Geol. Soc. 19, 201-207.
- , 1965. Origin of ultrabasic and basic gneiss masses in the Lewisian. Geol. Mag. 102, 296-314.
- , 1966. Reply to Bowes et al. (1966). Geol. Mag. 103, 284.
- , 1967. Mineral parageneses in ultrabasic rocks. In Ultramafic and related rocks (pp. 393-404), ed. P. J. Wyllie. Wiley, N.Y., 464 pp.
- , 1968a. The bearing of phase equilibria studies in synthetic and natural systems on the origin of basic and ultrabasic rocks. Earth-Sci. Rev. 4, 69-133.
- , 1968b. Are ocean floor basalts primary magmas? Nature 220, 683-686.

*Note This paper is referred to throughout most of the text as O'Hara (1961).

- ONSAGER, L., 1949. Theories and problems of liquid diffusion.
Ann. N.Y. Acad. Sci. 46, 241-265.
- PARK, R. G., 1964. The structural history of the Lewisian rocks
of Gairloch, Wester Ross, Scotland. Q. Jl. Geol.
Soc. Lond. 120, 397-433.
- , 1966. Nature and origin of Lewisian basic rocks
of Gairloch, Ross-shire. Scott. J. Geol. 2, 179-199.
- PECK, L. C., 1964. Systematic analysis of silicates. U.S. Geol.
Surv. Bull. 1170, 89 pp.
- PINUS, G. V., V. A. KUZNETSOV, and I. M. VOLOKHOV, 1958. Giper-
bazitii Altae-Sayanskoi Skladyatoi Oblastii.
Akad. Nauk. S.S.S.R. (Sibirskii Otdelenie, Institut
Geologii Geofizikii), 295 pp.
- PHILLIPS, A. H., and H. H. HESS, 1936. Metamorphic differentiation
at contacts between serpentinite and siliceous country
rock. Am. Miner. 21, 333-362.
- PLATEN, H. von, 1965. Experimental anatexis and the genesis of
migmatites. In Controls of metamorphism (pp. 203-
218), eds. W. S. Pitcher and G. W. Flinn. Oliver and
Boyd, Edin., 368 pp.
- READ, H. H., 1934. On zoned associations of talc, actinolite,
chlorite, and biotite in Unst, Shetland Islands.
Min. Mag. 23, 519-540.
- SABINE, P. A., and J. V. WATSON, 1965. Isotopic age-determinations
from the British Isles, 1955-64. Q. Jl. Geol. Soc.
Lond. 121, 477-533.

- SANDELL, E. B., 1959. Colorimetric determination of traces of metals. Interscience, N.Y. 1032.
- SHEPPARD, S. M. F., 1968. Zoned ultrabasic bodies in Skye. Scott. J. Geol. 4, 85-87.
- SØRENSEN, H., 1954. The border relations of the dunite at Siorarsuit, Sukkertoppen district, West Greenland. Medd. om Grønland 135, No. 4.
- STEWART, D. B., 1957. The system $\text{CaAl}_2\text{Si}_2\text{O}_8\text{-SiO}_2\text{-H}_2\text{O}$. Carnegie Inst. Wash. Y.B. 56, 214-216.
- SUTTON, J., and J. V. WATSON, 1950. The pre-Torridonian metamorphic history of the Loch Torridon and Scourie areas in the North-West Highlands, and its bearing on the chronological classification of the Lewisian. Q. Jl. Geol. Soc. Lond. 106, 241-307.
- , and ———, 1962. Further observations on the margin of the Laxfordian Complex of the Lewisian near Loch Laxford, Sutherland. Trans. Roy. Soc. Edin. 65, 89-106.
- TARNEY, J., 1963. Assynt dykes and their metamorphism. Nature 199, 672-674.
- TEALL, J. J. H., 1885. On the metamorphosis of dolerite into hornblende schist. Q. Jl. Geol. Soc. Lond. 41, 133-145.
- THAYER, T. P., 1967. Chemical and structural relations of ultramafic and felspathic rocks in Alpine intrusive complexes. In Ultramafic and related rocks (pp. 222-239), ed. P. J. Wyllie. Wiley, N.Y., 464 pp.

- THOMPSON, J. B., 1959. Local equilibrium in metasomatic processes. In Researches in geochemistry (pp. 427-457), ed. P. H. Abelson. Wiley, N.Y., 511 pp.
- , 1967. Thermodynamic properties of simple solutions. In Researches in geochemistry (2) (pp. 340-361), ed. P. H. Abelson. Wiley, N.Y., 633 pp.
- WADSWORTH, W. J., 1961. The layered ultrabasic rocks of southwest Rhum. Phil. Trans. Roy. Soc., Ser. B. 244, 21-64.
- WAGER, L. R., 1956. A chemical definition of fractionation stages as a basis for comparison of Hawaiian, Hebridean, and other lavas. Geochim. Cosmochim. Acta 2 217-248.
- WALKER, F., and A. POLDERVAART, 1949. Karroo Dolerites of the Union of South Africa. Bull. Geol. Soc. Am. 60, 591-706.
- WATSON, J. V., 1965. 'Lewisian' Ch. 2 (pp. 50-78) of The Geology of Scotland, ed. G. Y. Craig. Oliver and Boyd, Edin., 556 pp.
- WESTOLL, N. D. S., 1968. Ph.D. Thesis, Univ. of Edinburgh.
- WEILL, D. F., and W. S. FYFE, 1964. A discussion of the Khorzhinskii and Thompson treatments of thermodynamic equilibrium in open systems. Geochim. Cosmochim. Acta 28, 565-576.
- , and —————, 1967. On equilibrium thermodynamics of open systems and the phase rule (A reply to D. S. Khorzhinskii). Geochim. Cosmochim. Acta 31, 1167-1176.

WILSON, A. D., 1955. A new method for the determination of ferrous iron in rocks and minerals. Bull. Geol. Surv. G.B. 2.

YODER, H. S., 1955. Role of water in metamorphism. In The Crust of the Earth (pp. 505-523), ed. A. Poldervaart. Geol. Soc. Amer. Spec. Pap. 62, 762 pp.

—————, D. B. STEWART, and J. R. SMITH, 1957. Ternary feldspars. Carnegie Inst. Wash. Y.B. 56, 206-214.

ACKNOWLEDGEMENTS

I would like to thank Dr. M.J. O'Hara for suggesting the topic for study, and for his constant supervision and friendly advice. Also Dr. E.L.P. Mercy and Dr. M.R.W. Johnson for their supervision during the early stages of the work, and Professor F.H. Stewart for making available facilities in the Grant Institute of Geology, and for his tolerance in permitting an extension of the period of study.

Thanks are also due to the following: Mr. M.J. Saunders and Mr. G.R. Angell for advice concerning methods of analysis; Dr. J.V.P. Long for making available an electron probe, and assistance with its operation; and numerous other workers on the Lewisian of Sutherland, with whom many fruitful discussions were held, in particular, Mr. B.C. Barooah, Mr. P.K. Chowdhary, and Mr. W. Wheatley.

I gratefully acknowledge receipt of a maintenance grant from the Natural Environment Research Council (formerly D.S.I.R.) during the first three years of this work.